

Colloidal Transport in Porous Media

Modeling and Analysis

Kolloidaler Transport in porösen Medien

Modellierung und Analysis

Der Naturwissenschaftlichen Fakultät
der Friedrich-Alexander-Universität Erlangen-Nürnberg
zur

Erlangung des Doktorgrades Dr. rer. nat.

vorgelegt von

Nadja Ray

aus Erlangen

Als Dissertation genehmigt von der Naturwissenschaftlichen Fakultät der
Friedrich-Alexander-Universität Erlangen-Nürnberg

Tag der mündlichen Prüfung: 27.5.2013

Vorsitzender des Promotionsorgans: Prof. Dr. Johannes Barth

Gutachter: Prof. Dr. Peter Knabner

Gutachter: Prof. Dr. Ben Schweizer

Gutachter: Prof. Dr. Grégoire Allaire

Contents

Zusammenfassung	vii
Abstract	xi
1 Introduction	1
1.1 Motivation	1
1.2 Aim	5
1.3 Outline of the thesis	7
2 Basic models	9
2.1 Pore-scale models	10
2.1.1 Special cases	12
2.1.2 Model Problem P	16
2.1.3 Dimensionless form of Problem P	18
2.1.4 Analysis of Problem P	22
2.2 Effective models	27
2.2.1 Darcy's law	27
2.2.2 Transport equations	28
2.2.3 Linear systems	29
2.2.4 Effective model equations, Problem P_0	29
2.2.5 Analytical investigations	31
2.2.6 Non-negativity and boundedness in $L^\infty((0, T) \times \Omega)$	33
2.2.7 Existence and uniqueness	43
2.3 Concluding remarks	54
3 The concept of homogenization	55
3.1 Introduction	55

3.1.1	Introduction to upscaling methods	57
3.1.2	Method of volume averaging	57
3.1.3	Homogenization methods	57
3.1.4	Extension into Ω	64
3.2	Overview existing literature	65
4	Homogenization of Problem P	67
4.1	Pore-scale model P_ε	68
4.1.1	Definition and existence of weak solutions of Problem P_ε	71
4.2	Neumann case	73
4.2.1	ε -independent a priori estimates in the Neumann case	73
4.2.2	Homogenization in the Neumann case	82
4.2.3	Conclusion	95
4.3	Dirichlet Case	97
4.3.1	ε -independent a priori estimates in the Dirichlet case	97
4.3.2	Homogenization in the Dirichlet case	102
4.3.3	Conclusion	108
4.4	Concluding remarks	109
5	Homogenization of Problem P including an evolving microstructure	113
5.1	Introduction	113
5.2	Extensions of periodic upscaling	114
5.3	Pore-scale model	115
5.3.1	Mass conservation laws	116
5.3.2	Reaction rate	118
5.3.3	Level set function	118
5.3.4	Outline of the pore-scale model	119
5.4	Periodic homogenization	119
5.4.1	Evolving pore geometry	119
5.4.2	Scaled model equations	119
5.4.3	Two-scale asymptotic expansion	121
5.4.4	Lowest order problems of the asymptotic expansion	122
5.4.5	Next order problems of the asymptotic expansion	123
5.4.6	Zeroth order transport problem of the asymptotic expansion	125
5.4.7	Upscaling results	128

5.4.8	Properties of the coefficient functions	130
5.4.9	Backtransformation	132
5.5	Numerical Results	132
5.5.1	Representation of the interaction potential and the geometry in a radially symmetric setting	133
5.5.2	Computation of effective coefficients	135
5.6	Concluding remarks	139
6	Discussion and Outlook	141
A	Notation	145
A.1	Basic notation	145
A.2	Domain related quantities	147
A.3	Function spaces	148
A.4	(Differential) operators	150
A.5	Physical quantities	151
A.6	Dimensionless numbers and characteristic quantities	154
	Bibliography	155
	Declaration	167
	Curriculum vitae	169

Acknowledgement

First of all, I would like to express my sincere gratitude to Prof. Dr. Peter Knabner for making it possible to join his working group and doing research in a really fascinating and interdisciplinary field. He gave me considerable freedom to work and follow my own ideas, but supported me with his knowledge whenever necessary and kept me on the right track during my PhD. Moreover, he motivated and constantly encouraged me to take new initiatives.

I would like to express my warmest gratitude to Prof. Dr. Christof Eck, who, first of all, entrusted me with the idea of doing a PhD. Since he was a very gifted teacher, I learned a lot from him on (methods of) mathematical modeling and the understanding of physical processes. Till he past away far too early he has been an extraordinary supervisor who never refused to patiently join long lasting discussions although having serious health problems.

Moreover, I would like to take the opportunity to thank Prof. Dr. Grégoire Allaire and Prof. Dr. Ben Schweizer for reviewing this thesis and for their interest in my work. Further thanks are reserved for Prof. Dr. Nicole Marheineke and Prof. Dr. Wolfgang Borchers who kindly agreed to act as examiners in the defence of the thesis.

Special thanks are reserved for Dr. Tycho van Noorden with whom I had the opportunity to work, in particular, during his time at the University of Erlangen-Nuremberg. He was always ready to discuss patiently any questions and problems I faced him with. I really admire his deep understanding of mathematical modeling and physics.

I would like to express my gratitude to Dr. Adrian Muntean for his kind hospitality at the Technical University of Eindhoven, Netherlands, and our fruitful collaboration. His enthusiasm inspired my work and kept me motivated.

Moreover, I would like to thank my colleagues Prof. Dr. Nicole Marheineke, Prof. Dr. Willi Merz, Prof. Dr. Florin Radu and, in particular, Dr. Maria Neuss-Radu who have always been a source of advice and help. Prof. Dr. Kai-Uwe Totsche I would like to

thank for the insightful and inspiring discussions in hydrogeological applications and processes.

Florian Frank, with whom I shared the office for more than 4 years, I would like to thank for the good times and discussions we had, the insight he provided me into numerical approaches and the discussions on the interplay of numerics and analysis. He always had a helping hand for my countless problems with the computer, Latex, etc. He certainly soon became more than just a colleague and collaborator. Moreover, I would like to thank Matthias Herz with whom I had long lasting and stimulating discussions and a fruitful collaboration.

I would like to thank the secretaries, Cornelia Kloss and Astrid Bigott and also Dr. Alexander Prechtel and Fabian Klingbeil who had time to resolve all the smaller and bigger problems and highly contributed to a pleasant working atmosphere. Moreover, I would like to express my warmest gratitude to all my colleagues at the Chair of Applied Mathematics I. It was really a pleasure to work in this excellent working group and always finding an open door for discussions of problems and having enjoyable breaks.

For the support by the scholarships of the Office of Gender and Diversity at the University of Erlangen-Nuremberg, the Deutsche Telekomstiftung, in person Christiane Frense-Heck and Rainer Franke, and the Studienstiftung des Deutschen Volkes, in person Dr. Weyand and Prof. Dr. Stein-Kecks, I am very gratefully. These allowed me to concentrate on my research independently of financial worries and to join interesting workshops, seminars and summer schools, not to mention the fruitful exchange with further PhD students.

All my dear friends who supported my professional and personal development and kept me motivated deserve my deepest gratitude. Moreover, I would like to thank my parents Dr. Kisha Ray and Jürgen Kintscher, my brothers Nicolas Ray and Felix Ray, and my family for their continuous support and encouragement in so many ways.

And, last but not least, I would like to thank my husband Dr. Alexander Thekale for proof reading the manuscript of this work. He kept me motivated and encouraged me through his never ending support in any means. Most of all, I would like to thank him for his infinite and precious love.

Titel, Zusammenfassung und Aufbau der Arbeit

Kolloidaler Transport in Porösen Medien – Modellierung und Analysis

Zusammenfassung Die vorliegende Arbeit beschäftigt sich mit der mathematischen Modellierung und Analyse von Fließ- und Transportprozessen unter Berücksichtigung (elektrischer) Wechselwirkungen in porösen Medien. Im Einzelnen sollen folgende Aspekte in ein mathematisches Modell integriert und untersucht werden: Erstens die räumlich heterogene Struktur des porösen Mediums und zweitens die Wechselwirkungen und das Zusammenspiel der physikochemischen Prozesse zwischen Fluid, geladenen kolloidalen Partikeln sowie ihrem Transport und der Feststoffmatrix. Ziel der Arbeit ist es, ein tieferes Verständnis der wesentlichen Aspekte und relevanten physikalischen Prozesse zu erlangen, die auf unterschiedlichen räumlichen Skalen Einfluss auf die Kolloiddynamik in porösen Medien nehmen. Da die räumliche Struktur des stark heterogenen Mediums auf sinnvollen Raum- und Zeitskalen nicht exakt aufgelöst werden kann, und damit direkte numerische Simulationen nicht möglich sind, ist der Kernpunkt der Arbeit aussagekräftige mathematische Modelle für eine effektive Beschreibung des Fließverhaltens und der Transportprozesse abzuleiten.

Der Fokus dieser Arbeit liegt in weiten Teilen auf der Untersuchung von Effekten, die aus elektrostatischen Wechselwirkungen resultieren, da diese sich in signifikanter Weise auf den kolloidalen Transport auswirken. Desweiteren wird in der vorliegenden Arbeit eine Modellerweiterung untersucht, die einer Veränderungen in der Porosität Rechnung trägt. Diese zieht wiederum eine Rückkopplung auf Fließ- und Transportgeschehen mit sich.

In der vorliegenden Arbeit wird zunächst jeweils ein mathematisches Modell zur Beschreibung von Fließ- und Transportprozessen sowohl auf der Porenskala als auch auf makroskopischer Skala vorgestellt. Diese Modelle werden basierend auf Massen- und Impulsbilanzen abgeleitet und führen auf Systeme instationärer, nichtlinearer, voll gekoppelter partieller Differentialgleichungen: Das instationäre Stokes-Nernst-Planck-Poisson (SNPP) System und das instationäre Darcy-Nernst-Planck-Poisson (DNPP) System. Zwingend notwendig für alle weiteren Untersuchungen ist eine mathematische Analyse beider Systeme auf Existenz und Eindeutigkeit globaler schwacher Lösungen. Dazu wird ein Fixpunktansatz gewählt. Einen weiteren wesentlichen Schritt in der Untersuchung beider Systeme stellt die Ableitung von L^∞ -Abschätzungen für die Anzahldichten geladener kolloidaler Partikel mittels Moser-Iteration dar.

Um ein numerisch rechenbares mathematisches Modell zu erhalten, wird im Anschluss periodische Homogenisierung, oder genauer die Methode der Zweiskalenkonvergenz, auf das SNPP System erfolgreich angewendet. Dazu wird der Skalenparameter ε als Verhältnis zwischen Porendurchmesser und Abmessung des porösen Mediums definiert und der Grenzwert verschwindender Mikrostruktur, d.h. $\varepsilon \rightarrow 0$, untersucht. Der Skalenparameter ε wird genutzt, um die verschiedenen (Transport-)Terme zu skalieren, zu gewichten und miteinander in Beziehung zu setzen. Zwingend notwendig für die Ableitung äquivalenter effektiver Modelle im Rahmen der Zweiskalenkonvergenz ist es, dass ε -unabhängige a priori Abschätzungen gezeigt werden können. Effektive Koeffizienten (Porosität, Permeabilitätstensor und Diffusionstensor) werden mittels geeigneter Zellprobleme definiert, da dies erlaubt Informationen in direkter Weise von der Porenskala auf die makroskopische Skala zu übertragen. Schließlich wird die Struktur der Limesgleichungen in Abhängigkeit der gewählten Skalierungen und für unterschiedliche Randbedingungen diskutiert.

Darüberhinaus wird in der vorliegenden Arbeit eine Erweiterung des Stokes-Nernst-Planck Systems untersucht, um Wechselwirkungen und Reaktionen der kolloidalen Partikel mit der Feststoffmatrix in das mathematische Modell zu integrieren. Damit werden Porositätsveränderungen in das bestehende Modell einbezogen und Effekte des Porenverschlusses sowie Rückkopplungen an Fließ- und Transportgeschehen diskutiert. Um wiederum eine äquivalente effektive Modellbeschreibung zu erhalten, wird eine Erweiterung der Methode der formalen, asymptotischen Zweiskalenentwicklung angewandt, die mittels Level Set Formulierung der zeitlich veränderlichen flüssig-fest Grenzfläche habhaft wird. Zeit- und ortsabhängige Koeffizientenfunktionen sowie Zellprobleme werden definiert und im radialsymmetrischen Fall explizit berechnet.

Aufbau der Arbeit nach Kapiteln In Kapitel 1 der Arbeit wird die Bedeutung von porösen Medien und kolloidalen Partikeln in verschiedenen Anwendungsgebieten sowie die Vorteile der mathematischen Modellierung für alle weitere Untersuchungen diskutiert. Desweiteren werden die Kernfragen, die im Rahmen dieser Arbeit untersucht werden, herausgestellt und erörtert.

Im ersten Teil von Kapitel 2 wird zunächst ein mathematisches Modell eingeführt, welches das Fließgeschehen und den Transport geladener kolloidaler Teilchen auf der Porenskala beschreibt – das sogenannte Stokes-Nernst-Planck-Poisson (SNPP) System. Im Anschluss wird die zugehörige dimensionslose Form abgeleitet und Existenz und Eindeutigkeit schwacher Lösungen des Problems bewiesen. Darüber hinaus wird gezeigt, dass die Anzahldichten, die das SNPP System lösen, physikalisch sinnvolle Größen beschreiben, also nicht negativ und beschränkt sind. Im zweiten Teil des Kapitels wird ein effektives mathematisches Modell zur Beschreibung des Fließgeschehens und des Transports kolloidaler Teilchen diskutiert - das Darcy-Nernst-Planck-Poisson System, welches mittels Moser-Iteration und dem Fixpunktsatz von Tihonov ebenfalls analytisch untersucht wird.

In Kapitel 3 werden verschiedene Upscalingmethoden vorgestellt: Die Methode repräsentativer Elementarvolumen, die Methoden formaler asymptotischer Zweiskalenentwicklung und die Methode der Zweiskalenkonvergenz. Die beiden letzteren Methoden werden im Rahmen dieser Arbeit genutzt, um effektive Modelle abzuleiten. Dieses Kapitel wird mit einer mathematischen Beschreibung einer idealisierenden geometrischen Grundannahme und einem Literaturüberblick über Arbeiten, die sich mit der Homogenisierung des SNPP Systems und verwandter Systeme beschäftigt, beschlossen.

Kapitel 4 und Kapitel 5 stellen den Hauptteil der vorliegenden Arbeit dar. In Kapitel 4 wird die Methode der Zweiskalenkonvergenz auf das SNPP System angewandt. Dazu wird das Problem mittels Skalenparameter ε in einem Mehrskalenkontext formuliert. Zunächst werden a priori Abschätzungen gezeigt, die unabhängig von ε gelten. Im Anschluss werden gemittelte effektive Modelle abgeleitet, zu denen geeignete Zellprobleme und effektive Koeffizienten definiert werden. Im letzten Teil von Kapitel 4 verweisen wir auf einige numerische Ergebnisse, die die abgeleiteten theoretischen Resultate unterstreichen.

Kapitel 5 beschäftigt sich mit einer Erweiterung des Stokes-Nernst-Planck Systems und seiner Homogenisierung im Fall veränderlicher Mikrostrukturen, genauer gesagt, zeitlich veränderlicher flüssig-fest Grenzflächen. Hierzu werden aus dem Prinzip der

Massenerhaltung geeignete Randbedingungen auf der Grenzfläche abgeleitet. Eine Erweiterung der Methoden der formalen asymptotischen Zweiskalenentwicklung in einer Level Set Beschreibung, siehe [138], wird angewendet, um ein äquivalentes makroskopisches Modellproblem abzuleiten. Dieses Kapitel wird mit der Diskussion der effektiven Koeffizienten, für die Symmetrieeigenschaft und (gleichmäßige) positive Definitheit gezeigt werden, abgeschlossen. Im radialsymmetrischen Fall, d.h. insbesondere für radialsymmetrisches Interaktionspotential, werden diese Koeffizienten numerisch berechnet.

Die vorliegende Arbeit wird mit einigen Kommentaren und einem Ausblick auf mögliche weitere Forschungsaspekte in Kapitel 6 beschlossen.

Die folgenden Publikationen, bei denen N. Ray Hauptautor ist, enthalten Teile der in dieser Arbeit dargestellten Ergebnisse: [55, 113, 111, 110, 112]. Die Koautoren C. Eck, P. Knabner, A. Muntean und T. van Noorden haben im Rahmen ihrer Betreuungstätigkeit von N. Ray zu diesen Arbeiten beigetragen. Der zweite Teil von Kapitel 2 beruht auf [55] wobei ein Druckfehler in der Abschätzung der rechten Seite in der Moseriteration hier korrigiert wird. Beide Autoren N. Ray und M. Herz haben zu gleichen Teilen zum Entstehen der Arbeit [55] beigetragen. Kapitel 4 ist eine Erweiterung der Arbeiten [113, 110]. Insbesondere wird hier ein Druckfehler in der Skalierung der Poincaré-Ungleichung in [113] korrigiert. Kapitel 5 nimmt die in [111, 112] dargestellten Ergebnisse auf. F. Frank, der Koautor dieser Arbeit ist, trägt als insbesondere zu den Simulationen des Mehrskalenszenarios bei, die in [112] gezeigt werden.

Abstract

The scope of this thesis is the mathematical investigation and analysis of fluid flow and transport processes in porous media. In detail, the following aspects will be examined and incorporated in a mathematical model: 1) the heterogeneous spatial structure of the porous medium and 2) the interplay and coupling of processes between fluid flow, charged colloidal particles, their transport and the porous matrix.

The main aim of this thesis is to achieve a deeper understanding of the most significant aspects and relevant physical processes, which influence the colloidal dynamics within a porous medium on different spatial scales. Since the spatial structure of the highly heterogeneous porous medium cannot be resolved exactly on reasonable spatial and temporal scales, a direct numerical approach is unfeasible. For this reason, the main focus of this thesis is on deriving meaningful mathematical models that describe fluid flow and transport on a macroscopic, averaged scale.

Main parts of the work are concentrated on electric interactions, which significantly influence the transport of charged colloidal particles. Another question that is addressed in this thesis is the extension to a mathematical model that is capable of changes in porosity together with the back coupling to fluid flow and the change of transport properties of the porous medium.

First of all, mathematical models are introduced in order to describe fluid flow and transport processes on the pore-scale and on the macroscopic scale, respectively. Both of the models are based on physical principles such as balance of mass and of momentum and result in non-stationary, nonlinear, and fully coupled systems of partial differential equations. These two systems are the Stokes-Nernst-Planck-Poisson (SNPP) system and the Darcy-Nernst-Planck-Poisson (DNPP) system, respectively. For all further investigations, it is essential to guarantee unique existence of weak solutions of both mathematical models. To this end, a fixed point approach is applied and Moser's iteration technique is used in order to prove a L^∞ -estimate for the number densities of the charged colloidal particles.

In order to derive the desired meaningful effective mathematical models, periodic homogenization using the method of two-scale convergence is applied to the SNPP system. For this purpose, a small scale parameter ε is introduced as ratio between the pore diameter and the size of the porous medium. A scaling of the (transport) terms with ε is then performed and the limit of vanishing microstructure, i.e. $\varepsilon \rightarrow 0$, is investigated. In the derivation of equivalent effective models in the framework of two-scale convergence, it is essential to prove ε -independent a priori estimates. Moreover, an important step is to transfer information from the pore-scale to the macroscopic scale in a direct way. To this end, effective coefficients such as permeability, diffusion tensor, and porosity are defined by means of so-called cell problems. Finally, the structure of the limit equations is discussed for different boundary conditions and variable choices of scalings.

Finally, integrating the interaction and chemical reactions of the colloidal particles with the porous matrix to the Stokes-Nernst-Planck system, the mathematical model is extended in such a way that it captures changes in porosity, effects of pore clogging and a back coupling to fluid flow. In order to derive again an effective model description, two-scale asymptotic expansion in a level set framework is applied to include the evolving microstructure. Time and space dependent coefficient functions and cell problems are defined and calculated explicitly in a radially symmetric setting.

Chapter 1

Introduction

The scope of this thesis is the description and analysis of the dynamics of colloidal particles within a porous medium using mathematical modeling and upscaling techniques. We first motivate, in Section 1.1, why porous media and colloidal particles are of high practical relevance and why mathematical modeling approaches are beneficial for their analysis. In Section 1.2, we emphasize the specific aspects that will be investigated in this thesis and highlight their importance in certain applications. Concluding, in Section 1.3, we briefly outline the structure of the investigations within this thesis.

1.1 Motivation

Porous media. Porous media appear in many technical and biological applications as well as in engineering science. Examples of porous media that are produced by means of technical processes are concrete, ceramics and metal foam, just to mention a few. The most prominent example of a natural porous media is certainly the soil. Moreover, the research on flow and transport processes through porous media is of extreme practical interest: explicit attention has been paid, e.g., to the research of contaminant transport in the soil, transport through biological membranes, chromatography, filters or in the field of catalysis.

A *porous medium* is characterized by the heterogeneous spatial structure consisting of the *porous matrix* and the corresponding *pore space* (void space). In general, the pore space is filled by several phases (liquids and gases). In the natural underground, for example, soil air and soil water are both present in the so-called *unsaturated zone*, whereas in the so-called *saturated zone* (the *aquifer*) the pore space is completely filled

with water. In general, the distinct phases are not homogeneous. They can consist of several components and, especially in the liquid phase, various substances and chemical species can be dissolved.

In considering porous media, special attention has to be paid to the different spatial length scales that are inherent to the porous medium: there is at first the molecular scale on which chemical reactions take place. Secondly, there is the pore-scale (microscopic scale) on which the pore geometry is resolved explicitly and where physically relevant processes occur. And, last but not least, the macroscopic scale, where practically relevant phenomena occur and experimental observations are made, has to be taken into account.

Colloids. The word *colloid* is derived from the Greek words *κολλα*: glue and *ειδος*: shape. Already, Thomas Graham (1805-1869) established the term “colloid”. In 1854 he studied the passage of particles through membranes and, in contrast to crystalloids, he defined colloids to be those particles that could not diffuse through the membrane. A person who is also closely linked to colloid science is Wolfgang Ostwald. He was head of the first journal mainly dealing with this topic “Kolloidzeitschrift” (now Polymer and Colloid Science) in the year 1907 and was elected as the first chairman of the newly founded society “Kolloid-Gesellschaft” in 1922. Further names that are strongly related to this field are those of **D**erjaguin, **L**andau, **V**erwey, and **O**verbeek who developed the so-called DLVO theory [32, 142], which is devoted to the stability of colloidal systems. According to the International Union of Pure and Applied Chemistry, since 1971 colloids are defined by their size range which lies between $1nm$ and $1\mu m$ in at least one space dimension, [59]. Several attempts to classify colloids are undertaken: according to Staudinger, one distinguishes between the following classes of colloids due to their binding: dispersion colloid (dispersoid), molecular colloid, and association colloid. Further possibilities for classification are the behavior toward the dispersion medium such as lyophobic or lyophil, or properties such as geometry and shape. Often also the chemical composition such as inorganic (silicates, carbonates), organic (aggregates of organic soil substances, sooty particles) or biological (viruses, spores) are used as classification. It is important to note that a colloidal system always consists of two parts: the dispersed phase and the dispersion medium. Either of the parts may be solid, liquid, or gaseous. As the examples in Table 1.1 show, colloidal systems are found everywhere, in lifeless nature such as smoke and porous rock, in living matter such as bones and blood, and in technical applications as used, e.g., in the food, pharmaceutical and cosmetic industry, paints and printing, waste water treatment etc. [56, 51].

dispersed phase	dispersion medium	example
liquid	gaseous	mist, hair spray
solid	gaseous	smoke
gaseous	liquid	foam
liquid	liquid	milk, mayonnaise
solid	liquid	paint, toothpaste, blood
gaseous	solid	pumice, styrofoam
liquid	solid	ice cream
solid	solid	cranberry (gold ruby) glass

Table 1.1: Examples of colloidal systems

In geoscientific applications, and more precisely, in the context of colloidal transport within the soil, many interesting aspects are observed since colloids interact with each other, with the fluid flow, the porous matrix and further dissolved substances or chemical species. The (extended) DLVO theory was developed to describe such interactions. It relies on the analysis of the interplay between electrostatic interactions, London-van-der-Waals forces, and also further interaction forces such as Born repulsion, etc. Since van-der-Waals-forces are attractive, they result in flocculation or coagulation and act destabilizing whereas electrostatic forces are repulsive and act stabilizing on colloidal systems. An important aspect for the interaction of colloids is the variation of their electro-chemical properties. These may be influenced either electrostatically or sterically: factors that have an impact on the electrostatic properties are chemical reactions that affect functional groups, pH value and ionic strength of the surrounding dispersion medium or permanent charges. For steric hindrance, adsorption of polymers is the main influencing factor.

We mention just a few more specific, geoscientific examples in which colloids play a major role: the mobilization of substances, e.g. contaminants, structural changes in the pore space and clogging of pores. More precisely, colloids are of interest at least in three perspectives: firstly, colloids such as bacteria, viruses or spores are themselves undesirable, e.g., in drinking water. Secondly, it has been observed experimentally that (organic) colloidal particles are highly relevant in the exploration of transport phenomena within the soil [88, 101]. Due to their size range, surface properties play a crucial role in comparison to bulk properties. Based on their surface morphology, colloids act similar to the soil matrix and bind dissolved substances and transport them through the porous medium. In the soil, especially organic colloids are important since they mobilize and facilitate the transport of contaminant such as radio nuclides or heavy metals. On the other hand, colloids are also used to lower and control the activity of contaminants. In the field of wastewater treatment, colloids play a role since

they may decrease the effectiveness of filters by clogging. Thirdly, adsorption processes at the soil matrix can occur, which depend on different factors such as ionic strength, surface morphology, texture and structure of colloids and the soil matrix. This aspect is, among others, relevant since it goes along with a change of the structure of the porous matrix or even clogging of pores can occur. This leads to a back coupling to fluid flow since the pore space that is accessible for fluid flow and transport are changed.

Mathematical Modeling. In mathematical modeling, starting from an explicit (physical) problem, a well defined mathematical task is set up using mathematical concepts and language. The challenge hereby is to balance between accurateness, solvability, computational speed and value of the model. Therefore it is necessary to make simplifications, approximations and assumptions. Furthermore, certain effects have to be neglected that are not relevant for the objective of the underlying problem. Despite of this demanding task, a mathematical model helps to explain and understand a problem and allows to study the effects of different aspects or components. Moreover, a mathematical model can be used to predict the behavior of these components. For this reasons, mathematical modeling has been applied in many areas of the natural and engineering sciences. To get at least an overview on many different topics, we refer to [39] and the references therein. Also in the field of colloidal particles, many different model approaches have been studied in the literature:

Mathematical models and corresponding numerical simulation concerning solute transport including ad- and desorption phenomena can be found, e.g., in [11, 64, 66], and [107]. Most models available in the literature that focus on colloidal particles and their influence on contaminant transport are based on mass balances and heuristic reaction or de- and adsorption rates. Multiphase (e.g. mobile and immobile phase), multicomponent (e.g. solid matrix and sorbed colloids, contaminants, mobile colloids and pore water) models are investigated, see e.g. the work of Bekhit [14, 13], Corapcioglu [29, 28, 30], and Lührmann [79]. Bekhit et al. [14] consider a two-phase system with one mobile phase including pore water, dissolved contaminant and mobile colloids as well as an immobile phase including the soil matrix and adsorbed colloids. Corapcioglu et al. propose a three phase model in [29] with two solid phases consisting of the matrix and the adsorbed colloids and a four phase model in order to account for the additional phase pore air in [28]. Extensions to a dual porosity approach can be found in [30]. In general, mass balances are established for the concentrations of the arising components. They are coupled by adsorption- and desorption rates, respectively.

In accordance with experimental data, free parameter and the rate functions are determined and a validation is done via comparison with experimental data. The main disadvantage in this modeling approach is that the microscopic scale is completely neglected.

On the other hand, colloid dynamics can be described on the level of the colloidal particle themselves [6, 141, 120]. However, direct particle tracking is limited to low concentrations and the resolution of the complex structure of and interaction between colloidal particles.

Another type of method that is found in the literature are so-called hybrid models which combine the continuum description of fluid flow with particle methods, [83, 68, 71, 114]. In this sense, there is a possibility to take into account the microscopic scale via coupling to the macroscopic model by parameters, boundary conditions or source terms that are calculated by means of auxiliary microscopic problems. This approach allows to couple the discrete and continuum scale directly and the microscopic sub-problems are solved using for example molecular dynamics simulations. The drawback of these model approaches is that the way of coupling is heuristically motivated and not derived from microscopic modeling principles.

Further methods to handle multi-scale problems that are driven from a numerical point of view are, among many others, multi-scale finite elements and heterogeneous multi-scale methods, see [35, 40, 90] and references cited therein.

1.2 Aim

The mathematical investigation of fluid flow and transport in porous media is challenging in many perspectives. The aspect that is most interesting from a modeling, analytical and numerical point of view is the interplay and coupling of processes between fluid flow, particles, their transport, and the porous matrix. Our mathematical investigations within this thesis aim at these complex systems. Exemplarily for such systems, colloidal systems and their relevance in contaminant transport in the soil have already been discussed in more detail in Section 1.1.

In main parts of this thesis we restrict ourselves to electric interaction forces. But nevertheless, our model approach is representative for more general mathematical models, i.e. models including further interaction potentials. The reduced model captures all characteristics of the physical problem such as coupling phenomena and nonlinear-

ities. Moreover, the reduced model allows a clear presentation and comprehensible investigations of the content of the thesis. The reason why we choose electrostatic interaction and focus on the investigation of the correlated phenomena is that these phenomena occur also in many further applications such as in the context of semiconductor devices [86, 140], transport through biological membranes [23, 91], battery design [99, 31], and many more. Thus, the considerations in this thesis comprise also questions arising in these important fields.

In addition to the (nonlinear) coupling of processes arising from the electrostatic interaction forces, the main difficulty lies in the fact that the processes take place in a highly heterogeneous porous medium. Obviously, the exact resolution of the geometry is not possible and, for this reason, a direct numerical approach for a reasonable microscopic mathematical model is unfeasible in practice for meaningful time and spatial scales. On the other hand, pure macroscopic models are based on heuristics and experimental observations, and are not validated from a microscopic point of view. Therefore, starting from a pore-scale model (a system of partial differential equations), an averaging procedure will be necessary to provide an effective model that allows the interpretation of observed phenomena and physically relevant forecasts.

We recall that one main goal of the thesis is to provide a reasonable mathematical model that describes fluid flow and transport phenomena on an averaged scale maintaining information from the microscopic scale. To achieve this goal, it is essential that we succeed to integrate information from the pore-scale to the macroscopic scale in a direct way. For this reason, we apply rigorous homogenization techniques in order to derive effective averaged macroscopic models. Besides the derivation of models that are in some sense equivalent to the underlying exact pore-scale model, we use an upscaling approach since it provides the possibility to validate and expand the understanding of already existing effective models. Another advantage of homogenization is that the relation between microscopic and macroscopic model is given explicitly. Furthermore, effective coefficients such as permeability, diffusion tensor and porosity are given in terms of the microscopic geometry. In this sense, information is transferred from the pore-scale to the macroscopic scale directly.

Another aspect that we intend to understand in this thesis is the relationship between different multi-scale problems, which gives deeper insight in the understanding of physical processes, of the interplay between such processes, and of phenomena including electric interaction. By means of rigorous homogenization this can be achieved by studying the influence of the powers of a (small) scale parameter ε which is used in

order to scale/balance the different terms in the governing system of partial differential equations. We point out again that the second main goal of this thesis is to investigate the scaling of the electric term in relation to further well understood (transport) terms such as diffusion and convection. From a mathematical point of view, we pay particular attention to the investigation of the influence of the scaling in ε on the structure of the effective limit equations.

In order to achieve an even deeper understanding of the relevant processes and to get detailed insight in the relevant physical phenomena as well as to guarantee unique existence of weak solutions of the mathematical problem description, we investigate both of the models – pore-scale and effective model – analytically.

Another question that we address in this thesis is the modeling of a change of porosity and the pore space and inherent with that the back coupling to fluid flow and the change of the transport properties of the porous medium. Applying extensions of homogenization methods to non-periodic and evolving geometries enables us to capture these effects and to integrate them in an effective mathematical model.

All these investigations take quite some effort due to the coupling of processes and nonlinearities coming along with the underlying physical problem.

1.3 Outline of the thesis

This thesis is organized as follows:

In the first part of Chapter 2, a mathematical model describing fluid flow and charged colloidal transport at the pore-scale is introduced – the Stokes-Nernst-Planck-Poisson (SNPP) system. For this system, a non-dimensional form is derived. Moreover, unique existence of weak solution of the SNPP system and physical properties such as non-negativity and boundedness of the number densities which solve the SNPP system are shown. In the second part of Chapter 2, we state an effective mathematical model – the Darcy-Nernst-Planck-Poisson (DNPP) system. It is also analytically investigated applying Moser’s iteration technique and a fixed point approach.

In Chapter 3, different upscaling methods are presented, namely the method of representative elementary volumes, the method of formal two-scale asymptotic expansion and the method of two-scale convergence. This chapter is completed by a mathematical description of the idealized geometrical setting and a review on the existing literature of the homogenization of the SNPP system and related problems.

Chapter 4 and Chapter 5 are the core of the thesis. In Chapter 4, homogenization is applied to the SNPP system using the method of two-scale convergence. Therefore, the SNPP system is formulated in a multi-scale framework by means of the small scale parameter ε . Furthermore, a priori estimates are shown that are independent of ε . An effective model is stated defining suitable cell problems and effective coefficients. In the last part of Chapter 4, we refer to some numerical simulations that illustrate the obtained theoretical results.

Chapter 5 is devoted to an extension of the Nernst-Planck-Poisson system and its homogenization in the case of an evolution of the microscopic geometry or, more precisely, of the evolution of the solid-liquid interface. Regarding these phenomena, appropriate boundary conditions on the evolving solid-liquid interface are derived which are non-standard. Applying an extension of the method of formal two-scale asymptotic expansion to a level set description, cf. [138], an equivalent macroscopic model description is derived. This chapter is concluded by a discussion of the effective coefficients, i.e. physical properties such as symmetry and (uniformly) positive definiteness are shown and numerical computations for a simplified model with radially symmetric interaction potential are presented.

The thesis is concluded by some comments and an outlook on possible further research topics in Chapter 6.

The following publications to which N. Ray has contributed to as principle author contain parts of the results presented within this thesis: [55, 113, 111, 110, 112]. C. Eck, P. Knabner, A. Muntean, and T. van Noorden who have co-authored these publications have contributed to these in the context of supervising N. Ray. The second part of Chapter 2 is based on [55], taking the advantage to correct a misprint in the estimate of the right hand side during Moser's iteration is corrected here. Both of the authors N. Ray and M. Herz have contributed equally to the publication [55]. Chapter 4 is an extension of [113, 110]. A misprint in [113] in the scaling of the Poincaré inequality is corrected here. Chapter 5 is based on [111, 112]. F. Frank who co-authored the paper contributed in particular to the simulation of the multi-scale scenario presented in [112].

Chapter 2

Basic models

This chapter is devoted to the mathematical description of fluid flow and transport of (charged) colloidal particles within a saturated porous medium. Since processes occur on the pore-scale, whereas observations and experiments are made on the macroscopic scale (see also Chapter 3), mathematical models can be set up at least on these two different scales. For this reason, we concentrate on pore-scale models in the first part of this chapter whereas, in the second part, effective models are discussed. A mathematical investigation of models on both scales helps to get a deeper understanding of the interplay of the relevant processes and to get detailed insight in physical phenomena on different spatial scales. Especially, the investigation of the relation between the pore-scale models and effective models enables us to get a complete picture of the various influences on transport of charged colloids in porous media, see also Chapter 4.

The first part of this chapter is organized as follows: in Section 2.1, a mathematical model describing fluid flow and transport at the pore-scale is introduced. Several simplifications and specifications are discussed in Section 2.1.1 to illustrate these model equations. Afterwards, in Section 2.1.2, model Problem P is defined, which forms the basis for all further investigations in this thesis. In Section 2.1.3, the non-dimensional form of model Problem P is derived. Unique existence of weak solutions and its physical properties are stated in Section 2.1.4.

In the second part of Chapter 2, we discuss effective descriptions of fluid flow and transport processes. In particular, in Section 2.2.4, we introduce an effective mathematical model, Problem P_0 which is strongly related to Problem P . For details see also Chapter 4. For this model, unique existence of weak solutions is proven in Section 2.2.5 by means of Moser's iteration technique and a fixed point approach.

2.1 Pore-scale models

In this section, a mathematical model at the pore-scale is introduced. This model describes fluid flow and the dynamics of (charged) colloidal particles within a porous medium. Following, for example, [41] and [141], we formulate a system of partial differential equations imposing the balance of mass as well as the conservation of electric charges. In addition to standard transport mechanisms (convection and diffusion), the colloidal particles are transported by colloidal forces. Following [141], the different kinds ($i = 1, \dots, k$) of particles are modeled in an Eulerian approach by number densities c_i . These densities are transported by means of the total velocity \mathbf{v}_i that results from two effects: Firstly, the colloidal particles are transported with the fluid phase, in which they are dispersed. Here, the quantity \mathbf{v}^{hydr} , which is equal to the velocity of the fluid within the porous medium, induces the usual forced convection. This term is the same for all kind of particles. Secondly, the drift term $\mathbf{v}_i^{\text{col}}$, that is different for all types of particles, is calculated from the colloidal force F_i^{col} via

$$\mathbf{v}_i^{\text{col}} = f_i F_i^{\text{col}}$$

with resistance coefficient f_i . In applications, f_i is related to the diffusivity D_i and the product of Boltzmann constant and absolute temperature $k_B T$ by the *Stokes-Einstein relation* $f_i = \frac{D_i}{k_B T}$ [141]. In general, F_i^{col} contains the combination of all colloidal forces such as van-der-Waals, electrostatic and further (non-)DLVO forces. Exemplarily, we specify the structure of F_i^{col} for the electrostatic interaction force:

$$F_i^{\text{col}} = F_i^{\text{el}} = -z_i e \nabla \phi^{\text{el}}, \quad (2.1)$$

i.e. it is directly related to the total charge $z_i e$ and the gradient of the overall electrostatic potential ϕ^{el} .

In summary, the total transport velocity \mathbf{v}_i of colloidal particles of type i is expressed by

$$\mathbf{v}_i = \mathbf{v}_i^{\text{col}} + \mathbf{v}^{\text{hydr}} = \frac{D_i}{k_B T} F_i^{\text{col}} + \mathbf{v}^{\text{hydr}}.$$

Substituting this expression into the convection-diffusion-reaction equation $\partial_t c_i + \nabla \cdot (\mathbf{v}_i c_i - D_i \nabla c_i) = R_i(\mathbf{c})$ for a number density c_i , results in the following *transport equations* for the number densities c_i of colloidal particles

$$\partial_t c_i + \nabla \cdot \left(\mathbf{v}^{\text{hydr}} c_i - D_i \nabla c_i + \frac{D_i}{k_B T} c_i F_i^{\text{col}} \right) = R_i(\mathbf{c}) \quad \text{in } (0, T) \times \Omega \quad (2.2a)$$

with $\mathbf{c} := (c_1, \dots, c_k)$. The right-hand sides R_i include chemical reactions among different kinds of particles, source terms, et cetera to the mathematical model.

On the boundary $\Gamma = \Gamma_D \cup \Gamma_F$ of the considered domain Ω , Dirichlet or no-flux boundary conditions are prescribed and also appropriate initial conditions c_i^0 are defined in order to close the mathematical model of transport of the colloidal particles¹.

$$c_i = 0 \quad \text{on } (0, T) \times \Gamma_D^{NP}, \quad (2.2b)$$

$$\left(-\mathbf{v}^{\text{hydr}} c_i + D_i \nabla c_i - \frac{D_i}{k_B T} c_i F_i^{\text{col}} \right) \cdot \boldsymbol{\nu} = 0 \quad \text{on } (0, T) \times \Gamma_F^{NP}, \quad (2.2c)$$

$$c_i = c_i^0 \quad \text{in } \{t = 0\} \times \Omega. \quad (2.2d)$$

Remark 2.1 (Thermodynamics). *The transport equation for species i can be written in mixed formulation via $\partial_t c_i + \nabla \cdot \mathbf{j}_i = R_i$, $\mathbf{j}_i = -\frac{D_i}{k_B T} c_i \nabla \mu_i$ with mass flux \mathbf{j}_i and chemical potential μ_i . For electrostatic interactions the chemical potential is given by $\mu_i := k_B T \ln c_i + z_i e \phi^{\text{el}}$.*

Remark 2.2. *The term F_i^{col} contains the combinations of all colloidal interaction forces resulting e.g. from (extended) DLVO theory. The most important ones are van-der-Waals attraction, Born repulsion and potentials which have electric origin, cf. (2.1). In Figure 2.1, the interplay of different DLVO forces acting on a colloidal particle is depicted. Furthermore, external forces and external electrical fields may be integrated in the mathematical model in a straightforward way, i.e., as additional transport/source/sink terms or boundary conditions.*

Since the Reynolds number (for its definition see Section 2.1.3) is typically low for colloidal systems [41], we determine the fluid velocity \mathbf{v}^{hydr} by solving the *Stokes equations* for incompressible fluid flow [39] with kinematic viscosity η and constant density ρ of the fluid. As forcing term on the right hand side we take into account the drift force density. Equations (2.3a), (2.3b) are supplemented by a no-slip boundary condition:

$$-\eta \Delta \mathbf{v}^{\text{hydr}} + \frac{1}{\rho} \nabla p = \frac{1}{\rho} \sum_i c_i F_i^{\text{col}} \quad \text{in } (0, T) \times \Omega, \quad (2.3a)$$

$$\nabla \cdot \mathbf{v}^{\text{hydr}} = 0 \quad \text{in } (0, T) \times \Omega, \quad (2.3b)$$

$$\mathbf{v}^{\text{hydr}} = 0 \quad \text{on } (0, T) \times \Gamma. \quad (2.3c)$$

¹The indexes, e.g. D, F , are used to specify the type of boundary conditions. The superscripts, e.g. NP , are used to specify the subproblem, e.g. the transport problem, to which the boundary conditions are related.

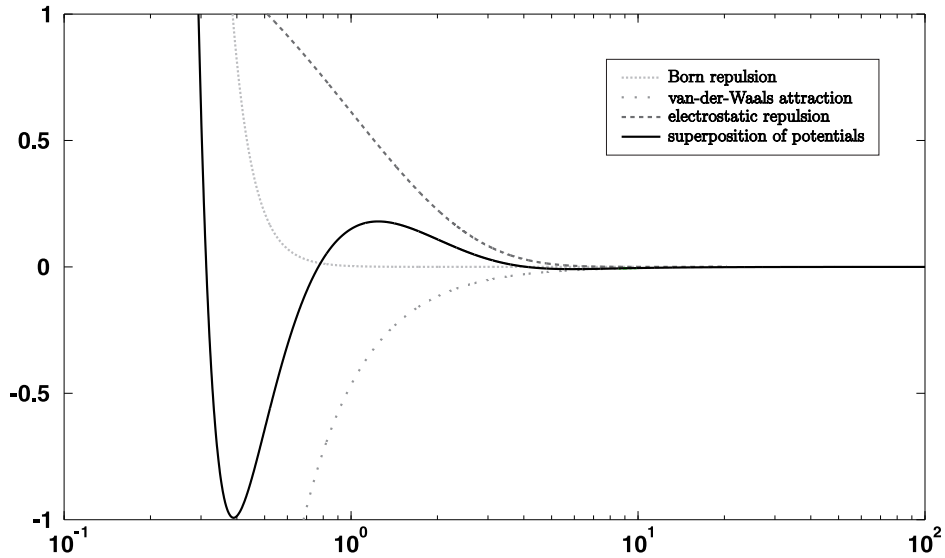


Figure 2.1: Schematic representation of superposition of DLVO forces.

2.1.1 Special cases

In the following, we discuss some simplifications and specifications of the above introduced system of coupled partial differential equations (2.2a), (2.3a). This provides a better understanding of the model problem and stresses the numerous challenges in its theoretical and numerical investigation. We first start with three well known examples in which the fluid flow is either a priori given or the chemical species are immobile. Furthermore, all colloidal interactions are neglected in the model description of the distribution of the number densities. This is followed by the description of problems including electric interaction phenomena – first without and then including convective effects, which results in a fully coupled system of partial differential equations. Special focus is then placed on the derivation of the Poisson-Boltzmann equation and the Boltzmann distribution by linearization of such a fully coupled stationary system. Finally, model Problem P is defined and discussed in some extent since it serves as a basis for all further investigations of this thesis.

1. *Convection-diffusion equation* for one single species ($k = 1, F^{\text{col}} = 0, R = 0$):

$$\partial_t c + \nabla \cdot (\mathbf{v}^{\text{hydr}} c - D \nabla c) = 0.$$

2. *Chemical reaction network I*: nonlinear system of coupled ordinary differential equations for $i = 1, \dots, k$ immobile species ($\mathbf{v}^{\text{hydr}} = 0, D_i = 0, F_i^{\text{col}} = 0$):

$$\partial_t c_i = R_i(\mathbf{c}).$$

3. *Chemical reaction network II (spatial model)*: nonlinear system of coupled partial differential equations for $i = 1, \dots, k$ mobile species ($F_i^{\text{col}} = 0$):

$$\partial_t c_i + \nabla \cdot (\mathbf{v}^{\text{hydr}} c_i - D_i \nabla c_i) = R_i(\mathbf{c}).$$

The reaction rates $R_i(\mathbf{c})$ in the chemical reaction networks I and II are often assumed to obey the mass action law, see, e.g., [39]. Analytical investigations of a combination/extension of the chemical reaction networks I and II with/to equilibrium and kinetic reactions and an effective numerical scheme can be found in [70]. The main challenge here is to handle the strong non-linearities since the reaction rates R_i contain products of powers of the number densities c_i in the case of mass action law.

4. *Van Roosbroeck system, semiconductor devices*: non-stationary drift-diffusion equation for holes (+) and electrons (-) ($i = \pm$, $\mathbf{v}^{\text{hydr}} = 0$, $F^{\text{col},\pm} = F^{\text{el},\pm}$):

$$\begin{aligned} \partial_t c^+ + \nabla \cdot \left(-D^+ \nabla c^+ - \frac{D^+ e}{k_B T} c^+ \nabla \phi^{\text{el}} \right) &= R^+(\mathbf{c}) && \text{in } (0, T) \times \Omega, \\ \partial_t c^- + \nabla \cdot \left(-D^- \nabla c^- + \frac{D^- e}{k_B T} c^- \nabla \phi^{\text{el}} \right) &= R^-(\mathbf{c}) && \text{in } (0, T) \times \Omega, \end{aligned}$$

where the reaction rate $R^\pm = -c^+ c^- + 1$ describes the annihilation/recreation reaction $X_+ + X_- \rightleftharpoons 0$ for the pairs of the electrons and holes. Furthermore, the number densities c^\pm undergo an electric drift due to their charge. The electric field ϕ^{el} which is created by the number densities of the electrons and holes is determined by *Poisson's equation* [39],

$$-\Delta \phi^{\text{el}} = \frac{e}{\epsilon_0 \epsilon_r} (c^+ - c^-). \quad (2.4)$$

For aspects on the modeling and analysis of the semiconductor equations, we refer the reader to the original work of van Roosbroeck [140], the work of Gajewski and Gröger, e.g. [48, 53], and to [86, 119] as well as to the references cited therein.

Remark 2.3. *The van Roosbroeck system has a dual gradient structure [89], i.e. $\partial_t \mathbf{c} = D_\mu \Psi^*(\mathbf{c}; -D_c \mathcal{E}(\mathbf{c}))$ with total (electric and free) energy \mathcal{E} and dual dissipation potential Ψ^* defined by*

$$\mathcal{E}(\mathbf{c}) := \int_\Omega \frac{\epsilon_0 \epsilon_r}{2} |\nabla \phi^{\text{el}}|^2 + k_B T c^+ (\log c^+ - 1) + k_B T c^- (\log c^- - 1) \, d\mathbf{x},$$

$$\Psi^*(\mathbf{c}; \boldsymbol{\mu}) := \int_{\Omega} \frac{D_-}{2k_B T} c^- |\nabla \mu_-|^2 + \frac{D_+}{2k_B T} c^+ |\nabla \mu_+|^2 + \frac{l(c^- c^+, 1)}{2} (\mu_- + \mu_+)^2 d\mathbf{x}$$

with

$$\boldsymbol{\mu} := \begin{pmatrix} \mu_+ \\ \mu_- \end{pmatrix}, \quad D_c \mathcal{E}(\mathbf{c}) = \begin{pmatrix} k_B T \log c^+ + e\phi^{\text{el}} \\ k_B T \log c^- - e\phi^{\text{el}} \end{pmatrix}$$

and

$$l(x, y) := \begin{cases} \frac{x-y}{\log x - \log y}, & x \neq y, \\ y, & x = y. \end{cases}$$

5. *Stokes-Nernst-Planck-Poisson system* for $i = 1, \dots, k$ species. Considering electric interaction forces, i.e. $F_i^{\text{col}, \pm} = F^- \cdot i \mathbf{e}_l, \pm$, the so-called *Nernst-Planck equations* [63, 80, 108] describe the transport of the charged particles:

$$\partial_t c_i + \nabla \cdot \left(\mathbf{v}^{\text{hydr}} c_i - D_i \nabla c_i - \frac{D_i z_i e}{k_B T} c_i \nabla \phi^{\text{el}} \right) = R_i(c). \quad (2.5a)$$

In the case of electric interaction, the forcing term in the Stokes equations is an electric force density and therefore (2.3a) transforms into

$$-\eta \Delta \mathbf{v}^{\text{hydr}} + \frac{1}{\rho} \nabla p = -\frac{1}{\rho} \sum_i z_i e c_i \nabla \phi^{\text{el}}. \quad (2.5b)$$

The electrostatic potential ϕ^{el} originating from the system itself is calculated using Poisson's equation. The effect on the electric field implied by the charged particles themselves is thereby included as right hand side, cf. (2.4) in item 4.

$$-\Delta \phi^{\text{el}} = \frac{1}{\epsilon_0 \epsilon_r} \sum_i z_i e c_i. \quad (2.5c)$$

6. *Boltzmann distribution, Poisson-Boltzmann equation*: the linearization of the Stokes-Nernst-Planck-Poisson system (2.5) in the stationary case and for $R_i = 0$ is well known in the engineering literature [41, 63, 80, 141] and also considered in the context of homogenization [4, 78, 94]. For the readers convenience, we recapitulate the linearization procedure here: Following the paper of O'Brian [102], we assume that the variables are linearized in the following way:

$$c_i = c_{i,\text{eq}} + \delta c_i, \quad \mathbf{v}^{\text{hydr}} = \mathbf{v}_{\text{eq}}^{\text{hydr}} + \delta \mathbf{v}^{\text{hydr}}, \quad p = p_{\text{eq}} + \delta p, \quad \phi^{\text{el}} = \phi_{\text{eq}}^{\text{el}} + \delta \phi^{\text{el}}. \quad (2.6)$$

The equilibrium values $c_{i,\text{eq}}, \phi_{\text{eq}}^{\text{el}}, \mathbf{v}_{\text{eq}}^{\text{hydr}}, p_{\text{eq}}$ which fulfill

$$\begin{aligned} -\nabla \cdot (-\mathbf{v}_{\text{eq}}^{\text{hydr}} c_{i,\text{eq}} + D_i \nabla c_{i,\text{eq}} + \frac{D_i z_i e}{k_B T} c_{i,\text{eq}} \nabla \phi_{\text{eq}}^{\text{el}}) &= 0, \\ -\eta \Delta \mathbf{v}_{\text{eq}}^{\text{hydr}} + \frac{1}{\rho} \nabla p_{\text{eq}} &= -\sum_i \frac{z_i e}{\rho} c_{i,\text{eq}} \nabla \phi_{\text{eq}}^{\text{el}}, \\ -\Delta \phi_{\text{eq}}^{\text{el}} &= \frac{1}{\epsilon_0 \epsilon_r} \sum_i z_i e c_{i,\text{eq}} \end{aligned} \quad (2.7)$$

for appropriate homogeneous boundary conditions are given by

$$c_{i,\text{eq}} = c_{i,\infty} e^{-\frac{z_i e}{k_B T} \phi_{\text{eq}}^{\text{el}}}, \quad \mathbf{v}_{\text{eq}}^{\text{hydr}} = 0, \quad \text{and} \quad p_{\text{eq}} = k_B T \sum_j c_{j,\text{eq}}. \quad (2.8)$$

The distribution for $c_{i,\text{eq}}$ in (2.8) is called *Boltzmann distribution*. Substituting (2.8) into (2.7), the so-called *Poisson-Boltzmann equation* is obtained to determine $\phi_{\text{eq}}^{\text{el}}$.

$$-\Delta \phi_{\text{eq}}^{\text{el}} = \frac{1}{\epsilon_0 \epsilon_r} \sum_i z_i e c_{i,\infty} e^{-\frac{z_i e}{k_B T} \phi_{\text{eq}}^{\text{el}}}. \quad (2.9)$$

Remark 2.4. *In the case of a z-z electrolyte, i.e. an solution with two oppositely charged species ($i = \pm$) with $z := z_+ = -z_-$ and $c_\infty := c_{\infty,+} = c_{\infty,-}$, the Poisson-Boltzmann equation (2.9) simplifies to*

$$-\Delta \phi_{\text{eq}}^{\text{el}} = -\frac{2ze}{\epsilon_0 \epsilon_r} c_\infty \sinh\left(\frac{ze}{k_B T} \phi_{\text{eq}}^{\text{el}}\right).$$

Inspired by the Boltzmann distribution (2.8) the following definition of the *ionic potential* is introduced

$$c_i := c_{i,\infty} e^{-\frac{z_i e}{k_B T} (\phi^{\text{el}} + \phi_i^{\text{ion}})}.$$

The linearization (2.6) and Taylor expansion in $\phi_{\text{eq}}^{\text{el}}$ leads to

$$\delta c_i = -\frac{z_i e}{k_B T} c_{i,\text{eq}} (\delta \phi^{\text{el}} + \phi_i^{\text{ion}}).$$

Substituting (2.6) and (2.8) into the stationary Stokes-Nernst-Planck-Poisson system (2.5) with $R_i = 0$, we obtain

$$-\nabla \cdot \left(-\delta \mathbf{v}^{\text{hydr}} \delta c_i + \frac{D_i z_i e}{k_B T} \delta c_{i,\text{eq}} \nabla \phi_i^{\text{ion}} \right) = 0, \quad (2.10)$$

$$-\eta \Delta \delta \mathbf{v}^{\text{hydr}} + \frac{1}{\rho} \nabla \delta p = - \sum_i \frac{z_i e}{\rho} (c_{i,\text{eq}} \nabla \delta \phi^{\text{el}} + \delta c_i \nabla \phi_{\text{eq}}^{\text{el}}). \quad (2.11)$$

$$-\Delta \delta \phi^{\text{el}} + \frac{1}{\epsilon_0 \epsilon_r} \sum_i \frac{z_i^2 e^2}{k_B T} c_{i,\text{eq}} \delta \phi^{\text{el}} = - \frac{1}{\epsilon_0 \epsilon_r} \sum_i \frac{z_i^2 e^2}{k_B T} c_{i,\text{eq}} \phi_i^{\text{ion}}, \quad (2.12)$$

The determination of $\delta \phi^{\text{el}}$ decouples from the system of partial differential equations determining δc_i , $\delta \mathbf{v}^{\text{hydr}}$, cf. (2.10), (2.11) and (2.13a) or (2.13b), respectively. In particular, there is no influence on the velocity field $\delta \mathbf{v}^{\text{hydr}}$ which can be seen by either of the following alternative considerations:

- The application of $\nabla \times$ to (2.11), as suggested in [102], implies

$$-\eta \Delta (\nabla \times \delta \mathbf{v}^{\text{hydr}}) = \sum_i \frac{z_i e}{\rho} \nabla c_{i,\text{eq}} \times \nabla \phi_i^{\text{ion}}, \quad (2.13a)$$

since $\nabla \times \nabla \psi = 0$ for any ψ .

- The definition of the overall pressure $P := \delta p + \sum_i z_i e c_{i,\text{eq}} (\delta \phi^{\text{el}} + \phi_i^{\text{ion}})$ in (2.11) [4], leads to

$$-\eta \Delta \delta \mathbf{v}^{\text{hydr}} + \frac{1}{\rho} \nabla P = - \sum_i \frac{z_i e}{\rho} c_{i,\text{eq}} \nabla \phi_i^{\text{ion}}. \quad (2.13b)$$

In summary, the equations (2.8), (2.10), (2.12), and (2.13a) or (2.13b) describe the linearized transport of the charged species.

2.1.2 Model Problem P

In this section, we define the *model Problem P* , which forms the basis of all further investigations within this thesis. In this sense, we set up model Problem P in such a way that all relevant processes are contained and, on the other hand, unnecessary technical overhead is avoided. Considering the transport of colloidal particles within a porous medium, e.g. the soil, we focus in the following on the electrostatic interaction. In more detail, this means that we neglect further colloidal forces as well as external forces or fields (see Chapter 5 for an approach containing further interaction potentials). Fur-

thermore, we consider two oppositely charged species (+/-) with the same absolute value of the charge number and the same diffusion coefficient, i.e $z := z_+ = -z_-$ and $D = D_+ = D_-$. In summary, we obtain a fully coupled system of partial differential equations consisting of the Nernst-Planck equations to describe the transport of the number densities of the particles - supplemented by incompressible Stokes equations and Poisson's equation to determine the fluid flow and the electric field, respectively. In addition to the coupling due to chemical reactions, a nonlinear coupling term $c\nabla\phi$ originates from the electric interaction. The latter enters the system of partial differential equations in two ways: Firstly, as forcing term in the Stokes equations and secondly as additional transport mechanism in the Nernst-Planck equations. This makes the problem non-trivial from a theoretical and numerical point of view and, in the context of (rigorous) homogenization, a quite actual research topic, see also Chapter 4. Moreover, model Problem P is suitable not only in describing colloidal dynamics in the soil but is of an increasing interest in mathematical models in many other fields, e.g. research on lithium ion batteries [99, 31, 27, 72] and biological applications such as transport of ions through membranes [23, 91, 97].

For ease of presentation, we omit the superscripts ^{hydr, el} and obtain the following system of coupled partial differential equation which is denoted by *Stokes-Nernst-Planck-Poisson (SNPP) system* or *Problem P* hereinafter².

Stokes equations (fluid flow)

$$-\eta\Delta\mathbf{v} + \frac{1}{\rho}\nabla p = -\frac{ze}{\rho}(c^+ - c^-)\nabla\phi \quad \text{in } (0, T) \times \Omega, \quad (2.14a)$$

$$\nabla \cdot \mathbf{v} = 0 \quad \text{in } (0, T) \times \Omega, \quad (2.14b)$$

$$\mathbf{v} = 0 \quad \text{on } (0, T) \times \Gamma, \quad (2.14c)$$

Nernst-Planck equations (transport of charged particles)

$$\partial_t c^\pm + \nabla \cdot \left(\mathbf{v}c^\pm - D\nabla c^\pm \mp \frac{Dze}{k_B T} c^\pm \nabla\phi \right) = R^\pm(\mathbf{c}) \quad \text{in } (0, T) \times \Omega, \quad (2.14d)$$

$$\left(-\mathbf{v}c^\pm + D\nabla c^\pm \pm \frac{Dze}{k_B T} c^\pm \nabla\phi \right) \cdot \boldsymbol{\nu} = 0 \quad \text{on } (0, T) \times \Gamma_F^{NP}, \quad (2.14e)$$

$$c^\pm = 0 \quad \text{on } (0, T) \times \Gamma_D^{NP}, \quad (2.14f)$$

$$c^\pm = c^{\pm,0} \quad \text{in } \{t = 0\} \times \Omega, \quad (2.14g)$$

²The indexes D, F, N are used to specify the boundary conditions of type Dirichlet, flux or Neumann. They can be chosen independently for each subproblem which is emphasized by the superscripts NP, P .

Poisson's equation (electrostatic potential)

$$-\Delta\phi = \frac{ze}{\epsilon_0\epsilon_r}(c^+ - c^-) \quad \text{in } (0, T) \times \Omega, \quad (2.14h)$$

$$\nabla\phi \cdot \boldsymbol{\nu} = \frac{1}{\epsilon_0\epsilon_r}\sigma \quad \text{on } (0, T) \times \Gamma_N^P. \quad (2.14i)$$

$$\phi = \phi_D \quad \text{on } (0, T) \times \Gamma_D^P, \quad (2.14j)$$

In (2.14), the notation \pm (and \mp) is used as abbreviation in order to present equations for both positively and negatively charged particles in one line. All the corresponding upper/lower signs have to be interpreted as first/second equation.

Remark 2.5. *Poisson's equation (2.14h) is supplemented by Neumann or Dirichlet boundary conditions, respectively. In the context of colloidal particles, these boundary conditions correspond to the surface charge density σ and the so-called zeta potential [108] which we denote in the following by ϕ_D . For applications in the field of geosciences, either of the boundary conditions is typically given, for example, by measurements. In the literature, the Dirichlet boundary condition (2.14f) for the transport problem is known as “perfect sink” boundary condition and the no-flux boundary condition (2.14e) supplements the so-called “no penetration” problem [41]. In applications it might also be reasonable to prescribe inhomogeneous inflow and outflow boundary conditions, e.g. $\mathbf{v} = \mathbf{v}_D$, $c^\pm = c_D^\pm$ on the inflow boundary Γ_{in} and $(\eta\nabla\mathbf{v} - p\mathbf{E}) \cdot \boldsymbol{\nu} = 0$, $D\nabla c^\pm \cdot \boldsymbol{\nu} = 0$ on the outflow boundary Γ_{out} [42, 62, 63]. We refer to [46] for computations of the corresponding system in such a framework.*

Remark 2.6. *The same system of equations is valid for the description of more than two species using the following notation and assumptions: Let I^+ and I^- denote the set of indexes of negatively and positively charged types of particles. If $D_i = D^+ = D$ for $i \in I^+$ and $D_i = D^- = D$ for $i \in I^-$ and $z_i = z^+ = z$ for $i \in I^+$ and $z_i = z^- = -z$ for $i \in I^-$, we define the collection of positively charged ions and negatively charged ions by $c^+ = \sum_{I^+} c_i$ and $c^- = \sum_{I^-} c_i$, respectively. Moreover, if the reaction rates can be expressed for the newly defined number densities c^\pm by $R^\pm(c^+, c^-) = \sum_{I^\pm} R_i(\mathbf{c})$ (e.g. for linear rates), we exactly obtain system (2.14).*

2.1.3 Dimensionless form of Problem P

In this section, we derive the non-dimensional form of Problem P following e.g. [141], i.e., we transform model Problem P in its representation in dimensionless variables.

Using this approach, we first of all reduce the number of parameters. However, more important is that we derive characteristic properties of the system which reveal the correlation of physical processes. A further advantage of the non-dimensionalization procedure is that we determine intrinsic constants of the system. In order to start with the non-dimensionalization procedure, we denote the dimensionless quantities with superscript $*$ and define their relation to the characteristic scales of length, time, velocity, pressure, number density and electrostatic potential L, t_c, V, P, C and Φ , respectively, to be $x^* = x/L$, $t^* = t/t_c$, $\mathbf{v}^* = \mathbf{v}_{\text{hydr}}/V$, $p^* = p/P$, $c^{\pm,*} = c^{\pm}/C$, and $\phi^* = \phi/\Phi$. Therefore, Problem P transforms into the following form:

$$\begin{aligned}
-\frac{\eta V}{L^2} \Delta_{x^*} \mathbf{v}^* + \frac{P}{\rho L} \nabla_{x^*} p^* &= -\frac{zeC\Phi}{\rho L} (c^{+,*} - c^{-,*}) \nabla_{x^*} \phi^*, \\
\frac{V}{L} \nabla_{x^*} \cdot \mathbf{v}^* &= 0, \\
V \mathbf{v}^* &= 0, \\
\frac{C}{t_c} \partial_{t^*} c^{\pm,*} + \frac{1}{L} \nabla_{x^*} \cdot \left(VC \mathbf{v}^* c^{\pm,*} - \frac{DC}{L} \nabla_{x^*} c^{\pm,*} - \frac{DzeC\Phi}{k_B T L} c^{\pm,*} \nabla_{x^*} \phi^* \right) &= R^{\pm}, \\
\left(\frac{DC}{L} \nabla_{x^*} c^{\pm,*} + \frac{DzeC\Phi}{k_B T L} c^{\pm,*} \nabla_{x^*} \phi^* \right) \cdot \boldsymbol{\nu} &= 0, \\
Cc^{\pm,*} &= c^{\pm,0}, \\
-\frac{\Phi}{L^2} \Delta_{x^*} \phi^* &= \frac{zeC}{\epsilon_0 \epsilon_r} (c^{+,*} - c^{-,*}), \\
\frac{\Phi}{L} \nabla_{x^*} \phi^* \cdot \boldsymbol{\nu} &= \frac{1}{\epsilon_0 \epsilon_r} \sigma, \\
\Phi \phi^* &= \phi_D.
\end{aligned}$$

We multiply the Stokes equation by L/V^2 , Poisson's equation by L^2/Φ and the transport equations by $L/(CV)$. Defining the *Reynolds number* $Re := \frac{LV}{\eta\rho}$, the *Peclet number* $Pe := \frac{LV}{D}$, and the *Stouhal number* $St := \frac{L}{Vt_c}$, we obtain

$$\begin{aligned}
-\frac{1}{Re} \Delta_{x^*} \mathbf{v}^* + \frac{P}{\rho V^2} \nabla_{x^*} p^* &= -\frac{zeC\Phi}{\rho V^2} (c^{+,*} - c^{-,*}) \nabla_{x^*} \phi^*, \\
\nabla_{x^*} \cdot \mathbf{v}^* &= 0, \\
\mathbf{v}^* &= 0, \\
St \partial_{t^*} c^{\pm,*} + \nabla_{x^*} \cdot \left(\mathbf{v}^* c^{\pm,*} - \frac{1}{Pe} (\nabla_{x^*} c^{\pm,*} - \frac{ze\Phi}{k_B T} c^{\pm,*} \nabla_{x^*} \phi^*) \right) &= \frac{L}{CV} R^{\pm}, \\
\left(\frac{1}{Pe} \left(\nabla_{x^*} c^{\pm,*} - \frac{ze\Phi}{k_B T} c^{\pm,*} \nabla_{x^*} \phi^* \right) \right) \cdot \boldsymbol{\nu} &= 0,
\end{aligned}$$

$$\begin{aligned}
c^{\pm,*} &= c^{\pm,0}/C, \\
-\Delta_{x^*} \phi^* &= \frac{zeCL^2}{\epsilon_0 \epsilon_r \Phi} (c^{+,*} - c^{-,*}), \\
\nabla_{x^*} \phi^* \cdot \boldsymbol{\nu} &= \frac{\Phi}{L \epsilon_0 \epsilon_r} \sigma =: \sigma^*, \\
\phi^* &= \phi_D / \Phi.
\end{aligned}$$

In order to further simplify these equations, we insert certain kinds of assumptions on the relations between the characteristic dimensions. First, we assume that $\Phi = \phi_D$, $C = c_0^\pm = c_0$ and $V = L/t_c$. The last assumption implies $St = 1$, which is also an implicit definition of the time scale. In order to obtain further reasonable relations, we apply the *Buckingham Pi Theorem* [39] first for the characteristic pressure P and later on for the characteristic potential Φ . This means that we write P as a product of exponents of the characteristic scales and physical parameters, i.e.

$$P = V^\alpha \eta^\beta \rho^\gamma (ze)^\delta C^\vartheta \Phi^\lambda.$$

Comparing the different exponents for the characteristic scales and solving the resulting system of linear equations results in

$$P = V^{2-3\vartheta+\lambda} \eta^{3\vartheta-3\lambda} \rho^{1-\lambda} (ze)^\lambda C^\vartheta \Phi^\lambda.$$

With the special choice of $\vartheta = \lambda = 0$ the following well known relation is obtained:

$$P = V^2 \rho. \tag{2.15}$$

We apply the same procedure for the characteristic potential Φ , although it is also related to the Dirichlet boundary value via $\Phi = \phi_D$

$$\Phi = C^\alpha D^\beta V^\gamma (ze)^\delta (k_B T)^\epsilon.$$

Comparing the different exponents for the characteristic scales and solving the resulting linear system of equations, we obtain

$$\Phi = C^\alpha D^{3\alpha} V^{-3\alpha} (ze)^{-1} (k_B T)^1.$$

With the choice of $\alpha = 0$, it follows

$$\Phi = \phi_D = \varphi \frac{k_B T}{ze}. \quad (2.16)$$

Here we introduced the parameter φ , since the characteristic value has already been set as ϕ_D , see also Remark 2.8. This relation is especially useful if there is no Dirichlet boundary condition or if $\phi_D = 0$.

We now explicitly calculate the *Debye length* κ [41, 63, 108, 141] for two species c^\pm with charge numbers $z^\pm = \pm z$ via

$$\kappa^2 := \frac{e^2}{\epsilon_0 \epsilon_r k_B T} \sum_{i=\pm} c_i z_i^2 = \frac{2c_0 (ze)^2}{\epsilon_0 \epsilon_r k_B T}. \quad (2.17)$$

Applying (2.15), (2.16), and (2.17), we obtain, in summary, the following dimensionless system of partial differential equations:

$$\begin{aligned} -\frac{1}{Re} \Delta_{x^*} \mathbf{v}^* + \nabla_{x^*} p^* &= -\frac{\varphi k_B T C t_c^2}{\rho L^2} (c^{+,*} - c^{-,*}) \nabla_{x^*} \phi^*, \\ \nabla_{x^*} \cdot \mathbf{v}^* &= 0, \\ \mathbf{v}^* &= 0, \\ \partial_{t^*} c^{\pm,*} + \nabla_{x^*} \cdot \left(\mathbf{v}^* c^{\pm,*} - \frac{1}{Pe} (\nabla_{x^*} c^{\pm,*} + \varphi c^{\pm,*} \nabla_{x^*} \phi^*) \right) &= \frac{L}{CV} R^\pm, \\ \left(\frac{1}{Pe} (\nabla_{x^*} c^{\pm,*} + \varphi c^{\pm,*} \nabla_{x^*} \phi^*) \right) \cdot \boldsymbol{\nu} &= 0, \\ c^{\pm,*} &= 1, \\ -\Delta_{x^*} \phi^* &= \frac{1}{2\varphi} (\kappa L)^2 (c^{+,*} - c^{-,*}), \\ \nabla_{x^*} \phi^* \cdot \boldsymbol{\nu} &= \sigma^*, \\ \phi^* &= 1. \end{aligned}$$

Remark 2.7. For a simple mass-conserving reaction $X_+ \rightleftharpoons X_-$ with rate coefficients equal to k , linear rates $R^\pm = \mp k(c^+ - c^-)$ result from the mass action law and couple the transport problems for $c^{\pm,*}$. It holds $[K] = 1/T$, and with $k^* = k/K$ we obtain

$$\frac{L}{CV} R^\pm = \mp \frac{LC}{CV} K k^* (c^{+,*} - c^{-,*}).$$

If the reaction time corresponds to the time scale chosen above ($St=1$), we set $K=1/t_c$, which yields

$$\frac{L}{CV}R^\pm = k^*(c^{+,*} - c^{-,*}) =: R^{\pm,*}.$$

Remark 2.8. In many applications, it holds $\varphi = 1$. At 20°C this correlates to a zeta-potential of 25 mV for a single charged particle.

2.1.4 Analysis of Problem P

In this Section, we summarize several analytical investigations concerning Problem P , i.e., we state the unique existence of weak solutions of Problem P and we show that the obtained number densities c^\pm are physically reasonable. The full SNPP system, extensions to the Navier-Stokes equations, subproblems or linearizations of the SNPP system have been investigated analytically for quite some time by Gajewski, Gröger and coworkers, see e.g. [48, 49, 47, 53], by Markowich [86], and by Roubicek [117, 118, 119]. Further contributions can be found, e.g., in [78, 126, 125]. Nevertheless, even the derivation of the SNPP system is still under consideration: The drift-diffusion (van Roosbroeck) subsystem is motivated in [89] taking the gradient structure into account and derived by means of a molecular model with methods from statistical physics in [130]. The system considered in [117] and [118] is derived thermodynamically consistent in [121]. Furthermore, recent extensions of the SNPP system for further effects such as size exclusion [20], nanopore blocking [19], and macromolecule dynamics [12] are found in the literature.

Assumptions on the data

To be able to state a result on the existence and uniqueness of weak solutions of Problem P , we assume the following additional restrictions.

- Assumption 2.9.**
1. *On the geometry:* We assume that $\Omega \subset \mathbb{R}^n$, $n \in \{1, 2, 3\}$ is a bounded and convex Lipschitz domain with boundary $\partial\Omega$.
 2. *On the coefficients:* We assume that the physical parameters $\eta, \rho, z, e, \epsilon_0, \epsilon_r, k_B T$, and D are strictly positive constants.
 3. *On the (initial) data:* We assume σ and ϕ_D to be constant and the initial data $c^{\pm,0}$

to be non-negative and bounded in L^∞ , i.e.

$$c^{\pm,0} \in L^\infty(\Omega) \quad \text{and} \quad c^{\pm,0}(x) \geq 0 \text{ for a.e. } x \in \Omega.$$

In the case of $\Gamma_D^P = \emptyset$, we assume the following compatibility condition for the initial data:

$$ze \int_{\Omega} c^{+,0} - c^{-,0} d\mathbf{x} = - \int_{\Gamma} \sigma d\mathbf{s}_{\mathbf{x}}.$$

If $\sigma = 0$, this implies global electro neutrality for the initial number densities.³

4. On the reaction rates: The reaction rates are assumed to have the following structure: $R^\pm(\mathbf{c}) = \mp(c^+ - c^-)$. Especially, they are linear and mass conservative.

Remark 2.10. In particular, item 2, 3 and 4 in Assumption 2.9, i.e. the assumptions on the initial data and physical parameters as well as on the reaction rates can be relaxed in a straightforward way using standard assumptions for the regularity of the given data. More general reaction rates can be treated assuming appropriate structural properties such as global Lipschitz continuity or mass conservation and non-negative productions rates of species whenever their number densities vanish, see, e.g., [119].

Remark 2.11. In the literature electro-neutrality ($\sum_i z_i e c_i = 1$) and volume additivity ($\sum_i c_i = 1$) are found as additional pointwise restriction to supplement the SNPP system or related systems. Both constraints are a possibility to directly guarantee physical properties such as non-negativity or boundedness.

The electro-neutrality ensures that the unique solution of Poisson's equation is $\phi \equiv 0$ in the case of $\sigma = 0$. An analogue statement holds for Stokes equations, i.e. the electric potential as well as the fluid flow are only driven by their boundary data and, if present, external forces. A discussion also in relation to the constant field assumption (i.e. $\nabla\phi = 0$) can be found in [81, 82, 60].

The additivity constraint is, e.g., discussed in [119, 118]. Following the lines there, it is seen that the assumption of electro-neutrality is strongly related to the volume additivity: Applying the electro-neutrality and assuming appropriate initial and boundary conditions as well as structural assumptions on the reaction rates, the volume additivity is a direct consequence of summing all the equations for the number densities.

³In the case of $\Gamma_{\text{out}} = \emptyset$ and an inhomogeneous inflow boundary condition for the velocity field, we assume in addition the following compatibility condition: $\int_{\Gamma_{\text{in}}} \mathbf{v}_D \cdot \boldsymbol{\nu} d\mathbf{s}_{\mathbf{x}} = 0$.

In the context of Problem P the constraints reduce to $e(c^+ - c^-) = 1$ and $c^+ + c^- = 1$, respectively. In both cases, either of the variables c^\pm can be expressed by the other one and consequently the system of partial differential equations (2.14) could be reduced. However, in the literature such a reduction is rarely used.

Existence and uniqueness of weak solutions

Subsequently, we define weak solutions of Problem P and state that Problem P admits a global unique weak solution. Furthermore, we show that the number densities c^\pm are reasonable quantities from a physical point of view.

We denote by $L^p(\Omega)$, $1 \leq p \leq \infty$ the standard Lebesgue spaces and by $H_0^1(\Omega)$ and $W^{p,q}(\Omega)$, $1 \leq p, q \leq \infty$ the standard Sobolev spaces [44]. Moreover, we set $V_0^1(\Omega) = \{\varphi \in H^1(\Omega) : \varphi = 0 \text{ on } \partial\Omega_D\}$, $H^p(\Omega) = W^{p,2}(\Omega)$, $H_0^2(\Omega) := H_0^1(\Omega) \cap H^2(\Omega)$ and define the extensions of Sobolev spaces to the time space cylinder analogously to [44, 119].

Multiplying the system of equations (2.14) with appropriate test functions and integrating by parts, we obtain the following weak formulation of Problem P :

$$\int_{\Omega} \eta \nabla \mathbf{v} : \nabla \boldsymbol{\psi} - \frac{1}{\rho} p \nabla \cdot \boldsymbol{\psi} \, d\mathbf{x} = -\frac{ze}{\rho} \int_{\Omega} (c^+ - c^-) \nabla \phi \cdot \boldsymbol{\psi} \, d\mathbf{x}, \quad \boldsymbol{\psi} \in (H_0^1(\Omega))^n, \quad (2.18a)$$

$$\int_{\Omega} (\nabla \cdot \mathbf{v}) \psi \, d\mathbf{x} = 0, \quad \psi \in L^2(\Omega), \quad (2.18b)$$

$$\begin{aligned} \langle \partial_t c^\pm, \psi \rangle_{(H^1)', H^1} + \int_{\Omega} \left(-\mathbf{v} c^\pm + D \nabla c^\pm \pm \frac{Dze}{k_B T} c^\pm \nabla \phi \right) \cdot \nabla \psi \, d\mathbf{x} \\ = \int_{\Omega} R^\pm(\mathbf{c}) \psi \, d\mathbf{x}, \quad \psi \in V_0^1(\Omega), \end{aligned} \quad (2.18c)$$

$$- \int_{\Omega} \Delta \phi \psi \, d\mathbf{x} = \int_{\Omega} \frac{ze}{\epsilon_0 \epsilon_r} (c^+ - c^-) \psi \, d\mathbf{x}, \quad \psi \in L^2(\Omega). \quad (2.18d)$$

Definition 2.12. ⁴ We call $(\mathbf{v}, p, \mathbf{c}, \phi)$ a weak solution of Problem P if $\mathbf{v} \in L^\infty(0, T; (H_0^1(\Omega))^n)$, $p \in L^\infty(0, T; L^2(\Omega)/\mathbb{R})$, $c^\pm \in L^\infty(0, T; L^2(\Omega)) \cap L^2(0, T; V_0^1(\Omega))$ with $\partial_t c^\pm \in L^2(0, T; (V_0^1(\Omega))')$, $\phi \in L^\infty(0, T; H_0^2(\Omega)/\mathbb{R})$, and equations (2.18) are satisfied.

⁴The notations $(\cdot)_0$ and $(\cdot)/\mathbb{R}$ are used to represent the definition of weak solutions for different choices of boundary conditions in one line. They are used in order to emphasize the suitable function spaces in the case of purely and homogeneous Dirichlet and Neumann boundary data, respectively. In particular, if $\partial\Omega = \Gamma_D$, it holds $V_0^1 = H_0^1$.

Remark 2.13. *The pressure field can be made unique prescribing, e.g., its mean value by $\int_{\Omega} p \, d\mathbf{x} = 0$. In the case of pure Neumann boundary data, for Poisson's equation, an analogue requirement is requested for the electrostatic potential to ensure uniqueness.*

Remark 2.14. *Weak problem formulations for the subproblems for further boundary conditions such as (inhomogeneous) inflow and outflow boundary conditions can be obtained as in [65, 109], see also Remark 2.5.*

However, arbitrary combinations of boundary conditions do not lead to the overall weak problem formulation given in (2.18): for the mixed boundary value problem of Poisson's equation, it is not clear whether a solution exists in H^2 [43]. Alternatively, the electrostatic problem can be formulated in H^1 and the L^∞ -regularity of c^\pm can be added to the definition of the weak solution instead, compare also [126]. In addition, the combination of outflow boundary conditions for the number densities and the fluid flow is delicate, since in this case the convective boundary integral remains in the weak formulation of the Nernst-Planck equation. A pointwise sign condition might be used in order to treat this term directly. However, for arbitrary right hand sides in Stokes equations as well as arbitrary boundary conditions for the electric potential such a condition may not be ensured. Similarly, the boundary integral resulting from the electric drift remains in the weak formulation of the Nernst-Planck equation. It can be estimated straightforward if a Neumann boundary condition for Poisson's equation is prescribed, but it is crucial to handle for Dirichlet type boundary conditions. Furthermore, in many proofs of existence of weak solutions of the above system, the number densities are used as test functions in Poisson's equation. In order to ensure that the number densities are admissible test functions and to estimate the boundary terms, it is often convenient to set $\Gamma_D^P = \Gamma_D^{NP}$ and $\Gamma_N^P = \Gamma_N^{NP} \cup \Gamma_F^{NP}$.

Periodic boundary condition for a linearized system are discussed in [4], whereas (in)homogeneous Dirichlet boundary are treated in [119, 117, 118]. The case of no-slip and no-flux boundary conditions is considered in [126] and a result concerning the combination of no-flux and Dirichlet boundary conditions for the number densities and Dirichlet/no-slip boundary conditions for the velocity field is stated in [127].

Summarizing the results from the literature, we can formulate the following theorem which states that Problem P admits existence of unique global weak solutions and is physically meaningful.

Theorem 2.15. *Let Assumption 2.9 hold. Then there exists a global unique weak solution $(\mathbf{v}, p, \mathbf{c}, \phi)$ of Problem P . Furthermore, the number densities c^\pm are non-negative*

and bounded from above. Moreover, the following a priori estimates hold ⁵:

$$\|\phi\|_{L^2((0,T)\times\Omega)} + \|\nabla\phi\|_{L^2((0,T)\times\Omega)} \leq C, \quad (2.19a)$$

$$\|\mathbf{v}\|_{L^2((0,T)\times\Omega)} + \|\nabla\mathbf{v}\|_{L^2((0,T)\times\Omega)} \leq C, \quad (2.19b)$$

$$\sum_{\pm} \max_{0 \leq t \leq T} \|c^{\pm}\|_{L^2(\Omega)} + \sum_{\pm} \|\nabla c^{\pm}\|_{L^2((0,T)\times\Omega)} + \sum_{\pm} \|\partial_t c^{\pm}\|_{L^2(0,T;(H_{(0)}^1(\Omega))')} \leq C. \quad (2.19c)$$

Proof. In [119, 117, 118, 126, 125] a Navier-Stokes-Nernst-Planck-Poisson (NSNPP) system is studied. Either of the proofs can be carried over directly to the Stokes-Nernst-Planck-Poisson system, see also [119, Exercise 12.29],[118]. Furthermore, extensions of the proofs to the boundary conditions defined for Problem P or to linear reaction rates are straight forward.

In [119, 117, 118] the NSNPP system with mass conservative reactions that are subjected to additional structural conditions is considered. Furthermore, a “reaction force” is added to the transport equation to guarantee the volume additivity constraint, see also Remark 2.11. To prove existence of weak solutions, in [117] a Galerkin approach and in [119, 118] Kakutani’s fixed point theorem is applied.

In [126, 125] a proof of existence of global weak and strong solutions of the NSNPP system without reactions and with homogeneous boundary conditions (i.e. $R^{\pm} = 0$, $\sigma = 0$, $\Gamma_D^{NP} = \emptyset$, $\Gamma_D^P = \emptyset$) is performed using Moser’s iteration and Schauder’s fixed point theorem. However, the work is in main parts just formal and in showing that the fixed point operator is well defined, Schmuck states that the right hand side of the flow problem $(c^+ - c^-)\nabla\phi$ is in $L^2((0,T) \times \Omega)$ for given $c \in L^4(0,T; L^2(\Omega))$ and $\phi \in L^4(0,T; H^2(\Omega))$. This is obviously wrong in three space dimensions. However, in the case of the (Navier-)Stokes equations, less regularity of the forcing term on the right hand side is needed in order to ensure the existence of a weak solution (\mathbf{v}, p) . Therefore, this part of the proof in [126, 125] can be corrected without any further changes. For a rigorous approach applying a fixed point theorem and Moser’s iteration to a similar system, we refer to [75] and Section 2.2.6. \square

Remark 2.16. *In the case of $\Gamma_D^{NP} = \emptyset$, i.e. a homogeneous flux boundary condition supplementing (2.14d), Problem P is mass conservative. Taking into account that $\sum_{\pm} R^{\pm} = 0$, cf. Assumption 2.9, item 4, this property is proven easily performing*

⁵Throughout this thesis, we denote by C a generic strict positive constant which nevertheless could change from line to line in our estimates. Remark, that here continuous dependence on the data for each subproblem is obtained. However, due to the nonlinear coupling of the system of equations, continuous dependence on the data for the whole problem formulation does not follow directly.

the following calculations:

$$\begin{aligned} \frac{d}{dt}m &= \frac{d}{dt} \int_{\Omega} \sum_{\pm} c^{\pm} d\mathbf{x} \\ &= \int_{\Omega} \sum_{\pm} (R^{\pm}(\mathbf{c}) + \nabla \cdot (-\mathbf{v}c^{\pm} + \nabla c^{\pm} \pm c^{\pm} \nabla \phi)) d\mathbf{x} \\ &= 0. \end{aligned}$$

2.2 Effective models

In this section, mathematical models are presented that describe fluid flow and transport phenomena on the scale of the porous medium. We refer to [10, 34, 62] for an extended discussion, motivation and derivation of Darcy's Law and the convection-diffusion-reaction equation. However, on the averaged macroscopic scale, the spatial structure of the porous medium is at first not taken into account explicitly. In the literature, constitutive laws of effective coefficients such as permeability tensor, diffusion (-dispersion) tensor, and porosity of the medium are used in order to integrate the spatial variability into a mathematical model, cf. Section 2.2.1 and Section 2.2.2. A direct relation of effective coefficients to the underlying geometrical setting is established for Darcy's Law and the diffusion equation in the context of homogenization, e.g., in [58], where explicit definitions of the permeability and diffusion tensor are found.

2.2.1 Darcy's law

To describe fluid flow on the macroscopic scale, Darcy's Law and its modifications are very popular:

$$\mathbf{v} = \frac{1}{\mu} \mathbf{K} \nabla p.$$

In the saturated case this equation is complemented by the incompressibility condition

$$\nabla \cdot \mathbf{v} = 0.$$

In an unsaturated porous medium, the so-called Richards equation [62, 115] is used to describe fluid flow. In both descriptions, the challenge in mathematical modeling is to find an appropriate constitutive law for the choice of the permeability tensor \mathbf{K} . In

applications, it is linked to the structure and geometry of the porous medium. More precisely, the permeability tensor is related to the fluid density ρ , the mean grain diameter of the soil d , and the dynamic viscosity of the fluid $\mu = \eta\rho$. For the scalar case, this relation reads [34]:

$$K = \alpha\rho d^2/\mu$$

with proportionality constant α . However, in general, a reduction of the permeability tensor \mathbf{K} to a scalar is not possible since preferred directions of the flow paths are neglected in such a simplified description. To account for these effects, in the anisotropic case, the permeability tensor \mathbf{K} remains a full tensor.

2.2.2 Transport equations

On the macroscopic scale, the transport of the number densities c of a chemical species is described by a convection-diffusion(-dispersion)-reaction equation. Using the mixed formulation with mass flux \mathbf{j} , this reads

$$\begin{aligned}\mathbf{j} &= -\mathbf{D}\nabla c + \mathbf{v}c, \\ \partial_t c + \nabla \cdot \mathbf{j} &= R(c).\end{aligned}$$

The mathematical modeling requires again a constitutive laws for the diffusion-(dispersion) tensor \mathbf{D} . As suitable approximations D^{eff} of \mathbf{D} in the scalar case, functions of the porosity θ and tortuosity τ are used in the literature [34]:

$$D^{\text{eff}} = \alpha\theta D \quad \text{or} \quad D^{\text{eff}} = \frac{\theta}{\tau}D.$$

Here, D is defined as bulk diffusion of the species in the fluid. In more than one space dimension, anisotropy has to be taken into account which again prevents the representation of the tensor \mathbf{D} by a scalar. A well known choice for a constitutive law in order to describe diffusion and dispersion, in the non-scalar case, is the Scheidegger tensor [124], which is given by

$$\mathbf{D} = - \left((\theta D + \beta_t \|\mathbf{j}\|_2) \mathbf{E} + (\beta_l - \beta_t) \frac{\mathbf{j} \otimes \mathbf{j}}{\|\mathbf{j}\|_2} \right)$$

with transversal dispersion coefficient β_t and longitudinal dispersion coefficient β_l , identity matrix \mathbf{E} , and bulk diffusion D .

2.2.3 Linear systems

In certain applications, it is necessary to include electric, thermal or further effects to the description of transport. To this end a linear flux-force relation is assumed [34, 10]:

$$\mathbf{j}_k = \sum_l \mathbf{L}_{kl} \mathbf{z}_l$$

with fluxes \mathbf{j}_k and driving forces \mathbf{z}_l . The driving forces can be of different nature such as number density, temperature, pressure or electric potential gradient. The corresponding fluxes are mass and heat flux, fluid velocity or electric current. The associated diagonal elements \mathbf{L}_{kk} represent the diffusion tensor and thermal, hydraulic and electric conductivity, whereas the non-diagonal elements describe cross coupling effects. For all these submatrices constitutive laws have to be defined, compare Section 2.2.1 and Section 2.2.2. Moreover, from thermodynamical principles, the matrices \mathbf{L}_{kl} have to account for Onsager's reciprocal principle [103] which states that the system matrix $\mathbf{L} = (\mathbf{L}_{kl})_{kl}$ is symmetric, i.e.

$$\mathbf{L}_{kl} = \mathbf{L}_{lk}.$$

For a $z - z$ electrolyte, as discussed in Section 2.1.2, the following linear flux-force relation is obtained, see e.g. [85]:

$$\begin{aligned} \mathbf{v} &= \mathbf{L}_{13} \nabla c^+ + \mathbf{L}_{14} \nabla c^- + \mathbf{L}_{11} \nabla p + \mathbf{L}_{12} \nabla \phi, \\ \mathbf{j}^+ &= \mathbf{L}_{33} \nabla c^+ + \mathbf{L}_{34} \nabla c^- + \mathbf{L}_{31} \nabla p + \mathbf{L}_{32} \nabla \phi, \\ \mathbf{j}^- &= \mathbf{L}_{43} \nabla c^+ + \mathbf{L}_{44} \nabla c^- + \mathbf{L}_{41} \nabla p + \mathbf{L}_{42} \nabla \phi, \\ \mathbf{i} &= \mathbf{L}_{23} \nabla c^+ + \mathbf{L}_{24} \nabla c^- + \mathbf{L}_{21} \nabla p + \mathbf{L}_{22} \nabla \phi. \end{aligned}$$

Remark 2.17. *Investigations considering Onsager's reciprocal relation are undertaken in [78, 4] in the context of homogenization of the stationary linearized system, cf. Section 2.1.1. Here, explicit formulae are derived for the system matrices and the symmetry property has been shown. Furthermore, positive definiteness of submatrices and the overall system matrix, respectively, has to be proven.*

2.2.4 Effective model equations, Problem P_0

In general, a linear relation as described in Section 2.2.3 is not expected to be obtained. In analogy to the pore-scale model (Problem P in Section 2.1.2), the following

nonlinear system of partial differential equations can be used to describe fluid flow and transport of charged colloidal particles on the macroscopic scale. Henceforth, the following system (2.20) is denoted by *Problem P₀* or *Darcy-Nernst-Planck-Poisson (DNPP) system*.

Darcy's Law

$$\mathbf{K}^{-1}\mathbf{v} = -\frac{1}{\eta\rho}(\nabla p + ze(c^+ - c^-)\nabla\phi) \quad \text{in } (0, T) \times \Omega, \quad (2.20a)$$

$$\nabla \cdot \mathbf{v} = 0 \quad \text{in } (0, T) \times \Omega, \quad (2.20b)$$

$$\mathbf{v} \cdot \boldsymbol{\nu} = 0 \quad \text{on } (0, T) \times \partial\Omega. \quad (2.20c)$$

Nernst-Planck equations

$$\theta\partial_t c^\pm + \nabla \cdot \left(\mathbf{v}c^\pm - D\mathbf{D}\nabla c^\pm \mp \frac{Dze}{k_B T} \mathbf{D}c^\pm \nabla\phi \right) = \mp\theta R^\pm(\mathbf{c}) \quad \text{in } (0, T) \times \Omega, \quad (2.20d)$$

$$c^\pm = 0 \quad \text{on } (0, T) \times \partial\Omega, \quad (2.20e)$$

*Poisson's equation*⁶

$$-\nabla \cdot (\epsilon_0\epsilon_r \mathbf{D}\nabla\phi) = \sigma + \theta ze(c^+ - c^-) \quad \text{in } (0, T) \times \Omega, \quad (2.20f)$$

$$\phi = 0 \quad \text{on } (0, T) \times \partial\Omega. \quad (2.20g)$$

with porosity θ , permeability tensor \mathbf{K} , diffusion tensor \mathbf{D} , and background charge density σ and appropriate initial conditions. For a derivation of the system of partial differential equations (2.20) by means of homogenization technique, we refer to Chapter 4, see also [4, 127] for related investigations.

Remark 2.18. *In (2.20), we restrict ourselves to the case of homogeneous (Dirichlet) boundary data for ease of presentation. Note that this setting is consistent with the derivation of the boundary conditions from those of Problem P by means of homogenization methods, see Chapter 4 and also the discussion in Remark 2.2, Remark 2.5, Remark 2.14, and Remark 4.2, Remark 4.4. Analogue results as stated in Theorem 2.23, Theorem 2.24, Theorem 2.28 and Theorem 2.31 are obtained for system (2.20) with further linear (and homogeneous) boundary conditions since Problem P₀ and its subproblems are well defined for more general boundary conditions, see also Remark 2.26. In applications, it might, e.g., be reasonable to prescribe inflow and outflow boundary conditions, i.e. $\mathbf{v} \cdot \boldsymbol{\nu} = -g, c^\pm = c_D^\pm$ on the inflow boundary*

⁶Here, σ is an averaged quantity, i.e. $[\sigma] = \frac{C}{m^2} \frac{m^2}{m^3} = \frac{C}{m^3}$, compare also Section 4.2.

and $p = 0, D\nabla c^\pm \cdot \nu = 0$ on the outflow boundary [62, 77]. We refer to [46] for computations of the corresponding system in such a framework.

2.2.5 Analytical investigations

This section is concerned with the analytical investigation of Problem P_0 , i.e. we prove existence of a unique global weak solution. The crucial point in treating the system of partial differential equations (2.20) is its nonlinear coupling by means of the electric force term. It enters Problem P_0 in two ways: firstly, as forcing term in Darcy's Law (2.20a), and secondly, as additional transport mechanism for the number densities (2.20d). In summary, this feedback mechanism results in a two sided coupled system of partial differential equations, which makes the problem interesting not only by means of applications but also from a mathematical point of view. Although effective models are highly relevant due to their applicability, an analytical treatment of the nonlinear DNPP system is still lacking in the literature. The strategy in the analytical investigations of Problem P_0 is similar to investigations that can be found in the literature for the SNPP system, related systems or extensions to the Navier-Stokes equations, see discussion in Section 2.1.4 and the proof of Theorem 2.15.

After the statement of basic assumptions on the data and the definition of weak solutions, we prove a L^∞ -estimate for the number densities c^\pm using Moser's iteration technique. In addition to the fact that the obtained number densities c^\pm are physically reasonable, the benefit of this estimate is at least threefold: firstly, it allows the application of Tihonov's fixed point theorem, which we will use in order to prove existence of weak solutions. Secondly, we prove uniqueness of the weak solutions due to this higher regularity. This result is, in particular, essential for the statement of convergence of the whole sequence in homogenization theory, see Chapter 4. Thirdly, the improved regularity is the basis for error estimates in the context of homogenization theory, see discussion in Section 4.4 and Chapter 6.

Assumptions on the data

To be able to prove a result on the existence and uniqueness of weak solutions of Problem P_0 , we state the following assumption:

Assumption 2.19. *1. On the geometry: We assume that $\Omega \subset \mathbb{R}^n$, $n \in \{1, 2, 3\}$ is a bounded and convex Lipschitz domain with boundary $\partial\Omega$.*

2. On the (initial) data: We assume that the physical parameter $\eta, \rho, D, z, e, k_B T, \theta$, and $\epsilon_0 \epsilon_r$ are strictly positive constants, that σ is an arbitrary constant, and that the initial data $c^{\pm,0}$ are non-negative and bounded in L^∞ , i.e.

$$c^{\pm,0} \in L^\infty(\Omega) \quad \text{and} \quad c^{\pm,0}(x) \geq 0 \quad \text{for a.e. } x \in \Omega.$$

3. On the coefficients: We assume that the coefficients are symmetric positive definite and bounded matrices, i.e.,

$$\begin{aligned} \sum_{ij} a_i \mathbf{D}_{ij} a_j &\geq \alpha_D |\mathbf{a}|^2, & \forall \mathbf{a} \in \mathbb{R}^n, \\ \sum_{ij} a_i \mathbf{K}_{ij}^{-1} a_j &\geq \alpha_K |\mathbf{a}|^2, & \forall \mathbf{a} \in \mathbb{R}^n, \\ \sum_{ij} a_i \mathbf{D}_{ij} b_j &\leq C_D |\mathbf{a}| |\mathbf{b}|, & \forall \mathbf{a}, \mathbf{b} \in \mathbb{R}^n, \\ \sum_{ij} a_i \mathbf{K}_{ij}^{-1} b_j &\leq C_K |\mathbf{a}| |\mathbf{b}|, & \forall \mathbf{a}, \mathbf{b} \in \mathbb{R}^n \end{aligned}$$

with strict positive constants $\alpha_K, \alpha_D, C_K, C_D$.

4. On the reaction rates: The reaction rates are assumed to have the following structure: $R^\pm(\mathbf{c}) = \mp(c^+ - c^-)$. Especially, they are linear and mass conservative.

Remark 2.20. We point out again that, in this thesis, we focus on the electric interaction in flow and transport processes and therefore impose linear reaction rates (Assumption 2.19, 4.) to our model which are mass conservative, compare also Assumption 2.9, 4. Further reaction terms with appropriate growth or sign conditions, e.g. globally Lipschitz continuous rates, can be handled in a similar way. In the context of homogenization, closed form expressions for the definition of the porosity θ , the permeability tensor \mathbf{K} , and diffusion tensor \mathbf{D} are given explicitly in terms of the underlying geometry and by means of the solutions of so-called cell problems, see Chapter 4. In that chapter, also symmetry and positive definiteness of the tensors are discussed, cf. item 3 in Assumption 2.19. As in the context of Chapter 5, item 3 in Assumption 2.19 may be generalized for \mathbf{x} -dependent coefficients. In this case, uniform positive definiteness and uniform boundedness allows for an analog treatment of the following investigations of Problem P_0 . Moreover, item 2 in Assumption 2.19 can be relaxed in a straightforward way using standard assumptions for the regularity of the coefficients, in particular for θ and σ .

Weak solutions

In addition to the standard Lebesgue spaces $L^p(\Omega)$, $1 \leq p \leq \infty$, the standard Sobolev spaces $H_{(0)}^p(\Omega)$, $H^{-1}(\Omega)$, $1 \leq p \leq \infty$ [44], and their extensions to the time-space cylinder, we introduce the function space [22, 43],

$$H_{\text{div},0}^1(\Omega) := \{\boldsymbol{\varphi} \in (L^2(\Omega))^n, \nabla \cdot \boldsymbol{\varphi} \in L^2(\Omega), \boldsymbol{\varphi} \cdot \boldsymbol{\nu} = 0 \text{ on } \partial\Omega_D\}.$$

As a remark note that here $\partial\Omega = \partial\Omega_D$ holds.

Multiplying the system of equations (2.20) with appropriate test functions and integrating by parts, we obtain the following weak formulation of Problem P_0 :

$$\int_{\Omega} \mathbf{K}^{-1} \mathbf{v} \cdot \boldsymbol{\psi} \, d\mathbf{x} = \int_{\Omega} \frac{1}{\eta\rho} p \nabla \cdot \boldsymbol{\psi} - \frac{1}{\eta\rho} z e (c^+ - c^-) \nabla \phi \cdot \boldsymbol{\psi} \, d\mathbf{x}, \quad \boldsymbol{\psi} \in H_{\text{div},0}^1(\Omega), \quad (2.21a)$$

$$\int_{\Omega} (\nabla \cdot \mathbf{v}) \psi \, d\mathbf{x} = 0, \quad \psi \in L^2(\Omega), \quad (2.21b)$$

$$\theta \langle \partial_t c^{\pm}, \psi \rangle_{H^{-1}(\Omega), H_0^1(\Omega)} + \int_{\Omega} \left(-\mathbf{v} c^{\pm} + D D \nabla c^{\pm} \pm \frac{D z e}{k_B T} c^{\pm} D \nabla \phi \right) \cdot \nabla \psi \, d\mathbf{x} = \int_{\Omega} \theta R^{\pm}(\mathbf{c}) \psi \, d\mathbf{x}, \quad \psi \in H_0^1(\Omega), \quad (2.21c)$$

$$- \int_{\Omega} \nabla \cdot (\epsilon_0 \epsilon_r D \nabla \phi) \psi \, d\mathbf{x} = \int_{\Omega} (\theta z e (c^+ - c^-) + \sigma) \psi \, d\mathbf{x}, \quad \psi \in L^2(\Omega). \quad (2.21d)$$

Definition 2.21. We call $(\mathbf{v}, p, \mathbf{c}, \phi)$ a weak solution of Problem P_0 if $\mathbf{v} \in L^2(0, T; (H_{\text{div},0}^1(\Omega))^n)$, $p \in L^2(0, T; L^2(\Omega)/\mathbb{R})$, $c^{\pm} \in L^{\infty}(0, T; L^2(\Omega)) \cap L^2(0, T; H_0^1(\Omega))$ with $\partial_t c^{\pm} \in L^2(0, T; H^{-1}(\Omega))$, $\phi \in L^{\infty}(0, T; H_0^2(\Omega))$, and equations (2.21) are satisfied.

Remark 2.22. Weak problem formulations for the subproblems for further boundary conditions such as (inhomogeneous) inflow and outflow boundary conditions (see Remark 2.18) are obtained similarly as in (2.21). However, arbitrary combinations of boundary conditions are delicate, compare also Remark 2.14.

2.2.6 Non-negativity and boundedness in $L^{\infty}((0, T) \times \Omega)$

In this section, we prove that the number densities c^{\pm} are non-negative and bounded from above, which ensures that these quantities are physically reasonable. Non-negativity is proven by standard arguments and in order to show the boundedness, we apply Moser's iteration technique [93, 92, 75].

Theorem 2.23. *Let $(\mathbf{v}, p, \mathbf{c}, \phi)$ be a weak solution of Problem P_0 according to Definition 2.21. Then, the number densities c^\pm are non-negative, i.e.*

$$c^\pm(t, x) \geq 0 \text{ for a.e. } t \in (0, T), x \in \Omega.$$

Proof. We test the Nernst-Planck equations (2.21c) with $\psi = c_\pm^\pm := \min(0, c^\pm) \in H_0^1(\Omega)$. This yields, after summation over \pm ,

$$\begin{aligned} & \sum_{\pm} \frac{\theta}{2} \frac{d}{dt} \|c_\pm^\pm\|_{L^2(\Omega)}^2 - \sum_{\pm} \frac{1}{2} \int_{\Omega} \mathbf{v} \cdot \nabla (c_\pm^\pm)^2 \, d\mathbf{x} + \sum_{\pm} \int_{\Omega} D \mathbf{D} \nabla c_\pm^\pm \cdot \nabla c_\pm^\pm \, d\mathbf{x} \\ &= - \sum_{\pm} \pm \frac{1}{2} \frac{Dze}{k_B T} \int_{\Omega} \mathbf{D} \nabla \phi \cdot \nabla (c_\pm^\pm)^2 \, d\mathbf{x} + \sum_{\pm} \mp \int_{\Omega} \theta (c^+ - c^-) c_\pm^\pm \, d\mathbf{x}, \\ & \iff I - II + III = -IV + V. \end{aligned}$$

Integral III is estimated due to the positive definiteness of \mathbf{D} , cf. Assumption 2.19, 3. By standard arguments, we obtain that $II = 0$ holds due to the incompressibility condition (2.21b) and the homogeneous boundary conditions of the velocity field \mathbf{v} . Moreover, integral V satisfies a sign condition due to the monotonicity of $(\cdot)_-$, i.e. $V \leq 0$ holds. Finally, we estimate integral IV applying the following interpolation inequality $\|\varphi\|_{L^3(\Omega_\varepsilon)} \leq C \|\varphi\|_{L^2(\Omega_\varepsilon)}^{1/2} \|\nabla \varphi\|_{L^2(\Omega_\varepsilon)}^{1/2}$ and also Young's inequality (4/3, 4). In summary, this leads to

$$\begin{aligned} & \sum_{\pm} \frac{\theta}{2} \frac{d}{dt} \|c_\pm^\pm\|_{L^2(\Omega)}^2 + \sum_{\pm} D \alpha_D \|\nabla (c_\pm^\pm)_-\|_{L^2(\Omega)}^2 \\ & \leq \sum_{\pm} \frac{1}{8 \alpha_D} \left(\frac{ze C_D}{k_B T} \right)^4 \|\nabla \Phi\|_{L^6(\Omega)}^4 \|c_\pm^\pm\|_{L^2(\Omega)}^2 + \frac{3}{8} \alpha_D D \|\nabla c_\pm^\pm\|_{L^2(\Omega)}. \end{aligned}$$

Adsorption of the gradient term as well as the application of Gronwall's Lemma [44], then concludes the proof of Theorem 2.23, together with the assumptions on the coefficients and the initial data $c^{\pm,0}$, cf. Assumption 2.19, 3 and 2. \square

Theorem 2.24. *Let $(\mathbf{v}, p, \mathbf{c}, \phi)$ be a weak solution of Problem P_0 according to Definition 2.21. Then the number densities c^\pm are bounded in $L^\infty((0, T) \times \Omega)$. Furthermore, the $L^\infty((0, T) \times \Omega)$ -norm is estimated by the $L^2((0, T) \times \Omega)$ -norm by means of the following relation:*

$$\sum_{\pm} \|c^\pm\|_{L^\infty((0, T) \times \Omega)} \leq C_{\text{Moser}} \sum_{\pm} \|c^\pm\|_{L^2((0, T) \times \Omega)} + 4 \max_{\pm} \|c^{\pm,0}\|_{L^\infty(\Omega)}$$

Proof. First of all, we formulate the Nernst-Planck equations (2.21c) for the difference $c^\pm - K$ with some constant $K \geq 0$ that is related to the initial values $c^{\pm,0}$ and will be specified at a later stage of this proof. Taking into account that the velocity field is divergence free (2.21b) and has homogeneous boundary values and inserting Poisson's equation (2.21d) for the electric potential, we obtain

$$\begin{aligned} & \theta \langle \partial_t(c^\pm - K), \psi \rangle_{H^{-1}(\Omega), H_0^1(\Omega)} \\ & + \int_{\Omega} \left(-\mathbf{v}(c^\pm - K) + D\mathbf{D}\nabla(c^\pm - K) \pm \frac{Dze}{k_B T}(c^\pm - K)\mathbf{D}\nabla\phi \right) \cdot \nabla\psi \, d\mathbf{x} \\ & = \mp\theta \left(1 + \frac{K\theta Dz^2 e^2}{k_B T \epsilon_0 \epsilon_r} \right) \int_{\Omega} (c^+ - c^-)\psi \, d\mathbf{x} \pm \frac{KDze}{k_B T \epsilon_0 \epsilon_r} \int_{\Omega} \sigma\psi \, d\mathbf{x}, \quad \psi \in H_0^1(\Omega). \end{aligned} \quad (2.22)$$

Subsequently, we apply Moser's iteration technique [93] and follow the procedure in [75] with a slightly modified test function. In agreement with Assumption 2.19, 2., we define

$$K_0 := \max_{\pm} \|c^{\pm,0}\|_{L^\infty(\Omega)} \quad (2.23)$$

and for $K_0 \leq K \leq M$, we define the cut-off function

$$(c_M^\pm - K)_+ := \max(\min(c^\pm - K, M - K), 0) = \begin{cases} M - K, & c^\pm \geq M, \\ c^\pm - K, & K < c^\pm < M, \\ 0, & c^\pm \leq K. \end{cases}$$

For arbitrary $\alpha \geq 0$, we use $\psi = (c_M^\pm - K)_+^{2\alpha}(c^\pm - K)_+ \in H_0^1(\Omega)$ as a test function in (2.22) and consider each term in (2.22) separately.

1. The convective term in (2.22) vanishes by standard arguments due to the incompressibility condition (2.21b) and the homogeneous boundary conditions of the velocity field \mathbf{v} , i.e.

$$\int_{\Omega} -\mathbf{v}(c^\pm - K) \cdot \nabla((c_M^\pm - K)_+^{2\alpha}(c^\pm - K)_+) \, d\mathbf{x} = 0.$$

2. For the diffusive term in (2.22), we apply the product and chain rule. Due to the positive definiteness of \mathbf{D} , cf. Assumption 2.19, item 3, we obtain

$$\begin{aligned} & \int_{\Omega} D\mathbf{D}\nabla(c^\pm - K) \cdot \nabla((c_M^\pm - K)_+^{2\alpha}(c^\pm - K)_+) \, d\mathbf{x} \\ & \geq D\alpha_D \frac{2\alpha}{(\alpha + 1)^2} \|\nabla(c_M^\pm - K)_+^{\alpha+1}\|_{L^2(\Omega)}^2 + D\alpha_D \|(c_M^\pm - K)_+^\alpha \nabla(c^\pm - K)_+\|_{L^2(\Omega)}^2. \end{aligned}$$

3. The drift term in (2.22) is manipulated using first the product and chain rule and then applying integration by parts. Inserting Poisson's equation (2.21d) finally leads to

$$\begin{aligned}
& \pm \int_{\Omega} \frac{Dze}{k_B T} (c^{\pm} - K) \mathbf{D} \nabla \phi \cdot \nabla \left((c_M^{\pm} - K)_+^{2\alpha} (c^{\pm} - K)_+ \right) d\mathbf{x} \\
&= \pm \int_{\Omega} \frac{Dze}{k_B T} \mathbf{D} \nabla \phi \cdot \left(\frac{1}{2} (c_M^{\pm} - K)_+^{2\alpha} \nabla (c^{\pm} - K)_+^2 + \frac{2\alpha}{2\alpha + 2} \nabla (c_M^{\pm} - K)_+^{2\alpha+2} \right) d\mathbf{x} \\
&= \pm \int_{\Omega} \frac{\theta D z^2 e^2}{2k_B T \epsilon_0 \epsilon_r} (c^+ - c^-) \left((c_M^{\pm} - K)_+^{2\alpha} (c^{\pm} - K)_+^2 + \frac{\alpha}{\alpha + 1} (c_M^{\pm} - K)_+^{2\alpha+2} \right) \\
&\quad + \frac{Dze\sigma}{2k_B T \epsilon_0 \epsilon_r} \left((c_M^{\pm} - K)_+^{2\alpha} (c^{\pm} - K)_+^2 + \frac{\alpha}{\alpha + 1} (c_M^{\pm} - K)_+^{2\alpha+2} \right) d\mathbf{x} \\
&=: \pm (I^{\pm} + II^{\pm}).
\end{aligned}$$

Summing over \pm , it holds $A_1 A_2 \geq 0$ due to the monotonicity properties of $(\cdot)_+$ with A_1 and A_2 being defined as

$$\begin{aligned}
A_1 &:= c^+ - c^-, \\
A_2 &:= \left[((c_M^+ - K)_+^{2\alpha} (c^+ - K)_+^2 - (c_M^- - K)_+^{2\alpha} (c^- - K)_+^2) \right. \\
&\quad \left. + \frac{\alpha}{\alpha + 1} ((c_M^+ - K)_+^{2\alpha+2} - (c_M^- - K)_+^{2\alpha+2}) \right].
\end{aligned}$$

Consequently, we obtain

$$\sum_{\pm} \pm I^{\pm} = I^+ - I^- = \frac{\theta D z^2 e^2}{2k_B T \epsilon_0 \epsilon_r} \int_{\Omega} A_1 A_2 d\mathbf{x} \geq 0.$$

Furthermore, the sum of the integrals $|II^+| + |II^-|$ is estimated in the following way:

$$\begin{aligned}
& |II^+| + |II^-| \\
&\leq \frac{Dze \|\sigma\|_{L^\infty((0,T) \times \Omega)}}{2k_B T \epsilon_0 \epsilon_r} \sum_{\pm} \int_{\Omega} \left| (c_M^{\pm} - K)_+^{2\alpha} (c^{\pm} - K)_+^2 + \frac{\alpha}{\alpha + 1} (c_M^{\pm} - K)_+^{2\alpha+2} \right| d\mathbf{x} \\
&= \frac{Dze \|\sigma\|_{L^\infty((0,T) \times \Omega)}}{2k_B T \epsilon_0 \epsilon_r} \sum_{\pm} \left(\|(c_M^{\pm} - K)_+^{\alpha} (c^{\pm} - K)_+\|_{L^2(\Omega)}^2 \right. \\
&\quad \left. + \frac{\alpha}{\alpha + 1} \|(c_M^{\pm} - K)_+^{\alpha+1}\|_{L^2(\Omega)}^2 \right).
\end{aligned}$$

4. Some additional technical effort is necessary, since a term of lower order is present on the right hand side of (2.22). This is because of the background charge density σ . The term of lower order is estimated as follows: defining $K > h$, $h > 0$, we obtain

$$\begin{aligned} & \left| \pm \frac{KDze}{k_B T \epsilon_0 \epsilon_r} \int_{\Omega} \sigma (c_M^{\pm} - K)_+^{2\alpha} (c^{\pm} - K)_+ \, d\mathbf{x} \right| \\ & \leq \frac{Dze \|\sigma\|_{L^\infty((0,T) \times \Omega)}}{k_B T \epsilon_0 \epsilon_r} \frac{K}{K-h} \int_{\Omega} (K-h) (c_M^{\pm} - K)_+^{2\alpha} (c^{\pm} - K)_+ \, d\mathbf{x} \\ & \leq \frac{Dze \|\sigma\|_{L^\infty((0,T) \times \Omega)}}{k_B T \epsilon_0 \epsilon_r} \frac{K}{K-h} \|(c_M^{\pm} - h)_+^\alpha (c^{\pm} - h)_+\|_{L^2(\Omega)}^2. \end{aligned}$$

In the last step, we consider the case of $c^{\pm} > K$, i.e. $K - h < c^{\pm} - h$, since otherwise the whole term is equal to zero by definition of $(c_M - K)_+$. Additionally, K is replaced by h in $(\cdot - K)_+$ since $K > h$ was set.

5. In order to estimate the sum of the remaining terms on the right hand side of (2.22), in particular the reactive term, we apply a similar argument as in item 3. Summing over \pm , it holds $B_1 B_2 \geq 0$ due to the monotonicity properties of $(\cdot)_+$ with B_1 and B_2 being defined as

$$\begin{aligned} B_1 & := c^+ - c^-, \\ B_2 & := (c_M^+ - K)_+^{2\alpha} (c^+ - K)_+ - (c_M^- - K)_+^{2\alpha} (c^- - K)_+. \end{aligned}$$

Consequently, we obtain

$$-\theta \left(1 + \frac{KDz^2 e^2}{k_B T \epsilon_0 \epsilon_r} \right) \int_{\Omega} B_1 B_2 \, d\mathbf{x} \leq 0.$$

6. Finally, we combine all the above considerations 1. to 5. and integrate the overall estimate with respect to time. Furthermore, all terms on the right hand side are expressed in terms of h instead of K . In summary, we reformulate (2.22) by

$$\begin{aligned} & \theta \sum_{\pm} \int_0^T \langle \partial_t (c^{\pm} - K), (c_M^{\pm} - K)_+^{2\alpha} (c^{\pm} - K)_+ \rangle_{H^{-1}(\Omega), H_0^1(\Omega)} \, dt \\ & + D\alpha_D \frac{2\alpha}{(\alpha+1)^2} \sum_{\pm} \|\nabla (c_M^{\pm} - K)_+^{\alpha+1}\|_{L^2((0,T) \times \Omega)}^2 \\ & + D\alpha_D \sum_{\pm} \|(c_M^{\pm} - K)_+^\alpha \nabla (c^{\pm} - K)_+\|_{L^2((0,T) \times \Omega)}^2 \end{aligned}$$

$$\begin{aligned}
&\leq \frac{Dze\|\sigma\|_{L^\infty((0,T)\times\Omega)}}{k_B T \epsilon_0 \epsilon_r} \frac{K}{K-h} \sum_{\pm} \|(c_M^\pm - h)_+^\alpha (c^\pm - h)_+\|_{L^2((0,T)\times\Omega)}^2 \\
&\quad + \frac{Dze\|\sigma\|_{L^\infty((0,T)\times\Omega)}}{2k_B T \epsilon_0 \epsilon_r} \sum_{\pm} \left(\|(c_M^\pm - h)_+^\alpha (c^\pm - h)_+\|_{L^2((0,T)\times\Omega)}^2 \right. \\
&\qquad\qquad\qquad \left. + \frac{\alpha}{\alpha+1} \|(c_M^\pm - h)_+^{\alpha+1}\|_{L^2((0,T)\times\Omega)}^2 \right) \\
&= \frac{Dze\|\sigma\|_{L^\infty((0,T)\times\Omega)}}{k_B T \epsilon_0 \epsilon_r} \left(\frac{1}{2} + \frac{K}{K-h} \right) \sum_{\pm} \|(c_M^\pm - h)_+^\alpha (c^\pm - h)_+\|_{L^2((0,T)\times\Omega)}^2 \\
&\quad + \frac{Dze\|\sigma\|_{L^\infty((0,T)\times\Omega)}}{2k_B T \epsilon_0 \epsilon_r} \frac{\alpha}{\alpha+1} \sum_{\pm} \|(c_M^\pm - h)_+^{\alpha+1}\|_{L^2((0,T)\times\Omega)}^2.
\end{aligned} \tag{2.24}$$

On the basis of (2.24), we start Moser's iteration⁷. To this end, we define the following sequences for $J \in \mathbb{N}_0$:

$$1 + \alpha_J := \left(\frac{n+2}{n} \right)^J = (5/3)^J, \tag{2.25}$$

$$K := K_{J+1}, \quad h := K_J = K_0 + (1 - 2^{-J})K_0, \tag{2.26}$$

$$K_0 := \max_{\pm} \|c^{\pm,0}\|_{L^\infty(\Omega)}. \tag{2.23}$$

Obviously, it holds $K_0 \leq K_J < 2K_0$, $J \in \mathbb{N}_0$ and $K_\infty = 2K_0$.

We now iterate over $J \in \mathbb{N}_0$:

Step 1 (base case $J = 0$): To start the induction, we set $J = 0$, ($\alpha_0 = 0$) and obtain from (2.24)

$$\begin{aligned}
&\frac{\theta}{2} \sum_{\pm} \max_{0 \leq t \leq T} \|(c^\pm - K_1)_+\|_{L^2(\Omega)}^2 + D\alpha_D \sum_{\pm} \|\nabla(c^\pm - K_1)_+\|_{L^2((0,T)\times\Omega)}^2 \\
&\leq \frac{Dze\|\sigma\|_{L^\infty((0,T)\times\Omega)}}{k_B T \epsilon_0 \epsilon_r} \left(\frac{1}{2} + \frac{K_1}{K_1 - K_0} \right) \sum_{\pm} \|(c^\pm - K_0)_+\|_{L^2((0,T)\times\Omega)}^2 \\
&=: \tilde{C}_0 \sum_{\pm} \|(c^\pm - K_0)_+\|_{L^2((0,T)\times\Omega)}^2
\end{aligned}$$

with $\tilde{C}_0 := \frac{Dze\|\sigma\|_{L^\infty((0,T)\times\Omega)}}{k_B T \epsilon_0 \epsilon_r} \left(\frac{1}{2} + \frac{K_1}{K_1 - K_0} \right)$. Note, that the initial values $(c^{\pm,0} - K_1)_+$ cancel here since $K_1 \geq K_0$ with K_0 being defined in (2.23).

⁷We assume $n = 3$. However, the same procedure is possible for $n = 1, 2$.

For $1 \leq p \leq \infty$, we denote in the following for a vector $\varphi = (\varphi_1, \varphi_2) \in \mathbb{R}^2$ the $L^p((0, T) \times \Omega)$ vector norm by

$$\begin{aligned} \|\varphi\|_{L^p((0,T)\times\Omega)} &:= \|(\varphi_1, \varphi_2)\|_{L^p((0,T)\times\Omega;\mathbb{R}^2)} := \left(\sum_{i=1}^2 \|\varphi_i\|_{L^p((0,T)\times\Omega)}^p \right)^{1/p}, \quad 1 \leq p < \infty, \\ \|\varphi\|_{L^\infty((0,T)\times\Omega)} &:= \|(\varphi_1, \varphi_2)\|_{L^\infty((0,T)\times\Omega;\mathbb{R}^2)} := \sum_{i=1}^2 \|\varphi_i\|_{L^\infty((0,T)\times\Omega)}, \quad p = \infty. \end{aligned}$$

With this definition and the above estimate, we obtain, applying Sobolev's embedding in the time-space cylinder [75]

$$\begin{aligned} &\|((c^+ - K_1)_+, (c^- - K_1)_+)\|_{L^{2\cdot 5/3}((0,T)\times\Omega;\mathbb{R}^2)} \\ &:= \left(\sum_{\pm} \|(c^\pm - K_1)_+\|_{L^{2\cdot 5/3}((0,T)\times\Omega)}^{2\cdot 5/3} \right)^{\frac{1}{2\cdot 5/3}} \\ &= \left(\sum_{\pm} \int_0^T \int_{\Omega} (c^\pm - K_1)_+^{2\cdot 5/3} \, d\mathbf{x} \, dt \right)^{\frac{1}{2\cdot 5/3}} \\ &\leq \left(\sum_{\pm} C_S \left(\max_{0 \leq t \leq T} \|(c^\pm - K_1)_+\|_{L^2(\Omega)} \right)^{2/3} \left(\|\nabla(c^\pm - K_1)_+\|_{L^2((0,T)\times\Omega)}^2 \right)^{\frac{1}{2\cdot 5/3}} \right)^{1/2} \\ &\leq C_S^{\frac{1}{2\cdot 5/3}} C_0^{1/2} \left(\sum_{\pm} \|(c^\pm - K_0)_+\|_{L^2((0,T)\times\Omega)}^2 \right)^{1/2} \\ &=: C_S^{\frac{1}{2\cdot 5/3}} C_0^{1/2} \|((c^+ - K_0)_+, (c^- - K_0)_+)\|_{L^2((0,T)\times\Omega;\mathbb{R}^2)}, \end{aligned}$$

where we used $\sum_{i=1}^2 (a_i)^{2/3} b_i \leq (\sum_{i=1}^2 a_i)^{2/3} (\sum_{i=1}^2 b_i)$, $a_i, b_i \geq 0$ and the definition $C_0 := \frac{\tilde{C}_0}{\min(D\alpha_D, \theta/2)}$.

Step 2 (induction hypothesis): We assume that the following induction hypothesis is already established for $J \in \mathbb{N}$.

$$\begin{aligned} &\|((c^+ - K_J)_+, (c^- - K_J)_+)\|_{L^{2\cdot(5/3)^J}((0,T)\times\Omega;\mathbb{R}^2)} \\ &\leq \prod_{j=0}^{J-1} C_S^{\frac{1}{2\cdot(5/3)^{j+1}}} C_j^{\frac{1}{2\cdot(5/3)^j}} \left(\sum_{\pm} \|(c^\pm - K_0)_+\|_{L^2((0,T)\times\Omega)}^2 \right)^{1/2} \\ &= \prod_{j=0}^{J-1} C_S^{\frac{1}{2\cdot(5/3)^{j+1}}} C_j^{\frac{1}{2\cdot(5/3)^j}} \|((c^+ - K_0)_+, (c^- - K_0)_+)\|_{L^2((0,T)\times\Omega;\mathbb{R}^2)} \end{aligned}$$

with the definitions ($j = 0, \dots, J - 1$)

$$C_j = \frac{\tilde{C}_j}{\min(D\alpha_D(2\alpha_j + 1)/(\alpha_j + 1)^2, \theta/(2\alpha_j + 2))},$$

$$\tilde{C}_j = \frac{Dze\|\sigma\|_{L^\infty((0,T)\times\Omega)}}{k_B T \epsilon_0 \epsilon_r} \left(\frac{K_{j+1}}{K_{j+1} - K_j} + \frac{1}{2} + \frac{1}{2} \frac{\alpha_j}{\alpha_j + 1} \right).$$

Step 3 (induction step $J \rightarrow J + 1$): Considering (2.24) for $J \in \mathbb{N}$ with $1 + \alpha_J = (3/5)^J$, we obtain

$$\begin{aligned} & \theta \sum_{\pm} \int_0^T \langle \partial_t(c^\pm - K_{J+1}), (c_M^\pm - K_{J+1})_+^{2\alpha_J} (c^\pm - K_{J+1})_+ \rangle_{H^{-1}(\Omega), H_0^1(\Omega)} dt \\ & \quad + D\alpha_D \frac{2\alpha_J}{(\alpha_J + 1)^2} \sum_{\pm} \|\nabla(c_M^\pm - K_{J+1})_+^{\alpha_J+1}\|_{L^2((0,T)\times\Omega)}^2 \\ & \quad \quad + D\alpha_D \sum_{\pm} \|(c_M^\pm - K_{J+1})_+^{\alpha_J} \nabla(c^\pm - K_{J+1})_+\|_{L^2((0,T)\times\Omega)}^2 \\ & \leq \frac{Dze\|\sigma\|_{L^\infty((0,T)\times\Omega)}}{k_B T \epsilon_0 \epsilon_r} \left(\frac{1}{2} + \frac{K_{J+1}}{K_{J+1} - K_J} \right) \sum_{\pm} \|(c_M^\pm - K_J)_+^{\alpha_J} (c^\pm - K_J)_+\|_{L^2((0,T)\times\Omega)}^2 \\ & \quad + \frac{Dze\|\sigma\|_{L^\infty((0,T)\times\Omega)}}{2k_B T \epsilon_0 \epsilon_r} \frac{\alpha_J}{\alpha_J + 1} \sum_{\pm} \|(c_M^\pm - K_J)_+^{\alpha_J+1}\|_{L^2((0,T)\times\Omega)}^2. \end{aligned}$$

We observe that the right hand side remains bounded for $M \rightarrow \infty$ due to the induction hypotheses, cf. Step 2 of the iteration. Considering this limit, we reformulate the equation above via

$$\begin{aligned} & \frac{\theta}{2\alpha_J + 2} \sum_{\pm} \max_{0 \leq t \leq T} \|(c^\pm - K_{J+1})_+^{\alpha_J+1}\|_{L^2(\Omega)}^2 \\ & \quad + D\alpha_D \frac{2\alpha_J + 1}{(\alpha_J + 1)^2} \sum_{\pm} \|\nabla(c^\pm - K_{J+1})_+^{\alpha_J+1}\|_{L^2((0,T)\times\Omega)}^2 \\ & \leq \frac{Dze\|\sigma\|_{L^\infty((0,T)\times\Omega)}}{k_B T \epsilon_0 \epsilon_r} \left(\frac{K_{J+1}}{K_{J+1} - K_J} + \frac{1}{2} + \frac{1}{2} \frac{\alpha_J}{\alpha_J + 1} \right) \sum_{\pm} \|(c^\pm - K_J)_+^{\alpha_J+1}\|_{L^2((0,T)\times\Omega)}^2 \\ & =: \tilde{C}_J \sum_{\pm} \|(c^\pm - K_J)_+^{\alpha_J+1}\|_{L^2((0,T)\times\Omega)}^2 \end{aligned}$$

Note that the time integral is calculated explicitly and that the initial values vanish here according to the definition of K_{J+1} , cf. (2.25).

As in Step 1 of the iteration, we apply Sobolev's embedding in the time-space cylinder [75] in order to obtain:

$$\begin{aligned}
& \|((c^+ - K_{J+1})_+, (c^- - K_{J+1})_+)\|_{L^{2 \cdot (5/3)^{J+1}}((0,T) \times \Omega; \mathbb{R}^2)} \\
& := \left(\sum_{\pm} \| (c^{\pm} - K_{J+1})_+ \|_{L^{2 \cdot (5/3)^{J+1}}}^{2 \cdot (5/3)^{J+1}} \right)^{\frac{1}{2 \cdot (5/3)^{J+1}}} \\
& = \left(\sum_{\pm} \int_0^T \int_{\Omega} (c^{\pm} - K_{J+1})_+^{2 \cdot (5/3)^{J+1}} \, d\mathbf{x} \, dt \right)^{\frac{1}{2 \cdot (5/3)^{J+1}}} \\
& \leq \left(\sum_{\pm} C_S \left(\max_{0 \leq t \leq T} \| (c^{\pm} - K_{J+1})_+^{(5/3)^J} \|_{L^2(\Omega)} \right)^{2/3} \right. \\
& \quad \left. \cdot \left(\| \nabla (c^{\pm} - K_{J+1})_+^{(5/3)^J} \|_{L^2((0,T) \times \Omega)}^2 \right)^{\frac{1}{2 \cdot (5/3)^{J+1}}} \right)^{\frac{1}{2 \cdot (5/3)^J}} \\
& \leq C_S^{\frac{1}{2 \cdot (5/3)^{J+1}}} C_J^{\frac{1}{2 \cdot (5/3)^J}} \left(\sum_{\pm} \| (c^{\pm} - K_J)_+ \|_{L^{2 \cdot (5/3)^J}((0,T) \times \Omega)}^{\frac{1}{2 \cdot (5/3)^J}} \right)^{\frac{1}{2 \cdot (5/3)^J}} \\
& =: C_S^{\frac{1}{2 \cdot (5/3)^{J+1}}} C_J^{\frac{1}{2 \cdot (5/3)^J}} \|((c^+ - K_J)_+, (c^- - K_J)_+)\|_{L^{2 \cdot (5/3)^J}((0,T) \times \Omega; \mathbb{R}^2)},
\end{aligned}$$

where we again used $\sum_{i=1}^2 (a_i)^{2/3} b_i \leq (\sum_{i=1}^2 a_i)^{2/3} (\sum_{i=1}^2 b_i)$, $a_i, b_i \geq 0$ and the definition

$$\begin{aligned}
C_J &= \frac{\tilde{C}_J}{\min(D\alpha_D(2\alpha_J + 1)/(\alpha_J + 1)^2, \theta/(2\alpha_J + 2))}, \\
\tilde{C}_J &= \frac{Dze\|\sigma\|_{L^\infty((0,T) \times \Omega)}}{k_B T \epsilon_0 \epsilon_r} \left(\frac{K_{J+1}}{K_{J+1} - K_J} + \frac{1}{2} + \frac{1}{2} \frac{\alpha_J}{\alpha_J + 1} \right).
\end{aligned}$$

Here, the induction hypothesis (Step 2) can be substituted directly, which leads to

$$\begin{aligned}
& \|((c^+ - K_{J+1})_+, (c^- - K_{J+1})_+)\|_{L^{2 \cdot (5/3)^{J+1}}((0,T) \times \Omega; \mathbb{R}^2)} \\
& \leq C_S^{\frac{1}{2 \cdot (5/3)^{J+1}}} C_J^{\frac{1}{2 \cdot (5/3)^J}} \prod_{j=0}^{J-1} C_S^{\frac{1}{2 \cdot (5/3)^{j+1}}} C_j^{\frac{1}{2 \cdot (5/3)^j}} \left(\sum_{\pm} \| (c^{\pm} - K_0)_+ \|_{L^2((0,T) \times \Omega)}^2 \right)^{1/2} \\
& = \prod_{j=0}^J C_S^{\frac{1}{2 \cdot (5/3)^{j+1}}} C_j^{\frac{1}{2 \cdot (5/3)^j}} \|((c^+ - K_0)_+, (c^- - K_0)_+)\|_{L^2((0,T) \times \Omega; \mathbb{R}^2)}.
\end{aligned}$$

Step 4 (Convergence of the constant): As last step of the iteration, we show

$$C_{\text{Moser}} := \prod_{j=0}^{\infty} C_S^{\frac{1}{2 \cdot (5/3)^{j+1}}} C_j^{\frac{1}{2 \cdot (5/3)^j}} \quad (2.27)$$

is finite, i.e. that the product $\prod_{j=0}^{J+1} C_S^{\frac{1}{2 \cdot (5/3)^{j+1}}} C_j^{\frac{1}{2 \cdot (5/3)^j}}$ does not blow up as $J \rightarrow \infty$. To this end we reformulate the infinite product as infinite sum by the identity [136]

$$\prod_{j=0}^{\infty} C_S^{\frac{1}{2 \cdot (5/3)^{j+1}}} C_j^{\frac{1}{2 \cdot (5/3)^j}} < \infty \Leftrightarrow \sum_{j=0}^{\infty} \log \left(C_S^{\frac{1}{2 \cdot (5/3)^{j+1}}} C_j^{\frac{1}{2 \cdot (5/3)^j}} \right) < \infty$$

and apply the following considerations:

$$\begin{aligned} C_j &= \frac{\tilde{C}_j}{\min(D\alpha_D(2\alpha_j + 1)/(\alpha_j + 1)^2, \theta/(2\alpha_j + 2))} \leq \frac{\tilde{C}_j}{\min(D\alpha_D, \theta/2)} (5/3)^j \\ &=: A_1 \tilde{C}_j (5/3)^j, \\ \tilde{C}_j &\leq \frac{Dze \|\sigma\|_{L^\infty((0,T) \times \Omega)} 2^{j+2}}{k_B T \epsilon_0 \epsilon_r} = \frac{Dze \|\sigma\|_{L^\infty((0,T) \times \Omega)} 2^{j+2}}{k_B T \epsilon_0 \epsilon_r} =: A_2 2^{j+2}. \end{aligned}$$

since $-\frac{1}{2} \left(1 - \frac{\alpha_j}{\alpha_j + 1}\right) \leq 0$. The ratio or root test ensures that the infinite sum

$$\sum_{j=0}^{\infty} \log \left(C_S^{\frac{1}{2 \cdot (5/3)^{j+1}}} C_j^{\frac{1}{2 \cdot (5/3)^j}} \right) \leq \sum_{j=0}^{\infty} (3/5)^j \left(\log A + j \log \left(\frac{10}{3} \right)^{1/2} \right)$$

with $A := C_S^{3/10} (4A_1 A_2)^{1/2}$ remains bounded. Consequently, we obtain $C_{\text{Moser}} < \infty$.

Since $K_\infty = 2K_0$ by definition, cf. (2.26), we obtain in the limit $J \rightarrow \infty$ due to $\|\varphi\|_{L^\infty((0,T) \times \Omega; \mathbb{R}^2)} = \lim_{p \rightarrow \infty} \|\varphi\|_{L^p((0,T) \times \Omega; \mathbb{R}^2)}$

$$\begin{aligned} \sum_{\pm} \|(c^\pm - 2K_0)_+\|_{L^\infty((0,T) \times \Omega)} &= \|((c^+ - 2K_0)_+, (c^- - 2K_0)_+)\|_{L^\infty((0,T) \times \Omega; \mathbb{R}^2)} \\ &\leq C_{\text{Moser}} \|((c^+ - K_0)_+, (c^- - K_0)_+)\|_{L^2((0,T) \times \Omega; \mathbb{R}^2)} \\ &:= C_{\text{Moser}} \left(\sum_{\pm} \|((c^\pm - K_0)_+)\|_{L^2((0,T) \times \Omega)}^2 \right)^{1/2} \\ &\leq C_{\text{Moser}} \sum_{\pm} \|(c^\pm - K_0)_+\|_{L^2((0,T) \times \Omega)} \\ &\leq C_{\text{Moser}} \sum_{\pm} \|c^\pm\|_{L^2((0,T) \times \Omega)} \end{aligned}$$

With the choice of K_0 from (2.23), we finally obtain the desired statement

$$\sum_{\pm} \|c^\pm\|_{L^\infty((0,T) \times \Omega)} \leq C_{\text{Moser}} \sum_{\pm} \|c^\pm\|_{L^2((0,T) \times \Omega)} + 4 \max_{\pm} \|c^{\pm,0}\|_{L^\infty(\Omega)}.$$

□

Remark 2.25. *Choosing $K_0 = K_1 = 0$, we directly obtain an energy estimate in Step 1 of the Moser iteration. Moreover, using c^\pm as test functions allows to treat the reactive term by a sign condition. For this reason, the energy estimates simplifies to*

$$\begin{aligned} \frac{\theta}{2} \frac{d}{dt} \sum_{\pm} \|c^\pm\|_{L^2(\Omega)}^2 + D\alpha_D \sum_{\pm} \|\nabla c^\pm\|_{L^2(\Omega)}^2 &\leq \left(\frac{Dze\|\sigma\|_{L^\infty((0,T)\times\Omega)}}{2k_B T \epsilon_0 \epsilon_r} \right) \sum_{\pm} \|c^\pm\|_{L^2(\Omega)}^2 \\ &=: C_{Energy} \sum_{\pm} \|c^\pm\|_{L^2(\Omega)}^2. \end{aligned} \quad (2.28)$$

Remark 2.26. *The constant C_S of the parabolic Sobolev embedding is given explicitly in [33]. In the case of homogeneous Dirichlet boundary data supplementing the Nernst-Planck equations, the Sobolev constant C_S depends only on the structure of $\partial\Omega$ and the space dimension. For Neumann boundary data (or more general boundary conditions), there is an additional time dependency of the form $C_S(T) \sim O(T^\delta)$ for some $\delta > 0$. On the other hand, the constants C_j are given explicitly, e.g., in the induction hypotheses. Hence, the Moser constant C_{Moser} defined in (2.27) is independent of the end time T and as a consequence the derived L^∞ -estimate holds true even for $T = \infty$.*

Remark 2.27. *In [126, 125] Moser's iteration technique has been applied at least formally for a Navier-Stokes-Nernst-Planck-Poisson system iterating over 2^j . However, considering the time-space dependencies this seems not to be appropriate when regarding the Moser iteration rigorously. Furthermore, we have proven a more subtle estimate here since the L^∞ -norm is estimated via the L^2 -norm and we extended the result to reaction rates as well as a background charge density which is meaningful for certain applications. For example in the context of semiconductor devices, it is related to a given doping profile [86, 119, 89].*

2.2.7 Existence and uniqueness

In this section, we prove the existence and uniqueness of a global weak solution of Problem P_0 , (2.21). In order to show local existence of weak solutions, a fixed point approach using Tihonov's fixed point theorem is applied. A bootstrapping argument is performed in order to extend the local existence result to a global one. Finally, we prove uniqueness of the weak solution using the L^∞ -estimate that has been derived in Section 2.2.6.

Theorem 2.28. *Let Assumption 2.19 hold. Then, there exists a global weak solution of Problem P_0 in the sense of Definition 2.21.*

Proof. The statement of Theorem 2.28 is proven by a fixed point approach. Therefore, we first construct an appropriate fixed point operator \mathcal{F} and then prove the assertions of Tihonov's fixed point theorem:

Theorem 2.29 (Tihonov fixed point theorem [144]). *Let $\mathcal{F} : K \subset X \rightarrow K$ be continuous, where K is a nonempty, compact, convex set in a locally convex space X . Then \mathcal{F} has a fixed point.*

Step 1 (Definition of the fixed point operator): We define the function space

$$X := L^\infty(0, T; L^2(\Omega)) \cap L^2(0, T; H_0^1(\Omega)) \cap H^1(0, T; H^{-1}(\Omega)) \cap L^\infty((0, T) \times \Omega).$$

X is a locally convex vector space with respect to the weak-* topology. On the other hand, supplemented with the following norm

$$\|\cdot\|_X := \|\cdot\|_{L^\infty(0, T; L^2(\Omega))} + \|\cdot\|_{L^2(0, T; H_0^1(\Omega))} + \|\cdot\|_{H^1(0, T; H^{-1}(\Omega))} + \|\cdot\|_{L^\infty((0, T) \times \Omega)},$$

the space X becomes a Banach space [50]. Moreover, we define the function space

$$X_0 := L^1(0, T; L^2(\Omega)) + L^2(0, T; H^{-1}(\Omega)) + H^{-1}(0, T; H^1(\Omega)) + L^1((0, T) \times \Omega).$$

Supplemented with the corresponding norm

$$\begin{aligned} \|\cdot\|_{X_0} \\ := \inf \left(\max \left(\|x_1\|_{L^1(0, T; L^2(\Omega))}, \|x_2\|_{L^2(0, T; H^{-1}(\Omega))}, \|x_3\|_{H^{-1}(0, T; H^1(\Omega))}, \|x_4\|_{L^1((0, T) \times \Omega)} \right) \right), \end{aligned}$$

the space X_0 becomes a Banach space [50]. Here, the infimum is taken over $X_0 \ni x_0 = x_1 + x_2 + x_3 + x_4$, $x_1 \in L^1(0, T; L^2(\Omega))$, $x_2 \in L^2(0, T; H^{-1}(\Omega))$, $x_3 \in H^{-1}(0, T; H^1(\Omega))$, $x_4 \in L^1((0, T) \times \Omega)$. Furthermore, it holds $(X_0)' = X$ [50].

For $R > 0$, we define the fixed point set K via

$$K := \{\varphi \in X : \|\varphi\|_X \leq R\} \subset X.$$

The set K has the following properties:

1. for $R > 0$, K is non-empty.
2. K is convex by definition.
3. K is countably compact with respect to the weak-* topology.

Note that here countably compact and sequentially compact are equivalent since the normed space $(X, \|\cdot\|_X)$ is a Banach space with separable predual X_0 [119]. This fact will be used when showing the continuity of the fixed point operator \mathcal{F} at a later stage of the proof (cf. Step 4).

We define the fixed point operator \mathcal{F} by

$$\mathcal{F} := \mathcal{F}_3 \circ \mathcal{F}_2 \circ \mathcal{F}_1 : X \times X \rightarrow X \times X$$

with

1. $\mathcal{F}_1 : X \times X \rightarrow X \times X \times L^\infty(0, T; H_0^2(\Omega))$, $(\hat{c}^+, \hat{c}^-) \mapsto (\hat{c}^+, \hat{c}^-, \phi)$ with ϕ being solution of

$$-\int_{\Omega} \nabla \cdot (\epsilon_0 \epsilon_r \mathbf{D} \nabla \phi) \psi \, d\mathbf{x} = \int_{\Omega} (\theta z e (\hat{c}^+ - \hat{c}^-) + \sigma) \psi \, d\mathbf{x}, \quad \psi \in L^2(\Omega). \quad (2.29)$$

2. $\mathcal{F}_2 : X \times X \times L^\infty(0, T; H_0^2(\Omega)) \rightarrow X \times X \times L^\infty(0, T; H_0^2(\Omega)) \times L^\infty(0, T; (H_{\text{div},0}^1(\Omega))^n) \times L^\infty(0, T; L^2(\Omega/\mathbb{R}))$, $(\hat{c}^+, \hat{c}^-, \phi) \mapsto (\hat{c}^+, \hat{c}^-, \phi, \mathbf{v}, p)$ with (\mathbf{v}, p) being solutions of

$$\int_{\Omega} \mathbf{K}^{-1} \mathbf{v} \cdot \boldsymbol{\psi} \, d\mathbf{x} = \int_{\Omega} \frac{1}{\eta \rho} p \nabla \cdot \boldsymbol{\psi} - \frac{1}{\eta \rho} z e (\hat{c}^+ - \hat{c}^-) \nabla \phi \cdot \boldsymbol{\psi} \, d\mathbf{x}, \quad \boldsymbol{\psi} \in H_{\text{div},0}^1(\Omega), \quad (2.30)$$

$$\int_{\Omega} (\nabla \cdot \mathbf{v}) \psi \, d\mathbf{x} = 0, \quad \psi \in L^2(\Omega). \quad (2.31)$$

3. $\mathcal{F}_3 : X \times X \times L^\infty(0, T; H_0^2(\Omega)) \times L^\infty(0, T; (H_{\text{div},0}^1(\Omega))^n) \times L^\infty(0, T; L^2(\Omega/\mathbb{R})) \rightarrow X \times X$, $(\hat{c}^+, \hat{c}^-, \phi, \mathbf{v}, p) \mapsto (c^+, c^-)$ with c^\pm being solutions of

$$\begin{aligned} \theta \langle \partial_t c^\pm, \psi \rangle_{H^{-1}(\Omega), H_0^1(\Omega)} + \int_{\Omega} \left(-\mathbf{v} c^\pm + \mathbf{D} \nabla c^\pm \pm \mathbf{D} \frac{z e}{k_B T} c^\pm \nabla \phi \right) \cdot \nabla \psi \, d\mathbf{x} \\ = \int_{\Omega} \mp \theta (c^+ - c^-) \psi \, d\mathbf{x}, \quad \psi \in H_0^1(\Omega). \end{aligned} \quad (2.32)$$

Remark 2.30. For more general and nonlinear reaction rates R^\pm , it is more convenient to use $R^\pm(\hat{c}^+, \hat{c}^-)$ or $R^+(\hat{c}^+, \hat{c}^-)$ and $R^-(c^+, \hat{c}^-)$ in the reactive term of the fixed point operator \mathcal{F}_3 .

Step 2 (Well definiteness): The fixed point operator is well defined as a composition of the well defined operators $\mathcal{F}_1, \mathcal{F}_2, \mathcal{F}_3$:

- (i) The operator \mathcal{F}_1 is well defined: For $(\hat{c}^+, \hat{c}^-) \in X \times X$ there exists a unique solution $\phi \in L^\infty(0, T; H_0^2(\Omega))$ of the elliptic problem (2.29). This result follows directly from elliptic regularity theory, cf. [52], and the fact that t plays only the role of a parameter in the subproblem for ϕ .
- (ii) The operator \mathcal{F}_2 is well defined: For $(\hat{c}^+, \hat{c}^-, \phi) \in X \times X \times L^\infty(0, T; H_0^2(\Omega))$ the right hand side $\hat{c}^\pm \nabla \phi$ is an element of $L^\infty(0, T; L^2(\Omega))$. Using the mixed formulation of the fluid problem (2.30), (2.31) with t as parameter and applying saddle point theory, we obtain that the subproblem for the velocity field \mathbf{v} and the pressure p admits a unique solution $(\mathbf{v}, p) \in L^\infty(0, T; (H_{\text{div},0}^1(\Omega))^n) \times L^\infty(0, T; L^2(\Omega/\mathbb{R}))$. Hereby, the pressure field is only determined up to a constant. The solution can be made unique in $L^2(\Omega)$ if we assume, e.g., that the pressure field p has zero mean value, i.e. that $\int_\Omega p \, d\mathbf{x} = 0$ holds.
- (iii) The operator \mathcal{F}_3 is well defined: For $(\hat{c}^+, \hat{c}^-, \phi, \mathbf{v}, p) \in X \times X \times L^\infty(0, T; H_0^2(\Omega)) \times L^\infty(0, T; (H_{\text{div},0}^1(\Omega))^n) \times L^\infty(0, T; L^2(\Omega/\mathbb{R}))$ there exist unique solutions $(c^+, c^-) \in X \times X$ of the parabolic problem (2.32). This can be proven applying standard Galerkin method or Rothe method and the results of Theorem 2.23 and Moser's iteration technique, cf. Theorem 2.24.

Step 3 (Self mapping property): Let $(\hat{c}^+, \hat{c}^-) \in K \times K$, i.e. it holds $\|\hat{c}^\pm\|_X = \|\hat{c}^\pm\|_{L^\infty(0,T;L^2(\Omega))} + \|\hat{c}^\pm\|_{L^2(0,T;H_0^1(\Omega))} + \|\hat{c}^\pm\|_{H^1(0,T;H^{-1}(\Omega))} + \|\hat{c}^\pm\|_{L^\infty((0,T)\times\Omega)} \leq R$. Then the following a priori estimates hold:

1. For Poisson's equation (2.29), we use ϕ as a test function to obtain directly

$$\begin{aligned} \|\nabla \phi\|_{L^2((0,T)\times\Omega)} &\leq \frac{C_P T^{1/2}}{\epsilon_0 \epsilon_r \alpha_D} \|\theta z e (\hat{c}^+ - \hat{c}^-) + \sigma\|_{L^\infty(0,T;L^2(\Omega))} \\ &\leq \frac{C_P T^{1/2}}{\epsilon_0 \epsilon_r \alpha_D} (2\theta z e R + \|\sigma\|_{L^\infty(0,T;L^2(\Omega))}) \\ &=: B_1(T, R). \end{aligned} \tag{2.33}$$

2. Testing Darcy's law (2.30) with the velocity field \mathbf{v} , the following a priori estimate is valid:

$$\begin{aligned} \|\mathbf{v}\|_{L^2(0,T;H_{\text{div},0}^1(\Omega))} &= \|\mathbf{v}\|_{L^2((0,T)\times\Omega)} \\ &\leq \frac{ze}{\eta \rho \alpha_K} \|(\hat{c}^+ - \hat{c}^-) \nabla \phi\|_{L^2((0,T)\times\Omega)} \end{aligned} \tag{2.34}$$

$$\begin{aligned}
&\leq \frac{ze}{\eta\rho\alpha_K} \|\hat{c}^+ - \hat{c}^-\|_{L^\infty((0,T)\times\Omega)} \|\nabla\phi\|_{L^2((0,T)\times\Omega)} \\
&\leq \frac{ze}{\eta\rho\alpha_K} 2RB_1(T, R) \\
&=: B_2(T, R).
\end{aligned} \tag{2.35}$$

3. For the transport equations (2.32), we obtained the energy estimate (2.28). Here, Gronwall's lemma implies

$$\begin{aligned}
\max_{0\leq t\leq T} \sum_{\pm} \|c^\pm\|_{L^2(\Omega)}^2 &\leq \exp\left(\frac{2}{\theta}C_{\text{Energy}}T\right) \sum_{\pm} \|c^{\pm,0}\|_{L^2(\Omega)}^2 \\
&=: A_1(T) \sum_{\pm} \|c^{\pm,0}\|_{L^2(\Omega)}^2.
\end{aligned} \tag{2.36}$$

On the other hand, integration of (2.28) with respect to time yields

$$\begin{aligned}
&\sum_{\pm} \|\nabla c^\pm\|_{L^2((0,T)\times\Omega)}^2 \\
&\leq \frac{1}{D\alpha_D} C_{\text{Energy}}T \max_{0\leq t\leq T} \sum_{\pm} \|c^\pm\|_{L^2(\Omega)}^2 + \frac{\theta}{2D\alpha_D} \sum_{\pm} \|c^{\pm,0}\|_{L^2(\Omega)}^2 \\
&\leq \left(\frac{1}{D\alpha_D} C_{\text{Energy}}T A_1(T) + \frac{\theta}{2D\alpha_D}\right) \sum_{\pm} \|c^{\pm,0}\|_{L^2(\Omega)}^2 \\
&=: \left(A_2(T) + \frac{\theta}{2D\alpha_D}\right) \sum_{\pm} \|c^{\pm,0}\|_{L^2(\Omega)}^2.
\end{aligned}$$

Furthermore, Moser's iteration (cf. Theorem 2.24) yields in combination with $(a+b) \leq \sqrt{2}(a^2+b^2)^{1/2}$, $(a^2+b^2)^{1/2} \leq a+b$, $a, b \geq 0$ and estimate (2.36)

$$\begin{aligned}
&\sum_{\pm} \|c^\pm\|_{L^\infty((0,T)\times\Omega)} \\
&\leq C_{\text{Moser}}T^{1/2} \max_{0\leq t\leq T} \sum_{\pm} \|c^\pm\|_{L^2(\Omega)} + 4 \max_{\pm} \|c^{\pm,0}\|_{L^\infty(\Omega)} \\
&\leq \left(2\sqrt{2}C_{\text{Moser}}T^{1/2} A_1^{1/2}(T)|\Omega|^{1/2} + 4\right) \max_{\pm} \|c^{\pm,0}\|_{L^\infty(\Omega)} \\
&=: (A_3(T) + 4) \max_{\pm} \|c^{\pm,0}\|_{L^\infty(\Omega)}.
\end{aligned}$$

As last step, it remains to derive an estimation of the time derivatives. By definition, and with $(\sum_{i=1}^4 a_i)^2 \leq 4\sum_{i=1}^4 a_i^2$, $(\sum_{i=1}^4 a_i^2)^{1/2} \leq \sum_{i=1}^4 a_i$, $a_i \geq 0$ and $(a+b)^2 \leq 2(a^2+b^2)$, $a, b \geq 0$, we obtain

$$\begin{aligned}
& \sum_{\pm} \|\partial_t c^{\pm}\|_{L^2(0,T;H^{-1}(\Omega))} \\
& \leq 2\sqrt{2} \left(\sum_{\pm} \|c^{\pm}\|_{L^{\infty}((0,T)\times\Omega)} \|\mathbf{v}\|_{L^2((0,T)\times\Omega)} + C_D \sum_{\pm} \|\nabla c^{\pm}\|_{L^2((0,T)\times\Omega)} \right. \\
& \quad \left. + \frac{DzeC_D}{k_B T} \sum_{\pm} \|c^{\pm}\|_{L^{\infty}((0,T)\times\Omega)} \|\nabla\phi\|_{L^2((0,T)\times\Omega)} + 2\theta \sum_{\pm} \|c^{\pm}\|_{L^2((0,T)\times\Omega)} \right)
\end{aligned}$$

Substituting the estimates (2.33) and (2.34), we obtain

$$\begin{aligned}
& \sum_{\pm} \|\partial_t c^{\pm}\|_{L^2(0,T;H^{-1}(\Omega))} \\
& \leq \left(A_4(T, R) + 8\sqrt{2}C_D \left(\frac{\theta|\Omega|}{D\alpha_D} \right)^{1/2} \right) \max_{\pm} \|c^{\pm,0}\|_{L^{\infty}(\Omega)}
\end{aligned}$$

with the definitions $A_4(T, R) := 16\theta(2A_1(T)T|\Omega|)^{1/2} + 2\sqrt{2}(A_3(T) + 4)B_2(T, R) + 2\sqrt{2}\frac{Dze}{k_B T}C_D(A_3(T) + 4)B_1(T, R) + 16C_D(A_2(T)|\Omega|)^{1/2}$.

Combinig all the above estimates, we obtain a bound for the $\|\cdot\|_X$ -norm of the number densities c^{\pm} with the following structure:

$$\sum_{\pm} \|c^{\pm}\|_X \leq (C_1(T, R) + C_2) \max_{\pm} \|c^{\pm,0}\|_{L^{\infty}(\Omega)} \quad (2.37)$$

with $C_1(T, R) := 2(2A_1(T)|\Omega|)^{1/2}(1+T^{1/2}) + A_3(T) + 4(2|\Omega|A_2(T))^{1/2} + A_4(T, R)$ and $C_2 := 4 + 4\left(\frac{\theta|\Omega|}{D\alpha_D}\right)^{1/2} + 8C_D\left(\frac{\theta|\Omega|}{D\alpha_D}\right)^{1/2}$.

In summary, the estimates (2.37) provide that using the relation $\sum_{\pm} \|\hat{c}^{\pm}\|_X \leq 2R$ also $\sum_{\pm} \|c^{\pm}\|_X \leq 2R$ holds – at least for small end times T since $C_1(T, R) \rightarrow 0$ as $T \rightarrow 0$. This is achieved by making an appropriate choice of the radius R , e.g. as a multiple of $\max_{\pm} \|c^{\pm,0}\|_{L^{\infty}(\Omega)}^2$.

Step 4 (Continuity): We prove that the fixed point operator \mathcal{F} is weakly-* continuous. Hereby, we use the fact that countably compact and sequentially compact are equivalent in X [119]. We assume that

$$\hat{c}_k^{\pm} \xrightarrow{*} \hat{c}^{\pm} \quad \text{in } X$$

and intend to prove that

$$\mathcal{F}(\hat{c}_k^\pm) =: c_k^\pm \xrightarrow{*} c^\pm = \mathcal{F}(\hat{c}^\pm) \quad \text{in } X.$$

Since c_k^\pm is gained as a solution of the system of partial differential equations (2.29)-(2.32), the self mapping property (Step 3) implies

$$\|c_k^\pm\|_X \leq R$$

i.e. there exist weak-* convergent subsequences (c_k^+, c_k^-) that converge to some $(c^+, c^-) \in X \times X$. For ease of presentation, we denote these subsequences again by c_k^\pm . It remains to shown that c^\pm are the ‘‘right’’ limits, i.e. that they are also obtained as solutions of the system of partial differential equations (2.29)-(2.32). To be more concrete, we intend to prove that $c^\pm = \mathcal{F}(\hat{c}^\pm)$.

As preliminary remark, note that due to the compact embedding of X into $L^2(0, T; L^{6-\delta}(\Omega))$, $\delta > 0$ [119], it holds, in particular, that

$$\begin{aligned} \hat{c}_k^\pm &\rightarrow \hat{c}^\pm && \text{in } L^2((0, T) \times \Omega), \\ \hat{c}_k^\pm &\rightarrow \hat{c}^\pm && \text{in } L^2(0, T; L^3(\Omega)). \end{aligned}$$

We consider each term of the Nernst-Planck equation (2.32) separately with $\psi \in H_0^1(\Omega)$:

1. The evolution term converges since c_k^\pm is a priori bounded in $L^2(0, T; H^{-1}(\Omega))$ and hence for the subsequence $c_k^\pm \in L^2(0, T; H^{-1}(\Omega))$ it holds:

$$\int_0^T \theta \langle \partial_t (c_k^\pm - c^\pm), \psi \rangle dt \rightarrow 0$$

2. The diffusive term converges since c_k^\pm is a priori bounded in $L^2(0, T; H^1(\Omega))$, i.e. ∇c_k^\pm is bounded in $L^2((0, T) \times \Omega)$ and therefore weak convergence holds true for the subsequence $\nabla c_k^\pm \in L^2((0, T) \times \Omega)$:

$$\int_0^T \int_\Omega DD \nabla (c_k^\pm - c^\pm) \cdot \nabla \psi \, d\mathbf{x} \, dt \rightarrow 0$$

3. For the drift term we perform the following manipulations

$$\int_0^T \int_\Omega \frac{Dze}{k_B T} (c_k^\pm \mathbf{D} \nabla \phi_k - c^\pm \mathbf{D} \nabla \phi) \cdot \nabla \psi \, dt \, dt$$

$$\begin{aligned}
&= \int_0^T \int_{\Omega} \frac{Dze}{k_B T} (c_k^{\pm} \mathbf{D}\nabla(\phi_k - \phi) + (c_k^{\pm} - c^{\pm}) \mathbf{D}\nabla\phi) \cdot \nabla\psi \, dt \, dt \\
&\leq \frac{Dze}{k_B T} C_D \|c_k^{\pm}\|_{L^{\infty}((0,T)\times\Omega)} \|\nabla(\phi_k - \phi)\|_{L^2((0,T)\times\Omega)} \|\psi\|_{L^2((0,T)\times\Omega)} \\
&\quad + \int_0^T \int_{\Omega} \frac{Dze}{k_B T} (c_k^{\pm} - c^{\pm}) \mathbf{D}\nabla\phi \cdot \nabla\psi \, dt \, dt \\
&\rightarrow 0
\end{aligned}$$

The argument for the statement of convergence in the last step of the estimate is twofold: Firstly, with the a priori estimate (2.33) it holds

$$\|\nabla(\phi_k - \phi)\|_{L^2((0,T)\times\Omega)} \leq \frac{\theta ze C_P}{\epsilon_0 \epsilon_r \alpha_D} \|(\hat{c}_k^+ - \hat{c}^+) - (\hat{c}_k^- - \hat{c}^-)\|_{L^2((0,T)\times\Omega)} \rightarrow 0.$$

This means that $\nabla(\phi_k - \phi)$ converges strongly to 0 in $L^2((0,T)\times\Omega)$, while all other terms remain bounded. Secondly, it holds $\mathbf{D}\nabla\phi \cdot \nabla\psi \in L^1((0,T)\times\Omega)$ and $c_k^{\pm} - c^{\pm} \in L^{\infty}((0,T)\times\Omega) = (L^1((0,T)\times\Omega))'$ is weakly-* convergent, i.e.

$$\left\langle \frac{Dze}{k_B T} (c_k^{\pm} - c^{\pm}), \mathbf{D}\nabla\phi \cdot \nabla\psi \right\rangle_{(L^1((0,T)\times\Omega))', L^1((0,T)\times\Omega)} \rightarrow 0$$

4. The argumentation to prove convergence of the convective term is similar to that one of the drift term, cf. 3.

$$\begin{aligned}
&\int_0^T \int_{\Omega} (-\mathbf{v}_k c_k^{\pm} + \mathbf{v} c^{\pm}) \cdot \nabla\psi \, dt \, dt \\
&= \int_0^T \int_{\Omega} (-\mathbf{v}_k + \mathbf{v}) c_k^{\pm} + \mathbf{v} (c^{\pm} - c_k^{\pm}) \cdot \nabla\psi \, dt \, dt \\
&\leq \|c_k^{\pm}\|_{L^{\infty}((0,T)\times\Omega)} \|\mathbf{v}_k - \mathbf{v}\|_{L^2((0,T)\times\Omega)} \|\psi\|_{L^2((0,T)\times\Omega)} \\
&\quad + \int_0^T \int_{\Omega} (c^{\pm} - c_k^{\pm}) \mathbf{v} \cdot \nabla\psi \, dt \, dt \\
&\rightarrow 0
\end{aligned}$$

The justification of the last step of the estimate is again twofold: Firstly, with the a priori estimate (2.34) it holds

$$\begin{aligned}
&\|\mathbf{v}_k - \mathbf{v}\|_{L^2((0,T)\times\Omega)} \\
&\leq \frac{ze}{\eta \rho \alpha_K} \|(\hat{c}_k^{\pm} \nabla\phi_k - \hat{c}^{\pm} \nabla\phi)\|_{L^2((0,T)\times\Omega)} \\
&= \frac{ze}{\eta \rho \alpha_K} \|(\hat{c}_k^{\pm} - \hat{c}^{\pm}) \nabla\phi_k + \hat{c}^{\pm} \nabla(\phi_k - \phi)\|_{L^2((0,T)\times\Omega)}
\end{aligned}$$

$$\begin{aligned}
&\leq \frac{ze}{\eta\rho\alpha_K} \|(\hat{c}_k^\pm - \hat{c}^\pm)\|_{L^2(0,T;L^3(\Omega))} \|\nabla\phi_k\|_{L^\infty(0,T;L^6(\Omega))} \\
&\quad + \frac{ze}{\eta\rho\alpha_K} \|\hat{c}^\pm\|_{L^\infty((0,T)\times\Omega)} \|\nabla(\phi_k - \phi)\|_{L^2((0,T)\times\Omega)} \\
&\rightarrow 0.
\end{aligned}$$

This means that $\mathbf{v}_k - \mathbf{v}$ converges strongly to zero in $L^2((0, T) \times \Omega)$ by assumption, while all other terms remain bounded. Secondly, it holds $\mathbf{v} \cdot \nabla\psi \in L^1((0, T) \times \Omega)$ and $c_k^\pm - c^\pm \in L^\infty((0, T) \times \Omega) = (L^1((0, T) \times \Omega))'$ is weakly-* convergent, i.e.

$$\langle (c^\pm - c_k^\pm), \mathbf{v} \cdot \nabla\psi \rangle_{(L^1((0,T)\times\Omega))', L^1((0,T)\times\Omega)} \rightarrow 0$$

Step 5 (Global solution): In order to obtain a global instead of a local existence result, we apply a bootstrapping argument. To this end, we assume that the time interval $[0, T]$ is arbitrary large and decompose it in k -subintervals $[T_i, T_{i+1}]$, $i \in \{0, \dots, k-1\}$ with $0 =: T_0 < T_1 < \dots < T_k < T_k := T$ such that on each time interval $[T_i, T_{i+1}]$ Step 1. - 5. are fulfilled. Hence, solutions $c_{0,i}^\pm$ exist on the each of the time intervals $[T_i, T_{i+1}]$, $i \in \{0, \dots, k-1\}$. These solutions satisfy the a priori estimates from Step 3 and are non-negative and bounded in L^∞ according to Theorem 2.23 and 2.24. Therefore, it is admissible to take $c_{0,i}^\pm(T_{i+1})$ as initial values for the system of partial differential equation that has $c_{0,i+1}^\pm$ as a solutions. With the uniqueness from Step 2 this leads to a continuation of the solution on the whole time interval $[0, T]$ and thus to a global weak solution according to Definition 2.21. \square

Theorem 2.31. *The solution of Problem P_0 in the sense of Definition 2.21 is unique.*

Proof. We assume that there are two weak solutions $(\mathbf{v}_1, p_1, \phi_1, \mathbf{c}_1)$ and $(\mathbf{v}_2, p_2, \phi_2, \mathbf{c}_2)$ of Problem P_0 , (2.20), in the sense of Definition 2.21 which correspond to the same initial values $c^{\pm,0}$. Let furthermore c_1^\pm, c_2^\pm be bounded in $L^\infty((0, T) \times \Omega)$ according to Section 2.2.6. We denote by $\Delta\mathbf{v} := \mathbf{v}_1 - \mathbf{v}_2$, $\Delta p := p_1 - p_2$, $\Delta\phi := \phi_1 - \phi_2$, and $\Delta c^\pm := c_1^\pm - c_2^\pm$ the differences of the solutions. We test the transport equations for the differences Δc^\pm , i.e. the differences of (2.21c), with Δc^\pm and obtain

$$\begin{aligned}
&\frac{\theta}{2} \frac{d}{dt} \|\Delta c^\pm\|_{L^2(\Omega)}^2 + D\alpha_D \|\nabla\Delta c^\pm\|_{L^2(\Omega)}^2 \\
&\quad + \int_{\Omega} (\Delta\mathbf{v}c_1^\pm + \mathbf{v}_2\Delta c^\pm) \cdot \nabla\Delta c^\pm \pm \frac{Dze}{k_B T} (c_1^\pm \mathbf{D}\nabla\Delta\phi - \Delta c^\pm \mathbf{D}\nabla\phi_2) \cdot \nabla\Delta c^\pm \, d\mathbf{x} \\
&= \mp\theta \int_{\Omega} (\Delta c^+ - \Delta c^-) \Delta c^\pm \, d\mathbf{x}.
\end{aligned}$$

Here, we take into account that the velocity field is divergence free (2.21b) and has homogeneous boundary data. Moreover, we consider the sum over \pm which results in a cancellation of the reactive term according to a sign condition. With Hölder's inequality this finally leads to

$$\begin{aligned}
& \frac{\theta}{2} \frac{d}{dt} \sum_{\pm} \|\Delta c^{\pm}\|_{L^2(\Omega)}^2 + D\alpha_D \sum_{\pm} \|\nabla \Delta c^{\pm}\|_{L^2(\Omega)}^2 \\
& \leq \sum_{\pm} \left(\|\Delta \mathbf{v}\|_{L^2(\Omega)} \|c_1^{\pm}\|_{L^\infty(\Omega)} \|\nabla \Delta c^{\pm}\|_{L^2(\Omega)} \right. \\
& \quad \left. + \frac{DzeC_D}{k_B T} \|c_1^{\pm}\|_{L^\infty(\Omega)} \|\nabla \Delta \phi\|_{L^2(\Omega)} \|\nabla \Delta c^{\pm}\|_{L^2(\Omega)} \right. \\
& \quad \left. + \frac{DzeC_D}{k_B T} \|\Delta c^{\pm}\|_{L^3(\Omega)} \|\nabla \phi_2\|_{L^6(\Omega)} \|\nabla \Delta c^{\pm}\|_{L^2(\Omega)} \right) \\
& \leq \|\Delta \mathbf{v}\|_{L^2(\Omega)} \max_{\pm} \|c_1^{\pm}\|_{L^\infty(\Omega)} \sum_{\pm} \|\nabla \Delta c^{\pm}\|_{L^2(\Omega)} \\
& \quad + \frac{DzeC_D}{k_B T} \|\nabla \Delta \phi\|_{L^2(\Omega)} \max_{\pm} \|c_1^{\pm}\|_{L^\infty(\Omega)} \sum_{\pm} \|\nabla \Delta c^{\pm}\|_{L^2(\Omega)} \\
& \quad + \left(\frac{DzeC_D}{k_B T} \|\nabla \phi_2\|_{L^6(\Omega)} C_{\text{Int}} \right)^4 C(\delta) \sum_{\pm} \|\Delta c^{\pm}\|_{L^2(\Omega)}^2 + \delta \sum_{\pm} \|\nabla \Delta c^{\pm}\|_{L^2(\Omega)}^2.
\end{aligned} \tag{2.38}$$

In the last step of the estimate, we applied the following interpolation inequality $\|\varphi\|_{L^3(\Omega)} \leq C_{\text{Int}} \|\varphi\|_{L^2(\Omega)}^{1/2} \|\nabla \varphi\|_{L^2(\Omega)}^{1/2}$ [44] and also Young's inequality [44].

We consider now the following stability estimates (see also the a priori estimates (2.33), (2.34)), which are estimated analog to (2.38) by the interpolation inequality and Young's inequality (4, 4/3) [44].

$$\begin{aligned}
\|\nabla \Delta \phi\|_{L^2(\Omega)} & \leq \frac{\theta ze C_P}{\epsilon_0 \epsilon_r \alpha_D} \|\Delta c^+ - \Delta c^-\|_{L^2(\Omega)} \leq \frac{\theta ze C_P}{\epsilon_0 \epsilon_r \alpha_D} \sum_{\pm} \|\Delta c^{\pm}\|_{L^2(\Omega)}, \\
\|\Delta \mathbf{v}\|_{L^2(\Omega)} & \leq \frac{ze}{\eta \rho \alpha_K} \left(\|(\Delta c^+ - \Delta c^-) \nabla \phi_2\|_{L^2(\Omega)} + \|(c_1^+ - c_1^-) \nabla \Delta \phi\|_{L^2(\Omega)} \right) \\
& \leq \frac{ze}{\eta \rho \alpha_K} \left(\sum_{\pm} \|\Delta c^{\pm}\|_{L^3(\Omega)} \|\nabla \phi_2\|_{L^6(\Omega)} + \sum_{\pm} \|c_1^{\pm}\|_{L^\infty(\Omega)} \|\nabla \Delta \phi\|_{L^2(\Omega)} \right) \\
& \leq \left(\frac{ze}{\eta \rho \alpha_K} \|\nabla \phi_2\|_{L^6(\Omega)} C_{\text{Int}} \right)^2 C(\delta) \sum_{\pm} \|\Delta c^{\pm}\|_{L^2(\Omega)} + \delta \sum_{\pm} \|\nabla \Delta c^{\pm}\|_{L^2(\Omega)} \\
& \quad + \frac{2\theta z^2 e^2 C_P}{\epsilon_0 \epsilon_r \alpha_K \alpha_D \eta \rho} \max_{\pm} \|c_1^{\pm}\|_{L^\infty(\Omega)} \sum_{\pm} \|\Delta c^{\pm}\|_{L^2(\Omega)},
\end{aligned}$$

Substituting these stability estimates in (2.38), we obtain

$$\begin{aligned}
& \frac{\theta}{2} \frac{d}{dt} \sum_{\pm} \|\Delta c^{\pm}\|_{L^2(\Omega)}^2 + \alpha_D \sum_{\pm} \|\nabla \Delta c^{\pm}\|_{L^2(\Omega)}^2 \\
& \leq \left(\left(\frac{ze}{\eta\rho\alpha_K} \|\nabla\phi_2\|_{L^6(\Omega)} C_{\text{Int}} \right)^2 C(\delta) \sum_{\pm} \|\Delta c^{\pm}\|_{L^2(\Omega)} + \delta \sum_{\pm} \|\nabla \Delta c^{\pm}\|_{L^2(\Omega)} \right. \\
& \quad \left. + \frac{2\theta z^2 e^2 C_P}{\epsilon_0 \epsilon_r \alpha_K \alpha_D \eta \rho} \max_{\pm} \|c_1^{\pm}\|_{L^\infty(\Omega)} \sum_{\pm} \|\Delta c^{\pm}\|_{L^2(\Omega)} \right) \max_{\pm} \|c_1^{\pm}\|_{L^\infty(\Omega)} \sum_{\pm} \|\nabla \Delta c^{\pm}\|_{L^2(\Omega)} \\
& \quad + \frac{\theta D z^2 e^2 C_P C_D}{\epsilon_0 \epsilon_r k_B T \alpha_D} \sum_{\pm} \|\Delta c^{\pm}\|_{L^2(\Omega)} \max_{\pm} \|c_1^{\pm}\|_{L^\infty(\Omega)} \sum_{\pm} \|\nabla \Delta c^{\pm}\|_{L^2(\Omega)} \\
& \quad + \left(\frac{DzeC_D}{k_B T} \|\nabla\phi_2\|_{L^6(\Omega)} C_{\text{Int}} \right)^4 C(\delta) \sum_{\pm} \|\Delta c^{\pm}\|_{L^2(\Omega)}^2 + \delta \|\nabla \Delta c^{\pm}\|_{L^2(\Omega)}^2 \\
& \leq A \sum_{\pm} \|\Delta c^{\pm}\|_{L^2(\Omega)}^2 + (7 + 2 \max_{\pm} \|c_1^{\pm}\|_{L^\infty(\Omega)}) \delta \sum_{\pm} \|\nabla \Delta c^{\pm}\|_{L^2(\Omega)}^2.
\end{aligned}$$

Here, we used the basic relation $(a + b)^2 \leq 2(a^2 + b^2)$ and introduced the following definition:

$$\begin{aligned}
A = & 2 \left(\frac{ze}{\eta\rho\alpha_K} \|\nabla\phi_2\|_{L^6(\Omega)} C_{\text{Int}} \right)^4 \left(\max_{\pm} \|c_1^{\pm}\|_{L^\infty(\Omega)} \right)^2 C^3(\delta) \\
& + 2 \left(\frac{2\theta z^2 e^2 C_P}{\epsilon_0 \epsilon_r \alpha_K \alpha_D \eta \rho} \right)^2 \left(\max_{\pm} \|c_1^{\pm}\|_{L^\infty(\Omega)} \right)^4 C(\delta) \\
& + 2 \left(\frac{\theta D z^2 e^2 C_P C_D}{\epsilon_0 \epsilon_r k_B T \alpha_D} \max_{\pm} \|c_1^{\pm}\|_{L^\infty(\Omega)} \right)^2 C(\delta) \\
& + \left(\frac{DzeC_D}{k_B T} \|\nabla\phi_2\|_{L^6(\Omega)} C_{\text{Int}} \right)^4 C(\delta).
\end{aligned}$$

Adsorption with $\alpha_D - (7 + 2 \max_{\pm} \|c_1^{\pm}\|_{L^\infty(\Omega)}) \delta \geq \frac{\alpha_D}{2}$ implies

$$\frac{d}{dt} \sum_{\pm} \|\Delta c^{\pm}\|_{L^2(\Omega)}^2 + \sum_{\pm} \|\nabla \Delta c^{\pm}\|_{L^2(\Omega)}^2 \leq \frac{A}{\min(\theta/2, D\alpha_D/2)} \sum_{\pm} \|\Delta c^{\pm}\|_{L^2(\Omega)}^2.$$

Gronwall's Lemma [44] then yields

$$\max_{0 \leq t \leq T} \left(\sum_{\pm} \|\Delta c^{\pm}\|_{L^2(\Omega)}^2 \right) \leq \exp \left(\int_0^T \frac{A}{\min(\theta/2, D\alpha_D/2)} dt \right) \left(\sum_{\pm} \|\Delta c^{\pm,0}\|_{L^2(\Omega)}^2 \right) = 0.$$

Since A does only depend on the physical parameters, $\|\nabla\phi_2\|_{L^6(\Omega)}^4$, $\|c_1^\pm\|_{L^\infty(\Omega)}^2$ and $\|c_1^\pm\|_{L^\infty(\Omega)}^4$, the right hand side in the above estimate is well defined and for this reason, the statement of Theorem 2.31 is proven. \square

2.3 Concluding remarks

In this chapter, we considered the mathematical description of fluid flow and transport of charged colloidal particles within a saturated porous medium on different spatial scales. First of all, a mathematical model at the pore-scale, the Stokes-Nernst-Planck-Poisson system (Problem P), was introduced and several simplifications and specifications were discussed. Moreover, its non-dimensional form was derived, unique existence of weak solutions and physical properties of its solutions were stated. In the second part of this chapter, the effective descriptions of fluid flow and transport processes were discussed. In particular, the Darcy-Nernst-Planck-Poisson system (Problem P_0), was introduced and its unique existence of weak solutions was established. In the context of homogenization, these analytical results form the starting point for error estimates and are the basis of numerical schemes. In [46], both the pore-scale model, Problem P , and the effective model, Problem P_0 , cf. Section 2.1.2 and Section 2.2.4, have been investigated numerically. Solving these problems is computationally challenging due to the mass balances that have to be fulfilled and the diverse boundary conditions. A fully discrete numerical scheme capable of approximating the quantities of interest was used in [46] applying Rothe's method and the implicit Euler method. The spatial discretization is performed on unstructured triangular grids by lowest order mixed finite elements. The most crucial point is that appropriate fixed point iterations have to be constructed depending on the nature of the nonlinear couplings between the subsystems for fluid flow, transport, and electrostatic potential. For details of the discretization and the numerical toolbox HyPHM, we refer to [46].

Chapter 3

The concept of homogenization

3.1 Introduction

In many applications, transport phenomena are of interest on different time and length scales. Separate time scales arise, [87], since the transport processes convection, diffusion, and drift involve different characteristic times, cf. Section 2.1.3. Moreover, the reaction constants in realistic chemical reactions network are often of different orders of magnitude. However, in the remainder of this work we neglect the separation of time scales and focus on the different length scales that come along quite naturally in the context of transport in heterogeneous porous media, see [116], Figure 3.1, and Figure 3.2.

Firstly, there is the macroscopic length scale (the field or laboratory scale) in the order of m to km or cm to dm , respectively, on which experiments are designed and observations are made. Secondly, there is the microscopic scale (the pore-scale) in the order of nm to μm , on which the physical processes take place. We characterize the separation of these two length scales by a small, dimensionless parameter ε that is

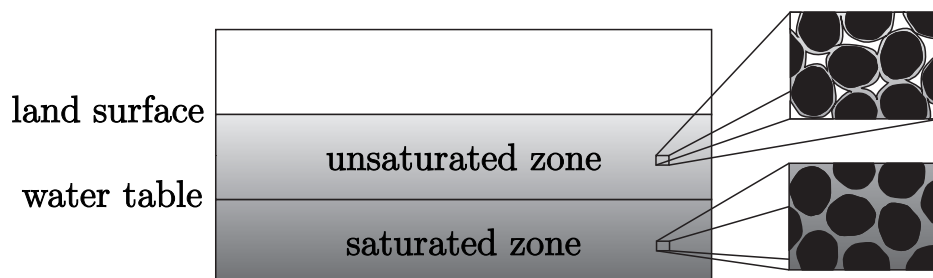


Figure 3.1: Schematic representation of a natural soil

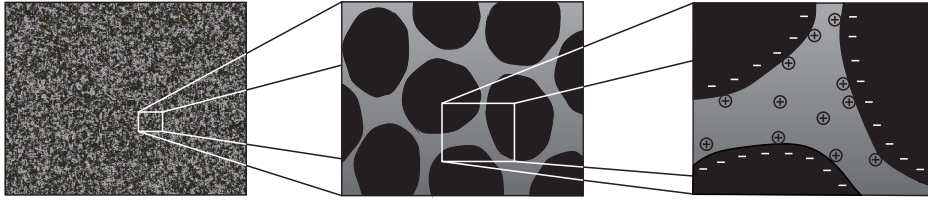


Figure 3.2: Schematic representation of different scales within a natural soil

related to the ratio between a characteristic macroscopic length L and a characteristic microscopic length l by

$$\varepsilon := \frac{l}{L}. \quad (3.1)$$

Generally, it is assumed that phenomena are described accurately by an “exact” mathematical model on the pore-scale. However, direct numerical simulations of this model problem resolving the complex heterogeneous geometrical structure of the porous medium are not possible unless choosing very small time or length scales, which is not reasonable for most applications. Moreover, in practice, one is typically less interested in the detailed behavior on the pore-scale but in the prediction and understanding of observable phenomena on the field/laboratory scale.

The aim, in applying an upscaling procedure, is to obtain an effective, averaged model that is in some sense equivalent to the underlying exact pore-scale model. More precisely, starting from the pore-scale model, a mathematical model on the macroscopic scale is deduced, which is capable by a numerical scheme. Furthermore, using an upscaling technique allows to validate and expand the understanding of existing effective models. For this reason, such an approach is applied to the SNPP system at a later stage of this thesis and we give a short review of the most common upscaling methods in this chapter.

The remainder of the chapter is organized as follows: In the first part, Section 3.1.1, different upscaling methods are presented, namely the *method of representative elementary volumes*, the *method of formal two-scale asymptotic expansion* and the *method of two-scale convergence*. This part is completed by a mathematical description of an idealized geometrical setting in Section 3.1.3 and the definition of extension in Section 3.1.4. In the second part, in Section 3.2, a review on the existing literature of the upscaling of model Problem P and related problems is given.

3.1.1 Introduction to upscaling methods

In the following, we recapitulate different upscaling methods that are well known in the literature, namely averaging by the *method of representative elementary volumes* and two homogenization methods: the *method of formal two-scale asymptotic expansion* and the *method of two-scale convergence*.

3.1.2 Method of volume averaging

In the method of volume averaging [143], an (oscillating) function φ which describes the behavior of a physical quantity properly on the pore-scale is smoothed by taking its local average

$$\bar{\varphi}(\mathbf{x}) := \int_{V(\mathbf{x})} \varphi(\mathbf{y}) \, d\mathbf{y}$$

over some *representative elementary volume (REV)* $V(\mathbf{x})$. The averaged function $\bar{\varphi}$ then describes the physical properties on a macroscopic scale and the pore-scale model equations are all written in terms of averaged quantities. This finally provides an effective model description for the considered physical quantities. The crucial point in using the method of representative elementary volumes is that the REV has to be small compared to the size of the porous medium and, at the same time, it has to be large compared to the size of a single pore or grain in order to capture all geometrical characteristics of the porous medium, see Figure 3.3.

3.1.3 Homogenization methods

In contrast to the method of volume averaging which is also very popular in the engineering sciences, in mathematics homogenization methods have been developed. Instead of considering the pore-scale problem $P : \mathcal{L}\varphi = f$, i.e. a system of partial differential equations with differential operator \mathcal{L} , solution φ and force term f defined on a real porous medium, and averaging over REVs, in homogenization one is working with the family of problems $P_\varepsilon : \mathcal{L}_\varepsilon\varphi_\varepsilon = f_\varepsilon$ with solutions φ_ε parametrized and indexed by the scale parameter ε [3]. Moreover, problem P_ε is defined on the periodic (and perforated) geometry with characteristic length ε . Then, the limit $\varepsilon \rightarrow 0$ is taken, i.e. the problem is analyzed for vanishing microstructure instead of taking explicit averages. Thereby, the problem formulation on the pore-scale is transformed

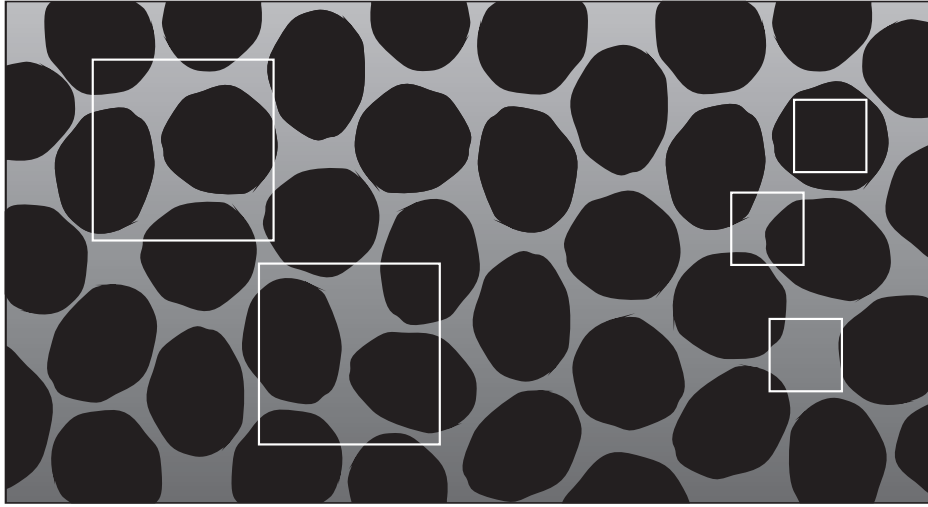


Figure 3.3: Reasonable choice of a REV that captures characteristics of the porous medium (left) and inappropriate choice (right)

into effective equations $P_0 : \bar{\mathcal{L}}\bar{\varphi}_0 = \bar{f}_0$ on the macroscopic scale. For an schematic illustration see also Figure 3.4.

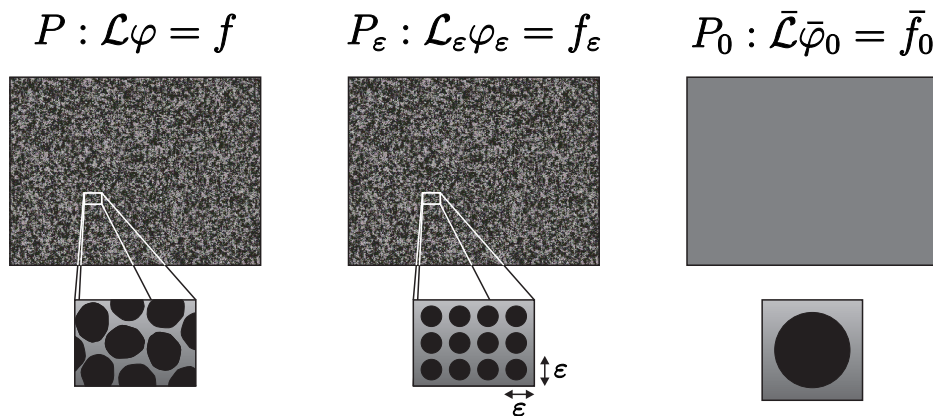


Figure 3.4: Schematic representation of the homogenization procedure

The homogenization methods of two-scale asymptotic expansion and two-scale convergence are more rigorous than the method of representative elementary volumes. On the other hand, several restrictive assumptions such as periodicity are made. This means that the real porous medium is replaced by a periodic idealized version, cf. Figure 3.4. However, several attempts can be found in the literature how to relax the restriction of periodicity again. For references and a short discussion, we refer to Chapter 5. Another point one should be aware of is that for natural porous media the complete and detailed geometrical description is never available and therefore approximative assumptions are made or stochastic descriptions are used. Moreover, in certain experimental settings or

technical applications, periodicity is not necessarily a restriction at all, see, e.g., [76]. In contrast to assuming constitutive laws for physical parameters, see Section 2.2.1 and Section 2.2.2, one main benefit of the homogenization methods is that explicit formulae for averaged coefficients such as permeability tensor and diffusion tensor are obtained defining appropriate so-called cell problems. The unit cells on which these cell problems are defined represent the underlying microscopic geometry similar to the REV in the method of representative elementary volumes, see Figure 3.5. For this reason, the relation between effective averaged coefficients and the underlying heterogeneous geometry is clarified. In other words, the information regarding the microstructure is retained in the effective model description by means of averaged coefficients, which is often sufficient in practice.



Figure 3.5: Schematic picture of different representative two dimensional unit cells. from left to right: solid phase consisting of several non-connected parts, platy clays (cf. [133]), idealized anisotropic and isotropic material

Before presenting the homogenization methods in more detail, we need to introduce some notation on the underlying geometrical setting.

Geometrical Setting

In this section, the notation that comes along with the multi-scale framework of problems treated by homogenization theory is defined. The idealized underlying geometry which characterizes the highly heterogeneous structure of the porous medium is depicted schematically for two space dimensions in Figure 3.6.

We consider a convex domain $\Omega \subset \mathbb{R}^n$, $n \in \{2, 3\}$ and construct a perforated domain Ω_ε with an associated periodic microstructure representing the porous medium. The idealized porous medium is given by the periodic composition of shifted and scaled *standard unit cells* $Y = [-\frac{1}{2}, +\frac{1}{2}]^n$. The unit cell Y is made up of two open sets, see Figure 3.6: The liquid part Y_l and the solid part Y_s such that $\bar{Y}_l \cup \bar{Y}_s = \bar{Y}$, $Y_l \cap Y_s = \emptyset$, and $\bar{Y}_l \cap \bar{Y}_s = \Gamma$. Since the unit cell Y represents the underlying microstructure of the porous medium, the solid part Y_s may have a complex structure or may even consist

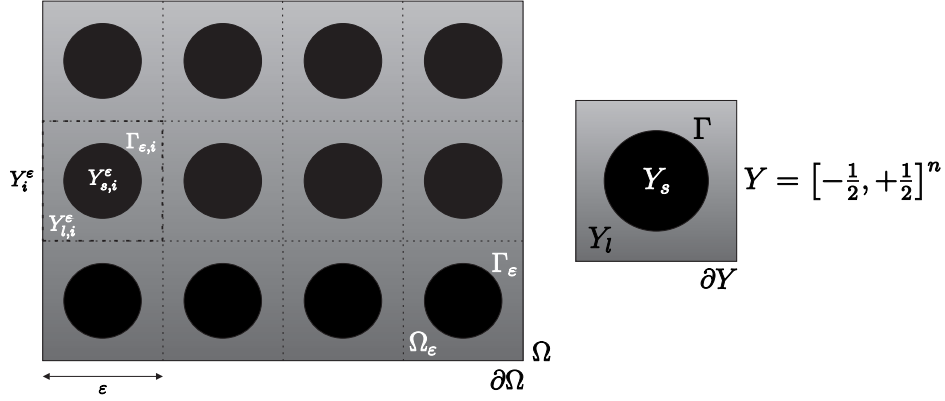


Figure 3.6: Periodic representation of a porous medium (left) and standard unit cell (right)

of several non-connected parts, cf. Section 3.1.2 and Figure 3.5. For simplicity, the solid is represented schematically by circles in Figure 3.6. We define the ratio of pore size to domain size by ε and call $\varepsilon \ll 1$ the scale parameter, cf. (3.1). We assume the macroscopic domain Ω to be covered by a regular mesh of size ε consisting of ε scaled and shifted cells Y_i^ε that are divided analogously into a scaled fluid part, solid part and corresponding boundary. Let us denote these by $Y_{l,i}^\varepsilon$, $Y_{s,i}^\varepsilon$, and $\Gamma_{\varepsilon,i}$, respectively. The fluid part (pore space), the solid part (solid matrix), and the inner boundary of the porous medium are defined by

$$\Omega_\varepsilon := \bigcup_i Y_{l,i}^\varepsilon, \quad \Omega \setminus \overline{\Omega_\varepsilon} := \bigcup_i Y_{s,i}^\varepsilon, \quad \text{and} \quad \Gamma_\varepsilon := \bigcup_i \Gamma_{\varepsilon,i},$$

respectively. We assume that Ω_ε is connected and has Lipschitz boundary. This is, e.g., achieved if the solid part Y_s is smooth enough and does not touch or intersect the boundary of the unit cell Y . If, in addition, we assume that Ω is completely covered by ε -scaled unit cells Y_i^ε , it holds in particular $\partial\Omega \cap \Gamma_\varepsilon = \emptyset$, see again Figure 3.6. We refer to [24] and the discussion of the references [1] and [5] therein for alternative approaches to weaken these restrictive geometrical assumptions such as introducing security zones close to the boundary, deriving appropriate estimates far from the boundary, or developing strategies in order to omit direct extensions of the variables into the holes. Note as a remark, that the solid part cannot be connected in a two-dimensional setting under the assumption that the pore space is connected. This is, however, physically reasonable since otherwise the fluid flow and transport would be blocked. On the other hand, in the three-dimensional case, both the solid matrix and the pore space may be connected at the same time.

Method of formal two-scale asymptotic expansion

Having these notations at hand, we introduce the method of two-scale asymptotic expansion. A mathematical description can be found, e.g., in [15, 123] and for a further application to basic flow and transport problems we refer, e.g., to [58].

The aim of the method of formal two-scale asymptotic expansion is to obtain at least formally the limit equations $P_0 : \bar{\mathcal{L}}\bar{\varphi}_0 = \bar{f}_0$ of the family of problems $P_\varepsilon : \mathcal{L}_\varepsilon\varphi_\varepsilon = f_\varepsilon$ for $\varepsilon \rightarrow 0$. To this end, we introduce in addition to the global, macroscopic (“slow”) variable \mathbf{x} , the microscopic (“fast”) variable \mathbf{y} . Due to the scale separation, these variables are connected via the relation $\mathbf{y} = \mathbf{x}/\varepsilon$. As a consequence, applying the chain rule, the expansion of the spatial gradient, divergence and Laplace operator reads

$$\nabla_\varepsilon = \nabla_{\mathbf{x}} + \frac{1}{\varepsilon}\nabla_{\mathbf{y}}, \quad \nabla_\varepsilon \cdot = \nabla_{\mathbf{x}} \cdot + \frac{1}{\varepsilon}\nabla_{\mathbf{y}} \cdot, \quad \Delta_\varepsilon = \Delta_{\mathbf{x}} + \frac{2}{\varepsilon}\nabla_{\mathbf{x}} \cdot \nabla_{\mathbf{y}} + \frac{1}{\varepsilon^2}\Delta_{\mathbf{y}}. \quad (3.2)$$

Further spatial derivatives are calculated analogously applying the chain rule. Moreover, we postulate that the solutions φ_ε are expanded in series of the scale parameter ε , i.e.

$$\varphi_\varepsilon(t, \mathbf{x}) = \varphi_0(t, \mathbf{x}, \mathbf{y}) + \varepsilon\varphi_1(t, \mathbf{x}, \mathbf{y}) + \varepsilon^2\varphi_2(t, \mathbf{x}, \mathbf{y}) + \dots, \quad \mathbf{y} = \mathbf{x}/\varepsilon. \quad (3.3)$$

Applying the expansions (3.2), (3.3) to the model problems $P_\varepsilon : \mathcal{L}_\varepsilon\varphi_\varepsilon = f_\varepsilon$ and analyzing successively the different orders in ε^k , $k \in \mathbb{Z}$, a so-called two-scale homogenized problem is obtained. The desired macroscopic homogenized problem description $P_0 : \bar{\mathcal{L}}\bar{\varphi}_0 = \bar{f}_0$ is derived from the two-scale homogenized problem after averaging with respect to \mathbf{y} . Here, effective coefficients are defined in terms of solutions of auxiliary cell problems. In general, these are set up according to a linear representations of the higher order term φ_1 by means of the zero order term φ_0 .

In summary, two different types of problems remain to be solved: the macroscopic problem P_0 , which is defined in the variable \mathbf{x} together with the cell problems, which have \mathbf{y} as main variable. In this way, the slow (macroscopic) and the fast (microscopic) variables are separated owing to the assumed scale separation.

Remark 3.1. *In general, cell problems have to be solved in every time and space point of the macroscopic domain. This is of course computationally very demanding and without a good solution strategy as hopeless as trying to solve the exact model problem on the highly heterogeneous domain. However, in many cases the cell problems can*

be computed in parallel or decouple from the effective equations and can therefore be precomputed. In summary, solving the homogenized model is more flexible and for this reason advantageous compared to solving the original model problem.

Remark 3.2. An extension of the method of formal two-scale asymptotic expansion to evolving microstructures will be discussed and applied in Chapter 5.

Method of two-scale convergence

As second homogenization method, we present the method of two-scale convergence which has been proposed by Nguetseng in [100] and further developed by Allaire in [3]. An introduction to this topic and the application of the method to basic model equations can be found, for example, in [24] and [58].

Contrary to the previously introduced upscaling methods, the method of two-scale convergence provides a rigorous justification of the existence of the zero order term in the ansatz (3.3). It is therefore strongly related to the method of formal two-scale asymptotic expansion. The main drawback of the latter method is that it does not provide any proof that the assumption of the ansatz (3.3) is valid and that the correct limit problem is obtained. In the method of two-scale convergence, the derivation and verification of the homogenization results are combined in one single step.

We state now the definition of a new type of convergence, the *two-scale convergence* as well as the basic compactness result for oscillating functions being defined on a time-space cylinder, see, e.g., also [84] and [98].

Definition 3.3. A sequence of functions $\{\varphi_\varepsilon\}$ in $L^2((0, T) \times \Omega)$ is said to two-scale converge to a limit φ_0 belonging to $L^2((0, T) \times \Omega \times Y)$ if, for any function ψ in $\mathcal{D}((0, T) \times \Omega; C_{per}^\infty(Y))$, we have

$$\lim_{\varepsilon \rightarrow 0} \int_0^T \int_\Omega \varphi_\varepsilon(t, \mathbf{x}) \psi\left(t, \mathbf{x}, \frac{\mathbf{x}}{\varepsilon}\right) d\mathbf{x} dt = \int_0^T \int_{\Omega \times Y} \varphi_0(t, \mathbf{x}, \mathbf{y}) \psi(t, \mathbf{x}, \mathbf{y}) d\mathbf{y} d\mathbf{x} dt.$$

In short notation we write $\varphi_\varepsilon \xrightarrow{2} \varphi_0$.

A sequence of functions $\{\varphi_\varepsilon\}$ in $L^2((0, T) \times \Gamma_\varepsilon)$ is said to two-scale converge to a limit φ_0 belonging to $L^2((0, T) \times \Omega \times \Gamma)$ if, for any function ψ in $\mathcal{D}((0, T) \times \Omega; C_{per}^\infty(\Gamma))$, we have

$$\lim_{\varepsilon \rightarrow 0} \varepsilon \int_0^T \int_{\Gamma_\varepsilon} \varphi_\varepsilon(t, \mathbf{x}) \psi\left(t, \mathbf{x}, \frac{\mathbf{x}}{\varepsilon}\right) ds_{\mathbf{x}} dt = \int_0^T \int_{\Omega \times \Gamma} \varphi_0(t, \mathbf{x}, \mathbf{y}) \psi(t, \mathbf{x}, \mathbf{y}) ds_{\mathbf{y}} d\mathbf{x} dt.$$

Here, $\mathcal{D}((0, T) \times \Omega; C_{\text{per}}^\infty(Y))$ and $\mathcal{D}((0, T) \times \Omega; C_{\text{per}}^\infty(\Gamma))$ denote the function spaces of infinitely smooth functions having compact support in $(0, T) \times \Omega$ with values in the space of infinitely differentiable functions that are periodic in Y and Γ , respectively. The following compactness results allow to extract converging subsequences from bounded sequences and therefore yield the possibility to pass to the two-scale limit provided that suitable *a priori* estimates are shown.

Theorem 3.4. 1. Let $\{\varphi_\varepsilon\}$ be a bounded sequence in $L^2((0, T) \times \Omega)$. Then there exists a function φ_0 in $L^2((0, T) \times \Omega \times Y)$ such that, up to a subsequence, φ_ε two-scale converges to φ_0 .

2. Let $\{\varphi_\varepsilon\}$ be a bounded sequence in $L^2(0, T; H^1(\Omega))$. Then there exist functions φ_0 in $L^2(0, T; H^1(\Omega))$ and φ_1 in $L^2((0, T) \times \Omega; H_{\text{per}}^1(Y))$ such that, up to a subsequence, φ_ε and $\nabla\varphi_\varepsilon$ two-scale converge to φ_0 and $\nabla_{\mathbf{x}}\varphi_0 + \nabla_{\mathbf{y}}\varphi_1$, respectively.

3. Let $\{\varphi_\varepsilon\}$ and $\{\varepsilon\nabla\varphi_\varepsilon\}$ be a bounded sequence in $L^2((0, T) \times \Omega)$. Then there exists a function φ_0 in $L^2((0, T) \times \Omega; H_{\text{per}}^1(Y))$ such that, up to a subsequence, φ_ε and $\varepsilon\nabla\varphi_\varepsilon$ two-scale converge to φ_0 and $\nabla_{\mathbf{y}}\varphi_0$, respectively.

4. Let $\{\varphi_\varepsilon\}$ be a bounded sequence in $L^2((0, T) \times \Gamma_\varepsilon)$. Then there exists a function φ_0 in $L^2((0, T) \times \Omega \times \Gamma)$ such that, up to a subsequence, φ_ε two-scale converges to φ_0 .

Proof. For a proof of the time independent case, we refer, e. g., to [3], [98] and [100]. The proof transfers directly to the time dependent case since t plays only the role of a parameter. \square

In order to derive the desired macroscopic and homogenized problem description $P_0 : \bar{\mathcal{L}}\bar{\varphi}_0 = \bar{f}_0$, first of all appropriate ε -independent *a priori* estimates for problem $P_\varepsilon : \mathcal{L}_\varepsilon\varphi_\varepsilon = f_\varepsilon$ have to be proven. Using then oscillating test functions in the weak formulation of problem $P_\varepsilon : \mathcal{L}_\varepsilon\varphi_\varepsilon = f_\varepsilon$ and passing to the two-scale limit $\varepsilon \rightarrow 0$ by means of Theorem 3.4 and Definition 3.3 automatically provides the weak formulation of the two-scale homogenized problem. The correct homogenized limit problem $P_0 : \bar{\mathcal{L}}\bar{\varphi}_0 = \bar{f}_0$ is obtained as in the method of formal two-scale asymptotic expansion by defining auxiliary cell problems as well as effective coefficients, compare also the corresponding paragraph in Section 3.1.3.

3.1.4 Extension into Ω

One difficulty in applying the method of two-scale convergence is that a priori estimates are usually derived within the perforated domain Ω_ε , cf. Figure 3.4 and Figure 3.6. An extension of the estimates and to this end also of functions into Ω is necessary, such that the compactness Theorem 3.4 can be applied and limits can be identified in function spaces on Ω . Such extensions are quite standard and have been applied and discussed, e.g. in [1, 3, 25, 26, 57, 58]. Thereby, the following two types of extensions are mainly used:

1. Trivial extension by zero

Definition 3.5. Let φ_ε be any function in $H^1(\Omega_\varepsilon)$. We define its extension by zero into $\Omega \setminus \Omega_\varepsilon$ in the following way:

$$E_0(\varphi_\varepsilon) := \begin{cases} \varphi_\varepsilon & \text{in } \Omega_\varepsilon, \\ 0 & \text{in } \Omega \setminus \Omega_\varepsilon. \end{cases}$$

With this definition, the following theorem holds:

Theorem 3.6. For a function $\varphi_\varepsilon \in X(\Omega_\varepsilon)$, $X = L^2$ or $X = H_0^1$, defined on the perforated domain Ω_ε and norm $\|\cdot\|_X$ given, it holds for its trivial extension $E_0(\varphi_\varepsilon)$

$$\|E_0(\varphi_\varepsilon)\|_{X(\Omega)} = \|\varphi_\varepsilon\|_{X(\Omega_\varepsilon)}.$$

2. More crucial extensions

Theorem 3.7. Let $V_0^1(\Omega_\varepsilon) := \{\varphi \in H^1(\Omega_\varepsilon) : \varphi = 0 \text{ on } \partial\Omega\}$. There exists a linear extension operator $E \in \mathcal{L}(V_0^1(\Omega_\varepsilon), H_0^1(\Omega))$, such that

$$\|E(\varphi_\varepsilon)\|_{H^1(\Omega)}^2 := \|E(\varphi_\varepsilon)\|_{L^2(\Omega)}^2 + \|\nabla E(\varphi_\varepsilon)\|_{L^2(\Omega)}^2 \leq C \|\varphi_\varepsilon\|_{H^1(\Omega_\varepsilon)}^2.$$

Proof. For the construction of the extension and the proof of Theorem 3.7, we refer the reader to [25, 26, 57]. \square

Remark 3.8. The extension by zero of a $H^1(\Omega_\varepsilon)$ function is in general in $L^2(\Omega)$. Only in the case that zero boundary data is prescribed on the complete boundary $\partial\Omega_\varepsilon = \Gamma_\varepsilon \cup \partial\Omega$ it also belongs to $H^1(\Omega)$. Guaranteeing this regularity in general is the main advantage of the second approach.

We define the characteristic function χ_ε of the porous medium via

$$\chi_\varepsilon(\mathbf{x}) = \chi\left(\frac{\mathbf{x}}{\varepsilon}\right) := \chi_{\Omega_\varepsilon}(\mathbf{x}) := \begin{cases} 1 & \mathbf{x} \in \Omega_\varepsilon, \\ 0 & \mathbf{x} \in \Omega \setminus \Omega_\varepsilon. \end{cases}$$

and let

$$\chi(\mathbf{y}) := \chi_{Y_l}(\mathbf{y}) := \begin{cases} 1 & \mathbf{y} \in Y_l, \\ 0 & \mathbf{y} \in Y_s, \end{cases} \quad (3.4)$$

be the characteristic function of the liquid part in the unit cell Y . The convergence properties of the characteristic function and its product with a strongly converging sequence are stated in the following theorem.

Theorem 3.9. *If the sequence $\{\varphi_\varepsilon\}$ converges strongly to φ_0 in $L^2((0, T) \times \Omega)$, then the sequence of the product with the corresponding characteristic function $\{\chi_\varepsilon \varphi_\varepsilon\}$ converges two-scale to $\chi(\mathbf{y})\varphi_0(t, \mathbf{x})$.*

Proof. Since $\chi_\varepsilon \varphi_\varepsilon$ is equal to zero in $\Omega \setminus \Omega_\varepsilon$, the two-scale limit has the structure $\chi(\mathbf{y})\varphi_0(t, \mathbf{x}, \mathbf{y})$. The strong convergence of φ_ε yields the \mathbf{y} -independency of φ_0 . \square

Remark 3.10. *The method of two-scale convergence will be applied in Chapter 4 to model problem P .*

3.2 Overview existing literature

Using mathematical homogenization theory, different kinds of coupled models have been investigated and derived. In addition to the combination of fluid flow and convective-diffusive transport, the coupling among different kinds of species by chemical reactions have been discussed for example in [58], see also the references cited therein. Further cross couplings of the water flow by heat, chemical or electrical transport are studied formally in [8]. It is worth to mention that a nonlinear coupling quite analogous to the one of our problem occurs in a totally different context – the phase-field models of Allen-Cahn type. For more details on the modeling, analysis, and averaging of such models, see [36, 37, 38]. Investigations concerning variable scaling and their influence on the limit equations is illustrated (by means of formal two-scale asymptotic homogenization) in [7], where different choices of ranges of the Péclet

number are considered. In the same spirit, but this time rigorously, different scale ranges are examined for a linear diffusion-reaction system with interfacial exchange in [106].

Electric effects and therefore the Stokes-Nernst-Planck-Poisson system and its deviations are still topic of recent research papers due to their variable applications, cf. Section 2: Formal upscaling attempts are reported, for instance, in [9, 8, 78, 95, 94, 96]. It is worth pointing out that [95, 94, 96] succeeded to compute (again formally) microstructure effects on the deforming, swelling clay. Moreover, hybrid mixture theory has been applied to swelling porous media with charged particles in [128] and [129]. In the field of lithium batteries upscaling has been applied in [27, 72]; an application of volume averaging and formal two-scale asymptotic expansion to ion transport in cementitious materials can be found in [122] and [18], respectively. As, in general, the interest is increasing in biological applications, the SNPP system and its deviations attract attention, e.g., in the context of ion transport through membrane channels. With focus on rigorous homogenization of this problem some effort has been undertaken in [97].

In spite of such an extraordinary interest and good formal asymptotic understanding of the situation, rigorous homogenization results seem to be quite rare. Only recently, Markus Schmuck published a paper concerning the rigorous upscaling of a non-scaled Stokes-Nernst-Planck-Poisson system, [127]. Furthermore, Allaire et al. studied the stationary and linearized case (cf. Section 2.1.1, item 6) in [4].

In Chapter 4 and Chapter 5 of this thesis, we present results on the upscaling of the SNPP system that go beyond the investigations known from literature: In Chapter 4, we rigorously investigate the limit $\varepsilon \rightarrow 0$ of the non-stationary SNPP system using the method of two-scale convergence (cf. Section 3.1.3). The main contribution lies in the investigation of the structure of the limit problems for different choices of scalings in the scale parameter ε . Furthermore, we discuss the influence that different choices of the boundary condition, which are present for colloidal systems in the engineering literature, exert on the limit systems. In Chapter 5, we consider an extension of the Stokes-Nernst-Planck system to an evolving microstructure using a level set formulation. The benefit of this modeling approach is that it provides an explicit description of the evolving solid-liquid interface. In order to derive again an effective model description, two-scale asymptotic expansion in a level set framework is applied.

Chapter 4

Homogenization of Problem P

This chapter deals with the periodic homogenization of the non-stationary Stokes-Nernst-Planck-Poisson system (2.14). First of all, the SNPP system is incorporated in a multi-scale framework, i.e. a family of model Problems P_ε is defined on the heterogeneous domain Ω_ε , cf. Section 3.1.3 and Figure 3.6. To this end, the (small) scale parameter ε is introduced, which describes not only the geometry, but also scales and balances the different terms in the governing system of partial differential equations. In particular, we focus on the scaling of those terms, that have electrostatic origin and study the balance between electrostatic drift and further well understood transport mechanisms such as diffusion and convection. Since the SNPP system is of interest in various kinds of applications, we cover different choices of scalings using the set of parameter $(\alpha_1, \alpha_2, \alpha_3, \beta, \gamma)$.

The objective of this chapter is to rigorously investigate the limit $\varepsilon \rightarrow 0$ of the family of Problems P_ε using the method of two-scale convergence, cf. Section 3.1.3. The focus thereby lies on the coupling between the colloidal transport, the fluid flow and the electrostatic potential. The crucial and demanding challenge is that we have to ensure, that the passage to the limit $\varepsilon \rightarrow 0$ in the nonlinear terms $c_\varepsilon^\pm \nabla \phi_\varepsilon$ and $c_\varepsilon^\pm \mathbf{v}_\varepsilon$ is possible. This is achieved by proving appropriate ε -independent a priori estimates for the velocity \mathbf{v}_ε , the pressure p_ε , the number densities c_ε^\pm and the electrostatic potential ϕ_ε . Here, the essential step is to show L^∞ -estimates for the number densities c_ε^\pm which guarantee a strong convergence property.

Finally, we show that the Darcy-Nernst-Planck-Poisson (DNPP) system (2.20) and its modifications are obtained as upscaling result. Effective coefficients such as permeability tensor, diffusion tensor and porosity are defined in terms of solutions of auxiliary

cell problems. In this sense, information of the underlying geometrical structure enters the effective model description. In our investigations, we highlight the influence of the scaling in ε on both the a priori estimates and the structure of the limit problems. Furthermore, we discuss the influence of the choice of different kinds of boundary conditions for the transport equations such as “perfect sink” and “no penetration” and boundary conditions of type Neumann and Dirichlet, respectively, for the electrostatic potential.

In addition to the advantage of a rigorous derivation of effective models, one benefit of our investigations is that effective models are derived, which go beyond those relying on linear relations, cf. Section 2.2.3. All the non-linearities are maintained and the fully coupled structure of the SNPP system is preserved unless specific terms cancel out due to their weak emphasis (scaling) in the model Problem P_ε . Moreover, our approach provides the possibility to directly compare effective models that result from a different scaling of the terms in the pore-scale model. This gives deeper insight in the understanding of physical processes and the interplay of phenomena including electric interaction on different spatial scales.

The chapter is organized as follows: In Section 4.1, the Stokes-Nernst-Planck-Poisson system, which is the starting point of our investigations, is incorporated in a multi-scale framework. The problem with boundary conditions of type Neumann and Dirichlet, resp., for the electrostatic potential are studied separately, but with the same strategy. Basic, ε -independent a priori estimates are shown in Theorem 4.10 and Theorem 4.33. In Section 4.2.2 and Section 4.3.2, the “equivalent” effective equations are obtained investigating rigorously the limit $\varepsilon \rightarrow 0$ applying the method of two-scale convergence. The main results of the upscaling procedure are presented in Theorem 4.16, Theorem 4.19, Theorem 4.22 and Theorem 4.35, Theorem 4.38, Theorem 4.41, respectively. The limit equations are discussed with emphasis on their structure in Remark 4.18, Remark 4.21, Remark 4.25 and Remark 4.37, Remark 4.40, Remark 4.43, respectively and also in Section 4.2.3 and Section 4.3.3. Finally, Chapter 4 is concluded in Section 4.4 by some discussions – also on numerical simulations, that underline the achieved theoretical results.

4.1 Pore-scale model P_ε

In this section, Problem P , (2.14), is included in a multi-scale framework and investigated analytically. The definition of the idealized underlying geometry which char-

acterizes the highly heterogeneous porous medium is depicted in Figure 3.6. The (small) scale parameter ε and the parameter set $(\alpha_1, \alpha_2, \alpha_3, \beta, \gamma)$ are introduced to scale/balance the different terms in the governing system of partial differential equations. These scalings are chosen in such a way that reasonable mathematical limits are obtained. Moreover, they can, e.g., be motivated by the choice of the values of the characteristic numbers in the dimensionless form of Problem P , see Section 2.1.3. However, since the SNPP system is used to describe various kinds of applications, different choices of scaling are relevant depending on the underlying physical problem. For ease of presentation, we do not take into account all the all physical parameters explicitly in the following. Then, the resulting multi-scale problem, i.e. the following system of scaled partial differential equations, is denoted by *Problem P_ε* and reads:

Scaled Stokes equations

$$-\varepsilon^2 \Delta \mathbf{v}_\varepsilon + \nabla p_\varepsilon = -\varepsilon^{\alpha_1} (c_\varepsilon^+ - c_\varepsilon^-) \nabla \phi_\varepsilon \quad \text{in } (0, T) \times \Omega_\varepsilon, \quad (4.1a)$$

$$\nabla \cdot \mathbf{v}_\varepsilon = 0 \quad \text{in } (0, T) \times \Omega_\varepsilon, \quad (4.1b)$$

$$\mathbf{v}_\varepsilon = 0 \quad \text{on } (0, T) \times (\Gamma_\varepsilon \cup \partial\Omega), \quad (4.1c)$$

Scaled Nernst-Planck equations

$$\partial_t c_\varepsilon^\pm + \nabla \cdot (\varepsilon^\beta \mathbf{v}_\varepsilon c_\varepsilon^\pm - \varepsilon^\gamma \nabla c_\varepsilon^\pm \mp \varepsilon^{\alpha_2} c_\varepsilon^\pm \nabla \phi_\varepsilon) = R_\varepsilon^\pm(\mathbf{c}_\varepsilon) \quad \text{in } (0, T) \times \Omega_\varepsilon, \quad (4.1d)$$

$$(-\varepsilon^\beta \mathbf{v}_\varepsilon c_\varepsilon^\pm + \varepsilon^\gamma \nabla c_\varepsilon^\pm \pm \varepsilon^{\alpha_2} c_\varepsilon^\pm \nabla \phi_\varepsilon) \cdot \boldsymbol{\nu} = 0 \quad \text{on } (0, T) \times \Gamma_\varepsilon \cup \partial\Omega_F, \quad (4.1e)$$

$$c_\varepsilon^\pm = 0 \quad \text{on } (0, T) \times \partial\Omega_D, \quad (4.1f)$$

$$c_\varepsilon^\pm = c^{\pm,0} \quad \text{in } \{t = 0\} \times \Omega_\varepsilon, \quad (4.1g)$$

Scaled Poisson's equation

$$-\varepsilon^{\alpha_3} \Delta \phi_\varepsilon = c_\varepsilon^+ - c_\varepsilon^- \quad \text{in } (0, T) \times \Omega_\varepsilon, \quad (4.1h)$$

$$\varepsilon^{\alpha_3} \nabla \phi_\varepsilon \cdot \boldsymbol{\nu} = \varepsilon \sigma \quad \text{on } (0, T) \times \Gamma_{\varepsilon, N}, \quad (4.1i)$$

$$\phi_\varepsilon = \phi_D \quad \text{on } (0, T) \times \Gamma_{\varepsilon, D} \cup \partial\Omega_D, \quad (4.1j)$$

$$\varepsilon^{\alpha_3} \nabla \phi_\varepsilon \cdot \boldsymbol{\nu} = 0 \quad \text{on } (0, T) \times \partial\Omega_N. \quad (4.1k)$$

As a remark note, that depending on the application either of the boundary conditions (4.1i) and (4.1j) is applied on Γ_ε ¹. In particular, a partition of Γ_ε into Dirichlet *and*

¹The indexes N, D are used to specify the type of boundary conditions on $\partial\Omega$ and Γ_ε , respectively. Here, in order to avoid further technicalities, an independent partition of $\partial\Omega$ into $\partial\Omega_D$ and $\partial\Omega_N, \partial\Omega_F$ for the individual subproblems is not considered

Neumann type is not considered here. If the boundary condition (4.1i) is considered, we call it the *Neumann case*, whereas the choice of (4.1j) is denoted as *Dirichlet case*. Both of the cases are meaningful in geoscientific applications, see [41] and Remark 2.5. We refer to Remark 2.5 and Remark 2.14 for an extended discussion on further boundary conditions. In the field of homogenization, different non-homogeneous boundary conditions also in the context of electrostatic interaction are discussed, e.g. in [4, 21, 57, 127].

Remark 4.1. *The characteristic dimensionless numbers which have been introduced in Section 2.1.3, can be related to the choice of scaling in (4.1) via*

$$\begin{aligned} Re := O(\varepsilon^{-2}), \quad St := O(\varepsilon^{-\beta}), \quad StPe := O(\varepsilon^{-\gamma}), \quad \frac{\varphi kTC\tau^2}{\rho L^2} := O(\varepsilon^{\alpha_1}), \\ \frac{StPe}{\varphi} := O(\varepsilon^{-\alpha_2}), \quad \text{and} \quad \frac{1}{2\varphi}(\kappa L)^2 := O(\varepsilon^{-\alpha_3}). \end{aligned}$$

Remark 4.2. *We could also add an additional scaling factor for the reactive terms in (4.1d). However, we concentrate here on the role of the electrostatic potential ϕ_ε and the interplay of electric drift with the transport processes of convection and diffusion. The same choice of scaling in the equations for c_ε^+ and c_ε^- is especially justified in the case that both types of particles have similar properties except of the sign of the charge. The parameter set $(\alpha_1, \alpha_2, \alpha_3, \beta, \gamma)$ can be chosen arbitrarily in the beginning. However, in order to pass rigorously to the limit $\varepsilon \rightarrow 0$ their ranges have to be restricted at a later stage of our investigations. Recently, in [4], Allaire et al. study a stationary and linearized SNPP system with periodic boundary condition on the exterior boundary which corresponds to the parameter set $(\alpha_1 = 0, \alpha_2 = 0, \alpha_3 = 2, \beta = 0, \gamma = 0)$. In [127], Schmuck considers the case $(\alpha_1 = 0, \alpha_2 = 0, \alpha_3 = 0, \beta = 0, \gamma = 0)$ using transmission conditions for the electrostatic potential on an uncharged interface Γ_ε and a combination of no-flux and Dirichlet boundary conditions on the exterior boundary. Considering the non-stationary, fully coupled nonlinear system of partial differential equations with inhomogeneous boundary conditions and also as large as possible ranges of parameters, we extend the investigations known from the literature.*

On the outer boundary $\partial\Omega$, we assume a combination of homogeneous flux and Dirichlet boundary conditions for the number densities c_ε^\pm as well as a no-slip boundary condition for the velocity field \mathbf{v}_ε on both the outer boundary $\partial\Omega$ and the inner boundary Γ_ε since, in our investigations, we focus on the role of the electrostatic potential ϕ_ε on the dynamics of colloidal particles. However, periodic and inhomogeneous flux and Dirichlet boundary conditions could be treated analogously, cf. [4, 58, 57, 127].

For a discussion on different boundary conditions for the number densities on the inner boundary and their influence on the results of the homogenization procedure we refer to Section 4.4.

Remark 4.3. We could also introduce the parameter set $(\tilde{\alpha}_1, \tilde{\alpha}_2, 1, \beta, \gamma) = (\alpha_1 - \alpha_3, \alpha_2 - \alpha_3, 1, \beta, \gamma) \in \mathbb{R}^5$ for the Neumann and $(\tilde{\alpha}_1, \tilde{\alpha}_2, 1, \beta, \gamma) = (\alpha_1 - \alpha_3 + 1, \alpha_2 - \alpha_3 + 1, 1, \beta, \gamma) \in \mathbb{R}^5$ for the Dirichlet case, compare the a priori estimates in Theorem 4.10 and Theorem 4.33. This would reduce the number of parameter from five to four in each case. However, both cases can be handled simultaneously when choosing $(\alpha_1, \alpha_2, \alpha_3, \beta, \gamma) \in \mathbb{R}^5$ and therefore allows for a more compact presentation of the forthcoming technical calculations.

4.1.1 Definition and existence of weak solutions of Problem P_ε

In this Section, we define weak solutions of Problem P_ε and summarize analytical investigations concerning the unique existence of weak solutions of model Problem P_ε .

Assumptions on the data

To be able to state a result on the existence and uniqueness of weak solutions of Problem P_ε , we assume the following additional restrictions in analogy to Assumption 2.9. We refer to Remark 2.10 for a discussion how these restrictions can be released.

Assumption 4.4. 1. *On the geometry:* We assume a perforated domain $\Omega_\varepsilon \subset \Omega \subset \mathbb{R}^n$, $n \in \{1, 2, 3\}$ according to Section 3.1.3 with $\partial\Omega_D \neq \emptyset$.

2. *On the coefficients:* We assume that all the physical parameters $\mu, \epsilon_0, \epsilon_r, k, T, D$ are strictly positive. For ease of presentation, we suppress them in the following investigations.

3. *On the (initial) data:* We assume σ, ϕ_D to be constant and the initial data $c^{\pm,0}$ to be non-negative and bounded in L^∞ independently of ε , i.e. there exists $\Lambda > 0$, such that

$$0 \leq c^{\pm,0}(x) \leq \Lambda, \quad \text{for a.e. } x \in \Omega.$$

In the case of $\partial\Omega_D = \emptyset$, $\Gamma_D = \emptyset$, we assume the following compatibility condition

for the initial data:

$$\int_{\Omega_\varepsilon} c^{+,0} - c^{-,0} \, d\mathbf{x} = \int_{\Gamma_\varepsilon} \sigma \, ds_{\mathbf{x}}.$$

If $\sigma = 0$, this implies global electro neutrality for the initial number densities.

4. On the reaction rates: The reaction rates are assumed to have the following structure: $R_\varepsilon^\pm(\mathbf{c}_\varepsilon) = \mp(c_\varepsilon^+ - c_\varepsilon^-)$. Especially, they are linear and mass conservative.

In addition to the standard Lebesgue spaces $L^p(\Omega_\varepsilon)$, $1 \leq p \leq \infty$ and the standard Sobolev spaces $W^{p,q}(\Omega_\varepsilon)$, $1 \leq p, q \leq \infty$, [44], we introduce the following function space, [26],

$$V_0^1(\Omega_\varepsilon) = \{\varphi \in H^1(\Omega_\varepsilon) : \varphi = 0 \text{ on } \partial\Omega_D\}.$$

We denote by $V^{-1}(\Omega_\varepsilon)$ its dual, i.e. $V^{-1} := (V_0^1)'$.

In analogy to Definition 2.12, we define weak solutions of Problem P_ε : We multiply (4.1) with appropriate test function to obtain

$$\int_{\Omega_\varepsilon} \varepsilon^2 \nabla \mathbf{v}_\varepsilon : \nabla \boldsymbol{\psi} - p_\varepsilon \nabla \cdot \boldsymbol{\psi} \, d\mathbf{x} = - \int_{\Omega_\varepsilon} \varepsilon^{\alpha_1} (c_\varepsilon^+ - c_\varepsilon^-) \nabla \phi_\varepsilon \cdot \boldsymbol{\psi} \, d\mathbf{x}, \quad \boldsymbol{\psi} \in (H_0^1(\Omega_\varepsilon))^n, \quad (4.2a)$$

$$\int_{\Omega_\varepsilon} (\nabla \cdot \mathbf{v}_\varepsilon) \psi \, d\mathbf{x} = 0, \quad \psi \in L^2(\Omega_\varepsilon), \quad (4.2b)$$

$$\begin{aligned} \langle \partial_t c_\varepsilon^\pm, \psi \rangle_{V^{-1}, V_0^1} + \int_{\Omega_\varepsilon} (-\varepsilon^\beta \mathbf{v}_\varepsilon c_\varepsilon^\pm + \varepsilon^\gamma \nabla c_\varepsilon^\pm \pm \varepsilon^{\alpha_2} c_\varepsilon^\pm \nabla \phi_\varepsilon) \cdot \nabla \psi \, d\mathbf{x} \\ = \int_{\Omega_\varepsilon} R_\varepsilon^\pm(\mathbf{c}_\varepsilon) \psi \, d\mathbf{x}, \quad \psi \in V_0^1(\Omega_\varepsilon), \end{aligned} \quad (4.2c)$$

$$- \int_{\Omega_\varepsilon} \varepsilon^{\alpha_3} \Delta \phi_\varepsilon \psi \, d\mathbf{x} = \int_{\Omega_\varepsilon} (c_\varepsilon^+ - c_\varepsilon^-) \psi \, d\mathbf{x}, \quad \psi \in L^2(\Omega_\varepsilon). \quad (4.2d)$$

Definition 4.5.² We call $(\mathbf{v}_\varepsilon, p_\varepsilon, c_\varepsilon^\pm, \phi_\varepsilon)$ a weak solution of Problem P_ε if $\mathbf{v}_\varepsilon \in L^\infty(0, T; (H_0^1(\Omega_\varepsilon))^n)$, $p_\varepsilon \in L^\infty(0, T; L^2(\Omega_\varepsilon)/\mathbb{R})$, $c_\varepsilon^\pm \in L^\infty(0, T; L^2(\Omega_\varepsilon)) \cap L^2(0, T; V_0^1(\Omega_\varepsilon))$ with $\partial_t c_\varepsilon^\pm \in L^2(0, T; V^{-1}(\Omega_\varepsilon))$, $\phi_\varepsilon \in L^\infty(0, T; H_{(0)}^2(\Omega_\varepsilon/\mathbb{R}))$, and equations (4.2) are satisfied.

With the assumptions stated in Assumption 4.4, Theorem 2.15 directly ensures the validity of the following theorem:

²Compare the definition and footnote in Definition 2.12.

Theorem 4.6. *Let Assumption 4.4 be valid. Then, for each $\varepsilon > 0$ there exists a unique global weak solution of Problem P_ε in the sense of Definition 4.5. Furthermore, the number densities are non-negative and bounded in $L^\infty((0, T) \times \Omega_\varepsilon)$.*

A priori estimates that are ε -independent are essential requirements for the application of Theorem 3.4 and Definition 3.3 and therefore for the homogenization of Problem P_ε by the method of two-scale convergence. That the a priori estimates in Theorem 2.19 can be carried over directly to Problem P_ε with a constant C independent of ε is anything but granted. Since these uniform estimates are the basis for all considerations that follow, we present their derivation to some extent with focus on the ε dependencies. A crucial point is to have uniform estimate of the number densities in $L^\infty((0, T) \times \Omega_\varepsilon)$. Having this estimate at hand, all a priori estimates and their ε dependencies are derived by standard calculations.

In comparison to the literature, the estimates provided here are advantageous since we require no additional restriction such as electro-neutrality or volume-additivity, cf. Remark 2.11 in the case of homogeneous Neumann boundary conditions, see also [126]. Furthermore, we discuss L^∞ -estimates in the case of inhomogeneous Neumann or Dirichlet boundary data for the electrostatic potential.

In the following two subsections, we consider the case of Neumann and Dirichlet boundary condition for the electrostatic potential separately.

4.2 Neumann case

In this Section, we consider the upscaling of Problem P_ε in the case of Neumann boundary data for the electrostatic potential on Γ_ε , cf. (4.1i) and homogeneous Dirichlet boundary data on the outer boundary $\partial\Omega$, cf. (4.1j). This choice corresponds to a physical problem in which the surface charge density of the porous medium is prescribed. First of all, we prove ε -independent *a priori* estimates. Thereafter, an extension of the problem and of the variables to the whole domain Ω is defined and its upscaling is performed applying the method of two-scale convergence, see Section 3.1.3.

4.2.1 ε -independent a priori estimates in the Neumann case

Subsequently, we derive ε -independent a priori estimates. We state in advance the (scaled) Poincaré inequalities for function $\varphi_\varepsilon \in V_0^1(\Omega_\varepsilon)$ and $\varphi_\varepsilon \in H_0^1(\Omega_\varepsilon)$, respectively:

$$\|\varphi_\varepsilon\|_{L^2(\Omega_\varepsilon)} \leq C_P \|\nabla \varphi_\varepsilon\|_{L^2(\Omega_\varepsilon)}, \quad \varphi_\varepsilon \in V_0^1(\Omega_\varepsilon) \quad (4.3)$$

and

$$\|\varphi_\varepsilon\|_{L^2(\Omega_\varepsilon)} \leq C_P^0 \varepsilon \|\nabla \varphi_\varepsilon\|_{L^2(\Omega_\varepsilon)}, \quad \varphi_\varepsilon \in H_0^1(\Omega_\varepsilon), \quad (4.4)$$

respectively. For a proof of these inequalities, we refer, e.g., to [26, 58].

Moreover, the following inequality is often used to estimate the boundary integral of a function $\varphi_\varepsilon \in H^1(\Omega_\varepsilon)$, see, e.g., [57]:

$$\varepsilon \|\varphi_\varepsilon\|_{L^2(\Gamma_\varepsilon)}^2 \leq C \left(\|\varphi_\varepsilon\|_{L^2(\Omega_\varepsilon)}^2 + \varepsilon^2 \|\nabla \varphi_\varepsilon\|_{L^2(\Omega_\varepsilon)}^2 \right) \quad (4.5)$$

with some constant $C \in \mathbb{R}_+$ independent of ε .

As a first, auxiliary step, non-negativity and boundedness of the number densities c_ε^\pm in $L^\infty((0, T) \times \Omega_\varepsilon)$ are proven, which are uniform in the scale parameter ε .

Theorem 4.7. *Let $(\mathbf{v}_\varepsilon, p_\varepsilon, c_\varepsilon^\pm, \phi_\varepsilon)$ be a weak solution of Problem P_ε in the Neumann case according to Definition 4.5. Let furthermore Assumption 4.4 hold. If $\sigma \neq 0$, we additionally assume $\alpha_2 - \alpha_3 \geq 0$ and $\alpha_2 - \alpha_3 - \gamma + 2 \geq 0$. Then the number densities are non-negative uniformly in ε , i.e.*

$$c_\varepsilon^\pm(t, \mathbf{x}) \geq 0 \quad \text{for a.e. } t \in (0, T), \quad \mathbf{x} \in \Omega_\varepsilon.$$

Proof. In analogy to the proof of Theorem 2.23, we test the Nernst-Planck equations (4.2c) with $(c_\varepsilon^\pm)_- := \min(0, c_\varepsilon^\pm)$. This yields after summation over \pm

$$\begin{aligned} & \sum_{\pm} \frac{1}{2} \frac{d}{dt} \|(c_\varepsilon^\pm)_-\|_{L^2(\Omega_\varepsilon)}^2 - \sum_{\pm} \int_{\Omega_\varepsilon} \frac{1}{2} \varepsilon^\beta \mathbf{v}_\varepsilon \cdot \nabla (c_\varepsilon^\pm)_-^2 \, d\mathbf{x} + \sum_{\pm} \varepsilon^\gamma \|\nabla (c_\varepsilon^\pm)_-\|_{L^2(\Omega_\varepsilon)}^2 \\ &= - \sum_{\pm} \int_{\Omega_\varepsilon} \pm \frac{1}{2} \varepsilon^{\alpha_2} \nabla \phi_\varepsilon \cdot \nabla (c_\varepsilon^\pm)_-^2 \, d\mathbf{x} + \sum_{\pm} \mp \int_{\Omega} (c_\varepsilon^+ - c_\varepsilon^-) (c_\varepsilon^\pm)_- \, d\mathbf{x} \\ &\iff: I - II + III = -IV + V. \end{aligned}$$

The convective integral II cancels by standard calculations due to the incompressibility (4.2b) and the no-slip boundary condition. Moreover, integral V is non-positive due to the monotonicity of $(\cdot)_-$, i.e. $V \leq 0$ holds.

The drift term, integral IV , is rewritten using integration by parts and Poisson's equation (4.2d):

$$\begin{aligned}
& - \int_{\Omega_\varepsilon} \frac{1}{2} \varepsilon^{\alpha_2} \nabla \phi_\varepsilon \cdot \nabla \left((c_\varepsilon^+)_-^2 - (c_\varepsilon^-)_-^2 \right) d\mathbf{x} \\
& = \int_{\Gamma_\varepsilon} \frac{1}{2} \varepsilon^{\alpha_2 - \alpha_3} \varepsilon \sigma \left(|(c_\varepsilon^-)_-|^2 - |(c_\varepsilon^+)_-|^2 \right) ds_{\mathbf{x}} \\
& \quad - \int_{\Omega_\varepsilon} \frac{1}{2} \varepsilon^{\alpha_2 - \alpha_3} (c_\varepsilon^+ - c_\varepsilon^-) \left(|(c_\varepsilon^+)_-|^2 - |(c_\varepsilon^-)_-|^2 \right) d\mathbf{x} \\
& =: IV_a + IV_b.
\end{aligned}$$

Integral IV_b is non-positive due to the monotonicity and properties of $(\cdot)_-$ and 2 and integral IV_a is estimated as follows:

$$\begin{aligned}
IV_a & = \int_{\Gamma_\varepsilon} \frac{1}{2} \varepsilon^{\alpha_2 - \alpha_3} \varepsilon \sigma \left(|(c_\varepsilon^-)_-|^2 - |(c_\varepsilon^+)_-|^2 \right) ds_{\mathbf{x}} \\
& \leq \frac{1}{2} \varepsilon^{\alpha_2 - \alpha_3} \|\sigma\|_{L^\infty(\Gamma_\varepsilon)} \sum_{\pm} \varepsilon \|(c_\varepsilon^\pm)_-\|_{L^2(\Gamma_\varepsilon)}^2 \\
& \leq \frac{1}{2} \varepsilon^{\alpha_2 - \alpha_3} \|\sigma\|_{L^\infty(\Gamma_\varepsilon)} C \sum_{\pm} \left(\|(c_\varepsilon^\pm)_-\|_{L^2(\Omega_\varepsilon)}^2 + \varepsilon^2 \|\nabla(c_\varepsilon^\pm)_-\|_{L^2(\Omega_\varepsilon)}^2 \right).
\end{aligned}$$

For the inequality in the last step we used relation (4.5). Combing all the above considerations and adsorption of the gradient term, finally leads to

$$\begin{aligned}
\frac{1}{2} \frac{d}{dt} \sum_{\pm} \|(c_\varepsilon^\pm)_-\|_{L^2(\Omega_\varepsilon)}^2 + \left(\varepsilon^\gamma - \frac{1}{2} \varepsilon^{\alpha_2 - \alpha_3 + 2} \|\sigma\|_{L^\infty(\Gamma_\varepsilon)} C \right) \sum_{\pm} \|\nabla c_\varepsilon^\pm\|_{L^2(\Omega_\varepsilon)}^2 \\
\leq \frac{1}{2} \varepsilon^{\alpha_2 - \alpha_3} \|\sigma\|_{L^\infty(\Gamma_\varepsilon)} C \sum_{\pm} \|(c_\varepsilon^\pm)_-\|_{L^2(\Omega_\varepsilon)}^2.
\end{aligned}$$

In the case of $\alpha_2 - \alpha_3 \geq 0$ and $\varepsilon^\gamma - \frac{1}{2} \varepsilon^{\alpha_2 - \alpha_3 + 2} \|\sigma\|_{L^\infty(\Gamma_\varepsilon)} C \geq \frac{1}{2} \varepsilon^\gamma$, i.e. $\alpha_2 - \alpha_3 - \gamma + 2 \geq 0$ and $\varepsilon \leq \varepsilon_0 := \left(\frac{1}{\|\sigma\|_{L^\infty(\Gamma_\varepsilon)} C} \right)^{\frac{1}{\alpha_2 - \alpha_3 - \gamma + 2}}$, Gronwall's lemma, [44], implies the statement of Theorem 4.7 since the initial number densities are non-negative according to Assumption 4.4 and all terms remain well defined as $\varepsilon \rightarrow 0$. \square

Remark 4.8. *In the case of $\sigma = 0$, the additional constraints on the parameters in Theorem 4.7 are unnecessary. See also the discussions in Remark 4.28, Remark 4.31 for modifications of the model problem in order to avoid constraints on the parameter set.*

Theorem 4.9. *Let $(\mathbf{v}_\varepsilon, p_\varepsilon, c_\varepsilon^\pm, \phi_\varepsilon)$ be a weak solution of Problem P_ε in the Neumann case according to Definition 4.5. Let furthermore Assumption 4.4 and $\gamma \leq 0$ hold. If $\sigma \neq 0$, we additionally assume $\alpha_2 - \alpha_3 \geq 0$ and $\alpha_2 - \alpha_3 - \gamma + 2 \geq 0$ hold. Then, the number densities are bounded from above uniformly in ε .*

Proof. In the case of homogeneous Neumann boundary conditions for the electrostatic potential, the boundedness of the number densities c_ε^\pm has been proven rather formally in [126] by Moser's iteration technique, see also Section 2.2.6. Opposed to this quite technical approach, a straight forward way to prove the statement of Theorem 4.9 in the case of homogeneous Neumann boundary conditions, i.e. if $\sigma = 0$, is to show that a maximum principle holds true:

For this reason, we choose $(c_\varepsilon^\pm - \Lambda)_+ := \max(0, c_\varepsilon^\pm - \Lambda)$ as test function in (4.2c) and obtain after summation over \pm

$$\begin{aligned} & \sum_{\pm} \frac{1}{2} \frac{d}{dt} \|(c_\varepsilon^\pm - \Lambda)_+\|_{L^2(\Omega_\varepsilon)}^2 - \sum_{\pm} \int_{\Omega_\varepsilon} \varepsilon^\beta \mathbf{v}_\varepsilon c_\varepsilon^\pm \cdot \nabla (c_\varepsilon^\pm - \Lambda)_+ \, d\mathbf{x} \\ & \qquad \qquad \qquad + \sum_{\pm} \varepsilon^\gamma \|\nabla (c_\varepsilon^\pm - \Lambda)_+\|_{L^2(\Omega_\varepsilon)}^2 \\ & = - \sum_{\pm} \pm \int_{\Omega_\varepsilon} \varepsilon^{\alpha_2} c_\varepsilon^\pm \nabla \phi_\varepsilon \cdot \nabla (c_\varepsilon^\pm - \Lambda)_+ \, d\mathbf{x} + \sum_{\pm} \mp \int_{\Omega_\varepsilon} (c_\varepsilon^+ - c_\varepsilon^-) (c_\varepsilon^\pm - \Lambda)_+ \, d\mathbf{x} \\ & \iff: I - II + III = -IV + V. \end{aligned}$$

The convective integral II cancels by standard calculations due to the incompressibility condition (4.2b) and the no-slip boundary condition. Moreover, integral V is non-positive due to the monotonicity of $(\cdot)_+$, i.e. $V \leq 0$ holds. It remains to consider the drift term, integral IV . Using the identity $c_\varepsilon^\pm \nabla \phi_\varepsilon \cdot \nabla (c_\varepsilon^\pm - \Lambda)_+ = (c_\varepsilon^\pm - \Lambda) \nabla \phi_\varepsilon \cdot \nabla (c_\varepsilon^\pm - \Lambda)_+ + \Lambda \nabla \phi_\varepsilon \cdot \nabla (c_\varepsilon^\pm - \Lambda)_+ = \nabla \phi_\varepsilon \cdot \frac{1}{2} \nabla (c_\varepsilon^\pm - \Lambda)_+^2 + \Lambda \nabla \phi_\varepsilon \cdot \nabla (c_\varepsilon^\pm - \Lambda)_+$, integration by parts and inserting Poisson's equation (4.2d), we obtain

$$\begin{aligned} -IV & = - \int_{\Omega_\varepsilon} \varepsilon^{\alpha_2 - \alpha_3} (c_\varepsilon^+ - c_\varepsilon^-) \left(\frac{1}{2} (c_\varepsilon^+ - \Lambda)_+^2 - \frac{1}{2} (c_\varepsilon^- - \Lambda)_+^2 \right) \\ & \qquad \qquad \qquad + \left(\Lambda (c_\varepsilon^+ - \Lambda)_+ - \Lambda (c_\varepsilon^- - \Lambda)_+ \right) \, d\mathbf{x} \\ & \leq 0 \end{aligned}$$

Here, the homogeneous Neumann boundary condition for the electrostatic potential prevents the occurrence of boundary terms. Moreover, the sign condition of integral IV is valid due to the monotonicity of $(\cdot)_+$ and $(\cdot)^2$.

Altogether, we have

$$\sum_{\pm} \left(\frac{1}{2} \frac{d}{dt} \|(c_{\varepsilon}^{\pm} - \Lambda)_+\|_{L^2(\Omega_{\varepsilon})}^2 + \varepsilon^{\gamma} \|\nabla(c_{\varepsilon}^{\pm} - \Lambda)_+\|_{L^2(\Omega_{\varepsilon})}^2 \right) \leq 0.$$

Then, Gronwall's lemma, [44], implies the statement of Theorem 4.9 since the initial number densities are bounded from above by Λ according to Assumption 4.4.

In the case of inhomogeneous Neumann boundary conditions as defined in Assumption 4.4, i.e. $\sigma \neq 0$, we prove boundedness in $L^{\infty}((0, T) \times \Omega_{\varepsilon})$ without any additional constraints opposed to [118]. To this end, we rigorously apply Moser iteration technique, see [75, 93, 92] and also Section 2.2. Although the procedure is quite analog to the proof of Theorem 2.24, we represent it for the sake of clearness. Subsequently, our aim is to examine in detail the ε dependency of the L^{∞} estimate, which is essential in order to homogenize the SNPP system later on. Therefore, we use test functions $(c_{\varepsilon}^{\pm})^{2\alpha+1}$, cf. Section 2.2.6 and estimate the $L^{2\alpha+1}((0, T) \times \Omega_{\varepsilon})$ norm of the number densities c_{ε}^{\pm} and consider the limit $\alpha \rightarrow \infty$. As a remark note, that our choice of test functions is admissible due to the statement in Theorem 4.6 and for this reason, the following calculations are less technical than those in the proof of Theorem 2.24.

$$\begin{aligned} \langle \partial_t c_{\varepsilon}^{\pm}, (c_{\varepsilon}^{\pm})^{2\alpha+1} \rangle_{V^{-1}, V_0^1} + \int_{\Omega_{\varepsilon}} (-\varepsilon^{\beta} \mathbf{v}_{\varepsilon} c_{\varepsilon}^{\pm} + \varepsilon^{\gamma} \nabla c_{\varepsilon}^{\pm} \pm \varepsilon^{\alpha_2} c_{\varepsilon}^{\pm} \nabla \phi_{\varepsilon}) \cdot \nabla (c_{\varepsilon}^{\pm})^{2\alpha+1} \, d\mathbf{x} \\ = \mp \int_{\Omega_{\varepsilon}} (c_{\varepsilon}^+ - c_{\varepsilon}^-) (c_{\varepsilon}^{\pm})^{2\alpha+1} \, d\mathbf{x} \end{aligned} \quad (4.6)$$

1. The velocity term in (4.6) cancels due to standard arguments, i.e.

$$\int_{\Omega_{\varepsilon}} -\varepsilon^{\beta} \mathbf{v}_{\varepsilon} c_{\varepsilon}^{\pm} \cdot \nabla (c_{\varepsilon}^{\pm})^{2\alpha+1} \, d\mathbf{x} = 0.$$

2. For the diffusive term in (4.6), we apply the product and chain rule in order to obtain

$$\int_{\Omega_{\varepsilon}} \varepsilon^{\gamma} \nabla c_{\varepsilon}^{\pm} \cdot \nabla (c_{\varepsilon}^{\pm})^{2\alpha+1} \, d\mathbf{x} = \frac{2\alpha + 1}{(\alpha + 1)^2} \varepsilon^{\gamma} \|\nabla (c_{\varepsilon}^{\pm})^{\alpha+1}\|_{L^2(\Omega)}^2.$$

3. The drift term in (4.6) is manipulated using first the product and chain rule and then applying integration by parts. Substituting Poisson's equation (4.2d) finally leads to

$$\pm \int_{\Omega_{\varepsilon}} \varepsilon^{\alpha_2} c_{\varepsilon}^{\pm} \nabla \phi_{\varepsilon} \cdot \nabla (c_{\varepsilon}^{\pm})^{2\alpha+1} \, d\mathbf{x}$$

$$\begin{aligned}
&= \pm \frac{2\alpha + 1}{2\alpha + 2} \varepsilon^{\alpha_2 - \alpha_3} \int_{\Omega_\varepsilon} (c_\varepsilon^+ - c_\varepsilon^-) (c_\varepsilon^\pm)^{2\alpha+2} d\mathbf{x} + \int_{\Gamma_\varepsilon} \varepsilon \sigma (c_\varepsilon^\pm)^{2\alpha+2} ds_x \\
&=: \pm (I^\pm + II^\pm)
\end{aligned}$$

After summation over \pm , $\sum_{\pm} \pm I^\pm$ fulfills a sign condition due to the monotonicity of $(\cdot)^{2\alpha+2}$, i.e $\sum_{\pm} \pm I^\pm = I^+ - I^- \geq 0$ holds. The integrals II^\pm are estimated by means of (4.5) and Young's inequality (2, 2) as follows:

$$\begin{aligned}
|\mp II^\pm| &= \left| \int_{\Gamma_\varepsilon} \frac{2\alpha + 1}{2\alpha + 2} \varepsilon^{\alpha_2 - \alpha_3} \varepsilon \sigma (c_\varepsilon^\pm)^{2\alpha+2} ds_x \right| \\
&\leq \varepsilon^{\alpha_2 - \alpha_3} \frac{2\alpha + 1}{4} C \|\sigma\|_{L^\infty(\Gamma_\varepsilon)}^2 \|(c_\varepsilon^\pm)^{\alpha+1}\|_{L^2(\Omega_\varepsilon)}^2 \\
&\quad + \delta \varepsilon^{\alpha_2 - \alpha_3 + 2} \frac{2\alpha + 1}{(\alpha + 1)^2} \|\nabla (c_\varepsilon^\pm)^{\alpha+1}\|_{L^2(\Omega_\varepsilon)}^2
\end{aligned}$$

4. We sum over \pm in order to estimate the reactive term in (4.6):

$$\sum_{\pm} \mp \int_{\Omega_\varepsilon} (c_\varepsilon^+ - c_\varepsilon^-) (c_\varepsilon^\pm)^{2\alpha+1} d\mathbf{x} \leq 0.$$

Here, again a sign condition is fulfilled according to the monotonicity property of $(\cdot)^{2\alpha+1}$.

Combining all the above estimates 1.-4. and adsorption of the gradient term in 3., finally leads to

$$\begin{aligned}
&\frac{1}{2\alpha + 2} \frac{d}{dt} \sum_{\pm} \|(c_\varepsilon^\pm)^{\alpha+1}\|_{L^2(\Omega_\varepsilon)}^2 \\
&\quad + \left(\frac{2\alpha + 1}{(\alpha + 1)^2} \varepsilon^\gamma - \delta \varepsilon^{\alpha_2 - \alpha_3 + 2} \frac{2\alpha + 1}{(\alpha + 1)^2} \right) \sum_{\pm} \|\nabla (c_\varepsilon^\pm)^{2k-1}\|_{L^2(\Omega_\varepsilon)}^2 \\
&\leq \varepsilon^{\alpha_2 - \alpha_3} \frac{2\alpha + 1}{4} C \|\sigma\|_{L^\infty(\Gamma_\varepsilon)}^2 \sum_{\pm} \|(c_\varepsilon^\pm)^{\alpha+1}\|_{L^2(\Omega_\varepsilon)}^2
\end{aligned}$$

In the case of $\alpha_2 - \alpha_3 \geq 0$, $\alpha_2 - \alpha_3 - \gamma + 2 \geq 0$ and $\delta \leq 1/2$, all terms remain well defined, even for $\varepsilon \rightarrow 0$.

Proceeding the Moser iteration as in the proof of Theorem 2.24, we obtain

$$\sum_{\pm} \|c_\varepsilon^\pm\|_{L^{2 \cdot (5/3)^j}((0,T) \times \Omega_\varepsilon)} \leq \prod_{j=0}^J \left(\frac{C_S}{\varepsilon^\gamma} \right)^{\frac{1}{2 \cdot (5/3)^{j+1}}} C_j^{\frac{1}{2 \cdot (5/3)^j}} \sum_{\pm} \|c_\varepsilon^\pm\|_{L^2((0,T) \times \Omega_\varepsilon)}$$

with $C_j := \varepsilon^{\alpha_2 - \alpha_3} \frac{1}{2} (2 \cdot (5/3)^j - 1) (5/3)^j C \|\sigma\|_{L^\infty((0,T) \times \Gamma_\varepsilon)}^2 + \|(c_\varepsilon^\pm, 0)^{(5/3)^j}\|_{L^2(\Omega_\varepsilon)}^2$. With the definition $C_{\text{Moser}} := \prod_{j=0}^{\infty} C_S^{\frac{1}{2 \cdot (5/3)^{j+1}}} C_j^{\frac{1}{2 \cdot (5/3)^j}}$, the convergence property of C_{Moser} for $\alpha \rightarrow \infty$ is investigated by the root/ratio test as in the proof of Theorem 2.24. In particular, the constant C_{Moser} does not depend on the scale parameter ε if $\gamma \leq 0$ and therefore, remains bounded even for $\varepsilon \rightarrow 0$. Remark, that we assumed in step j of the Moser iteration that $\sum_{\pm} \|(c_\varepsilon^\pm)^{(5/3)^j}\|_{L^2(\Omega_\varepsilon)}^2 \geq 1$ in order to subsume the initial value in the constant C_j . If, on the other hand, it would hold $\sum_{\pm} \|(c_\varepsilon^\pm)^{(5/3)^j}\|_{L^2(\Omega_\varepsilon)}^2 \leq 1$ for every j , the statement would already be proven. \square

In the following theorem, we state ε -independent a priori estimates for the Neumann case. These strongly rely on the estimates derived in Theorem 4.7 and Theorem 4.9 and are the basis of the upscaling procedure which is presented in Section 4.2.2. As a remark, note that in the case of $\sigma \neq 0$ the range of the parameters $\alpha_2, \alpha_3, \gamma$ is restricted according to Theorem 4.7 and Theorem 4.9.

Theorem 4.10. *Let Assumption 4.4 and Theorem 4.7 and Theorem 4.9 hold. Then, the following a priori estimates hold in the Neumann case.*

$$\varepsilon^{\alpha_3} \|\phi_\varepsilon\|_{L^2((0,T) \times \Omega_\varepsilon)} + \varepsilon^{\alpha_3} \|\nabla \phi_\varepsilon\|_{L^2((0,T) \times \Omega_\varepsilon)} \leq C. \quad (4.7)$$

In the case $\alpha_1 - \alpha_3 \geq 0$, it holds

$$\|\mathbf{v}_\varepsilon\|_{L^2((0,T) \times \Omega_\varepsilon)} + \varepsilon \|\nabla \mathbf{v}_\varepsilon\|_{L^2((0,T) \times \Omega_\varepsilon)} \leq C. \quad (4.8)$$

If additionally $\beta \geq 0$, $\gamma \geq 0$ and $\alpha_2 - \alpha_3 \geq 0$ hold and if $\alpha_2 - \alpha_3 - \gamma + 2 \geq 0$ is fulfilled in the case of $\sigma \neq 0$, it holds

$$\max_{0 \leq t \leq T} \sum_{\pm} \|c_\varepsilon^\pm\|_{L^2(\Omega_\varepsilon)} + \varepsilon^{\gamma/2} \sum_{\pm} \|\nabla c_\varepsilon^\pm\|_{L^2((0,T) \times \Omega_\varepsilon)} + \sum_{\pm} \|\partial_t c_\varepsilon^\pm\|_{L^2(0,T; V^{-1}(\Omega_\varepsilon))} \leq C. \quad (4.9)$$

In (4.7), (4.8), and (4.9), $C \in \mathbb{R}_+$ is a constant independent of ε .

Proof. We consider separately the a priori estimates for the electrostatic potential, the velocity field and the number densities and investigate the ε -dependencies carefully. Firstly, to derive the a priori estimate for the electrostatic potential, we test (4.2d) with ϕ_ε which leads to

$$\begin{aligned} & \varepsilon^{\alpha_3} \|\nabla \phi_\varepsilon\|_{L^2(\Omega_\varepsilon)}^2 \\ & \leq \varepsilon \|\sigma\|_{L^2(\Gamma_\varepsilon)} \|\phi_\varepsilon\|_{L^2(\Gamma_\varepsilon)} + \|c_\varepsilon^+ - c_\varepsilon^-\|_{L^2(\Omega_\varepsilon)} \|\phi_\varepsilon\|_{L^2(\Omega_\varepsilon)} \end{aligned}$$

$$\begin{aligned} &\leq \sqrt{\varepsilon} \|\sigma\|_{L^2(\Gamma_\varepsilon)} C (\|\phi_\varepsilon\|_{L^2(\Omega_\varepsilon)} + \varepsilon \|\nabla \phi_\varepsilon\|_{L^2(\Omega_\varepsilon)}) + \|c_\varepsilon^+ - c_\varepsilon^-\|_{L^2(\Omega_\varepsilon)} \|\phi_\varepsilon\|_{L^2(\Omega_\varepsilon)} \\ &\leq (C(C_P + \varepsilon) \sqrt{\varepsilon} \|\sigma\|_{L^2(\Gamma_\varepsilon)} + C_P \|c_\varepsilon^+ - c_\varepsilon^-\|_{L^2(\Omega_\varepsilon)}) \|\nabla \phi_\varepsilon\|_{L^2(\Omega_\varepsilon)}. \end{aligned}$$

Here, we used (4.5) and the Poincaré inequality (4.3). This results in

$$\varepsilon^{\alpha_3} \|\nabla \phi_\varepsilon\|_{L^2(\Omega_\varepsilon)} \leq C(C_P + \varepsilon) \sqrt{\varepsilon} \|\sigma\|_{L^2(\Gamma_\varepsilon)} + C_P \|c_\varepsilon^+ - c_\varepsilon^-\|_{L^2(\Omega_\varepsilon)} \leq C, \quad (\star)$$

since σ is constant according to Assumption 4.4 and the number densities c_ε^\pm are bounded uniformly in ε , see Theorem 4.7 and 4.9. Using once again the Poincaré inequality (4.3) leads directly to statement (4.7) after integration with respect to time. The constant C remains bounded ε -independently due to Theorem 4.7 and Theorem 4.9 and Assumption 4.4.

Secondly, to derive an a priori estimate for the velocity field, we test (4.2a) with \mathbf{v}_ε and apply the Poincaré inequality (4.4). This leads due to the incompressibility of \mathbf{v}_ε , (\star) and the ε -independent boundedness of c_ε^\pm according to Theorem 4.7 and 4.9 to

$$\begin{aligned} \varepsilon^2 \|\nabla \mathbf{v}_\varepsilon\|_{L^2(\Omega_\varepsilon)}^2 &\leq \varepsilon^{\alpha_1} \|(c_\varepsilon^+ - c_\varepsilon^-)\|_{L^\infty(\Omega_\varepsilon)} \|\nabla \phi_\varepsilon\|_{L^2(\Omega_\varepsilon)} \|\mathbf{v}_\varepsilon\|_{L^2(\Omega_\varepsilon)} \\ &\leq \varepsilon^{\alpha_1 - \alpha_3} \|(c_\varepsilon^+ - c_\varepsilon^-)\|_{L^\infty(\Omega_\varepsilon)} (C(C_P + \varepsilon) \sqrt{\varepsilon} \|\sigma\|_{L^2(\Gamma_\varepsilon)} \\ &\quad + C_P \|c_\varepsilon^+ - c_\varepsilon^-\|_{L^2(\Omega_\varepsilon)}) C_P^0 \varepsilon \|\nabla \mathbf{v}_\varepsilon\|_{L^2(\Omega_\varepsilon)}. \end{aligned}$$

Consequently, we obtain

$$\begin{aligned} &\varepsilon \|\nabla \mathbf{v}_\varepsilon\|_{L^2(\Omega_\varepsilon)} \\ &\leq \varepsilon^{\alpha_1 - \alpha_3} C_P^0 \|(c_\varepsilon^+ - c_\varepsilon^-)\|_{L^\infty(\Omega_\varepsilon)} (C(C_P + \varepsilon) \sqrt{\varepsilon} \|\sigma\|_{L^2(\Gamma_\varepsilon)} + C_P \|c_\varepsilon^+ - c_\varepsilon^-\|_{L^2(\Omega_\varepsilon)}) \\ &\leq C. \end{aligned}$$

Note that the right hand side remains bounded by a constant C that is independent of ε for $\varepsilon \rightarrow 0$ due to the estimates derived for the electrostatic potential, cf. (\star) , Theorem 4.7, and Theorem 4.9, if additionally $\alpha_1 - \alpha_3 \geq 0$ is postulated. Using once again the Poincaré inequality (4.4) leads after integration with respect to time directly to statement (4.8) and the constant C remains bounded ε -independently.

Thirdly, to derive an a priori estimate for the number densities, we test (4.2c) with c_ε^\pm to obtain, as a first step, an energy estimate. This allows to bound also the gradient of the number densities. Summing with respect to \pm , a sign condition for the reactive term and standard arguments for the convective term (compare the proof of Theorem 4.7

and Theorem 4.9), leads to

$$\frac{1}{2} \frac{d}{dt} \sum_{\pm} \|c_{\varepsilon}^{\pm}\|_{L^2(\Omega_{\varepsilon})}^2 + \varepsilon^{\gamma} \sum_{\pm} \|\nabla c_{\varepsilon}^{\pm}\|_{L^2(\Omega_{\varepsilon})}^2 \leq - \sum_{\pm} \int_{\Omega_{\varepsilon}} \pm \varepsilon^{\alpha_2} c_{\varepsilon}^{\pm} \nabla \phi_{\varepsilon} \cdot \nabla c_{\varepsilon}^{\pm} \, d\mathbf{x}.$$

Analogue to the proof of Theorem 4.7, we estimate the drift term using integration by parts, Poisson's equation (4.2d), and a sign condition.

$$\begin{aligned} \frac{1}{2} \frac{d}{dt} \sum_{\pm} \|c_{\varepsilon}^{\pm}\|_{L^2(\Omega_{\varepsilon})}^2 + \varepsilon^{\gamma} \sum_{\pm} \|\nabla c_{\varepsilon}^{\pm}\|_{L^2(\Omega_{\varepsilon})}^2 &\leq \frac{1}{2} \sum_{\pm} \varepsilon^{\alpha_2 - \alpha_3} \|\sigma\|_{L^{\infty}(\Gamma_{\varepsilon})} \varepsilon \|c_{\varepsilon}^{\pm}\|_{L^2(\Gamma_{\varepsilon})}^2 \\ &\leq \frac{1}{2} \sum_{\pm} \varepsilon^{\alpha_2 - \alpha_3} \|\sigma\|_{L^{\infty}(\Gamma_{\varepsilon})} C (\|c_{\varepsilon}^{\pm}\|_{L^2(\Omega_{\varepsilon})}^2 + \varepsilon^2 \|\nabla c_{\varepsilon}^{\pm}\|_{L^2(\Omega_{\varepsilon})}^2). \end{aligned}$$

In the last step of the above estimate, we used (4.5).

Adsorption of the gradient term with $\varepsilon^{\gamma} - \frac{1}{2} \varepsilon^{\alpha_2 - \alpha_3 + 2} \|\sigma\|_{L^{\infty}(\Gamma_{\varepsilon})} C \geq \frac{1}{2} \varepsilon^{\gamma}$, i.e. with $\varepsilon \leq \varepsilon_0 := \left(\frac{1}{C \|\sigma\|_{L^{\infty}(\Gamma_{\varepsilon})}} \right)^{\frac{1}{\alpha_2 - \alpha_3 - \gamma + 2}}$ and $\alpha_2 - \alpha_3 - \gamma + 2 \geq 0$, finally leads to

$$\frac{1}{2} \frac{d}{dt} \sum_{\pm} \|c_{\varepsilon}^{\pm}\|_{L^2(\Omega_{\varepsilon})}^2 + \frac{1}{2} \varepsilon^{\gamma} \sum_{\pm} \|\nabla c_{\varepsilon}^{\pm}\|_{L^2(\Omega_{\varepsilon})}^2 \leq \frac{1}{2} \varepsilon^{\alpha_2 - \alpha_3} \|\sigma\|_{L^{\infty}(\Gamma_{\varepsilon})} C \sum_{\pm} \|c_{\varepsilon}^{\pm}\|_{L^2(\Omega_{\varepsilon})}^2.$$

Gronwall's lemma, [44], and integration with respect to time gives the following estimate for the gradient of the number densities

$$\begin{aligned} &\sum_{\pm} \varepsilon^{\gamma} \|\nabla c_{\varepsilon}^{\pm}\|_{L^2((0,T) \times \Omega_{\varepsilon})}^2 \\ &\leq \left(1 + C \varepsilon^{\alpha_2 - \alpha_3} \|\sigma\|_{L^{\infty}(\Gamma_{\varepsilon})} \exp \left(\int_0^T C \varepsilon^{\alpha_2 - \alpha_3} \|\sigma\|_{L^{\infty}(\Gamma_{\varepsilon})} \, dt \right) \right) \sum_{\pm} \|c_{\varepsilon}^{\pm,0}\|_{L^2(\Omega_{\varepsilon})}^2 \\ &\leq C. \end{aligned}$$

The right hand side of the above estimate remains well defined for $\varepsilon \rightarrow 0$ if $\alpha_2 - \alpha_3 \geq 0$ holds. As a consequence, C does not depend on ε if $\alpha_2 - \alpha_3 \geq 0$ holds.

To conclude the proof of Theorem 4.10, we still need to derive estimates for the time derivatives $\partial_t c_{\varepsilon}^{\pm}$ of the number densities. Due to the definition of the V^{-1} norm and by means of the transport equations (4.2c), we obtain

$$\|\partial_t c_{\varepsilon}^{\pm}\|_{V^{-1}(\Omega_{\varepsilon})} = \sup_{\varphi \in V_0^1(\Omega_{\varepsilon}), \|\varphi\|_{V_0^1(\Omega_{\varepsilon})} \leq 1} \langle \partial_t c_{\varepsilon}^{\pm}, \varphi \rangle_{V^{-1}, V_0^1}$$

$$\begin{aligned}
&\leq \|c_\varepsilon^+\|_{L^2(\Omega_\varepsilon)} + \|c_\varepsilon^-\|_{L^2(\Omega_\varepsilon)} + (\varepsilon^\beta \|\mathbf{v}_\varepsilon\|_{L^2(\Omega_\varepsilon)} + \varepsilon^{\alpha_2} \|\nabla \phi_\varepsilon\|_{L^2(\Omega_\varepsilon)}) \|c_\varepsilon^\pm\|_{L^\infty(\Omega_\varepsilon)} \\
&\quad + \varepsilon^\gamma \|\nabla c_\varepsilon^\pm\|_{L^2(\Omega_\varepsilon)} \\
&\leq C,
\end{aligned}$$

The constant C is bounded uniformly in ε , in particular, for $\varepsilon \rightarrow 0$, if additionally $\beta, \gamma \geq 0$ and $\alpha_2 - \alpha_3 \geq 0$ hold. Integration with respect to time therefore yields the last statement of Theorem 4.10. \square

Remark 4.11. *In the literature, often $\tilde{\gamma} = \gamma/2$ is used in estimate (4.9).*

Remark 4.12. *The ε -independent L^∞ -estimate for the number densities c_ε^\pm , enters the proof of Theorem 4.10 whenever nonlinear terms appear, i.e. in two places: Firstly, the a priori estimate of the velocity field \mathbf{v}_ε and secondly the estimate of the time derivative of the number densities $\partial_t c_\varepsilon^\pm$. The L^∞ -estimate is essential here, since an alternative approach using estimates including higher order L^p -norms of the electrostatic potential and corresponding stability estimates can not be used. This is due to the fact, that, in general, it is not guaranteed that these regularity estimates are ε -independent, i.e. uniform in the scale parameter ε . However, such estimates and related questions are quite an actual research topic, [61, 131]. Note, that in the stationary SNPP problem and consequently for a prescribed and decoupled velocity field \mathbf{v}_ε , the L^∞ -estimate for the number densities would not be necessary.*

4.2.2 Homogenization in the Neumann case

In this section, we determine the limit $\varepsilon \rightarrow 0$ in the ε -scaled Stokes-Nernst-Planck-Poisson system (4.1). We consider the Neumann case, i.e. boundary conditions of Neumann type for the electrostatic potential on the interior boundary Γ_ε , and different choices of scaling $(\alpha_1, \alpha_2, \alpha_3, \beta, \gamma)$. To identify the macroscopic limit equations, which describe the effective fluid flow, transport of the number densities, and the behavior of the electrostatic potential, we apply the method of two-scale convergence, see Section 3.1.3.

In our investigations, we focus on the coupling of the partial differential equations (4.1) by means of electrostatic interaction and pay special attention to the treatment of the nonlinear terms $c_\varepsilon^\pm \nabla \phi_\varepsilon$ and $c_\varepsilon^\pm \mathbf{v}_\varepsilon$. For this reason, we choose the set of parameters $(\alpha_1, \alpha_2, \alpha_3, \beta, \gamma)$ in such a way that the ε -independent a priori estimates of Theorem 4.10 hold and also strong convergence for the number densities c_ε^\pm holds true. This is ensured by the a priori estimates in Theorem 4.10 and standard compact embedding

according to Aubin-Lions, [119, 132]. In particular, we assume that $\gamma = 0$ holds true for the remainder of this section.

Moreover, we define extensions of system (4.1) and its variables from the perforated domain Ω_ε to the whole domain Ω , cf. Theorem 3.6 and Theorem 3.7 and deduce the structure of their two-scale limits using the a priori estimates presented in Theorem 4.10.

First of all, we define effective tensors as well as auxiliary cell problems, which will arise during the process of homogenization in this section.

Definition 4.13. *We define the permittivity/diffusion tensor $\mathbf{D} = (D_{ij})_{i,j=1,\dots,n}$ by*

$$D_{ij} := \int_{Y_l} (\delta_{ij} + \partial_{y_i} \varphi_j) \, d\mathbf{y}, \quad (4.10)$$

whereby $\varphi_j = \varphi_j(\mathbf{y})$ are solutions of the following family of cell problems ($j = 1, \dots, n$)

$$-\Delta_{\mathbf{y}} \varphi_j = 0 \quad \text{in } Y_l, \quad (4.11a)$$

$$\nabla_{\mathbf{y}} \varphi_j \cdot \boldsymbol{\nu} = -\mathbf{e}_j \cdot \boldsymbol{\nu} \quad \text{on } \Gamma, \quad (4.11b)$$

$$\varphi_j \quad \text{periodic in } \mathbf{y}. \quad (4.11c)$$

We define the permeability tensor $\mathbf{K} = (K_{ij})_{i,j=1,\dots,n}$ by

$$K_{ij} = \int_{Y_l} (w_j)_i \, d\mathbf{y}, \quad (4.12)$$

whereby $\mathbf{w}_j = \mathbf{w}_j(\mathbf{y})$, $\pi_j = \pi_j(\mathbf{y})$ are solutions of the following family of cell problems ($j = 1, \dots, n$)

$$-\Delta_{\mathbf{y}} \mathbf{w}_j + \nabla_{\mathbf{y}} \pi_j = \mathbf{e}_j \quad \text{in } Y_l, \quad (4.13a)$$

$$\nabla_{\mathbf{y}} \cdot \mathbf{w}_j = 0 \quad \text{in } \Omega \times Y_l, \quad (4.13b)$$

$$\mathbf{w}_j = 0 \quad \text{in } Y_s, \quad (4.13c)$$

$$\mathbf{w}_j, \pi_j \quad \text{periodic in } \mathbf{y}. \quad (4.13d)$$

The a priori estimates that have been derived in Theorem 4.10 are at first only valid within the perforated domain Ω_ε . Therefore, extensions of the functions \mathbf{v}_ε , $\nabla \mathbf{v}_\varepsilon$, p_ε , ϕ_ε , $\nabla \phi_\varepsilon$, c_ε^\pm , ∇c_ε^\pm , and $\partial_t c_\varepsilon^\pm$ are necessary, such that appropriate a priori estimates are extended and that the limits for $\varepsilon \rightarrow 0$ are identified in function spaces on Ω . Besides

the notation and definitions of Section 3.1.4 we introduce the following extension of the pressure field p_ε , [4, 58]:

Definition 4.14. *Let $(\mathbf{v}_\varepsilon, p_\varepsilon, c_\varepsilon^\pm, \phi_\varepsilon)$ be a weak solution of Problem P_ε in the sense of Definition 4.5. The pressure field p_ε is extended via*

$$E_p(p_\varepsilon) := \begin{cases} p_\varepsilon & \text{in } \Omega_\varepsilon, \\ \frac{1}{|Y_{t,i}^\varepsilon|} \int_{Y_{t,i}^\varepsilon} p_\varepsilon \, d\mathbf{y} & \text{in each } Y_{s,i}^\varepsilon. \end{cases}$$

Using in addition the notation and definitions of extensions in Section 3.1.4, we transform Problem P_ε to a system of partial differential equations, which is defined on the whole domain Ω : We set

$$\tilde{\phi}_\varepsilon := \varepsilon^{\alpha_3} \phi_\varepsilon \quad (4.14)$$

and obtain the following problem formulation, which is the starting point of the homogenization procedure using the method of two-scale convergence.

$$\begin{aligned} \int_0^T \int_\Omega \varepsilon^2 \nabla E_0(\mathbf{v}_\varepsilon) : \nabla \boldsymbol{\psi} - E_p(p_\varepsilon) \nabla \cdot \boldsymbol{\psi} \, d\mathbf{x} \, dt \\ = - \int_0^T \int_{\Omega_\varepsilon} \varepsilon^{\alpha_1 - \alpha_3} E(c_\varepsilon^+ - c_\varepsilon^-) E_0(\nabla \tilde{\phi}_\varepsilon) \cdot \boldsymbol{\psi} \, d\mathbf{x} \, dt, \end{aligned} \quad (4.15)$$

$$\begin{aligned} \int_0^T \langle E_0(\partial_t c_\varepsilon^\pm), \boldsymbol{\psi} \rangle_{V^{-1}, V_0^1} \, dt + \int_0^T \int_\Omega \left(-\varepsilon^\beta E_0(\mathbf{v}_\varepsilon) E(c_\varepsilon^\pm) + \varepsilon^\gamma E_0(\nabla c_\varepsilon^\pm) \right. \\ \left. \pm \varepsilon^{\alpha_2 - \alpha_3} E(c_\varepsilon^\pm) E_0(\nabla \tilde{\phi}_\varepsilon) \right) \cdot \nabla \boldsymbol{\psi} \, d\mathbf{x} \, dt = \mp \int_0^T \int_\Omega \chi_\varepsilon E(c_\varepsilon^+ + c_\varepsilon^-) \varphi_3 \, d\mathbf{x} \, dt, \end{aligned} \quad (4.16)$$

$$\begin{aligned} \int_0^T \int_\Omega E_0(\nabla \tilde{\phi}_\varepsilon) \cdot \nabla \boldsymbol{\psi} \, d\mathbf{x} \, dt = \int_0^T \int_{\Gamma_\varepsilon} \varepsilon \sigma \boldsymbol{\psi} \, ds_{\mathbf{x}} \, dt \\ + \int_0^T \int_\Omega \chi_\varepsilon (E(c_\varepsilon^+) - E(c_\varepsilon^-)) \boldsymbol{\psi} \, d\mathbf{x} \, dt. \end{aligned} \quad (4.17)$$

Standard estimates for the pressure field in Stokes equations, following directly the procedure in [58] and including the electrostatic interaction [4], and Definition 4.14 ensure that the following theorem holds.

Theorem 4.15. *Let $(\mathbf{v}_\varepsilon, p_\varepsilon, c_\varepsilon^\pm, \phi_\varepsilon)$ be a solution of Problem P_ε and let $E_p(p_\varepsilon)$ denote the extension of the pressure field p_ε according to Definition 4.14. Then, the following uniform a priori estimate holds:*

$$\|E_p(p_\varepsilon)\|_{L^2((0,T) \times (\Omega/\mathbb{R}))} \leq C.$$

Together with the statements of Theorem 3.6 and Theorem 3.7, the perforated domain Ω_ε can be replaced by Ω in all the a priori estimates of Theorem 4.10.

For ease of presentation, we suppress the notation of the extensions in the following and proceed with the homogenization of the SNPP system in the Neumann case; see also [3] for a strategy in identifying the corresponding limit functions of the extensions. The homogenization is done in three steps: The three subproblems Poisson's equation, Stokes equations and Nernst-Planck equations are considered separately and consecutively. For each of these subproblems, a two-scale homogenized system is derived as a first step. This is followed by the definition of appropriate cell problems and the explicit representation of certain limit functions in terms of solutions of these cell problems and of further limit functions due to linear relations. Finally, macroscopic equations for the two-scale limits are derived defining effective tensors. For each subproblem, we discuss the structure of the macroscopic limit equations for different choices of the parameter set $(\alpha_1, \alpha_2, \alpha_3, \beta, \gamma)$.

Homogenization of Poisson's equation

The first step of the homogenization procedure is the investigation of Poisson's equation. Remind that we defined $\tilde{\phi}_\varepsilon := \varepsilon^{\alpha_3} \phi_\varepsilon$, cf. (4.14).

Theorem 4.16. *Let the a priori estimates of Theorem 4.10 be valid. Then the following two-scale limits are identified for the electrostatic potential $\tilde{\phi}_\varepsilon$ and its gradient $\nabla \tilde{\phi}_\varepsilon$: There exist functions $\tilde{\phi}_0 \in L^2(0, T; H^1(\Omega))$ and $\tilde{\phi}_1 \in L^2((0, T) \times \Omega; H_{per}^1(Y))$ such that, up to a subsequence,*

$$\begin{aligned} \tilde{\phi}_\varepsilon(t, \mathbf{x}) &\xrightarrow{2} \tilde{\phi}_0(t, \mathbf{x}), \\ \nabla \tilde{\phi}_\varepsilon(t, \mathbf{x}) &\xrightarrow{2} \nabla_{\mathbf{x}} \tilde{\phi}_0(t, \mathbf{x}) + \nabla_{\mathbf{y}} \tilde{\phi}_1(t, \mathbf{x}, \mathbf{y}). \end{aligned}$$

Proof. We consider the estimate (4.7) in Theorem 4.10 which implies

$$\|\tilde{\phi}_\varepsilon\|_{L^2(\Omega)} + \|\nabla \tilde{\phi}_\varepsilon\|_{L^2(\Omega)} \leq C.$$

Then, Theorem 3.4 ensures directly the existence of the two-scale limit functions $\tilde{\phi}_0$ and $\tilde{\phi}_1$ as stated in Theorem 4.16. \square

In the following theorem the partial differential equations which are fulfilled by the limits function $\tilde{\phi}_0$ according to Theorem 4.16 are presented.

Theorem 4.17. *Let $(\mathbf{v}_\varepsilon, p_\varepsilon, c_\varepsilon^\pm, \phi_\varepsilon)$ be a weak solution of Problem P_ε in the sense of Definition 4.5. Assume that c_ε^\pm converge strongly to c_0^\pm in $L^2((0, T) \times \Omega)$. Then, the two-scale limit $\tilde{\phi}_0$ of $\tilde{\phi}_\varepsilon$ according to Theorem 4.16 satisfies the following macroscopic limit equations:*

$$\begin{aligned} -\nabla_{\mathbf{x}} \cdot \left(\mathbf{D} \nabla_{\mathbf{x}} \tilde{\phi}_0 \right) &= \bar{\sigma}_0 + |Y_l| (c_0^+ - c_0^-) && \text{in } (0, T) \times \Omega, \\ \mathbf{D} \nabla_{\mathbf{x}} \tilde{\phi}_0 \cdot \boldsymbol{\nu} &= 0 && \text{on } (0, T) \times \partial\Omega_N, \\ \tilde{\phi}_0 &= 0 && \text{on } (0, T) \times \partial\Omega_D \end{aligned}$$

with $\bar{\sigma}_0 := \int_\Gamma \sigma \, ds_{\mathbf{y}}$.

Proof. Step 1 (two-scale homogenized system) To prove Theorem 4.17, we test Poisson's equation (4.17) with test function $\psi_0(t, \mathbf{x}) + \varepsilon \psi_1(t, \mathbf{x}, \frac{\mathbf{x}}{\varepsilon})$, $\psi_0 \in \mathcal{D}((0, T) \times \Omega)$, $\psi_1 \in \mathcal{D}((0, T) \times \Omega; C_{\text{per}}^\infty(Y))$ and obtain

$$\begin{aligned} &\int_0^T \int_\Omega \nabla \tilde{\phi}_\varepsilon(t, \mathbf{x}) \cdot \nabla \left(\psi_0(t, \mathbf{x}) + \varepsilon \psi_1 \left(t, \mathbf{x}, \frac{\mathbf{x}}{\varepsilon} \right) \right) \, d\mathbf{x} \, dt \\ &= \int_0^T \int_{\Gamma_\varepsilon} \varepsilon \sigma \left(\psi_0(t, \mathbf{x}) + \varepsilon \psi_1 \left(t, \mathbf{x}, \frac{\mathbf{x}}{\varepsilon} \right) \right) \, d\mathbf{x} \, dt \\ &\quad + \int_0^T \int_\Omega \chi_\varepsilon(\mathbf{x}) (c_\varepsilon^+(t, \mathbf{x}) - c_\varepsilon^-(t, \mathbf{x})) \left(\psi_0(t, \mathbf{x}) + \varepsilon \psi_1 \left(t, \mathbf{x}, \frac{\mathbf{x}}{\varepsilon} \right) \right) \, d\mathbf{x} \, dt. \end{aligned}$$

We pass to the two-scale limit $\varepsilon \rightarrow 0$ in the above equation using the convergence properties stated in Theorem 4.16 and postulated in Theorem 4.17:

$$\begin{aligned} &\int_0^T \int_{\Omega \times Y_l} \left(\nabla_{\mathbf{x}} \tilde{\phi}_0(t, \mathbf{x}) + \nabla_{\mathbf{y}} \tilde{\phi}_1(t, \mathbf{x}, \mathbf{y}) \right) \cdot \left(\nabla_{\mathbf{x}} \psi_0(t, \mathbf{x}) + \nabla_{\mathbf{y}} \psi_1(t, \mathbf{x}, \mathbf{y}) \right) \, d\mathbf{y} \, d\mathbf{x} \, dt \\ &= \int_0^T \int_{\Omega \times \Gamma} \sigma \psi_0(t, \mathbf{x}) \, ds_{\mathbf{y}} \, d\mathbf{x} \, dt \\ &\quad + \int_0^T \int_{\Omega \times Y_l} (c_0^+(t, \mathbf{x}) - c_0^-(t, \mathbf{x})) \psi_0(t, \mathbf{x}) \, d\mathbf{y} \, d\mathbf{x} \, dt. \end{aligned} \tag{*}$$

Step 2 (representation of $\tilde{\phi}_1$, cell problems) We choose $\psi_0(t, \mathbf{x}) = 0$ in (*), which leads, after integration by parts with respect to \mathbf{y} , to

$$\begin{aligned} -\nabla_{\mathbf{y}} \cdot \left(\nabla_{\mathbf{x}} \tilde{\phi}_0(t, \mathbf{x}) + \nabla_{\mathbf{y}} \tilde{\phi}_1(t, \mathbf{x}, \mathbf{y}) \right) &= 0 && \text{in } (0, T) \times \Omega \times Y_l, \\ \left(\nabla_{\mathbf{x}} \tilde{\phi}_0(t, \mathbf{x}) + \nabla_{\mathbf{y}} \tilde{\phi}_1(t, \mathbf{x}, \mathbf{y}) \right) \cdot \boldsymbol{\nu} &= 0 && \text{on } (0, T) \times \Omega \times \Gamma, \\ \tilde{\phi}_1(t, \mathbf{x}, \mathbf{y}) &&& \text{periodic in } \mathbf{y} \end{aligned}$$

and, for this reason, also to

$$-\Delta_{\mathbf{y}} \tilde{\phi}_1(t, \mathbf{x}, \mathbf{y}) = 0 \quad \text{in } (0, T) \times \Omega \times Y_l, \quad (4.18a)$$

$$\nabla_{\mathbf{y}} \tilde{\phi}_1(t, \mathbf{x}, \mathbf{y}) \cdot \boldsymbol{\nu} = -\nabla_{\mathbf{x}} \tilde{\phi}_0(t, \mathbf{x}) \cdot \boldsymbol{\nu} \quad \text{on } (0, T) \times \Omega \times \Gamma, \quad (4.18b)$$

$$\tilde{\phi}_1(t, \mathbf{x}, \mathbf{y}) \quad \text{periodic in } \mathbf{y}. \quad (4.18c)$$

Due to the linearity of the equations, we deduce the following representation of $\tilde{\phi}_1$:

$$\tilde{\phi}_1(t, \mathbf{x}, \mathbf{y}) = \sum_j \varphi_j(\mathbf{y}) \partial_{x_j} \tilde{\phi}_0(t, \mathbf{x}) \quad (4.19)$$

with φ_j being solutions of the standard family of $j = 1, \dots, n$ cell problems as defined in (4.11).

Step 3 (macroscopic equation for $\tilde{\phi}_0$) On the other hand, if we choose $\psi_1(t, \mathbf{x}, \mathbf{y}) = 0$ in (\star) , we read off, after integration by parts with respect to \mathbf{x} , the strong problem formulation for $\tilde{\phi}_0$:

$$\begin{aligned} \nabla_{\mathbf{x}} \cdot \left(\int_{Y_l} \nabla_{\mathbf{x}} \tilde{\phi}_0(t, \mathbf{x}) + \nabla_{\mathbf{y}} \tilde{\phi}_1(t, \mathbf{x}, \mathbf{y}) \, d\mathbf{y} \right) \\ = \int_{\Gamma} \sigma \, ds_{\mathbf{y}} + |Y_l| (c_0^+(t, \mathbf{x}) - c_0^-(t, \mathbf{x})) \quad \text{in } (0, T) \times \Omega, \\ \left(\int_{Y_l} \nabla_{\mathbf{x}} \tilde{\phi}_0(t, \mathbf{x}) + \nabla_{\mathbf{y}} \tilde{\phi}_1(t, \mathbf{x}, \mathbf{y}) \, d\mathbf{y} \right) \cdot \boldsymbol{\nu} = 0 \quad \text{on } (0, T) \times \partial\Omega_N. \end{aligned}$$

Substituting the representation (4.19) of $\tilde{\phi}_1$ into the equations stated above, finally yields

$$\begin{aligned} \nabla_{\mathbf{x}} \cdot \left(\mathbf{D} \nabla_{\mathbf{x}} \tilde{\phi}_0(t, \mathbf{x}) \right) &= \bar{\sigma}_0 + |Y_l| (c_0^+(t, \mathbf{x}) - c_0^-(t, \mathbf{x})) \quad \text{in } (0, T) \times \Omega, \\ \mathbf{D} \nabla_{\mathbf{x}} \tilde{\phi}_0(t, \mathbf{x}) \cdot \boldsymbol{\nu} &= 0 \quad \text{on } (0, T) \times \partial\Omega_N, \\ \tilde{\phi}_0(t, \mathbf{x}) &= 0 \quad \text{on } (0, T) \times \partial\Omega_D \end{aligned}$$

with diffusion tensor \mathbf{D} being defined in (4.10) and $\bar{\sigma}_0 := \int_{\Gamma} \sigma_0 \, ds_{\mathbf{y}}$. \square

Remark 4.18 (Modeling of ϕ_0). *The behavior of the electrostatic potential $\tilde{\phi}_0$ is described by a macroscopic Poisson's equation with permittivity tensor \mathbf{D} . The number densities c_0^{\pm} directly enter the Poisson's equation as forcing terms. Moreover, a background charge density is present in the case of $\sigma \neq 0$, which results from the inhomogeneous Neumann boundary data.*

In the case of $\alpha_3 = 0$, it holds $\tilde{\phi}_\varepsilon = \phi_\varepsilon$, (4.14), and therefore also $\tilde{\phi}_0 = \phi_0$. The case of $\alpha_3 < 0$ implies that ϕ_ε and $\nabla\phi_\varepsilon$ converge to zero. However, for any α_3 a meaningful effective equation can be derived for the two-scale limit $\tilde{\phi}_0$ of $\tilde{\phi}_\varepsilon$.

Homogenized Limit Problems for Stokes Equation

The next step in the homogenization procedure is the investigation of Stokes equations. Here, the treatment of the nonlinear coupling terms $c_\varepsilon^\pm \nabla\phi_\varepsilon$ is crucial. To ensure that the two-scale limit $\varepsilon \rightarrow 0$ can be determined, the strong convergence of the number densities c_ε^\pm is essential.

Theorem 4.19. *Let the a priori estimates of Theorem 4.10 and Theorem 4.15 be valid. Then the following two-scale limits are identified for the velocity field \mathbf{v}_ε and the gradient $\varepsilon\nabla\mathbf{v}_\varepsilon$: There exists $\mathbf{v}_0 \in L^2((0, T) \times \Omega; H_{per}^1(Y))$ such that, up to a subsequence,*

$$\begin{aligned}\mathbf{v}_\varepsilon(t, \mathbf{x}) &\xrightarrow{2} \mathbf{v}_0(t, \mathbf{x}, \mathbf{y}), \\ \varepsilon\nabla\mathbf{v}_\varepsilon(t, \mathbf{x}) &\xrightarrow{2} \nabla_{\mathbf{y}}\mathbf{v}_0(t, \mathbf{x}, \mathbf{y}).\end{aligned}$$

Furthermore, the following two-scale limit is identified for the pressure field p_ε : There exists $p_0(t, \mathbf{x}, \mathbf{y}) \in L^2((0, T) \times \Omega \times Y)$, such that up to a subsequence,

$$p_\varepsilon(t, \mathbf{x}) \xrightarrow{2} p_0(t, \mathbf{x}, \mathbf{y}).$$

Proof. We consider the estimate (4.8) in Theorem 4.10, which implies together with Theorem 3.4 the existence of the two-scale limit \mathbf{v}_0 as stated in Theorem 4.19. The existence of the two-scale limit of p_ε follows directly from Theorem 4.15. Furthermore, the convergence of p_ε to p_0 is even strong in $L^2(\Omega)/\mathbb{R}$, [58, 4]. \square

In the following theorem the partial differential equations which are fulfilled by the limits functions \mathbf{v}_0, p_0 according to Theorem 4.19 are presented for different ranges of the parameter set (α_1, α_3) .

Theorem 4.20. *Let $(\mathbf{v}_\varepsilon, p_\varepsilon, c_\varepsilon^\pm, \phi_\varepsilon)$ be a weak solution of Problem P_ε in the sense of Definition 4.5. Assume that c_ε^\pm converge strongly to c_0^\pm in $L^2((0, T) \times \Omega)$. Then, the two-scale limit of \mathbf{v}_ε according to Theorem 4.19 satisfies the following macroscopic limit equations:*

$$\begin{aligned}
\bar{\mathbf{v}}_0 &= -\mathbf{K} \left(\nabla_{\mathbf{x}} p_0 + \begin{cases} (c_0^+ - c_0^-) \nabla_{\mathbf{x}} \tilde{\phi}_0, & \alpha_1 = \alpha_3 \\ 0, & \alpha_1 > \alpha_3 \end{cases} \right) && \text{in } (0, T) \times \Omega, \\
\nabla_{\mathbf{x}} \cdot \bar{\mathbf{v}}_0 &= 0 && \text{in } (0, T) \times \Omega, \\
\bar{\mathbf{v}}_0 \cdot \boldsymbol{\nu} &= 0 && \text{on } (0, T) \times \partial\Omega.
\end{aligned}$$

Proof. Step 1 (p_0 independent of \mathbf{y}) We choose $\varepsilon\psi(t, \mathbf{x}, \frac{\mathbf{x}}{\varepsilon})$, $\psi \in \mathcal{D}((0, T) \times \Omega; C_{\text{per}}^\infty(Y))$ as test function in (4.15), which yields

$$\begin{aligned}
&\int_0^T \int_{\Omega} \varepsilon \nabla \mathbf{v}_\varepsilon(t, \mathbf{x}) \cdot \varepsilon^2 \nabla \psi \left(t, \mathbf{x}, \frac{\mathbf{x}}{\varepsilon} \right) - p_\varepsilon(t, \mathbf{x}) \varepsilon \nabla \cdot \psi \left(t, \mathbf{x}, \frac{\mathbf{x}}{\varepsilon} \right) \, d\mathbf{x} \, dt \\
&= \int_0^T \int_{\Omega} -\varepsilon^{\alpha_1+1} (c_\varepsilon^+(t, \mathbf{x}) - c_\varepsilon^-(t, \mathbf{x})) \nabla \phi_\varepsilon(t, \mathbf{x}) \psi \left(t, \mathbf{x}, \frac{\mathbf{x}}{\varepsilon} \right) \, d\mathbf{x} \, dt.
\end{aligned}$$

We pass to the two-scale limit $\varepsilon \rightarrow 0$ in the above equation using the convergence properties stated in Theorem 4.19 and postulated in Theorem 4.20. As a consequence, we obtain

$$\int_0^T \int_{\Omega \times Y_l} -p_0(t, \mathbf{x}, \mathbf{y}) \nabla_{\mathbf{y}} \cdot \psi(t, \mathbf{x}, \mathbf{y}) \, d\mathbf{y} \, d\mathbf{x} \, dt = 0,$$

which, after integration by parts with respect to \mathbf{y} , directly leads to

$$p_0(t, \mathbf{x}, \mathbf{y}) = p_0(t, \mathbf{x}). \tag{4.20}$$

Step 2 (two-scale homogenized system) First of all, we define the following function space \mathcal{V} , [58]

$$\begin{aligned}
\mathcal{V} := &\left\{ \psi \in \mathcal{D}((0, T) \times \Omega; C_{\text{per}}^\infty(Y)) : \nabla_{\mathbf{y}} \cdot \psi = 0 \text{ in } (0, T) \times \Omega \times Y_l, \right. \\
&\nabla_{\mathbf{x}} \cdot \int_{Y_l} \psi \, d\mathbf{y} = 0 \text{ in } (0, T) \times \Omega, \psi = 0 \text{ in } (0, T) \times \Omega \times Y_s, \\
&\left. \int_{Y_l} \psi \, d\mathbf{y} \cdot \boldsymbol{\nu} = 0 \text{ on } (0, T) \times \partial\Omega \right\} \\
&\subset L^2((0, T) \times \Omega, H_{\text{per}}^1(Y))
\end{aligned}$$

and choose $\psi(t, \mathbf{x}, \frac{\mathbf{x}}{\varepsilon}) \in \mathcal{V}$ as test function in (4.15):

$$\begin{aligned} & \int_0^T \int_{\Omega} \varepsilon \nabla \mathbf{v}_{\varepsilon}(t, \mathbf{x}) \cdot \varepsilon \nabla \psi \left(t, \mathbf{x}, \frac{\mathbf{x}}{\varepsilon} \right) - p_{\varepsilon}(t, \mathbf{x}) \nabla \cdot \psi \left(t, \mathbf{x}, \frac{\mathbf{x}}{\varepsilon} \right) \, d\mathbf{x} \\ &= \int_0^T \int_{\Omega} -\varepsilon^{\alpha_1} (c_{\varepsilon}^+(t, \mathbf{x}) - c_{\varepsilon}^-(t, \mathbf{x})) \nabla \phi_{\varepsilon}(t, \mathbf{x}) \psi \left(t, \mathbf{x}, \frac{\mathbf{x}}{\varepsilon} \right) \, d\mathbf{x}. \end{aligned}$$

We again pass to the two-scale limit $\varepsilon \rightarrow 0$ using the convergence properties stated in Theorem 4.19 and postulated in Theorem 4.20 in order to obtain

$$\begin{aligned} & \int_0^T \int_{\Omega \times Y_l} \nabla_{\mathbf{y}} \mathbf{v}_0 \cdot \nabla_{\mathbf{y}} \psi - p_0 \nabla_{\mathbf{x}} \cdot \psi \, d\mathbf{y} \, d\mathbf{x} \\ &= \left\{ \begin{array}{ll} \int_0^T \int_{\Omega \times Y_l} -(c_0^+ - c_0^-) (\nabla_{\mathbf{x}} \tilde{\phi}_0 + \nabla_{\mathbf{y}} \tilde{\phi}_1) \psi \, d\mathbf{y} \, d\mathbf{x}, & \alpha_1 = \alpha_3 \\ 0, & \alpha_1 > \alpha_3 \end{array} \right\}. \end{aligned}$$

In addition, we used the fact that for $\psi \in \mathcal{V}$, it holds $\nabla_{\mathbf{y}} \cdot \psi = 0$. The property $p_0 = p_0(t, \mathbf{x})$, (4.20), yields together with the property $\nabla_{\mathbf{x}} \cdot \int_{Y_l} \psi \, d\mathbf{y} = 0$, since $\psi \in \mathcal{V}$, the following identity:

$$\int_0^T \int_{\Omega} -p_0(t, \mathbf{x}) \nabla_{\mathbf{x}} \cdot \left(\int_{Y_l} \psi(t, \mathbf{x}, \mathbf{y}) \, d\mathbf{y} \right) \, d\mathbf{x} \, dt = 0.$$

Finally, integration by parts with respect to \mathbf{y} leads to the following two-scale homogenized system:

$$\begin{aligned} & -\Delta_{\mathbf{y}} \mathbf{v}_0 + \nabla_{\mathbf{x}} p_0 + \nabla_{\mathbf{y}} p_1 \\ &= \left\{ \begin{array}{ll} -(c_0^+ - c_0^-) (\nabla_{\mathbf{x}} \tilde{\phi}_0 + \nabla_{\mathbf{y}} \tilde{\phi}_1), & \alpha_1 = \alpha_3 \\ 0, & \alpha_1 > \alpha_3 \end{array} \right\} & \text{in } (0, T) \times \Omega \times Y_l \\ & \nabla_{\mathbf{y}} \cdot \mathbf{v}_0 = 0 & \text{in } (0, T) \times \Omega \times Y_l \\ & \nabla_{\mathbf{x}} \cdot \int_{Y_l} \mathbf{v}_0 \, d\mathbf{y} = 0 & \text{in } (0, T) \times \Omega \\ & \int_{Y_l} \mathbf{v}_0 \, d\mathbf{y} \cdot \boldsymbol{\nu} = 0 & \text{on } (0, T) \times \partial\Omega \\ & \mathbf{v}_0 = 0 & \text{on } (0, T) \times \Omega \times Y_s. \end{aligned}$$

Here, the properties of the orthogonal of \mathcal{V} , [58], ensures the existence of a function $p_1 \in L^2((0, T) \times \Omega; L^2(Y_l)/\mathbb{R})$. Furthermore, following [58] allows to identify the pressure p_0 directly.

Step 3 (transformation $\tilde{p}_1 = p_1 + (c_0^+ - c_0^-)\tilde{\phi}_1$, representation of \mathbf{v}_0 , cell problems) We define the modified pressure

$$\tilde{p}_1 = \begin{cases} p_1 + (c_0^+ - c_0^-)\tilde{\phi}_1, & \alpha_1 = \alpha_3, \\ 0, & \alpha_1 > \alpha_3. \end{cases}$$

With this definition and due to the linearity of the equations, \mathbf{v}_0 is represented by

$$\begin{aligned} & \mathbf{v}_0(t, \mathbf{x}, \mathbf{y}) \\ &= - \sum_j \mathbf{w}_j(\mathbf{y}) \left(\partial_{x_j} p_0(t, \mathbf{x}) + \begin{cases} (c_0^+(t, \mathbf{x}) - c_0^-(t, \mathbf{x})) \partial_{x_j} \tilde{\phi}_0(t, \mathbf{x}), & \alpha_1 = \alpha_3 \\ 0, & \alpha_1 > \alpha_3 \end{cases} \right) \end{aligned}$$

with \mathbf{w}_j being solutions of the $j = 1, \dots, n$ cell problems (4.13).

Step 4 (macroscopic equation for $\bar{\mathbf{v}}_0$) We define the averaged velocity field by

$$\bar{\mathbf{v}}_0(t, \mathbf{x}) = \int_{Y_1} \mathbf{v}_0(t, \mathbf{x}, \mathbf{y}) \, d\mathbf{y}. \quad (4.21)$$

This leads directly to, [58],

$$\begin{aligned} \nabla_{\mathbf{x}} \cdot \bar{\mathbf{v}}_0 &= 0 && \text{in } (0, T) \times \Omega, \\ \bar{\mathbf{v}}_0 \cdot \boldsymbol{\nu} &= 0 && \text{on } (0, T) \times \partial\Omega, \end{aligned}$$

and, after integration with respect to \mathbf{y} , to

$$\begin{aligned} \bar{\mathbf{v}}_0(t, \mathbf{x}) &= -\mathbf{K} \left(\nabla_{\mathbf{x}} p_0(t, \mathbf{x}) \right. \\ &\quad \left. + \begin{cases} (c_0^+(t, \mathbf{x}) - c_0^-(t, \mathbf{x})) \nabla_{\mathbf{x}} \tilde{\phi}_0(t, \mathbf{x}), & \alpha_1 = \alpha_3 \\ 0, & \alpha_1 > \alpha_3 \end{cases} \right) \quad \text{in } (0, T) \times \Omega \end{aligned}$$

with permeability tensor \mathbf{K} being defined in (4.12). □

Remark 4.21 (Modeling of $\bar{\mathbf{v}}_0$). *Depending on the choice of the scale range, the homogenization of Stokes equations leads to two structurally different limit systems: In the case of $\alpha_1 = \alpha_3$, we derive an extended incompressible Darcy's law. In addition to the pressure gradient, another forcing term occurs due to the electrostatic potential $\tilde{\phi}_0$ (see Theorem 4.16 and Remark 4.18) and the distribution of the number densities c_0^\pm . In the case of $\alpha_1 > \alpha_3$, the electrostatic potential has no influence on the macroscopic velocity $\bar{\mathbf{v}}_0$, which is then determined by a standard Darcy's law.*

Homogenized Limit Problems for the Nernst-Planck Equations

The third and last step in the homogenization procedure is the investigation of the Nernst-Planck equations. Analogously to the homogenization of the Stokes equations in the previous paragraph, the treatment of the nonlinear coupling terms $c_\varepsilon^\pm \nabla \phi_\varepsilon$ and $c_\varepsilon^\pm \mathbf{v}_\varepsilon$ is again crucial and the strong convergence of the number densities c_ε^\pm is essential. Therefore, we first of all formulate the following theorem:

Theorem 4.22. *Let the a priori estimates of Theorem 4.10 be valid. Then the following two-scale limits are identified for the number densities c_ε^\pm and their gradients ∇c_ε^\pm . There exist functions $c_0^\pm(t, \mathbf{x}) \in L^2((0, T); H^1(\Omega))$ and $c_1(t, \mathbf{x}, \mathbf{y}) \in L^2((0, T) \times \Omega; H_{per}^1(Y))$ such that (up to a subsequence)*

$$\begin{aligned} c_\varepsilon^\pm(t, \mathbf{x}) &\rightarrow c_0^\pm(t, \mathbf{x}) \text{ strongly in } L^2((0, T) \times \Omega), \\ \nabla c_\varepsilon^\pm(t, \mathbf{x}) &\xrightarrow{2} \nabla_{\mathbf{x}} c_0^\pm(t, \mathbf{x}) + \nabla_{\mathbf{y}} c_1^\pm(t, \mathbf{x}, \mathbf{y}). \end{aligned}$$

Proof. The statement of strong convergence holds true due to the extension of the number densities c_ε^\pm with the properties defined in Theorem 3.7, the a priori estimates (4.9), and Aubin-Lions compact embedding lemma, [119, 132] since we restrict ourselves to the case of $\gamma = 0$. The existence of the two-scale limits follows directly from the a priori estimates (4.9) that have already been previously formulated in Theorem 4.10. \square

Remark 4.23. *The strong convergence of the number densities c_ε^\pm in $L^2(0, T; L^2(\Omega))$ enables us to pass to the limit $\varepsilon \rightarrow 0$ also in the convective and drift term of the Nernst-Planck equations (4.16).*

In the following theorem the partial differential equations which are fulfilled by the limits functions c_0^\pm according to Theorem 4.22 are presented and different ranges of the scaling parameter $(\alpha_2, \alpha_3, \beta)$ are emphasized.

Theorem 4.24. *Let $(\mathbf{v}_\varepsilon, p_\varepsilon, c_\varepsilon^\pm, \phi_\varepsilon)$ be a weak solution of Problem P_ε in the sense of Definition 4.5. Assume that $\nabla \tilde{\phi}_\varepsilon$ and v_ε two-scale converge to $\nabla_{\mathbf{x}} \tilde{\phi}_0 + \nabla_{\mathbf{y}} \tilde{\phi}_1$ and \mathbf{v}_0 , respectively as stated in Theorem 4.16 and Theorem 4.19.*

Then the two-scale limits of the number densities as stated in Theorem 4.22 satisfy the following macroscopic limit equations:

$$\begin{aligned}
& |Y_l| \partial_t c_0^\pm + \nabla_{\mathbf{x}} \cdot \left(\begin{cases} \bar{\mathbf{v}}_0 c_0^\pm, & \beta = 0 \\ 0, & \beta > 0 \end{cases} - \mathbf{D} \nabla_{\mathbf{x}} c_0^\pm \right. \\
& \quad \left. \pm \begin{cases} \mathbf{D} c_0^\pm \nabla_{\mathbf{x}} \tilde{\phi}_0, & \alpha_2 = \alpha_3 \\ 0, & \alpha_2 > \alpha_3 \end{cases} \right) = \mp |Y_l| (c_0^+ - c_0^-) \quad \text{in } (0, T) \times \Omega, \\
& \left(\begin{cases} \bar{\mathbf{v}}_0 c_0^\pm, & \beta = 0 \\ 0, & \beta > 0 \end{cases} - \mathbf{D} \nabla_{\mathbf{x}} c_0^\pm \right. \\
& \quad \left. \pm \begin{cases} \mathbf{D} c_0^\pm \nabla_{\mathbf{x}} \tilde{\phi}_0, & \alpha_2 = \alpha_3 \\ 0, & \alpha_2 > \alpha_3 \end{cases} \right) \cdot \boldsymbol{\nu} = 0 \quad \text{on } (0, T) \times \partial\Omega_N, \\
& \quad c_0^\pm = 0 \quad \text{on } (0, T) \times \partial\Omega_D.
\end{aligned}$$

Proof. Step 1 (two-scale homogenized system) We choose $\psi_0(t, \mathbf{x}) + \varepsilon \psi_1(t, \mathbf{x}, \frac{\mathbf{x}}{\varepsilon})$, $\psi_0 \in \mathcal{D}((0, T) \times \Omega)$, $\psi_1 \in \mathcal{D}((0, T) \times \Omega; C_{\text{per}}^\infty(Y))$ as test function in the Nernst-Planck equations (4.16) and obtain:

$$\begin{aligned}
& \int_0^T \left\langle \partial_t c_\varepsilon^\pm(t, \mathbf{x}), \left(\psi_0(t, \mathbf{x}) + \varepsilon \psi_1\left(t, \mathbf{x}, \frac{\mathbf{x}}{\varepsilon}\right) \right) \right\rangle_{V^{-1}, V_0^1} dt + \int_0^T \int_\Omega (-\varepsilon^\beta \mathbf{v}_\varepsilon(t, \mathbf{x}) c_\varepsilon^\pm(t, \mathbf{x}) \\
& \quad + \nabla c_\varepsilon^\pm(t, \mathbf{x}) \pm \varepsilon^{\alpha_2 - \alpha_3} c_\varepsilon^\pm(t, \mathbf{x}) \nabla \tilde{\phi}_\varepsilon(t, \mathbf{x})) \cdot \nabla \left(\psi_0(t, \mathbf{x}) + \varepsilon \psi_1\left(t, \mathbf{x}, \frac{\mathbf{x}}{\varepsilon}\right) \right) d\mathbf{x} dt \\
& = \int_0^T \int_\Omega \mp \chi_\varepsilon(\mathbf{x}) (c_\varepsilon^+(t, \mathbf{x}) - c_\varepsilon^-(t, \mathbf{x})) \left(\psi_0(t, \mathbf{x}) + \varepsilon \psi_1\left(t, \mathbf{x}, \frac{\mathbf{x}}{\varepsilon}\right) \right) d\mathbf{x} dt. \quad (*)
\end{aligned}$$

Due to convergence properties stated in Theorem 4.22, the postulates in Theorem 4.24, and the statement of Theorem 3.9, we pass to the two-scale limit $\varepsilon \rightarrow 0$, which yields

$$\begin{aligned}
& |Y_l| \int_0^T \left\langle \partial_t c_0^\pm(t, \mathbf{x}), \psi_0(t, \mathbf{x}) \right\rangle_{V^{-1}, V_0^1} dt + \int_{\Omega \times Y_l} \left(\begin{cases} -\mathbf{v}_0(t, \mathbf{x}, \mathbf{y}) c_0^\pm(t, \mathbf{x}), & \beta = 0 \\ 0, & \beta > 0 \end{cases} \right. \\
& \quad \left. + (\nabla c_0^\pm(t, \mathbf{x}) + \nabla_{\mathbf{y}} c_1^\pm(t, \mathbf{x}, \mathbf{y})) \pm \begin{cases} c_0^\pm (\nabla_{\mathbf{x}} \tilde{\phi}_0 + \nabla_{\mathbf{y}} \tilde{\phi}_1), & \alpha_2 = \alpha_3 \\ 0, & \alpha_2 > \alpha_3 \end{cases} \right) \\
& \quad \cdot (\nabla_{\mathbf{x}} \psi_0(t, \mathbf{x}) + \nabla_{\mathbf{y}} \psi_1(t, \mathbf{x}, \mathbf{y})) d\mathbf{y} d\mathbf{x} dt \\
& = \int_0^T \int_{\Omega \times Y_l} \mp (c_0^+(t, \mathbf{x}) - c_0^-(t, \mathbf{x})) \psi_0(t, \mathbf{x}) d\mathbf{y} d\mathbf{x} dt.
\end{aligned}$$

Step 2 (transformation $\tilde{c}_1^\pm := c_1^\pm \pm c_0^\pm \tilde{\phi}_1$, representation of \tilde{c}_1^\pm , cell problems)

We define

$$\tilde{c}_1^\pm = c_1^\pm \pm \begin{cases} c_0^\pm \tilde{\phi}_1, & \alpha_2 = \alpha_3 \\ 0, & \alpha_2 > \alpha_3 \end{cases}.$$

We choose $\psi_0 \equiv 0$ in (\star) , which leads, after integration by parts with respect to \mathbf{y} , to

$$\begin{aligned} -\Delta_{\mathbf{y}}\tilde{c}_1^\pm(t, \mathbf{x}, \mathbf{y}) &= 0 && \text{in } (0, T) \times \Omega \times Y_l, \\ \nabla_{\mathbf{y}}\tilde{c}_1^\pm(t, \mathbf{x}, \mathbf{y}) \cdot \boldsymbol{\nu} &= \left(-\nabla_{\mathbf{x}}c_0^\pm(t, \mathbf{x}) \right. && \text{on } (0, T) \times \Omega \times \Gamma, \\ &\quad \mp \left. \begin{cases} c_0^\pm(t, \mathbf{x})\nabla_{\mathbf{x}}\tilde{\phi}_0(t, \mathbf{x}), & \alpha_2 = \alpha_3 \\ 0, & \alpha_2 > \alpha_3 \end{cases} \right) \cdot \boldsymbol{\nu} \\ \tilde{c}_1^\pm(t, \mathbf{x}, \mathbf{y}) &&& \text{periodic in } \mathbf{y}. \end{aligned}$$

Due to the linearity of the equations, we deduce the following representations of c_1^\pm :

$$\tilde{c}_1^\pm(t, \mathbf{x}, \mathbf{y}) = \sum_j \varphi_j(\mathbf{y})\partial_{x_j}c_0^\pm(t, \mathbf{x}) \pm \begin{cases} c_0^\pm\partial_{x_j}\tilde{\phi}_0, & \alpha_2 = \alpha_3 \\ 0, & \alpha_2 > \alpha_3 \end{cases}, \quad (4.22)$$

whereby φ_j are the solution of the $j = 1, \dots, n$ standard cell problems (4.11).

Step 3 (macroscopic equation for c_0^\pm) On the other hand, if choosing $\psi_1(t, \mathbf{x}, \mathbf{y}) = 0$ in (\star) , we read off the strong problem formulation for c_0^\pm , after integration by parts with respect to \mathbf{x} and after substituting the representation (4.22) of \tilde{c}_1^\pm :

$$\begin{aligned} |Y_l|\partial_t c_0^\pm(t, \mathbf{x}) + \nabla_{\mathbf{x}} \cdot \left(\begin{cases} \bar{\mathbf{v}}_0(t, \mathbf{x})c_0^\pm(t, \mathbf{x}), & \beta = 0 \\ 0, & \beta > 0 \end{cases} - \mathbf{D}\nabla_{\mathbf{x}}c_0^\pm(t, \mathbf{x}) \right. \\ \left. \pm \begin{cases} \mathbf{D}c_0^\pm(t, \mathbf{x})\nabla_{\mathbf{x}}\tilde{\phi}_0(t, \mathbf{x}), & \alpha_2 = \alpha_3 \\ 0, & \alpha_2 > \alpha_3 \end{cases} \right) = \mp |Y_l|(c_0^+(t, \mathbf{x}) - c_0^-(t, \mathbf{x})) \quad \text{in } (0, T) \times \Omega, \\ \left(\begin{cases} \bar{\mathbf{v}}_0(t, \mathbf{x})c_0^\pm(t, \mathbf{x}), & \beta = 0 \\ 0, & \beta > 0 \end{cases} - \mathbf{D}\nabla_{\mathbf{x}}c_0^\pm(t, \mathbf{x}) \right. \\ \left. \pm \begin{cases} \mathbf{D}c_0^\pm(t, \mathbf{x})\nabla_{\mathbf{x}}\tilde{\phi}_0(t, \mathbf{x}), & \alpha_2 = \alpha_3 \\ 0, & \alpha_2 > \alpha_3 \end{cases} \right) \cdot \boldsymbol{\nu} = 0 \quad \text{on } (0, T) \times \partial\Omega_N, \\ c_0^\pm = 0 \quad \text{on } (0, T) \times \partial\Omega_D, \end{aligned}$$

with \mathbf{D} and $\bar{\mathbf{v}}_0$ being defined in (4.10) and (4.21), respectively. \square

Remark 4.25 (Modeling of c_0^\pm). *Depending on the scaling parameters, structurally different types of limit equations arise for the macroscopic transport description: In the case of $\beta = 0$ and $\alpha_2 = \alpha_3$, the transport of the number densities is given by the Nernst-Planck equations. In the case of $\beta = 0$ and $\alpha_2 > \alpha_3$, the respective equations simplify to convection-diffusion-reaction equations, whereas for $\beta > 0$ and $\alpha_2 = \alpha_3$ the drift-diffusion equation is obtained. If, on the other hand $\beta > 0$ and $\alpha_2 > \alpha_3$ holds true, the transport equations reduce even further to diffusion-reaction equations.*

4.2.3 Conclusion

In Section 4.2.2, we considered the rigorous homogenization of the Stokes-Nernst-Planck-Poisson system (4.1) by the method of two-scale convergence. In more detail, we investigated the two-scale limit $\varepsilon \rightarrow 0$ for the Neumann case (i.e. for given surface charge σ on Γ_ε) and for different ranges of the set of scale parameters $(\alpha_1, \alpha_2, \alpha_3, \beta, \gamma)$. In virtue of the general a priori estimates that have been shown for a large range of the parameter set, we derived the corresponding two-scale limits of Problem P_ε .

Depending on the scaling parameters $(\alpha_1, \alpha_2, \alpha_3, \beta, \gamma)$, we classified *conceptually different types of limit systems* that range from a nonlinear, fully coupled system of partial differential equations to a description of the transport of the number densities which completely decouples from fluid flow and electrostatic potential. For the three subproblems, the different structures of the resulting effective limit equations, which come along with the specific choice of the scaling and the parameter set, are underlined in Remark 4.18, Remark 4.21, and Remark 4.25. Subsequently, we summarize the results for different specific choices: We recover the effective model introduced in Section 2.2.4, the Darcy-Nernst-Planck-Poisson system, if we choose the parameter set $(0, 0, 0, 0, 0)$. In the case of $\alpha_2 = \alpha_3, \beta = 0$, the transport of the number densities is given by the Nernst-Planck equations. Thereby, the limits $\tilde{\phi}_0$ of the electrostatic potential and $\bar{\mathbf{v}}_0$ of the velocity field are given in Theorem 4.16 and Theorem 4.19. If $\alpha_1 = \alpha_3$, the homogenization procedure yields a fully coupled system of partial differential equation: The number densities determine the electrostatic potential and both enter the equation for the fluid flow, which itself enters the convective term of the transport equation. In the case $\alpha_2 > \alpha_3$, the electrostatic potential has no direct influence on the macroscopic number densities. The equations for the number densities simplify to a convection-diffusion-reaction equation. If, in addition, $\beta > 0$ holds, the transport equations reduce even further to a diffusion-reaction equation and the transport equations decouple completely from the fluid flow and the electric potential. If, on the other hand, $\beta = 0$, depending on the choice of α_1 , the effective equations might be coupled in one direction: If $\alpha_1 > \alpha_3$, the fluid flow is calculated separately and independently of the number densities and the electrostatic potential but enters the convective term in the transport equations. Moreover, the number densities are needed in order to determine the electrostatic potential. In Figure 4.1 and Figure 4.2, the structures of the different limit models are illustrated.

One of the essential points in the upscaling procedure is the strong convergence property of the number densities c_ε^\pm . It also provides that their two-scale limit c_0^\pm are

β \diagdown α_2	$\alpha_2 = \alpha_3$	$\alpha_2 > \alpha_3$
extended Darcy's law $\beta = 0$	Nernst-Planck equation	convection-diffusion-reaction equation
Darcy's law $\beta > 0$	drift-diffusion-reaction equation	diffusion-reaction equation

Figure 4.1: Schematic representation of upscaling results

β \diagdown α_1	$\alpha_1 = \alpha_3$	$\alpha_1 > \alpha_3$
$\beta = 0$	transport and fluid flow fully coupled	transport and fluid flow one sided coupled: fluid flow depends on transport
$\beta > 0$	transport and fluid flow one sided coupled: transport depends on fluid flow	transport and fluid flow decoupled

Figure 4.2: Schematic representation of upscaling results

independent of the oscillating, fast variable \mathbf{y} . Therefore, it is reasonable to define the following meaningful auxiliary variables $\tilde{p}_1 = p_1 + (c_0^+ - c_0^-)\tilde{\phi}_1$ and $\tilde{c}_1^\pm := c_1^\pm \pm c_0^\pm \tilde{\phi}_1$. These variables enable us to extract certain cell problems, which need to be solved in order to provide closed-form expressions for the effective macroscopic coefficients \mathbf{D} and \mathbf{K} and allow for a macroscopic representation of the homogenized limit problems. The benefit of the homogenization approach hereby lies in the fact that these averaged coefficients are directly related to the underlying geometry and transfer information to the macroscopic scale that is contained in the problem description on a microscopic level.

Note as a remark, that the families of auxiliary cell problems (4.11) in the homogenization of the electrostatic and the transport problem are identical and for this reason yield the same solutions and also the same macroscopic coefficients \mathbf{D} (up to the constant parameters that we have suppressed for the ease of presentation).

In comparison to the literature, see Section 3.2, we are able here to rigorously handle the non-stationary fully coupled nonlinear system of partial differential equations (4.1) with linear reaction rates and inhomogeneous boundary data.

4.3 Dirichlet Case

In this Section, we consider the upscaling of Problem P_ε in the case of Dirichlet boundary data for the electrostatic potential on Γ_ε , cf. (4.1i), and boundary conditions of Neumann or Dirichlet type on the outer boundary $\partial\Omega$, see the discussion in Remark 4.32. This corresponds to a physical problem in which the surface potential of the porous medium is prescribed. In applications in the geosciences this boundary condition is related to the specification of the so-called zeta potential. In order to derive macroscopic and homogenized problem descriptions, we proceed as in the Neumann case, i.e. we first state ε -independent a priori estimates. Thereafter, an extension of the problem to the whole domain Ω is defined and its upscaling is performed applying the method of two-scale convergence, see Section 3.1.3.

4.3.1 ε -independent a priori estimates in the Dirichlet case

As a first, auxiliary step, conditions are discussed such that the number densities are non-negative and bounded in $L^\infty((0, T) \times \Omega_\varepsilon)$ uniformly with respect to the scale parameter ε . Analogously to the Neumann case, the L^∞ estimate will be the basis for ε -independent a priori estimates which, on the other hand, are the starting point for the upscaling procedure.

We modify the drift term in the Nernst-Planck equation by replacing the number densities c_ε^\pm with the cut off functions

$$\tilde{c}_\varepsilon^\pm := \max(0, c_\varepsilon^\pm) \begin{cases} 0 & c_\varepsilon^\pm < 0 \\ c_\varepsilon^\pm & 0 \leq c_\varepsilon^\pm \end{cases}$$

and consequently obtain

$$\partial_t c_\varepsilon^\pm + \nabla \cdot (\varepsilon^\beta \mathbf{v}_\varepsilon c_\varepsilon^\pm - \varepsilon^\gamma \nabla c_\varepsilon^\pm \mp \varepsilon^{\alpha_2} \tilde{c}_\varepsilon^\pm \nabla \phi_\varepsilon) = \mp (c_\varepsilon^+ - c_\varepsilon^-) \quad \text{in } (0, T) \times \Omega_\varepsilon, \quad (4.23a)$$

$$(-\varepsilon^\beta \mathbf{v}_\varepsilon c_\varepsilon^\pm + \varepsilon^\gamma \nabla c_\varepsilon^\pm \pm \varepsilon^{\alpha_2} \tilde{c}_\varepsilon^\pm \nabla \phi_\varepsilon) \cdot \boldsymbol{\nu} = 0 \quad \text{in } (0, T) \times (\Gamma_\varepsilon \cup \partial\Omega), \quad (4.23b)$$

$$c_\varepsilon^\pm = c^{\pm, 0} \quad \text{in } \{t = 0\} \times \Omega_\varepsilon. \quad (4.23c)$$

The modified system consisting of (4.23), (4.1a)–(4.1c), and (4.1h), (4.1j)–(4.1k) is referred here as Problem \tilde{P}_ε . The weak solution of Problem \tilde{P}_ε is defined analogously to Definition 4.5.

Remark 4.26. *The weak solution of Problem \tilde{P}_ε is also a weak solution of Problem P_ε . Furthermore, all non-negative weak solutions of Problem P_ε are also weak solutions of Problem \tilde{P}_ε . As stated in Theorem 4.6 Problem P_ε has a unique solution for each ε which is the non-negative one. Therefore both problems are equivalent. However, for the proof of uniqueness higher regularities of the number densities or of the electrostatic potential, respectively, have to be postulated. For these we cannot guarantee uniformity in the scale parameter ε , compare also the proof of Theorem 2.31 and Remark 4.29.*

Theorem 4.27. *Let $(\mathbf{v}_\varepsilon, p_\varepsilon, \phi_\varepsilon, c_\varepsilon^+, c_\varepsilon^-)$ be a weak solution of Problem \tilde{P}_ε in the Dirichlet case. Let furthermore Assumption 4.4 hold. Then the number densities are non-negative uniformly in ε .*

Proof. The proof of Theorem 4.27 is analogous to the proof of Theorem 4.7. However, using $(c_\varepsilon^\pm)_- := \min(0, c_\varepsilon^\pm)$ as a test function, the drift term is evaluated directly due to the definition of $\tilde{c}_\varepsilon^\pm$:

$$\pm \int_{\Omega_\varepsilon} \varepsilon^{\alpha_2} \tilde{c}_\varepsilon^\pm \nabla \phi_\varepsilon \cdot \nabla (c_\varepsilon^\pm)_- = 0.$$

□

Remark 4.28. *Considering the modified Problem \tilde{P}_ε also in the Neumann case, see Section 4.2, the requirement of the additional constraints in Theorem 4.7 is not necessary.*

Remark 4.29. *The crucial point in the Dirichlet case is the following: For the original problem P_ε , in the Dirichlet case, an ε -independent estimate can not be achieved applying the methods used in the Neumann case. Especially the advantage in handling the drift term using integration by parts which has been used several times in the Neumann case, cannot be applied in the same way for the Dirichlet case. This is due to the change in the boundary conditions, especially on Γ_ε .*

In the Dirichlet case, the drift term could be estimated as follows:

$$\begin{aligned} & \int_{\Omega_\varepsilon} \varepsilon^{\alpha_2} c_\varepsilon^\pm \nabla \phi_\varepsilon \cdot \nabla (c_\varepsilon^\pm)^{2\alpha+1} \, d\mathbf{x} \\ &= \int_{\Omega_\varepsilon} \varepsilon^{\alpha_2} \frac{2\alpha+1}{\alpha+1} (c_\varepsilon^\pm)^{\alpha+1} \nabla \phi_\varepsilon \cdot \nabla (c_\varepsilon^\pm)^{\alpha+1} \, d\mathbf{x} \\ &\leq \varepsilon^{\alpha_2} \frac{2\alpha+1}{\alpha+1} \| (c_\varepsilon^\pm)^{\alpha+1} \|_{L^3(\Omega_\varepsilon)} \| \nabla \phi_\varepsilon \|_{L^6(\Omega_\varepsilon)} \| \nabla (c_\varepsilon^\pm)^{\alpha+1} \|_{L^2(\Omega_\varepsilon)} \end{aligned}$$

Applying the interpolation inequality $\|\varphi\|_{L^3(\Omega_\varepsilon)} \leq C\|\varphi\|_{L^2(\Omega_\varepsilon)}^{1/2}\|\nabla\varphi\|_{L^2(\Omega_\varepsilon)}^{1/2}$ and Young's inequality (4/3, 4), we obtain

$$\begin{aligned} & \int_{\Omega_\varepsilon} \varepsilon^{\alpha_2} c_\varepsilon^\pm \nabla\phi_\varepsilon \cdot \nabla(c_\varepsilon^\pm)^{2\alpha+1} \, d\mathbf{x} \\ & \leq \varepsilon^{\alpha_2} \frac{2\alpha+1}{\alpha+1} \|(c_\varepsilon^\pm)^{\alpha+1}\|_{L^3(\Omega_\varepsilon)} \|\nabla\phi_\varepsilon\|_{L^6(\Omega_\varepsilon)} \|\nabla(c_\varepsilon^\pm)^{\alpha+1}\|_{L^2(\Omega_\varepsilon)} \\ & \leq \varepsilon^{\alpha_2} (2\alpha+1)(\alpha+1)^2 C \|(c_\varepsilon^\pm)^{\alpha+1}\|_{L^2(\Omega_\varepsilon)}^2 \|\nabla\phi_\varepsilon\|_{L^6(\Omega_\varepsilon)}^4 + \delta\varepsilon^{\alpha_2} \frac{2\alpha+1}{(\alpha+1)^2} \|\nabla(c_\varepsilon^\pm)^{\alpha+1}\|_{L^2(\Omega_\varepsilon)}^2 \end{aligned}$$

Proceeding the Moser iteration as in the proof of Theorem 4.9 or Theorem 2.24, the gradient term can be sorbed in every iteration step on the left hand side. The respective constants C_j in the Moser iteration are given in the Dirichlet case with the following dependencies: $C_j = C_j(\varepsilon^{\alpha_2}, \|\nabla\phi_\varepsilon\|_{L^\infty(0,T;L^6(\Omega_\varepsilon))}^4, (1+\alpha_j)^m)$, $m \leq 4$. With the same arguments as in the proof of Theorem 2.24, the overall constant $C_{Moser} := \prod_{j=0}^{\infty} C_S^{\frac{1}{2 \cdot (5/3)^{j+1}}} C_j^{\frac{1}{2 \cdot (5/3)^j}}$ remains bounded for fixed $\varepsilon > 0$. Moreover, the dependency on ε^{α_2} does not cause any problem, if additionally $\alpha_2 \geq 0$ holds. Note further, that the term $\|\nabla\phi_\varepsilon\|_{L^\infty(0,T;L^6(\Omega_\varepsilon))}^4$ is well defined for each $\varepsilon > 0$ according the definition of weak solutions of Problem P_ε in Definition 4.5. However, we cannot guarantee that this term is bounded ε -independent. This question and related investigations on higher regularity, which is uniform with respect to the scale parameter ε , are in fact still unsolved problems and also quite actual research topics, see, e.g., [61, 131].

One possibility to ensure that boundedness of the number densities in $L^\infty((0,T) \times \Omega_\varepsilon)$ remains true also in the Dirichlet case is to require additional constraints such as volume additivity, see Remark 2.11. In combination with non-negativity, this guarantees ε -independent boundedness of the number densities c_ε^\pm . Moreover, note as a remark, that volume additivity together with non-negativity is equivalent to boundedness in $L^\infty((0,T) \times \Omega_\varepsilon)$. Under the restriction of volume additivity, an obvious reduction of the considered system of equations can be undertaken: Applying the relation $c_\varepsilon^- = 1 - c_\varepsilon^+$, makes the equation for c_ε^- redundant.

Due the considerations in Remark 4.29, we obtain directly the following Theorem.

Theorem 4.30. *Let $(\mathbf{v}_\varepsilon, p_\varepsilon, \phi_\varepsilon, c_\varepsilon^+, c_\varepsilon^-)$ be a weak solution of Problem \tilde{P}_ε in the Dirichlet case. Let furthermore Assumption 4.4, Theorem 4.27, and the constraint of volume additivity, cf. Remark 2.11, hold. Then, the number densities are bounded from above uniformly in ε .*

Remark 4.31. *Considering the volume additivity constraint also in the Neumann case, see Section 4.2, the requirement of the additional constraints in Theorem 4.9 is not necessary.*

Before stating ε -independent a priori estimates in the Dirichlet case that are uniform with respect to the scale parameter ε , we define the transformed electrostatic potential $\phi_\varepsilon^{\text{hom}} := \phi_\varepsilon - g$ with $g|_{\Gamma_\varepsilon} = \phi_{D,\Gamma_\varepsilon}$ and $g|_{\partial\Omega} = \phi_{D,\partial\Omega}$ due to technical reasons.

Remark 4.32. 1. *In the case of $\partial\Omega_D = \emptyset$ or in the case of $\phi_{D,\Gamma_\varepsilon} = \phi_{D,\partial\Omega} = \text{const.}$ it holds $g \equiv \phi_{D,\Gamma_\varepsilon}$ on Ω . According to Assumption 4.4, we obtain $\Delta g = 0$.*

2. *In the case of $\phi_{D,\Gamma_\varepsilon} \neq \phi_{D,\partial\Omega}$, Δg has to be well defined even for $\varepsilon \rightarrow 0$.*

For ease of presentation, we only consider item 1 in Remark 4.32 with $\partial\Omega_D \neq \emptyset$ for the remainder of this chapter, see also Assumption 4.4. As a consequence, $\phi_\varepsilon^{\text{hom}}$ fulfills the following set of equations:

$$-\varepsilon^{\alpha_3} \Delta \phi_\varepsilon^{\text{hom}} = (c_\varepsilon^+ - c_\varepsilon^-) \quad \text{in } (0, T) \times \Omega_\varepsilon, \quad (4.24a)$$

$$\phi_\varepsilon^{\text{hom}} = 0 \quad \text{in } (0, T) \times \Gamma_\varepsilon \cup \partial\Omega_D, \quad (4.24b)$$

$$\varepsilon^{\alpha_3} \nabla \phi_\varepsilon^{\text{hom}} \cdot \boldsymbol{\nu} = 0 \quad \text{in } (0, T) \times \partial\Omega_N. \quad (4.24c)$$

Theorem 4.33. *Let Assumption 2.9 be valid. The following a priori estimates hold in the case of Dirichlet boundary conditions on Γ_ε for the electrostatic potential*

$$\varepsilon^{\alpha_3-2} \|\phi_\varepsilon^{\text{hom}}\|_{L^2((0,T) \times \Omega_\varepsilon)} + \varepsilon^{\alpha_3-1} \|\nabla \phi_\varepsilon^{\text{hom}}\|_{L^2((0,T) \times \Omega_\varepsilon)} \leq C. \quad (4.25)$$

In the case of $\alpha_1 - \alpha_3 + 1 \geq 0$, it holds

$$\|\mathbf{v}_\varepsilon\|_{L^2((0,T) \times \Omega_\varepsilon)} + \varepsilon \|\nabla \mathbf{v}_\varepsilon\|_{L^2((0,T) \times \Omega_\varepsilon)} \leq C. \quad (4.26)$$

In the case of $\beta \geq 0$, $\gamma \geq 0$, $\alpha_2 - (\alpha_3 - 1) \geq 0$, and $2\alpha_2 - 2(\alpha_3 - 1) - \gamma \geq 0$, it holds

$$\max_{0 \leq t \leq T} \sum_{\pm} \|c_\varepsilon^\pm\|_{L^2(\Omega_\varepsilon)} + \varepsilon^{\gamma/2} \sum_{\pm} \|\nabla c_\varepsilon^\pm\|_{L^2((0,T) \times \Omega_\varepsilon)} + \sum_{\pm} \|\partial_t c_\varepsilon^\pm\|_{L^2(0,T;V^{-1}(\Omega_\varepsilon))} \leq C. \quad (4.27)$$

In (4.25), (4.26) and (4.27), $C \in \mathbb{R}_+$ is a constant independent of ε .

Proof. We test equation (4.24a) with the translated potential $\phi_\varepsilon^{\text{hom}}$ and use the Poincaré inequality (4.4).

This leads to

$$\varepsilon^{\alpha_3} \|\nabla \phi_\varepsilon^{\text{hom}}\|_{L^2(\Omega_\varepsilon)}^2 \leq \|c_\varepsilon^+ - c_\varepsilon^-\|_{L^2(\Omega_\varepsilon)} \|\phi_\varepsilon^{\text{hom}}\|_{L^2(\Omega_\varepsilon)} \leq \|c_\varepsilon^+ - c_\varepsilon^-\|_{L^2(\Omega_\varepsilon)} \varepsilon C_P \|\nabla \phi_\varepsilon^{\text{hom}}\|_{L^2(\Omega_\varepsilon)},$$

which directly results in

$$\varepsilon^{\alpha_3-1} \|\nabla \phi_\varepsilon^{\text{hom}}\|_{L^2(\Omega_\varepsilon)} \leq C_P \|c_\varepsilon^+ - c_\varepsilon^-\|_{L^2(\Omega_\varepsilon)} \leq C.$$

Here, we have used the boundedness of the number densities c_ε^\pm provided by Theorem 4.9 with C being a constant independent of ε . Using again the Poincaré inequality (4.4), we obtain

$$\varepsilon^{\alpha_3-2} \|\phi_\varepsilon^{\text{hom}}\|_{L^2(\Omega_\varepsilon)} \leq C.$$

After integration with respect to time, the desired statement (4.25) follows directly. Furthermore, by means of Theorem 4.9, the constant C remains bounded ε -independently.

The rest of the statement in Theorem 4.33 follows analogously to the proof of Theorem 4.10. Only, in the energy estimate of the number densities c_ε^\pm , the drift term is estimated directly via

$$\begin{aligned} & \int_{\Omega_\varepsilon} \varepsilon^{\alpha_2} c_\varepsilon^\pm \nabla \phi_\varepsilon \cdot \nabla c_\varepsilon^\pm \, d\mathbf{x} \\ & \leq \varepsilon^{\alpha_2 - (\alpha_3 - 1) - \gamma/2} \|c_\varepsilon^\pm\|_{L^\infty(\Omega_\varepsilon)} \varepsilon^{(\alpha_3 - 1)} \|\nabla \phi_\varepsilon\|_{L^2(\Omega_\varepsilon)} \varepsilon^{\gamma/2} \|\nabla c_\varepsilon^\pm\|_{L^2(\Omega_\varepsilon)} \\ & \leq C \varepsilon^{2\alpha_2 - 2(\alpha_3 - 1) - \gamma} \|c_\varepsilon^\pm\|_{L^\infty(\Omega_\varepsilon)}^2 \varepsilon^{2(\alpha_3 - 1)} \|\nabla \phi_\varepsilon\|_{L^2(\Omega_\varepsilon)}^2 + \delta \varepsilon^\gamma \|\nabla c_\varepsilon^\pm\|_{L^2(\Omega_\varepsilon)}^2. \end{aligned}$$

Since due to the definition of the translated electrostatic potential and Theorem 4.33, it holds $\varepsilon^{\alpha_3-1} \|\nabla \phi_\varepsilon\|_{L^2(\Omega_\varepsilon)} = \varepsilon^{\alpha_3-1} \|\nabla \phi_\varepsilon^{\text{hom}}\|_{L^2(\Omega_\varepsilon)} \leq C$, the estimate (4.27) follows as in the proof of Theorem 4.10. \square

The a priori estimates that are derived in Theorem 4.33 are at first only valid within the perforated domain Ω_ε . Compare also the Neumann case which has been treated previously in Section 4.2.2. Therefore, an extension of the functions \mathbf{v}_ε , $\nabla \mathbf{v}_\varepsilon$, p_ε , ϕ_ε , $\nabla \phi_\varepsilon$, c_ε^\pm , $\partial_t c_\varepsilon^\pm$, and ∇c_ε^\pm is done analogously to Section 4.2.2 in such a way, that the perforated domain Ω_ε can be replaced by Ω in all the a priori estimates of Theorem 4.33. For ease of presentation, we suppress again the notation of the extensions in the following and proceed with the homogenization of the SNPP system in the Dirichlet case.

4.3.2 Homogenization in the Dirichlet case

In this section, we determine the limit $\varepsilon \rightarrow 0$ in the ε -scaled Stokes-Nernst-Planck-Poisson system (4.1). We consider the Dirichlet case, i.e. boundary conditions of Dirichlet type for the electrostatic potential on the interior boundary Γ_ε , and different choices of scaling $(\alpha_1, \alpha_2, \alpha_3, \beta, \gamma)$. We apply the method of two-scale convergence (see Section 3.1.3) in order to identify the macroscopic limit equations, which describe the effective fluid flow, the transport of the number densities, and the behavior of the electrostatic potential. As in Section 4.2.2, the homogenization is performed in three steps: The three subproblems Poisson's equation, Stokes equations and Nernst-Planck equations are considered separately and consecutively. For each of these subproblems, a two-scale homogenized system is derived as a first step. As in Section 4.2.2, we assume that $\gamma = 0$ and make use of the strong convergence property of the number densities in nonlinear terms $c_\varepsilon^\pm \nabla \Phi_\varepsilon$ and in the convective term $\mathbf{v}_\varepsilon c_\varepsilon^\pm$. This is followed by the definition of auxiliary cell problems and the explicit representation of certain limit functions in terms of solutions of these cell problems and of further limit functions due to linear relations. Finally, macroscopic equations for the two-scale limits are derived defining effective tensors. For each subproblem, we discuss the structure of the macroscopic limit equations for different choices of the parameter set $(\alpha_1, \alpha_2, \alpha_3, \beta, \gamma)$. In addition to the definition of auxiliary cell problems in Definition 4.13, we introduce the following family of cell problems.

Definition 4.34. *We define the following cell problem*

$$-\Delta_{\mathbf{y}} \varphi(\mathbf{y}) = 1 \quad \text{in } Y_l, \quad (4.28a)$$

$$\varphi(\mathbf{y}) = 0 \quad \text{on } \Gamma, \quad (4.28b)$$

$$\varphi \quad \text{periodic in } \mathbf{y}. \quad (4.28c)$$

Homogenized Limit Problems for Poisson's Equation

The first step of the homogenization procedure is the investigation of Poisson's equation. Similar to the Neumann case, cf. Section 4.2.2, we define $\tilde{\phi}_\varepsilon := \varepsilon^{\alpha_3-2} \phi_\varepsilon^{\text{hom}}$ which fulfills the following set of equations:

$$-\varepsilon^2 \Delta \tilde{\phi}_\varepsilon = c_\varepsilon^+ - c_\varepsilon^- \quad \text{in } (0, T) \times \Omega_\varepsilon, \quad (4.29)$$

$$\tilde{\phi}_\varepsilon = 0 \quad \text{on } (0, T) \times \Gamma_\varepsilon \cup \partial\Omega_D, \quad (4.30)$$

$$\varepsilon^2 \nabla \tilde{\phi}_\varepsilon \cdot \boldsymbol{\nu} = 0 \quad \text{on } (0, T) \times \partial\Omega_N. \quad (4.31)$$

We now state the structure of the two-scale limit of the rescaled electrostatic potential $\tilde{\phi}_\varepsilon$ as well as the corresponding limit equation.

Theorem 4.35. *Let the a priori estimates of Theorem 4.33 be valid. Then, the following two-scale limits are identified for the electrostatic potential $\tilde{\phi}_\varepsilon$ and the gradient $\varepsilon \nabla \tilde{\phi}_\varepsilon$: There exists $\tilde{\phi}_0 \in L^2((0, T) \times \Omega; H^1_{\text{per}}(Y))$ such that, up to a subsequence,*

$$\begin{aligned}\tilde{\phi}_\varepsilon(t, \mathbf{x}) &\xrightarrow{2} \tilde{\phi}_0(t, \mathbf{x}, \mathbf{y}), \\ \varepsilon \nabla \tilde{\phi}_\varepsilon(t, \mathbf{x}) &\xrightarrow{2} \nabla_{\mathbf{y}} \tilde{\phi}_0(t, \mathbf{x}, \mathbf{y}).\end{aligned}$$

Proof. We consider the estimate (4.25) in Theorem 4.33 which implies

$$\|\tilde{\phi}_\varepsilon\|_{L^2(\Omega)} + \varepsilon \|\nabla \tilde{\phi}_\varepsilon\|_{L^2(\Omega)} \leq C.$$

Theorem 3.4 then ensures the existence of the two-scale limit functions. \square

Theorem 4.36. *Let $(\mathbf{v}_\varepsilon, p_\varepsilon, c_\varepsilon^\pm, \phi_\varepsilon)$ be a weak solution of Problem P_ε in the sense of Definition 4.5. Assume that c_ε^\pm converge strongly to c_0^\pm in $L^2((0, T) \times \Omega)$. Then, the two-scale limit of $\tilde{\phi}_\varepsilon$ due to Theorem 4.35 satisfies the following macroscopic limit equation:*

$$\bar{\tilde{\phi}}_0 = \left(\int_{Y_l} \varphi_j d\mathbf{y} \right) (c_0^+ - c_0^-).$$

Proof. Step 1 (two-scale homogenized system) In order to prove Theorem 4.36, we choose $\psi(t, \mathbf{x}, \frac{\mathbf{x}}{\varepsilon})$, $\psi \in \mathcal{D}((0, T) \times \Omega; C^\infty_{\text{per}}(Y))$ as test function in (4.29) which leads to

$$\begin{aligned}& \int_0^T \int_\Omega \varepsilon \nabla \tilde{\phi}_\varepsilon(t, \mathbf{x}) \cdot \varepsilon \nabla \psi \left(t, \mathbf{x}, \frac{\mathbf{x}}{\varepsilon} \right) d\mathbf{x} dt \\ &= \int_0^T \int_\Omega (c_\varepsilon^+(t, \mathbf{x}) - c_\varepsilon^-(t, \mathbf{x})) \psi \left(t, \mathbf{x}, \frac{\mathbf{x}}{\varepsilon} \right) d\mathbf{x} dt.\end{aligned}$$

We then pass to the two-scale limit $\varepsilon \rightarrow 0$ using the properties we have stated in Theorem 4.35:

$$\begin{aligned}& \int_0^T \int_{\Omega \times Y_l} \left(\nabla_{\mathbf{y}} \tilde{\phi}_0(t, \mathbf{x}, \mathbf{y}) \cdot \nabla_{\mathbf{y}} \psi(t, \mathbf{x}, \mathbf{y}) \right) d\mathbf{y} d\mathbf{x} dt \\ &= \int_0^T \int_{\Omega \times Y_l} (c_0^+(t, \mathbf{x}) - c_0^-(t, \mathbf{x})) \psi(t, \mathbf{x}) d\mathbf{y} d\mathbf{x} dt.\end{aligned}$$

Step 3 (macroscopic equation for $\tilde{\phi}_0$) After integration by parts with respect to \mathbf{y} , the strong formulation for $\tilde{\phi}_0$ may be read off:

$$\begin{aligned} -\Delta_{\mathbf{y}}\tilde{\phi}_0(t, \mathbf{x}, \mathbf{y}) &= c_0^+(t, \mathbf{x}) - c_0^-(t, \mathbf{x}) && \text{in } (0, T) \times \Omega \times Y_l, \\ \tilde{\phi}_0 &= 0 && \text{in } (0, T) \times \Omega \times \Gamma, \\ \tilde{\phi}_0 &&& \text{periodic in } \mathbf{y}. \end{aligned}$$

Inserting the cell problem (4.28), we get

$$\bar{\phi}_0 = \int_{Y_l} \tilde{\phi}_0 \, d\mathbf{y} = \left(\int_{Y_l} \varphi \, d\mathbf{y} \right) (c_0^+ - c_0^-).$$

□

Remark 4.37 (Modeling of ϕ_0). *The macroscopic representation of $\bar{\phi}_0$ is directly related to the macroscopic number densities c_0^\pm .*

In the case of $\alpha_3 = 2$, it holds $\tilde{\phi}_\varepsilon = \phi_\varepsilon^{hom} = \phi_\varepsilon - \phi_D$ and therefore

$$\bar{\phi}_0 = \overline{\phi_0^{hom} + \phi_D} = \int_{Y_l} \phi_0^{hom} + \phi_D \, d\mathbf{y} = \left(\int_{Y_l} \varphi \, d\mathbf{y} \right) (c_0^+ - c_0^-) + |Y_l|\phi_D.$$

The case of $\alpha_3 < 1$ implies that ϕ_ε and $\nabla\phi_\varepsilon$ converge to ϕ_D and zero, respectively. However, for any parameter α_3 a meaningful effective equation is derived for the limit $\bar{\phi}_0$ of $\tilde{\phi}_\varepsilon$.

Homogenized Limit Problems for Stokes Equation

The next step in the homogenization procedure is the investigation of Stokes equations. Here, the treatment of the nonlinear coupling terms $c_\varepsilon^\pm \nabla\phi_\varepsilon$ is crucial. To ensure that the two-scale limit $\varepsilon \rightarrow 0$ can be determined, strong convergence of the number densities c_ε^\pm is required.

Theorem 4.38. *Let the a priori estimates of Theorem 4.33 be valid. Then, the following two-scale limits are identified for the velocity field \mathbf{v}_ε and the gradient $\varepsilon\nabla\mathbf{v}_\varepsilon$: There exists $\mathbf{v}_0 \in L^2((0, T) \times \Omega; H_{per}^1(Y))$ such that, up to a subsequence,*

$$\begin{aligned} \mathbf{v}_\varepsilon(t, \mathbf{x}) &\xrightarrow{2} \mathbf{v}_0(t, \mathbf{x}, \mathbf{y}), \\ \varepsilon\nabla\mathbf{v}_\varepsilon(t, \mathbf{x}) &\xrightarrow{2} \nabla_{\mathbf{y}}\mathbf{v}_0(t, \mathbf{x}, \mathbf{y}). \end{aligned}$$

Furthermore, the following two-scale limit is identified for the pressure field p_ε : There exists $p_0(t, \mathbf{x}, \mathbf{y}) \in L^2((0, T) \times \Omega \times Y)$, such that up to a subsequence,

$$p_\varepsilon(t, \mathbf{x}) \xrightarrow{2} p_0(t, \mathbf{x}, \mathbf{y}).$$

Proof. We consider the estimate (4.26) in Theorem 4.33 which implies according to Theorem 3.4 the existence of the two-scale limit \mathbf{v}_0 as stated in Theorem 4.38. The convergence for p_ε follows as in Theorem 4.19 and is even strong in $L^2(\Omega)/\mathbb{R}$, see, for example, [4, 58]. \square

Theorem 4.39. *Let $(\mathbf{v}_\varepsilon, p_\varepsilon, c_\varepsilon^\pm, \phi_\varepsilon)$ be a weak solution of Problem P_ε in the sense of Definition 4.5. Assume that c_ε^\pm converge strongly to c_0^\pm in $L^2((0, T) \times \Omega)$. Then, the two-scale limit of \mathbf{v}_ε according to Theorem 4.38 satisfies the following macroscopic limit equations:*

$$\begin{aligned} \bar{\mathbf{v}}_0 &= \int_{Y_l} \mathbf{v}_0 \, d\mathbf{y} = -\mathbf{K} \nabla_{\mathbf{x}} p_0 && \text{in } (0, T) \times \Omega, \\ \nabla_{\mathbf{x}} \cdot \bar{\mathbf{v}}_0 &= 0 && \text{in } (0, T) \times \Omega, \\ \bar{\mathbf{v}}_0 \cdot \boldsymbol{\nu} &= 0 && \text{on } (0, T) \times \partial\Omega. \end{aligned}$$

Proof. Step 1 (p_0 independent of \mathbf{y}) We choose $\varepsilon\psi(t, \mathbf{x}, \frac{\mathbf{x}}{\varepsilon})$, $\psi \in \mathcal{D}((0, T) \times \Omega; C_{\text{per}}^\infty(Y))$ as test function in (4.15) and obtain, analogously to the proof of Theorem 4.20, that $p_0 = p_0(t, \mathbf{x})$ holds.

Step 2 (two-scale homogenized system) We choose $\psi(t, \mathbf{x}, \frac{\mathbf{x}}{\varepsilon}) \in \mathcal{V}$ as test function in (4.15). As in the proof of Theorem 4.20, this leads in the two-scale limit $\varepsilon \rightarrow 0$ to

$$\begin{aligned} & \int_0^T \int_{\Omega \times Y_l} \nabla_{\mathbf{y}} \mathbf{v}_0 \cdot \nabla_{\mathbf{y}} \psi - p_0 \nabla_{\mathbf{x}} \cdot \psi \, d\mathbf{y} \, d\mathbf{x} \, dt \\ &= \left\{ \begin{array}{ll} \int_0^T \int_{\Omega \times Y_l} -(c_0^+ - c_0^-) \nabla_{\mathbf{y}} \phi_0 \psi \, d\mathbf{y} \, d\mathbf{x} \, dt, & \alpha_1 = \alpha_3 - 1 \\ 0, & \alpha_1 > \alpha_3 - 1 \end{array} \right\} \end{aligned}$$

We follow exactly the proof of Theorem 4.20. Integration by parts finally results in

$$\begin{aligned} & -\Delta_{\mathbf{y}} \mathbf{v}_0(t, \mathbf{x}, \mathbf{y}) + \nabla_{\mathbf{x}} p_0(t, \mathbf{x}) + \nabla_{\mathbf{y}} p_1(t, \mathbf{x}, \mathbf{y}) \\ &= \left\{ \begin{array}{ll} -(c_0^+(t, \mathbf{x}) - c_0^-(t, \mathbf{x})) \nabla_{\mathbf{y}} \tilde{\phi}_0(t, \mathbf{x}, \mathbf{y}), & \alpha_1 = \alpha_3 - 1 \\ 0, & \alpha_1 > \alpha_3 - 1 \end{array} \right\}. \end{aligned}$$

Step 3 (transformation $\tilde{p}_1 = p_1 + (c_0^+ - c_0^-)\tilde{\phi}_0$, representation of \mathbf{v}_0 , cell problems) In the case of $\alpha_1 = \alpha_3 - 1$, we define the modified pressure $\tilde{p}_1 = p_1 + (c_0^+ - c_0^-)\tilde{\phi}_0$ analogously to the proof of Theorem 4.20. This allows to represent the velocity field \mathbf{v}_0 by

$$\mathbf{v}_0(t, \mathbf{x}, \mathbf{y}) = - \sum_j \mathbf{w}_j(\mathbf{y}) \partial_{x_j} p_0(t, \mathbf{x})$$

with \mathbf{w}_j being solutions of the $j = 1, \dots, n$ cell problems (4.13).

Step 4 (macroscopic equation for $\bar{\mathbf{v}}_0$) By standard arguments [58] and similar to the proof of Theorem 4.20, we determine a standard incompressible Darcy's Law $\bar{\mathbf{v}}_0 = -\mathbf{K}\nabla p_0$ which finishes the proof of Theorem 4.39. \square

Remark 4.40 (Modeling of $\bar{\mathbf{v}}_0$). *The fluid flow is determined by a standard Darcy's law. There is no direct coupling to the electrostatic potential, since it is only present in the modified pressure term \tilde{p}_1 .*

Homogenized Limit Problems for the Nernst-Planck Equations

The third and last step in the homogenization procedure is the investigation of the Nernst-Planck equations. Here, we again make use of the strong convergence property of the number densities c_ε^\pm .

Theorem 4.41. *Let the estimates of Theorem 4.33 be valid. Then, the following two-scale limits are identified for the number densities c_ε^\pm and their gradients ∇c_ε^\pm : There exist functions $c_0(t, \mathbf{x}) \in L^2((0, T); H^1(\Omega))$ and $c_1(t, \mathbf{x}, \mathbf{y}) \in L^2((0, T) \times \Omega; H_{per}^1(Y))$ such that (up to a subsequence)*

$$\begin{aligned} c_\varepsilon^\pm(t, \mathbf{x}) &\rightarrow c_0(t, \mathbf{x}) \text{ strongly in } L^2((0, T) \times \Omega), \\ \nabla c_\varepsilon^\pm(t, \mathbf{x}) &\xrightarrow{2} \nabla_{\mathbf{x}} c_0(t, \mathbf{x}) + \nabla_{\mathbf{y}} c_1^\pm(t, \mathbf{x}, \mathbf{y}). \end{aligned}$$

Proof. The statement of strong convergence holds true due to the extension of the number densities c_ε^\pm with the properties defined in Theorem 3.7 and Aubin-Lions compact embedding lemma. The existence of the two-scale limit directly follow from Theorem 4.33. \square

Theorem 4.42. *Let $(\mathbf{v}_\varepsilon, p_\varepsilon, c_\varepsilon^\pm, \phi_\varepsilon)$ be a weak solution of Problem P_ε in the sense of Definition 4.5. Assume that $\varepsilon\nabla\phi_\varepsilon$ and v_ε two-scale converges as stated in Theorem 4.35*

and Theorem 4.38. Then, the two-scale limits of the number densities as stated in Theorem 4.41 satisfy the following macroscopic limit equations:

$$\begin{aligned} |Y_l| \partial_t c_0^\pm + \nabla_{\mathbf{x}} \cdot \left(\begin{cases} \bar{\mathbf{v}}_0 c_0^\pm, & \beta = 0 \\ 0, & \beta > 0 \end{cases} - \mathbf{D} \nabla_{\mathbf{x}} c_0^\pm \right) &= \mp |Y_l| (c_0^+ - c_0^-) && \text{in } (0, T) \times \Omega, \\ \left(\begin{cases} \bar{\mathbf{v}}_0 c_0^\pm, & \beta = 0 \\ 0, & \beta > 0 \end{cases} - \mathbf{D} \nabla_{\mathbf{x}} c_0^\pm \right) \cdot \boldsymbol{\nu} &= 0 && \text{on } (0, T) \times \partial\Omega_N, \\ c_0^\pm &= 0 && \text{on } (0, T) \times \partial\Omega_D. \end{aligned}$$

Proof. Step 1 (two-scale homogenized system) We choose $\psi_0(t, \mathbf{x}) + \varepsilon \psi_1\left(t, \mathbf{x}, \frac{\mathbf{x}}{\varepsilon}\right)$, $\psi_0 \in \mathcal{D}((0, T) \times \Omega)$, $\psi_1 \in \mathcal{D}((0, T) \times \Omega; C_{\text{per}}^\infty(Y))$ as test functions in the Nernst-Planck equations (4.2c).

$$\begin{aligned} &\int_0^T \left\langle \partial_t c_\varepsilon^\pm(t, \mathbf{x}), \left(\psi_0(t, \mathbf{x}) + \varepsilon \psi_1\left(t, \mathbf{x}, \frac{\mathbf{x}}{\varepsilon}\right) \right) \right\rangle_{V^{-1}, V_0^1} dt \int_0^T \int_\Omega (-\varepsilon^\beta \mathbf{v}_\varepsilon(t, \mathbf{x}) c_\varepsilon^\pm(t, \mathbf{x}) \\ &\quad + \varepsilon^\gamma \nabla c_\varepsilon^\pm(t, \mathbf{x}) \pm \varepsilon^{\alpha_2} c_\varepsilon^\pm \nabla \phi_\varepsilon(t, \mathbf{x})) \cdot \nabla \left(\psi_0(t, \mathbf{x}) + \varepsilon \psi_1\left(t, \mathbf{x}, \frac{\mathbf{x}}{\varepsilon}\right) \right) d\mathbf{x} dt \\ &= \mp \int_0^T \int_\Omega (c_\varepsilon^+(t, \mathbf{x}) - c_\varepsilon^-(t, \mathbf{x})) \left(\psi_0(t, \mathbf{x}) + \varepsilon \psi_1\left(t, \mathbf{x}, \frac{\mathbf{x}}{\varepsilon}\right) \right) d\mathbf{x} dt. \end{aligned}$$

Passage to the limit $\varepsilon \rightarrow 0$ yields as in the proof of Theorem 4.24

$$\begin{aligned} &|Y_l| \int_0^T \left\langle \partial_t c_0^\pm(t, \mathbf{x}), \psi_0(t, \mathbf{x}) \right\rangle_{V^{-1}, V_0^1} dt + \left(\begin{cases} -\mathbf{v}_0(t, \mathbf{x}, \mathbf{y}) c_0^\pm(t, \mathbf{x}), & \beta = 0 \\ 0, & \beta > 0 \end{cases} \right. \\ &\quad \left. + (\nabla c_0^\pm(t, \mathbf{x}) + \nabla_{\mathbf{y}} c_1^\pm(t, \mathbf{x}, \mathbf{y})) \pm \begin{cases} c_0^\pm \nabla_{\mathbf{y}} \phi_0(t, \mathbf{x}, \mathbf{y}), & \alpha_2 = \alpha_3 - 1 \\ 0, & \alpha_2 > \alpha_3 - 1 \end{cases} \right) \\ &\quad \cdot (\nabla_{\mathbf{x}} \psi_0(t, \mathbf{x}) + \nabla_{\mathbf{y}} \psi_1(t, \mathbf{x}, \mathbf{y})) d\mathbf{y} d\mathbf{x} dt \\ &= \int_0^T \int_{\Omega \times Y_l} R_0^\pm(c_0^+(t, \mathbf{x}), c_0^-(t, \mathbf{x})) \psi_0(t, \mathbf{x}) d\mathbf{y} d\mathbf{x} dt. \end{aligned} \quad (\star)$$

Step 2 (transformation $\tilde{c}_1^\pm := c_1^\pm \pm c_0^\pm \tilde{\phi}_0$, representation of \tilde{c}_1^\pm , cell problems)

Similarly to the redefinition of the pressure in Step 2 within the proof of Theorem 4.39, we define the modified number densities

$$\tilde{c}_1^\pm = c_1^\pm \pm \begin{cases} c_0^\pm \phi_0, & \alpha_2 = \alpha_3 - 1 \\ 0, & \alpha_2 > \alpha_3 - 1 \end{cases}$$

and choose $\psi_0 \equiv 0$ in (\star) , which leads, after integration by parts with respect to \mathbf{y} , to:

$$\begin{aligned} -\Delta_{\mathbf{y}} \tilde{c}_1^\pm(t, \mathbf{x}, \mathbf{y}) &= 0 && \text{in } (0, T) \times \Omega \times Y_l, \\ \nabla_{\mathbf{y}} \tilde{c}_1^\pm(t, \mathbf{x}, \mathbf{y}) \cdot \boldsymbol{\nu} &= -\nabla_{\mathbf{x}} c_0^\pm(t, \mathbf{x}) \cdot \boldsymbol{\nu} && \text{on } (0, T) \times \Omega \times \Gamma, \\ \tilde{c}_1^\pm(t, \mathbf{x}, \mathbf{y}) &&& \text{periodic in } \mathbf{y}. \end{aligned}$$

The linearity of the equation yields (4.22) as representations for \tilde{c}_1^\pm supplemented by the family of cell problems (4.11).

Step 3 (macroscopic equation for c_0^\pm) On the other hand, if choosing $\psi_1(t, \mathbf{x}, \mathbf{y}) = 0$ in (\star) , we read off the strong formulation for c_0^\pm after integration by parts with respect to \mathbf{x} and after substituting the representation (4.22) of \tilde{c}_1^\pm :

$$\begin{aligned} |Y_l| \partial_t c_0^\pm(t, \mathbf{x}) + \nabla_{\mathbf{x}} \cdot \left(\begin{cases} \bar{\mathbf{v}}_0(t, \mathbf{x}) c_0^\pm(t, \mathbf{x}), & \beta = 0 \\ 0, & \beta > 0 \end{cases} \right. \\ \left. - \mathbf{D} \nabla_{\mathbf{x}} c_0^\pm(t, \mathbf{x}) \right) = |Y_l| R_0^\pm(c_0^+(t, \mathbf{x}), c_0^-(t, \mathbf{x})) & \text{ in } (0, T) \times \Omega, \\ \left(\begin{cases} \bar{\mathbf{v}}_0(t, \mathbf{x}) c_0^\pm(t, \mathbf{x}), & \beta = 0 \\ 0, & \beta > 0 \end{cases} - \mathbf{D} \nabla_{\mathbf{x}} c_0^\pm(t, \mathbf{x}) \right) \cdot \boldsymbol{\nu} = 0 & \text{ on } (0, T) \times \partial\Omega_N, \\ c_0^\pm = 0 & \text{ on } (0, T) \times \partial\Omega_D, \end{aligned}$$

with $\bar{\mathbf{v}}_0, D$ being defined in (4.10) and (4.21), respectively. \square

Remark 4.43 (Modeling of c_0^\pm). *The transport of the number densities is determined by a convection-diffusion-reaction equation. There is no direct coupling to the electrostatic potential, since it is only present in the modified higher order terms of the number densities \tilde{c}_1^\pm .*

4.3.3 Conclusion

In Section 4.3.2, we considered the rigorous homogenization of the Stokes-Nernst-Planck-Poisson system (4.1) by the method of two-scale convergence. In more detail, we investigated the two-scale limit $\varepsilon \rightarrow 0$ for the Dirichlet case, i.e. for given surface (zeta) potential on Γ_ε and for different ranges of the set of scale parameters $(\alpha_1, \alpha_2, \alpha_3, \beta, \gamma)$. In virtue of the general a priori estimates that have been shown for a large range of the parameter set, we derived the corresponding two-scale limits of Problem P_ε .

There is no direct coupling of fluid flow and transport to the electrostatic potential in

any of the considered ranges of the scaling parameters. Although the determination of the electrostatic potential is directly related to the macroscopic number densities, it is only present in the redefined higher order pressure p_1 and number densities \tilde{c}_1^\pm . In particular, the pressure field compensates the effect of the electrostatic potential and the macroscopic velocity field $\bar{\mathbf{v}}_0$ remains unchanged. Depending on the scaling parameters β , the effective equations might be coupled in one direction or decoupled: If $\beta = 0$, the fluid flow enters the convective term in the transport equations whereas if $\beta > 0$ transport is described by diffusion-reaction equations. Compare also the results of the Neumann case which are schematically depicted in Figure 4.1 and Figure 4.2.

As it was the case for the Neumann boundary condition, see Section 4.2, one of the essential points in the upscaling procedure is the strong convergence property of the number densities c_ε^\pm . Consequently, their two-scale limits c_0^\pm are independent of the oscillating, fast variable \mathbf{y} and, analogously to Section 4.2. For this reason, we are in the position to define the following reasonable auxiliary variables $\tilde{p}_1 = p_1 + (c_0^+ - c_0^-)\tilde{\phi}_0$ and $\tilde{c}_1^\pm := c_1^\pm \pm c_0^\pm \phi_0$ in order to extract certain cell problems. Their solutions again determine the effective macroscopic coefficients \mathbf{D} and \mathbf{K} and allow for a macroscopic representation of the homogenized limit problems.

4.4 Concluding remarks

Finally, in order to conclude the discussion of the homogenization results of Section 4.2 and Section 4.3, we point out the following general aspects:

- In the colloid literature, the so-called perfect sink boundary condition is often applied for the number densities instead of the no-penetration boundary condition, i.e. $c_\varepsilon^\pm = 0$ on $(0, T) \times \Gamma_\varepsilon$, see also Remark 2.5. In the framework of homogenization, as considered in this chapter, this choice of boundary condition would lead together with the strong convergence property of the number densities to the two-scale limit $c_0^\pm \equiv 0$. As a consequence, this approach does not provide a meaningful model description of charged transport in a porous medium.

In our investigations in Section 4.2 and also in Section 4.3, it was essential that the number densities converge strongly. However, if we cannot guarantee strong convergence for the number densities c_ε^\pm , we can at least determine the limit system in those cases, in which the nonlinear terms, i.e. the convective and the electric force terms, converge to zero. As a consequence, a diffusion-reaction system arises as macroscopic description of transport.

It is worth noting that, using two-scale convergence, we could not pass to the limit $\varepsilon \rightarrow 0$ for all choices of the parameter ranges. However, in these cases formal two-scale asymptotic expansions can be applied in order to pass formally to the limit $\varepsilon \rightarrow 0$ using, e.g., the transformation $u^\pm := \exp(\mp\phi) c^\pm$. These transformations are well known in the context of drift-diffusion problems, compare, for example, [119, 86]. We refer also to Chapter 5 for the application of such transformations.

- All derived limit systems of Section 4.2 and Section 4.3 are well defined from an analytical point of view, i.e. there exist global, unique weak solutions. The most complex limit system, the fully coupled nonlinear Darcy-Nernst-Planck-Poisson system, has already been investigated in Section 2.2.4. Analogue proofs as those of Theorem 2.23, Theorem 2.24 and Theorem 2.28, Theorem 2.31 carry over directly to the reduced limit systems that are obtained in Section 4.2 and Section 4.3 for different choices of scaling. Since, in particular, also uniqueness has been proven, convergence of the whole sequences instead of only subsequences is guaranteed in every case.
- The main benefit of the homogenization approach is that effective model equations are derived from microscopic modeling principles in a mathematical rigorous way. Effective coefficients, which are the crucial point in macroscopic modeling (cf. Section 2.2), are defined by means of the solutions of auxiliary cell problems. In this sense also the geometrical structure enters the effective model description.

Our main contribution in this chapter is that we managed to analyze a quite large range of the parameter set $(\alpha_1, \alpha_2, \alpha_3, \beta, \gamma)$ and different (non homogeneous) boundary conditions that are meaningful for certain applications. Moreover, we studied the influence of both, on general a priori estimates and also on the results of the homogenization procedure. In this sense, our investigations go beyond those known from the literature, see Section 3.2.

The following question now arises naturally: *Given a particular scenario of colloidal transport in the soil, which is the best/most reasonable mathematical (limit) model that should be considered?* In order to get a qualitatively deeper understanding, both, the pore-scale model and the effective limit equations have been investigated numerically for different choices of the scale range $(\alpha_1, \alpha_2, \alpha_3)$ in [46]. There, the convergence in the scale parameter ε is studied qualitatively and quantitatively. To this end, a

numerical discretization using mixed finite elements was applied for both, the macroscopic problems and the cell problems. One advantage of this approach is that the flux unknowns are computed directly which are required for the computation of the effective macroscopic tensors. For more details of the discretization, we refer to Section 2.3 and [46]. Since in geosciences so-called column experiments are a standard way to examine flow, transport, or material properties, in [46] the rate of convergence in ε was studied qualitatively by comparing the mass outflow curves. To this end, the temporal and spatial discretization parameters as well as the iteration tolerance were chosen sufficiently small to exclude discretization and splitting errors. In order to reduce the computation cost from quadratic to linear order in $1/\varepsilon$, all simulations were performed on stripes of length 1 and vertical height ε with periodic boundary conditions on $(0, 1) \times \{0, \varepsilon\}$, see also [138].

In [46], it was shown that the mean outflow curves converge for decreasing ε to their limits for all considered parameter sets $(\alpha_1, \alpha_2, \alpha_3)$ quite fast. Moreover, the impact of electrodynamic interactions, also with respect to reactivity, was investigated in [46]: Depending on the sign of charge an increased residence time in the domain or an acceleration of either of the charged species was observed. This fact emphasizes that electrodynamic effects have a severe impact on kinetic reactions which arises from a spatial redistribution of mass.

However, answering the above question is not limited to prescribing the precise values for the choice of the appropriate boundary conditions and for the scale range $(\alpha_1, \alpha_2, \alpha_3, \beta, \gamma)$. It also requires a careful calibration and adjustment by experimental measurements and also a parameter identification procedure may need to be done to make the model quantitatively. Moreover, corrector/error estimates will be needed in order to make it possible to quantitatively compare the effective solutions/problem descriptions with the oscillatory solution/microscopic model. First numerical results in this direction are obtained in [46] for different choices of scaling parameters. Moreover, also interior estimates and influence of boundary terms on the corrector estimates have been studied in [46]. This numerical estimation of convergence rates provides a first insight in the applicability of the homogenized systems, since those have not yet been accomplished analytically in a rigorous manner for the full SNPP-system. Only first analytical investigations for a simplified problem in the context of the Nernst-Planck-Poisson system have been published in [126].

Chapter 5

Homogenization of Problem P including an evolving microstructure

5.1 Introduction

Until now, we considered problems and mathematical models and their investigation as well as their homogenization in rigid porous media with periodic geometry, cf. Chapter 2 and Chapter 4. However, in several applications the porous medium contain multiple phases that evolve in time. As examples, we just mention unsaturated flow, where the gaseous and liquid phases evolve and two/multi-phase flow where two or more liquids and/or gases evolve, [54]. On the other hand, an evolution of the solid phase can occur. This is the case if, the porous matrix itself is compressible [16] or varies due to attachment/detachment processes or due to chemical reactions [74, 77].

Any change of the underlying geometry leads directly to a change of the pore space that is accessible for the phases and inherent with that of the transport properties of the porous medium. In certain applications, these effects need to be captured in a mathematical model, especially if the variation of the porous matrix is not negligible, i.e. the pore geometry cannot be assumed to be constant in time.

In the context of colloidal transport within the soil, interaction potentials between particles and the porous matrix are present and surface reactions take place. To be more concrete colloids undergo repulsive and attractive forces (consisting of electric repulsion, Born repulsion, van-der-Waals attraction and further (non-)DLVO forces). As long as the total interaction potential is attractive, attachment of colloidal particles to the porous matrix is facilitated, whereas, if the total interaction potential is repulsive,

detachment from the porous matrix is favorable. Finally, the (irreversible) binding of colloids to the surface is summarized by a surface reaction rate f . Since the thickness of the attached layer can lead to significant changes of the underlying geometry, we extend the pore-scale model Problem P in this section for such phenomena.

Since the evolution of the geometry is, in general, by no means uniform, extensions of homogenization methods to non-periodic and evolving geometries need to be considered.

5.2 Extensions of periodic upscaling

In the context of non-periodic homogenization, the first approaches in stochastic homogenization were undertaken in [69], [104], which is still an actual research topic, see, for example, [17, 73].

An approach for homogenization with evolving microstructure has been proposed in [105]. Here, the mathematical model equations are transformed onto a constant periodic reference configuration, where standard homogenization techniques as described in Section 3.1.1 can be applied. This procedure is quite similar to the approach known in continuum mechanics, [39]. The main drawback of this method is that it is not clear how changes in topology can be handled.

In the theory of swelling porous media, the porous matrix is considered as deformable medium which can be described, e.g., by linear elasticity. In the context of Problem P formal two-scale asymptotic expansions has been applied in [95, 94] for such a setting. The application of linear elasticity is, however, restricted to small deformations only. Furthermore, the evolving interface is not modeled explicitly.

In [36], a phase field approach for liquid-solid phase transitions with dendritic microstructure is analyzed and treated via homogenization theory. In [2] formal homogenization for a sharp interface model describing phase changes in solids is performed.

An ansatz in handling evolving microstructures using a level set formulation has been invented by van Noorden in [138] for a two-dimensional setting in the context of crystal precipitation and dissolution. This method will be applied here since it provides an explicit description of the evolving solid-liquid interface. Furthermore, attachment/detachment processes generate a change in the geometry rather than a (linear elastic) deformation of porous medium itself. To conclude, it can be stated that this methods is less restrictive than other methods and adapts best to our model problem.

This chapter is organized as follows: In Section 5.3, we extend Problem P in such a way that the evolution of the microscopic geometry or more precisely of the evolution of the solid-liquid interface is captured. This is dictated by a reaction rate that corresponds to the detachment and attachment processes of colloidal particles that have been transported to the porous matrix by the transport mechanism described in Section 2.1. Regarding these phenomena, we put some effort in the derivation of appropriate boundary conditions on the evolving solid-liquid interface which are non-standard. In Section 5.4.4, Section 5.4.5, and Section 5.4.6 we derive an equivalent macroscopic model description for the pore-scale model. To this end, we use an extension of the method of formal two-scale asymptotic expansion introduced in Section 3.1.3 to a level set description, cf. [138]. In Section 5.4.7, we discuss the results of the averaging procedure: We show physical properties of the effective coefficients such as symmetry and (uniform) positive definiteness, respectively. We furthermore point out that our model is a consistent extension of the well known description of transport without evolving microstructure and without interaction potential. The chapter is concluded with the numerical computation of the averaged coefficients and simulations results for a simplified radially symmetric setting in Section 5.5.

5.3 Pore-scale model

In Section 2.1, a pore-scale model describing colloidal transport processes and fluid flow within a porous medium was introduced. The corresponding model equations are repeated here for the sake of clarity:

$$\partial_t c + \nabla \cdot \left(\mathbf{v}^{\text{hydr}} c - D \nabla c - \frac{D}{k_B T} c \nabla \phi^{\text{col}} \right) = 0, \quad t \in (0, T), \quad \mathbf{x} \in \Omega(t), \quad (5.1)$$

$$-\eta \Delta \mathbf{v}^{\text{hydr}} + \frac{1}{\rho} \nabla p = -\frac{1}{\rho} c \nabla \phi^{\text{col}}, \quad t \in (0, T), \quad \mathbf{x} \in \Omega(t), \quad (5.2a)$$

$$\nabla \cdot \mathbf{v}^{\text{hydr}} = 0, \quad t \in (0, T), \quad \mathbf{x} \in \Omega(t), \quad (5.2b)$$

where we set $F^{\text{col}} = -\frac{D}{k_B T} \nabla \phi^{\text{col}}$.

Here, we assume that the total interaction potential ϕ^{col} is a given function which describes the interaction of colloidal particles with the porous matrix. Since we concentrate on the effects resulting from this interaction, we suppose that the interaction between the colloidal particles plays a secondary role compared to the interaction

between colloidal particles and the porous matrix. This assumption is for example reasonable for very dilute solution where enough equally favorable adsorption sites are available for attachment. In general, the colloids undergo repulsive and attractive forces (consisting of electric repulsion, Born repulsion, van-der-Waals attraction and further (non-)DLVO forces, see Section 2.1 and Figure 2.1). As long as the total potential is attractive, attachment to the porous matrix is favorable, whereas, if the total potential is repulsive, detachment from the porous matrix is favorable. Finally, the (irreversible) binding of colloids to the surface is summarized by a surface reaction rate f .

In Section 5.5, we will study the case of a radial symmetrically interaction potential that depends only on the distance between a colloidal particle and the porous matrix.

5.3.1 Mass conservation laws

Due to the interaction and reaction of the colloidal particles with the porous matrix, a change of the underlying geometry occurs. A crucial point in completing the pore-scale model (5.1), (5.2), is the derivation of appropriate and physically reasonable boundary conditions on the solid-liquid interface. To this end, we demand a mass conservation law at the evolving interface and therefore consider the conservation of total mass of the colloidal particles. Since the porous matrix is often of the same nature as the colloidal particles, we have in the one-dimensional case, cf. Figure 5.1:

$$\frac{d}{dt} \left(\int_0^{s(t)} c(t, x) dx + \int_{s(t)}^1 \frac{1}{m^{\text{col}}} \rho_s dx \right) = 0$$

with density ρ_s of the solid phase including attached particles. Inserting the differential equation for c (a one-dimensional analogue of (5.1)), applying the chain rule and the fundamental theorem of calculus it follows

$$-v^{\text{hydr}} c + D \partial_x c + \frac{D}{k_B T} c \partial_x \phi^{\text{col}} + c \partial_t s - \frac{1}{m^{\text{col}}} \rho_s \partial_t s = 0.$$

In the n -dimensional case, an analogous result holds true. Instead of $\partial_t s$, we introduce the normal velocity v_ν of the evolving interface and obtain

$$\left(-\mathbf{v}^{\text{hydr}} c + D \nabla c + \frac{D}{k_B T} c \nabla \phi^{\text{col}} \right) \cdot \boldsymbol{\nu} + v_\nu \left(c - \frac{1}{m^{\text{col}}} \rho_s \right) = 0, \quad t \in (0, T), \quad \mathbf{x} \in \Gamma(t). \quad (5.3)$$

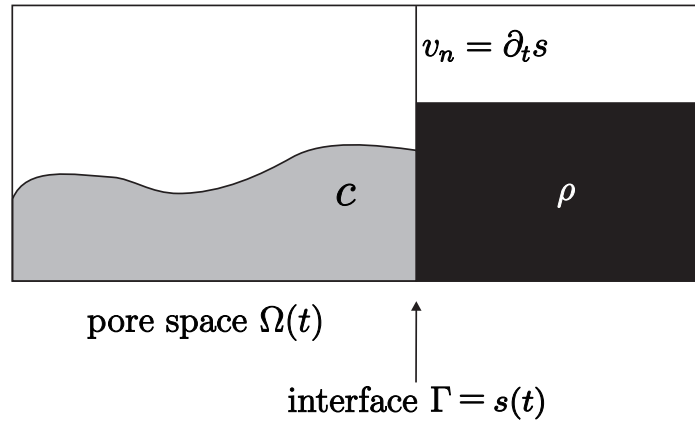


Figure 5.1: Schematic representation for the derivation of boundary conditions by mass conservation.

Remark 5.1. *In the case of $v_\nu = 0$, a “no flux condition” on the soil boundary holds true, which supplements the so-called “no penetration” model, [41]. In the case of $v_\nu \neq 0$, the mass flux toward or away from the soil boundary results in a growth or shrinkage of the solid phase, respectively. Equation (5.1) together with the conservation law (5.3) and an appropriate choice of the initial condition c^0 describes the dynamics of the colloidal particles properly.*

In order to close the model (5.1)-(5.3), we define appropriate boundary conditions for Stokes equations (5.2), namely, we supplement them by a no-slip boundary condition at the porous matrix, i.e.

$$\mathbf{v}^{\text{hydr}} = \frac{\rho - \rho_s}{\rho} v_\nu \boldsymbol{\nu}, \quad t \in (0, T), \quad \mathbf{x} \in \Gamma(t). \quad (5.4)$$

The coefficient $\frac{\rho - \rho_s}{\rho}$ is determined by the change in volume during the transition between liquid and solid part which comes along with the attachment to and detachment processes from the porous matrix, respectively.

Finally, the evolution of the solid-liquid interface needs to be characterized. The evolution of the microscopic geometry or, more precisely, the evolution of the solid-liquid interface is dictated by a surface reaction rate f that corresponds to the detachment and attachment processes of colloidal particles that have been transported to the porous matrix by the transport mechanism convection, diffusion and drift. Consequently, we assume

$$v_\nu = -\frac{m^{\text{col}}}{\rho_s} f(c, \rho_s), \quad t \in (0, T), \quad \mathbf{x} \in \Gamma(t). \quad (5.5)$$

5.3.2 Reaction rate

The surface reaction rate f strongly depends on the processes and reactions taking place directly at the interface. After colloidal particles have been transported to the soil boundary by the processes described in Section 2.1, chemical reaction can bind these particles (irreversibly). However, the accurate and detailed description of these processes is very challenging since there are numerous factors influencing the chemical reaction, see, e.g., [135, 134]. Therefore, structural assumptions on the reaction rate have to be made, depending, for example, on experimental observations. We state exemplarily some possible choices of f :

1. If f is exclusively a function of the number density of the colloids and the reaction obeys the mass action law with rate constant k , the reaction rate takes the form $f(c, \rho_s) = f(c) = kc^m$.
2. If f depends on both the the number density of the colloids and the soil density, a linear relation (or linearization of a nonlinear process, respectively) can be assumed, i.e. $f(c, \rho_s) = k_f c - k_b \rho_s$ with rate constants k_f, k_b .
3. For more sophisticated rates using a set-valued Heaviside graph for dissolution processes see [67, 137] and in the context of homogenization see [138].

5.3.3 Level set function

As a last step of modeling, we determine the distribution of solid and liquid part by a level set function

$$L(t, \mathbf{x}) \begin{cases} > 0 & \text{liquid part,} \\ = 0 & \text{interface,} \\ < 0 & \text{solid part,} \end{cases}$$

fulfilling the following partial differential equation

$$\partial_t L + v_\nu |\nabla L| = 0, \quad t \in (0, T), \quad \mathbf{x} \in \Omega(t), \quad (5.6a)$$

$$L = L^0, \quad \mathbf{x} \in \Omega(0). \quad (5.6b)$$

Then the interface between liquid and solid part is defined by $\Gamma(t) = \{\mathbf{x} : L(t, \mathbf{x}) = 0\}$ and the liquid part is given by $\Omega_l(t) = \{\mathbf{x} : L(t, \mathbf{x}) > 0\}$.

5.3.4 Outline of the pore-scale model

The overall pore-scale model (5.1)–(5.6) describes the transport of colloidal particles taking into account the processes convection, diffusion, and drift according to the total interaction potential ϕ^{col} . The model is formulated in a level set framework in order to include effects of an evolving microstructure, which result from attachment and detachment processes on the solid-liquid interface described by the surface reaction rate f . System (5.1)–(5.6) is derived from physical principles such as mass conservation and provides a first approach in taking into account aspects that cover a wide range of processes into one single model. The considered model provides a profound insight into the colloidal dynamics and the processes which result in a change of porosity and therefore of the pore space that is accessible for the fluid within the soil. Moreover, our model is a step toward the understanding of structural changes in the porous matrix.

5.4 Periodic homogenization

5.4.1 Evolving pore geometry

We consider a perforated domain as defined in Section 3.1.3, see also Figure 3.6. In the non-rigid framework, the unit cell $Y = [-\frac{1}{2}, +\frac{1}{2}]^2$ is made up of two open sets which vary in time: the liquid part $Y_l = Y_l(t, \mathbf{x})$ and the solid part $Y_s = Y_s(t, \mathbf{x})$. At initial time $t = 0$, we assume that the solid part has circular shape for ease of presentation and does not touch or intersect the boundary of the unit cell Y , i.e. the fluid part is connected. For a discussion of more general geometrical settings, we refer to the discussion in Section 3.1.3. Analogously to Section 3.1.3, we define $Y_{\varepsilon,l}^{ij} = Y_{\varepsilon,l}^{ij}(t, \mathbf{x})$, $Y_{\varepsilon,s}^{ij} = Y_{\varepsilon,s}^{ij}(t, \mathbf{x})$, and $\Gamma_{\varepsilon}^{ij} = \Gamma_{\varepsilon}^{ij}(t, \mathbf{x})$. The fluid part/pore space, the solid part, and the interior boundary of the porous medium are defined by

$$\begin{aligned} \Omega_{\varepsilon} = \Omega_{\varepsilon}(t, \mathbf{x}) &:= \bigcup_{ij} Y_{\varepsilon,l}^{ij}, & \Omega \setminus \overline{\Omega}_{\varepsilon} = \Omega \setminus \overline{\Omega}_{\varepsilon}(t, \mathbf{x}) &:= \bigcup_{ij} Y_{\varepsilon,s}^{ij}, \\ & & \text{and } \Gamma_{\varepsilon} &= \Gamma_{\varepsilon}(t, \mathbf{x}) := \bigcup_{ij} \Gamma_{\varepsilon}^{ij}. \end{aligned}$$

5.4.2 Scaled model equations

In this section, we reformulate the system consisting of (5.1)–(5.6) within the multi-scale framework that has been introduced in Chapter 3 and Section 5.4.1. As in Sec-

tion 4.1, the different terms are scaled with the scale parameter ε and, in summary, we derive the following pore-scale model:

Stokes equations.

$$-\varepsilon^2 \eta \Delta \mathbf{v}_\varepsilon^{\text{hydr}} + \frac{1}{\rho} \nabla p_\varepsilon = -\varepsilon \frac{1}{\rho} c_\varepsilon \nabla \phi_\varepsilon^{\text{col}}, \quad t \in (0, T), \quad \mathbf{x} \in \Omega_\varepsilon(t), \quad (5.7a)$$

$$\nabla \cdot \mathbf{v}_\varepsilon^{\text{hydr}} = 0, \quad t \in (0, T), \quad \mathbf{x} \in \Omega_\varepsilon(t), \quad (5.7b)$$

$$\mathbf{v}_\varepsilon^{\text{hydr}} = -\varepsilon \frac{\rho - \rho_s}{\rho \rho_s} f(c_\varepsilon, \rho_s) \boldsymbol{\nu}_\varepsilon, \quad t \in (0, T), \quad \mathbf{x} \in \Gamma_\varepsilon(t), \quad (5.7c)$$

$$\mathbf{v}_\varepsilon^{\text{hydr}} = 0. \quad t \in (0, T), \quad \mathbf{x} \in \partial\Omega. \quad (5.7d)$$

Nernst-Planck equation.

$$\partial_t c_\varepsilon - \nabla \cdot (-\mathbf{v}_\varepsilon^{\text{hydr}} c_\varepsilon + D \nabla c_\varepsilon + \frac{D}{k_B T} c_\varepsilon \nabla \phi_\varepsilon^{\text{col}}) = 0, \quad t \in (0, T), \quad \mathbf{x} \in \Omega_\varepsilon(t), \quad (5.8a)$$

$$\begin{aligned} & (-\mathbf{v}_\varepsilon^{\text{hydr}} c_\varepsilon + D \nabla c_\varepsilon + \frac{D}{k_B T} c_\varepsilon \nabla \phi_\varepsilon^{\text{col}}) \cdot \boldsymbol{\nu}_\varepsilon \\ & -\varepsilon \frac{m^{\text{col}}}{\rho_s} f(c_\varepsilon, \rho_s) (c_\varepsilon - \frac{1}{m^{\text{col}}} \rho_s) = 0, \quad t \in (0, T), \quad \mathbf{x} \in \Gamma_\varepsilon(t), \end{aligned} \quad (5.8b)$$

$$(-\mathbf{v}_\varepsilon^{\text{hydr}} c_\varepsilon + D \nabla c_\varepsilon + \frac{D}{k_B T} c_\varepsilon \nabla \phi_\varepsilon^{\text{col}}) \cdot \boldsymbol{\nu} = 0, \quad t \in (0, T), \quad \mathbf{x} \in \partial\Omega, \quad (5.8c)$$

$$c_\varepsilon = c^0. \quad \mathbf{x} \in \Omega_\varepsilon(0). \quad (5.8d)$$

Level set equation.

$$\partial_t L_\varepsilon - \varepsilon \frac{m^{\text{col}}}{\rho_s} f(c_\varepsilon, \rho_s) |\nabla L_\varepsilon| = 0, \quad t \in (0, T), \quad \mathbf{x} \in \Omega, \quad (5.9a)$$

$$L_\varepsilon = L^0. \quad \mathbf{x} \in \Omega. \quad (5.9b)$$

Remark 5.2. *For ease of presentation, we apply a no-flux boundary condition for the number density and a no-slip boundary condition for the fluid velocity on the exterior boundary $\partial\Omega$ of the computational domain. However, other linear boundary condition can be chosen on the exterior boundary without notable changes in the following calculations, see also Section 4.1, Remark 2.5, and Remark 2.14. Yet, the formal upscaling approach used here is more flexible, since a priori estimates that are based on weak formulations are not needed.*

5.4.3 Two-scale asymptotic expansion

Our main goal is now to determine a macroscopic model description starting from system (5.7)–(5.9). To this end, we intend to identify the limit $\varepsilon \rightarrow 0$ using an extension of the method of two-scale asymptotic expansion which described in Section 3.1.3. Along with the expansion of the spatial derivatives (3.2), all variable functions are expanded in series of the scale parameter ε , according to (3.3). Thus, we obtain

$$\mathbf{v}_\varepsilon^{\text{hydr}}(t, \mathbf{x}) = \mathbf{v}_0(t, \mathbf{x}, \mathbf{y}) + \varepsilon \mathbf{v}_1(t, \mathbf{x}, \mathbf{y}) + \varepsilon^2 \mathbf{v}_2(t, \mathbf{x}, \mathbf{y}) + \dots, \quad (5.10a)$$

$$p_\varepsilon(t, \mathbf{x}) = p_0(t, \mathbf{x}, \mathbf{y}) + \varepsilon p_1(t, \mathbf{x}, \mathbf{y}) + \varepsilon^2 p_2(t, \mathbf{x}, \mathbf{y}) + \dots, \quad (5.10b)$$

$$c_\varepsilon(t, \mathbf{x}) = c_0(t, \mathbf{x}, \mathbf{y}) + \varepsilon c_1(t, \mathbf{x}, \mathbf{y}) + \varepsilon^2 c_2(t, \mathbf{x}, \mathbf{y}) + \dots, \quad (5.10c)$$

$$\phi_\varepsilon^{\text{col}}(t, \mathbf{x}) = \phi_0(t, \mathbf{x}, \mathbf{y}) + \varepsilon \phi_1(t, \mathbf{x}, \mathbf{y}) + \varepsilon^2 \phi_2(t, \mathbf{x}, \mathbf{y}) + \dots, \quad \mathbf{y} = \mathbf{x}/\varepsilon. \quad (5.10d)$$

In addition to the expansions (3.2), (5.10), in the framework of a level set description, also the level set function L_ε itself and the normal vector $\boldsymbol{\nu}_\varepsilon$ have to be expanded due to the evolving microstructure. The expansion of the outer normal vector $\boldsymbol{\nu}_\varepsilon$ is expressed in terms of the level set function L_ε and for the two-dimensional setting, we obtain the following relations, see [138]:

$$L_\varepsilon(t, \mathbf{x}) = L_0(t, \mathbf{x}, \mathbf{y}) + \varepsilon L_1(t, \mathbf{x}, \mathbf{y}) + \varepsilon^2 L_2(t, \mathbf{x}, \mathbf{y}) + \dots, \quad \mathbf{y} = \mathbf{x}/\varepsilon, \quad (5.10e)$$

$$\boldsymbol{\nu}_\varepsilon = \boldsymbol{\nu}_0 + \varepsilon \boldsymbol{\nu}_1 + O(\varepsilon^2), \quad (5.10f)$$

$$\text{with } \boldsymbol{\nu}_0 = \frac{\nabla_{\mathbf{y}} L_0}{|\nabla_{\mathbf{y}} L_0|}, \quad \boldsymbol{\nu}_1 = \boldsymbol{\tau}_0 \frac{\boldsymbol{\tau}_0 \cdot (\nabla_{\mathbf{x}} L_0 + \nabla_{\mathbf{y}} L_1)}{|\nabla_{\mathbf{y}} L_0|} \quad (5.10g)$$

and $\boldsymbol{\tau}_0 := \boldsymbol{\nu}_0^\perp$ denoting the unit tangent on Γ_0 . We restrict ourselves to the two-dimensional setting here, since the representations (5.10g) together with the Lemmas 3.1 and 3.2 in [138] make it possible to simplify the following technical calculations considerably and to obtain reasonable upscaling results. Remind, that the zeroth order expansion L_0 of the level set function is also used to describe the zero order time evolving domain $Y_{l,0}(t, \mathbf{x}) := \{\mathbf{y} : L_0(t, \mathbf{x}, \mathbf{y}) > 0\}$ and interface $\Gamma_0(t, \mathbf{x}) := \{\mathbf{y} : L_0(t, \mathbf{x}, \mathbf{y}) = 0\}$, [138].

The expansions (3.2), (5.10a)–(5.10g) are the starting point for the homogenization procedure. We apply these expansions to our model problem and analyze the different orders in ε^k , $k \in \mathbb{Z}$, separately. For the sake of clearness, we split the derivation of the averaged model problem into several steps. The necessary technical calculations are performed in the following subsections.

5.4.4 Lowest order problems of the asymptotic expansion

In this section, we consider the lowest order terms of (5.7)–(5.9) that arise after substituting the expansions (3.2), (5.10a)–(5.10g).

Stokes equation of order $O(\varepsilon^{-1})$ (p_0 independent of \mathbf{y}). The lowest order problem of Stokes equation (5.7a) is of order ε^{-1} and yields that p_0 is a macroscopic variable since $\nabla_{\mathbf{y}} p_0 = 0$, i.e.

$$p_0(t, \mathbf{x}, \mathbf{y}) = p_0(t, \mathbf{x}). \quad (5.11)$$

Nernst-Planck equation of order $O(\varepsilon^{-2})$ and boundary condition of order $O(\varepsilon^{-1})$ (Transformation $c_0 = e^{-\frac{\phi_0}{k_B T}} u_0$, u_0 independent of \mathbf{y}). The transport equation (5.8a) of order ε^{-2} with boundary condition (5.8b) of order ε^{-1} reads

$$\begin{aligned} -\nabla_{\mathbf{y}} \cdot (D \nabla_{\mathbf{y}} c_0 + \frac{D}{k_B T} c_0 \nabla_{\mathbf{y}} \phi_0) &= 0, \\ (D \nabla_{\mathbf{y}} c_0 + \frac{D}{k_B T} c_0 \nabla_{\mathbf{y}} \phi_0) \cdot \boldsymbol{\nu}_0 &= 0. \end{aligned}$$

Applying the *transformation* $c_0(t, \mathbf{x}, \mathbf{y}) = e^{-\frac{\phi_0(t, \mathbf{x}, \mathbf{y})}{k_B T}} u_0(t, \mathbf{x}, \mathbf{y})$, which is well known from the stationary theory of semiconductor devices [86, 119], cf. also Section 2.1.1, item 6, leads to the following problem formulation

$$\begin{aligned} -\nabla_{\mathbf{y}} \cdot (D e^{-\frac{\phi_0}{k_B T}} \nabla_{\mathbf{y}} u_0) &= 0, \\ D e^{-\frac{\phi_0}{k_B T}} \nabla_{\mathbf{y}} u_0 \cdot \boldsymbol{\nu}_0 &= 0, \end{aligned}$$

which is uniquely solvable up to a constant (with respect to \mathbf{y}). Obviously, every macroscopic solution $u_0(t, \mathbf{x})$ is a solution of the above problem. Therefore, we derive the following form for the leading order term of the number density

$$c_0(t, \mathbf{x}, \mathbf{y}) = e^{-\frac{\phi_0(t, \mathbf{x}, \mathbf{y})}{k_B T}} u_0(t, \mathbf{x}) \quad (5.12)$$

with the transformed number density $u_0(t, \mathbf{x})$ being a macroscopic variable, i.e. being independent of \mathbf{y} .

Level set equation of order $O(\varepsilon^0)$. For the level set equation (5.9a), we obtain in order ε^0

$$\partial_t L_0 - \frac{m^{\text{col}}}{\rho_s} f(c_0, \rho_s) |\nabla_{\mathbf{y}} L_0| = 0.$$

5.4.5 Next order problems of the asymptotic expansion

Subsequently, we consider the next higher order terms in ε^k , $k \in \mathbb{Z}$ of (5.7) and (5.8).

Stokes equations of order $O(\varepsilon^0)$ and $O(\varepsilon^{-1})$ and boundary condition of order $O(\varepsilon^0)$ (Macroscopic equation for \mathbf{v}_0 , cell problems). The next order problem for Stokes equation (5.7a) is of order ε^0 , supplemented by the incompressibility condition (5.7b) of order ε^{-1} and boundary condition (5.7c) of order ε^0 :

$$\begin{aligned} -\eta\Delta_{\mathbf{y}}\mathbf{v}_0 + \frac{1}{\rho}\nabla_{\mathbf{y}}p_1 &= -\frac{1}{\rho}\nabla_{\mathbf{x}}p_0 - \frac{1}{\rho}c_0\nabla_{\mathbf{y}}\phi_0, \\ \nabla_{\mathbf{y}} \cdot \mathbf{v}_0 &= 0, \\ \mathbf{v}_0 &= 0. \end{aligned}$$

After application of the chain rule, the definition of the modified pressure $\tilde{p}_1 := p_1 - \frac{k_B T}{m^{\text{col}}}c_0\phi_0$, and the substitution of the representation (5.12), we obtain

$$\begin{aligned} -\eta\Delta_{\mathbf{y}}\mathbf{v}_0 + \frac{1}{\rho}\nabla_{\mathbf{y}}\tilde{p}_1 &= -\frac{1}{\rho}\nabla_{\mathbf{x}}p_0, \\ \nabla_{\mathbf{y}} \cdot \mathbf{v}_0 &= 0, \\ \mathbf{v}_0 &= 0. \end{aligned}$$

Since (5.11) holds, for $j = 1, 2$, we define the following *cell problems* of Stokes type, [58]:

$$-\Delta_{\mathbf{y}}\mathbf{w}_j + \nabla_{\mathbf{y}}\pi_j = \mathbf{e}_j, \quad \mathbf{y} \in Y_{l,0}(t, \mathbf{x}), \quad (5.13a)$$

$$\nabla_{\mathbf{y}} \cdot \mathbf{w}_j = 0, \quad \mathbf{y} \in Y_{l,0}(t, \mathbf{x}), \quad (5.13b)$$

$$\mathbf{w}_j = 0, \quad \mathbf{y} \in \Gamma_0(t, \mathbf{x}), \quad (5.13c)$$

$$\mathbf{w}_j, \pi_j \text{ periodic in } \mathbf{y}. \quad (5.13d)$$

Due to the linearity of the problem, the leading order velocity term $\mathbf{v}_0(\mathbf{x}, \mathbf{y})$ is expressed in terms of the solutions \mathbf{w}_j of the cell problems (5.13) via

$$\mathbf{v}_0(\mathbf{x}, \mathbf{y}) = -\frac{1}{\eta\rho} \sum_j \mathbf{w}_j(\mathbf{y}) \partial_{x_j} p_0(\mathbf{x}). \quad (5.14)$$

Integrating with respect to \mathbf{y} , we get *Darcy's law* for the \mathbf{y} -averaged velocity $\bar{\mathbf{v}}_0(\mathbf{x})$, [58]:

$$\bar{\mathbf{v}}_0 := \int_{Y_{l,0}(t, \mathbf{x})} \mathbf{v}_0(\mathbf{x}, \mathbf{y}) \, d\mathbf{y} = -\frac{1}{\eta\rho} \mathbf{K} \nabla_{\mathbf{x}} p_0,$$

with *permeability tensor* $\mathbf{K} = (K_{ij})_{ij}$, $K_{ij} := \int_{Y_{i,0}(t,\mathbf{x})} w_j^i d\mathbf{y}$. This law is supplemented by the *compressibility condition*

$$\nabla_{\mathbf{x}} \cdot \bar{\mathbf{v}}_0 = \frac{\rho - \rho_s}{\rho} \int_{\Gamma_0(t,\mathbf{x})} \frac{m^{\text{col}}}{\rho_s} f(c_0, \rho_s) ds_{\mathbf{y}},$$

as shown in [138] and by the *boundary condition*

$$\bar{\mathbf{v}}_0 = 0.$$

In summary, we have obtained macroscopic equations describing the effective fluid flow. These are supplemented by the cell problems (5.13) in order to calculate the macroscopic coefficient function \mathbf{K} .

Nernst-Planck equation of order $O(\varepsilon^{-1})$ and boundary condition of order $O(\varepsilon^0)$ (Transformation $c_1 = e^{-\frac{\phi_0}{k_B T}} u_1$, representation of u_1 , cell problems).

The next order problem of the transport equation (5.8a) is of order ε^{-1} , and thus we obtain:

$$\begin{aligned} -\nabla_{\mathbf{y}} \cdot (-\mathbf{v}_0 c_0 + D \nabla_{\mathbf{y}} c_1 + D \nabla_{\mathbf{x}} c_0 + \frac{D}{k_B T} c_0 \nabla_{\mathbf{y}} \phi_1 + \frac{D}{k_B T} c_1 \nabla_{\mathbf{y}} \phi_0 + \frac{D}{k_B T} c_0 \nabla_{\mathbf{x}} \phi_0) \\ -\nabla_{\mathbf{x}} \cdot (D \nabla_{\mathbf{y}} c_0 + \frac{D}{k_B T} c_0 \nabla_{\mathbf{y}} \phi_0) = 0. \end{aligned}$$

This equation is supplemented by the boundary condition (5.8b) of order ε^0 . Consequently, this results in:

$$\begin{aligned} (-\mathbf{v}_0 c_0 + D \nabla_{\mathbf{y}} c_1 + D \nabla_{\mathbf{x}} c_0 + \frac{D}{k_B T} c_0 \nabla_{\mathbf{y}} \phi_1 + \frac{D}{k_B T} c_1 \nabla_{\mathbf{y}} \phi_0 + \frac{D}{k_B T} c_0 \nabla_{\mathbf{x}} \phi_0) \cdot \boldsymbol{\nu}_0 \\ + (D \nabla_{\mathbf{y}} c_0 + \frac{D}{k_B T} c_0 \nabla_{\mathbf{y}} \phi_0) \cdot \boldsymbol{\nu}_1 + \mathbf{y} \cdot \nabla_{\mathbf{x}} (D \nabla_{\mathbf{y}} c_0 + \frac{D}{k_B T} c_0 \nabla_{\mathbf{y}} \phi_0) \cdot \boldsymbol{\nu}_0 \\ + \lambda \boldsymbol{\nu}_0 \cdot \nabla_{\mathbf{y}} (D \nabla_{\mathbf{y}} c_0 + \frac{D}{k_B T} c_0 \nabla_{\mathbf{y}} \phi_0) \cdot \boldsymbol{\nu}_0 = 0. \end{aligned}$$

Since the boundary condition is applied on the space- and time-dependent interface $\Gamma_0(t, \mathbf{x})$, additional terms appear due to the evolution of the pore space [138]. Hereby, the parameter λ occurring in the boundary condition is related to the expansion of the level set function L_ε in the following way [138]:

$$\lambda = \frac{L_1}{|\nabla_{\mathbf{y}} L_0|} - \frac{\mathbf{y} \cdot \nabla_{\mathbf{x}} L_0}{|\nabla_{\mathbf{y}} L_0|}, \quad \mathbf{y} \in \Gamma_0(t, \mathbf{x}).$$

Using (5.12) and an analog *transformation* for c_1 , namely

$$c_1(t, \mathbf{x}, \mathbf{y}) = e^{-\frac{\phi_0(t, \mathbf{x}, \mathbf{y})}{k_B T}} u_1(t, \mathbf{x}, \mathbf{y}), \quad (5.15)$$

as well as the chain rule yields the following problem formulation:

$$\begin{aligned} -\nabla_{\mathbf{y}} \cdot (D e^{-\frac{\phi_0}{k_B T}} \nabla_{\mathbf{y}} (u_1 + \frac{1}{k_B T} u_0 \phi_1)) &= \nabla_{\mathbf{y}} \cdot (-\mathbf{v}_0 e^{-\frac{\phi_0}{k_B T}} u_0 + D e^{-\frac{\phi_0}{k_B T}} \nabla_{\mathbf{x}} u_0), \\ D e^{-\frac{\phi_0}{k_B T}} \nabla_{\mathbf{y}} (u_1 + \frac{1}{k_B T} u_0 \phi_1) \cdot \boldsymbol{\nu}_0 &= (\mathbf{v}_0 e^{-\frac{\phi_0}{k_B T}} u_0 - D e^{-\frac{\phi_0}{k_B T}} \nabla_{\mathbf{x}} u_0) \cdot \boldsymbol{\nu}_0. \end{aligned}$$

We define the modified and transformed first order number density \tilde{u}_1 by

$$\tilde{u}_1 := u_1 + \frac{1}{k_B T} u_0 \phi_1. \quad (5.16)$$

Furthermore, we define the *cell problems* in ξ_j^2 for $j = 1, 2$ by:

$$-\nabla_{\mathbf{y}} \cdot (e^{-\frac{\phi_0}{k_B T}} \nabla_{\mathbf{y}} \xi_j^2) = \nabla_{\mathbf{y}} \cdot (e^{-\frac{\phi_0}{k_B T}} \mathbf{e}_j), \quad \mathbf{y} \in Y_{l,0}(t, \mathbf{x}), \quad (5.17a)$$

$$e^{-\frac{\phi_0}{k_B T}} \nabla_{\mathbf{y}} \xi_j^2 \cdot \boldsymbol{\nu}_0 = -e^{-\frac{\phi_0}{k_B T}} \mathbf{e}_j \cdot \boldsymbol{\nu}_0, \quad \mathbf{y} \in \Gamma_0(t, \mathbf{x}), \quad (5.17b)$$

$$\xi_j^2 \text{ periodic in } \mathbf{y}, \quad (5.17c)$$

and the *cell problems* in ξ_j^1 for $j = 1, 2$ by:

$$-\nabla_{\mathbf{y}} \cdot (e^{-\frac{\phi_0}{k_B T}} \nabla_{\mathbf{y}} \xi_j^1) = \nabla_{\mathbf{y}} \cdot (e^{-\frac{\phi_0}{k_B T}} \mathbf{w}_j), \quad \mathbf{y} \in Y_{l,0}(t, \mathbf{x}), \quad (5.18a)$$

$$(e^{-\frac{\phi_0}{k_B T}} \nabla_{\mathbf{y}} \xi_j^1) \cdot \boldsymbol{\nu}_0 = -e^{-\frac{\phi_0}{k_B T}} \mathbf{w}_j \cdot \boldsymbol{\nu}_0, \quad \mathbf{y} \in \Gamma_0(t, \mathbf{x}), \quad (5.18b)$$

$$\xi_j^1 \text{ periodic in } \mathbf{y}, \quad (5.18c)$$

where we used the representation (5.14) of \mathbf{v}_0 . Hence the modified and transformed first order term \tilde{u}_1 is expressed by linearity of the problem in the following way:

$$\tilde{u}_1 = \sum_j \frac{1}{D \eta \rho} \xi_j^1(\partial_{x_j} p_0) u_0 + \xi_j^2 \partial_{x_j} u_0. \quad (5.19)$$

5.4.6 Zeroth order transport problem of the asymptotic expansion

Nernst-Planck equation of order $O(\varepsilon^0)$, boundary condition of order $O(\varepsilon^1)$ (Macroscopic transport equation for u_0). In order ε^0 , we have:

$$\begin{aligned}
& \partial_t c_0 - \nabla_{\mathbf{x}} \cdot (-\mathbf{v}_0 c_0 + D \nabla_{\mathbf{x}} c_0 + D \nabla_{\mathbf{y}} c_1 + \frac{D}{k_B T} c_0 \nabla_{\mathbf{x}} \phi_0 + \frac{D}{k_B T} c_0 \nabla_{\mathbf{y}} \phi_1 + \frac{D}{k_B T} c_1 \nabla_{\mathbf{y}} \phi_0) \\
& \quad - \nabla_{\mathbf{y}} \cdot (-\mathbf{v}_1 c_0 - \mathbf{v}_0 c_1 + D \nabla_{\mathbf{x}} c_1 + D \nabla_{\mathbf{y}} c_2) \\
& \quad - \frac{D}{k_B T} \nabla_{\mathbf{y}} \cdot (c_0 \nabla_{\mathbf{x}} \phi_1 + c_1 \nabla_{\mathbf{x}} \phi_0 + c_1 \nabla_{\mathbf{y}} \phi_1 + c_2 \nabla_{\mathbf{y}} \phi_0 + c_0 \nabla_{\mathbf{y}} \phi_2) = 0.
\end{aligned}$$

The boundary condition is of order ε^1 and in combination with the additional terms resulting of the evolving pore geometry [138], it reads:

$$\begin{aligned}
& (-\mathbf{v}_1 c_0 - \mathbf{v}_0 c_1 + D \nabla_{\mathbf{x}} c_1 + D \nabla_{\mathbf{y}} c_2) \cdot \boldsymbol{\nu}_0 \\
& + \frac{D}{k_B T} (c_0 \nabla_{\mathbf{x}} \phi_1 + c_1 \nabla_{\mathbf{x}} \phi_0 + c_1 \nabla_{\mathbf{y}} \phi_1 + c_2 \nabla_{\mathbf{y}} \phi_0 + c_0 \nabla_{\mathbf{y}} \phi_2) \cdot \boldsymbol{\nu}_0 \\
& + (-\mathbf{v}_0 e^{-\frac{\phi_0}{k_B T}} u_0 + D e^{-\frac{\phi_0}{k_B T}} \nabla_{\mathbf{y}} (u_1 + \frac{1}{k_B T} u_0 \phi_1) + D e^{-\frac{\phi_0}{k_B T}} \nabla_{\mathbf{x}} u_0) \cdot \boldsymbol{\nu}_1 \\
& + \mathbf{y} \cdot \nabla_{\mathbf{x}} (-\mathbf{v}_0 e^{-\frac{\phi_0}{k_B T}} u_0 + D e^{-\frac{\phi_0}{k_B T}} \nabla_{\mathbf{y}} (u_1 + \frac{1}{k_B T} u_0 \phi_1) + D e^{-\frac{\phi_0}{k_B T}} \nabla_{\mathbf{x}} u_0) \cdot \boldsymbol{\nu}_0 \\
& + \lambda \boldsymbol{\nu}_0 \cdot \nabla_{\mathbf{y}} (-\mathbf{v}_0 e^{-\frac{\phi_0}{k_B T}} u_0 + D e^{-\frac{\phi_0}{k_B T}} \nabla_{\mathbf{y}} (u_1 + \frac{1}{k_B T} u_0 \phi_1) + D e^{-\frac{\phi_0}{k_B T}} \nabla_{\mathbf{x}} u_0) \cdot \boldsymbol{\nu}_0 \\
& \quad - \frac{m^{\text{col}}}{\rho_s} f(c_0, \rho_s) (c_0 - \frac{1}{m^{\text{col}}} \rho_s) = 0.
\end{aligned}$$

Starting from the equations above, we derive a macroscopic description of the transport processes in the following way: Integrating with respect to \mathbf{y} , applying the above boundary condition, and the transformations (5.12) and (5.15), we obtain together with the definition (5.16):

$$\begin{aligned}
& \int_{Y_{i,0}(t,\mathbf{x})} \partial_t (e^{-\frac{\phi_0}{k_B T}} u_0) \, d\mathbf{y} + \int_{Y_{i,0}(t,\mathbf{x})} \nabla_{\mathbf{x}} \cdot \left(e^{-\frac{\phi_0}{k_B T}} (\mathbf{v}_0 u_0 - D \nabla_{\mathbf{x}} u_0 - D \nabla_{\mathbf{y}} \tilde{u}_1) \right) \, d\mathbf{y} \\
& \quad + \int_{\Gamma_0(t,\mathbf{x})} e^{-\frac{\phi_0}{k_B T}} (-\mathbf{v}_0 u_0 + D \nabla_{\mathbf{y}} \tilde{u}_1 + D \nabla_{\mathbf{x}} u_0) \cdot \boldsymbol{\nu}_1 \, ds_{\mathbf{y}} \\
& \quad + \int_{\Gamma_0(t,\mathbf{x})} \mathbf{y} \cdot \nabla_{\mathbf{x}} \left(e^{-\frac{\phi_0}{k_B T}} (-\mathbf{v}_0 u_0 + D \nabla_{\mathbf{y}} \tilde{u}_1 + D \nabla_{\mathbf{x}} u_0) \cdot \boldsymbol{\nu}_0 \right) \, ds_{\mathbf{y}} \\
& \quad + \int_{\Gamma_0(t,\mathbf{x})} \lambda \boldsymbol{\nu}_0 \cdot \nabla_{\mathbf{y}} \left(e^{-\frac{\phi_0}{k_B T}} (-\mathbf{v}_0 u_0 + D \nabla_{\mathbf{y}} \tilde{u}_1 + D \nabla_{\mathbf{x}} u_0) \cdot \boldsymbol{\nu}_0 \right) \, ds_{\mathbf{y}} \\
& \quad - \int_{\Gamma_0(t,\mathbf{x})} \frac{m^{\text{col}}}{\rho_s} f(e^{-\frac{\phi_0}{k_B T}} u_0, \rho_s) (e^{-\frac{\phi_0}{k_B T}} u_0 - \frac{1}{m^{\text{col}}} \rho_s) \, ds_{\mathbf{y}} = 0.
\end{aligned}$$

Applying Reynolds transport theorem [39] in order to interchange integration and spatial derivation, we get

$$\begin{aligned}
& \int_{Y_{i,0}(t,\mathbf{x})} \partial_t \left(e^{-\frac{\phi_0}{k_B T}} u_0 \right) d\mathbf{y} + \nabla_{\mathbf{x}} \cdot \int_{Y_{i,0}(t,\mathbf{x})} e^{-\frac{\phi_0}{k_B T}} (\mathbf{v}_0 u_0 - D \nabla_{\mathbf{x}} u_0 - D \nabla_{\mathbf{y}} \tilde{u}_1) d\mathbf{y} \\
& + \int_{\Gamma_0(t,\mathbf{x})} \frac{\nabla_{\mathbf{x}} L_0}{|\nabla_{\mathbf{y}} L_0|} e^{-\frac{\phi_0}{k_B T}} (\mathbf{v}_0 u_0 - D \nabla_{\mathbf{x}} u_0 - D \nabla_{\mathbf{y}} \tilde{u}_1) ds_{\mathbf{y}} \\
& + \int_{\Gamma_0(t,\mathbf{x})} e^{-\frac{\phi_0}{k_B T}} (-\mathbf{v}_0 u_0 + D \nabla_{\mathbf{y}} \tilde{u}_1 + D \nabla_{\mathbf{x}} u_0) \cdot \boldsymbol{\nu}_1 ds_{\mathbf{y}} \\
& + \int_{\Gamma_0(t,\mathbf{x})} \mathbf{y} \cdot \nabla_{\mathbf{x}} \left(e^{-\frac{\phi_0}{k_B T}} (-\mathbf{v}_0 u_0 + D \nabla_{\mathbf{y}} \tilde{u}_1 + D \nabla_{\mathbf{x}} u_0) \right) \cdot \boldsymbol{\nu}_0 ds_{\mathbf{y}} \\
& + \int_{\Gamma_0(t,\mathbf{x})} \lambda \boldsymbol{\nu}_0 \cdot \nabla_{\mathbf{y}} \left(e^{-\frac{\phi_0}{k_B T}} (-\mathbf{v}_0 u_0 + D \nabla_{\mathbf{y}} \tilde{u}_1 + D \nabla_{\mathbf{x}} u_0) \right) \cdot \boldsymbol{\nu}_0 ds_{\mathbf{y}} \\
& - \int_{\Gamma_0(t,\mathbf{x})} \frac{m^{\text{col}}}{\rho_s} f(e^{-\frac{\phi_0}{k_B T}} u_0, \rho_s) \left(e^{-\frac{\phi_0}{k_B T}} u_0 - \frac{1}{m^{\text{col}}} \rho_s \right) ds_{\mathbf{y}} = 0.
\end{aligned}$$

With (5.10g) and the Lemmas 3.1 and 3.2 in [138], which can be applied directly, several terms cancel out and we obtain

$$\begin{aligned}
& \int_{Y_{i,0}(t,\mathbf{x})} \partial_t \left(e^{-\frac{\phi_0}{k_B T}} u_0 \right) d\mathbf{y} + \nabla_{\mathbf{x}} \cdot \int_{Y_{i,0}(t,\mathbf{x})} e^{-\frac{\phi_0}{k_B T}} (\mathbf{v}_0 u_0 - D \nabla_{\mathbf{x}} u_0 - D \nabla_{\mathbf{y}} \tilde{u}_1) d\mathbf{y} \\
& - \int_{\Gamma_0(t,\mathbf{x})} \frac{1}{\rho_s} f(e^{-\frac{\phi_0}{k_B T}} u_0, \rho_s) \left(e^{-\frac{\phi_0}{k_B T}} u_0 - \frac{1}{m^{\text{col}}} \rho_s \right) ds_{\mathbf{y}} = 0.
\end{aligned}$$

Using Reynolds Transport Theorem [39] for the time derivative and the boundary condition for the normal velocity, we have

$$\begin{aligned}
& \partial_t \left(\int_{Y_{i,0}(t,\mathbf{x})} e^{-\frac{\phi_0}{k_B T}} u_0 d\mathbf{y} \right) + \nabla_{\mathbf{x}} \cdot \int_{Y_{i,0}(t,\mathbf{x})} e^{-\frac{\phi_0}{k_B T}} (\mathbf{v}_0 u_0 - D \nabla_{\mathbf{x}} u_0 - D \nabla_{\mathbf{y}} \tilde{u}_1) d\mathbf{y} \\
& + \int_{\Gamma_0(t,\mathbf{x})} \frac{m^{\text{col}}}{\rho_s} f(e^{-\frac{\phi_0}{k_B T}} u_0, \rho_s) \frac{1}{m^{\text{col}}} \rho_s ds_{\mathbf{y}} = 0.
\end{aligned}$$

Here, the cell problems (5.17) and (5.18) are substituted as usual [58], and we derive

$$\begin{aligned}
& \partial_t \left(\int_{Y_{i,0}(t,\mathbf{x})} e^{-\frac{\phi_0}{k_B T}} u_0 d\mathbf{y} \right) + \int_{\Gamma_0(t,\mathbf{x})} f(e^{-\frac{\phi_0}{k_B T}} u_0, \rho_s) ds_{\mathbf{y}} \\
& + \nabla_{\mathbf{x}} \cdot \int_{Y_{i,0}(t,\mathbf{x})} -\frac{1}{\eta \rho} e^{-\frac{\phi_0}{k_B T}} \sum_j (\mathbf{w}_j + \nabla_{\mathbf{y}} \xi_j^1) u_0 \partial_{x_j} p_0 d\mathbf{y} \\
& + \nabla_{\mathbf{x}} \cdot \int_{Y_{i,0}(t,\mathbf{x})} -D e^{-\frac{\phi_0}{k_B T}} \sum_j \partial_{x_j} u_0 (\mathbf{e}_j + \nabla_{\mathbf{y}} \xi_j^2) d\mathbf{y} = 0.
\end{aligned}$$

Together with the definition of appropriate coefficient functions, see Section 5.4.7, we obtain a macroscopic description of the transport processes of the transformed number density u_0 supplemented by the cell problems (5.17) and (5.18).

5.4.7 Upscaling results

In the previous subsections, we applied periodic homogenization to the system of partial differential equations (5.7)–(5.9) describing fluid flow and transport (by convection, diffusion and drift) of colloidal particles within a porous medium. We used a level set formulation in order to handle the evolving microstructure that results from the surface reactions of the colloidal particles with the porous matrix. As resulting system of the averaging procedure by two-scale asymptotic expansion, we obtained Darcy's law for a compressible fluid and a modified averaged convection-diffusion equation. These equations are supplemented by several families of microscopic cell problems. Starting from the solutions of the cell problems, we derived averaged coefficient functions which explicitly depend on the microscopic geometry and the interaction potential between porous matrix and particles. We summarize the upscaling results in the following theorem.

Theorem 5.3 (Upscaling results I). *The two-scale limits \mathbf{v}_0, p_0, u_0 satisfy the following averaged limit equations:*

Darcy's law describes the averaged water movement

$$\begin{aligned}\bar{\mathbf{v}}_0 &= -\frac{1}{\eta\rho}\mathbf{K}(t, \mathbf{x})\nabla_{\mathbf{x}}p_0, & t \in (0, T), \mathbf{x} \in \Omega, \\ \nabla_{\mathbf{x}} \cdot \bar{\mathbf{v}}_0 &= m^{\text{col}}\frac{\rho - \rho_s}{\rho\rho_s}F(t, \mathbf{x}), & t \in (0, T), \mathbf{x} \in \Omega\end{aligned}$$

with $\bar{\mathbf{v}}_0 = \bar{\mathbf{v}}_0(t, \mathbf{x})$, $p_0 = p_0(t, \mathbf{x})$, and $F(t, \mathbf{x})$ being defined by

$$F(t, \mathbf{x}) := \int_{\Gamma_0(t, \mathbf{x})} f(e^{-\phi_0(t, \mathbf{x}, \mathbf{y})}u_0(t, \mathbf{x}), \rho_s) ds_{\mathbf{y}}, \quad (5.20)$$

and permeability tensor $\mathbf{K}(t, \mathbf{x})$ being defined by

$$K_{ij}(t, \mathbf{x}) := \int_{Y_{i,0}(t, \mathbf{x})} (\mathbf{w}_j)_i(t, \mathbf{x}, \mathbf{y}) d\mathbf{y}$$

with \mathbf{w}_j being the solutions of the supplementary family of cell problems (5.13).

The averaged convection-diffusion equation for the transformed number density $u_0 = u_0(t, \mathbf{x})$ is given by

$$\partial_t(A(t, \mathbf{x})u_0) + \nabla_{\mathbf{x}} \cdot (\mathbf{V}(t, \mathbf{x})u_0) - \nabla_{\mathbf{x}} \cdot (\mathbf{D}\mathbf{D}(t, \mathbf{x})\nabla_{\mathbf{x}}u_0) + F(t, \mathbf{x}) = 0, \quad t \in (0, T), \mathbf{x} \in \Omega$$

with weighted porosity $A(t, \mathbf{x})$, effective transport velocity $\mathbf{V}(t, \mathbf{x})$, and diffusion tensor $\mathbf{D}(t, \mathbf{x})$ being defined by

$$\begin{aligned} A(t, \mathbf{x}) &:= \int_{Y_{l,0}(t, \mathbf{x})} e^{-\frac{\phi_0(t, \mathbf{x}, \mathbf{y})}{k_B T}} d\mathbf{y}, \\ \mathbf{V}(t, \mathbf{x}) &:= \sum_j \left(-\frac{1}{\eta\rho} \int_{Y_{l,0}(t, \mathbf{x})} e^{-\frac{\phi_0(t, \mathbf{x}, \mathbf{y})}{k_B T}} (\mathbf{w}_j(t, \mathbf{x}, \mathbf{y}) + \nabla_{\mathbf{y}}\xi_j^1(t, \mathbf{x}, \mathbf{y})) d\mathbf{y} \right) \partial_{x_j} p_0(t, \mathbf{x}) \\ &=: -\frac{1}{\eta\rho} \hat{\mathbf{K}}(t, \mathbf{x}) \nabla_{\mathbf{x}} p_0(t, \mathbf{x}), \\ \mathbf{D}_{ij}(t, \mathbf{x}) &:= \int_{Y_{l,0}(t, \mathbf{x})} e^{-\frac{\phi_0(t, \mathbf{x}, \mathbf{y})}{k_B T}} (\partial_{y_i} \xi_j^2(\mathbf{w}_j(t, \mathbf{x}, \mathbf{y}) + \delta_{ij})) d\mathbf{y} \end{aligned}$$

with $\mathbf{w}_j, \xi_j^1, \xi_j^2$ being the solutions of the supplementary families of cell problems (5.13), (5.17), (5.18).

Furthermore, the level set function $L_0 = L_0(t, \mathbf{x}, \mathbf{y})$ satisfies

$$\partial_t L_0 - \frac{m^{\text{col}}}{\rho_s} f(e^{-\frac{\phi_0(t, \mathbf{x}, \mathbf{y})}{k_B T}} u_0(t, \mathbf{x}), \rho_s) |\nabla_{\mathbf{y}} L_0| = 0, \quad t \in (0, T), \mathbf{x} \in \Omega, \mathbf{y} \in Y. \quad (5.21)$$

Remark 5.4 (Consistency). We consider the \mathbf{y} -averaged number density $\bar{c}_0(t, \mathbf{x}) := \int_{Y_{l,0}(t, \mathbf{x})} c_0(t, \mathbf{x}, \mathbf{y}) d\mathbf{y}$. By integration of (5.12) it holds

$$\bar{c}_0(t, \mathbf{x}) = A(t, \mathbf{x})u_0(t, \mathbf{x}). \quad (5.22)$$

If there were no interactions, i.e. $\phi = \phi_0 + \varepsilon\phi_1 + \dots \equiv 0$, and also no evolving microstructure, i.e. $v_{\nu} \equiv 0$, the averaged coefficient functions A, \mathbf{D} would reduce in fact to the time and space independent coefficients

$$A = |Y_l| \quad \text{and} \quad \mathbf{D}_{ij} = \int_{Y_l} (\partial_{y_i} \xi_j^2(\mathbf{y}) + \delta_{ij}) d\mathbf{y}$$

and \mathbf{V} would reduce to the Darcy velocity

$$\mathbf{V}(t, \mathbf{x}) = \int_{Y_l} \mathbf{v}_0(t, \mathbf{x}, \mathbf{y}) d\mathbf{y} = \bar{\mathbf{v}}_0(t, \mathbf{x})$$

since $e^{-\frac{\phi_0}{k_B T}} \equiv e^0 = 1$ and the solutions ξ_j^1 of the additional family of cell problems would be equal to zero. Moreover, $c_0 = u_0$ and $\bar{c}_0 = |Y_l|c_0$ would hold. The quantity $|Y_l|/|Y| = |Y_{l,0}|/|Y|$ equals the porosity of the porous medium. Since $|Y|$ equals one, we henceforth denote the porosity by $\theta = |Y_{l,0}|$. The derived model is therefore consistent with the well-known effective model for fluid flow and transport

$$\begin{aligned} \bar{\mathbf{v}}_0 &= -\mathbf{K}\nabla_{\mathbf{x}}p_0, & t \in (0, T), \mathbf{x} \in \Omega, \\ \nabla_{\mathbf{x}} \cdot \bar{\mathbf{v}}_0 &= 0, & t \in (0, T), \mathbf{x} \in \Omega, \\ \theta\partial_t\bar{c}_0 + \nabla_{\mathbf{x}} \cdot (\bar{\mathbf{v}}_0\bar{c}_0) - \nabla_{\mathbf{x}} \cdot (D\nabla_{\mathbf{x}}\bar{c}_0) &= \theta|\Gamma|f(\bar{c}_0, \rho_s), & t \in (0, T), \mathbf{x} \in \Omega, \end{aligned}$$

since the equations and the coefficient functions reduce to the well known two-scale description that is found for example in [58].

5.4.8 Properties of the coefficient functions

In the following, we discuss in more detail the value and interpretation of the derived model. First of all, we state that the obtained coefficient functions are physically meaningful.

Theorem 5.5 (Physical properties). *The weighted porosity A as defined in Theorem 5.3 is strictly positive. The diffusion tensor \mathbf{D} and the permeability tensor \mathbf{K} as defined in Theorem 5.3 are symmetric and (uniformly) positive definite.*

Proof. The statement for the weighted porosity A is true by definition. The statement for the permeability tensor \mathbf{K} follows directly as in [58]. In order to prove the statement for the diffusion tensor, we follow the ideas in [24] and [58]:

The diffusion tensor is reformulated via

$$\mathbf{D}_{ij} := \int_{Y_{l,0}(t,\mathbf{x})} e^{-\frac{\phi_0}{k_B T}} (\partial_{y_i}\xi_j^2 + \delta_{ij}) d\mathbf{y} = \int_{Y_{l,0}(t,\mathbf{x})} e^{-\frac{\phi_0}{k_B T}} (\nabla_{\mathbf{y}}\xi_j^2 + \mathbf{e}_j) \cdot \mathbf{e}_i d\mathbf{y}.$$

Considering ξ_j^2 as test function in the weak formulation of the cell problem (5.17), we obtain

$$\int_{Y_{l,0}(t,\mathbf{x})} e^{-\frac{\phi_0}{k_B T}} \mathbf{e}_i \cdot \nabla_{\mathbf{y}}\xi_j^2 d\mathbf{y} = - \int_{Y_{l,0}(t,\mathbf{x})} e^{-\frac{\phi_0}{k_B T}} \nabla_{\mathbf{y}}\xi_i^2 \cdot \nabla_{\mathbf{y}}\xi_j^2 d\mathbf{y}$$

Applying both of the above identities and using the equality while interchanging the

indexes, leads directly to the symmetry property of the diffusion tensor \mathbf{D} :

$$\begin{aligned} \mathbf{D}_{ij} &:= \int_{Y_{i,0}(t,\mathbf{x})} e^{-\frac{\phi_0}{k_B T}} (\nabla_{\mathbf{y}} \xi_j^2 + \mathbf{e}_j) \cdot \mathbf{e}_i \, d\mathbf{y} = \int_{Y_{i,0}(t,\mathbf{x})} e^{-\frac{\phi_0}{k_B T}} (-\nabla_{\mathbf{y}} \xi_j^2 \cdot \nabla_{\mathbf{y}} \xi_i^2 + \mathbf{e}_j \cdot \mathbf{e}_i) \, d\mathbf{y} \\ &= \int_{Y_{i,0}(t,\mathbf{x})} e^{-\frac{\phi_0}{k_B T}} (-\nabla_{\mathbf{y}} \xi_i^2 \cdot \nabla_{\mathbf{y}} \xi_j^2 + \mathbf{e}_i \cdot \mathbf{e}_j) \, d\mathbf{y} = \int_{Y_{i,0}(t,\mathbf{x})} e^{-\frac{\phi_0}{k_B T}} (\nabla_{\mathbf{y}} \xi_i^2 + \mathbf{e}_i) \cdot \mathbf{e}_j \, d\mathbf{y} \\ &= \mathbf{D}_{ji}. \end{aligned}$$

As a preliminary remark, we note that using ξ_j^2 as test function in the weak formulation of the cell problem (5.17) allows to formulate the following representation of “zero”.

$$\int_{Y_{i,0}(t,\mathbf{x})} e^{-\frac{\phi_0}{k_B T}} (\nabla_{\mathbf{y}} \xi_j^2 + \mathbf{e}_j) \cdot \nabla_{\mathbf{y}} \xi_i^2 \, d\mathbf{y} = 0.$$

Since $e^{-\frac{\phi_0}{k_B T}} > 0$ holds, we obtain the positive definiteness of the effective diffusion tensor \mathbf{D} performing the following calculations:

$$\begin{aligned} \sum_{ij} a_i \mathbf{D}_{ij} a_j &:= \sum_{ij} a_i \left(\int_{Y_{i,0}(t,\mathbf{x})} e^{-\frac{\phi_0}{k_B T}} (\partial_{y_i} \xi_j^2 + \delta_{ij}) \, d\mathbf{y} \right) a_j \\ &= \sum_{ij} a_i \left(\int_{Y_{i,0}(t,\mathbf{x})} e^{-\frac{\phi_0}{k_B T}} (\nabla_{\mathbf{y}} \xi_j^2 + \mathbf{e}_j) \cdot \mathbf{e}_i \, d\mathbf{y} \right) a_j \\ &= \sum_{ij} a_i \left(\underbrace{\int_{Y_{i,0}(t,\mathbf{x})} e^{-\frac{\phi_0}{k_B T}} (\nabla_{\mathbf{y}} \xi_j^2 + \mathbf{e}_j) \cdot \nabla_{\mathbf{y}} \xi_i^2 \, d\mathbf{y}}_{=0} \right. \\ &\quad \left. + \int_{Y_{i,0}(t,\mathbf{x})} e^{-\frac{\phi_0}{k_B T}} (\nabla_{\mathbf{y}} \xi_j^2 + \mathbf{e}_j) \cdot \mathbf{e}_i \, d\mathbf{y} \right) a_j \\ &= \sum_{ij} a_i \left(\int_{Y_{i,0}(t,\mathbf{x})} e^{-\frac{\phi_0}{k_B T}} (\nabla_{\mathbf{y}} \xi_j^2 + \mathbf{e}_j) \cdot (\nabla_{\mathbf{y}} \xi_i^2 + \mathbf{e}_i) \, d\mathbf{y} \right) a_j \\ &= \int_{Y_{i,0}(t,\mathbf{x})} \sum_i e^{-\frac{\phi_0}{2k_B T}} \nabla_{\mathbf{y}} (a_i (\xi_i^2 + y_i)) \cdot \sum_j e^{-\frac{\phi_0}{2k_B T}} \nabla_{\mathbf{y}} (a_j (\xi_j^2 + y_j)) \, d\mathbf{y} \\ &\geq 0 \end{aligned}$$

Uniform positive definiteness is shown in two steps, cf. [24]. First of all, we prove that $\sum_{ij} a_i \mathbf{D}_{ij} a_j$ is strictly positive. Otherwise it held $\sum_i e^{-\frac{\phi_0}{2k_B T}} \nabla_{\mathbf{y}} (a_i (\xi_i^2 + y_i)) = 0$, which implied that $\sum_i \nabla_{\mathbf{y}} (a_i (\xi_i^2 + y_i)) = 0$ and therefore $\sum_i a_i (\xi_i^2 + y_i)$ was constant. This statement is only true in the case of all a_i being zero, since ξ_i^2 is Y -periodic and on the other hand y_i is not, i.e., the strict positivity follows by contradiction.

Secondly, the mapping $f(\mathbf{a}, \mathbf{a}) := \sum_{ij} a_i \mathbf{D}_{ij} a_j$ is continuous on the circle $S^1 := \{\mathbf{a} : \|\mathbf{a}\| = 1\}$ and strict positive on the compact subset $S^1 \subset \mathbb{R}^N$ since $\mathbf{a} = 0 \notin S^1$. Therefore, the minimum value $0 < \alpha := \min_{S^1} f(\mathbf{a}, \mathbf{a})$ is taken and via the transformation $\mathbf{b} := \frac{\mathbf{a}}{\|\mathbf{a}\|}$ uniform positive definiteness follows by

$$\sum_{ij} b_i \mathbf{D}_{ij} b_j = \frac{1}{\|\mathbf{a}\|^2} \sum_{ij} a_i \mathbf{D}_{ij} a_j \geq \alpha > 0 \quad \Leftrightarrow \quad \sum_{ij} a_i \mathbf{D}_{ij} a_j \geq \alpha \|\mathbf{a}\|^2 > 0 .$$

This concludes the proof of Theorem 5.5. \square

5.4.9 Backtransformation

Upscaling result I, cf. Theorem 5.3, was formulated in terms of the transformed number density u_0 and the original unknown c_0 is regained in virtue of (5.12). Using (5.22), an equation for the averaged number density \bar{c}_0 is obtained directly:

Theorem 5.6 (Upscaling results II). *The averaged convection-diffusion equation for the averaged number density \bar{c}_0 is given by*

$$\partial_t(\bar{c}_0) + \nabla_{\mathbf{x}} \cdot \left(\tilde{\mathbf{V}}(t, \mathbf{x}) \bar{c}_0 - D \tilde{\mathbf{D}}(t, \mathbf{x}) \nabla_{\mathbf{x}} \bar{c}_0 \right) + \tilde{F}(t, \mathbf{x}) = 0, \quad t \in (0, T), \quad \mathbf{x} \in \Omega \quad (5.23)$$

with the newly defined effective coefficients $\tilde{\mathbf{V}}, \tilde{\mathbf{D}}, \tilde{F}$ that are given by $\tilde{\mathbf{V}}(t, \mathbf{x}) = \frac{\mathbf{v}}{A} - \mathbf{D} \nabla_{\mathbf{x}} \frac{1}{A}$, $\tilde{\mathbf{D}} = \frac{\mathbf{D}}{A}$ and $\tilde{F} = \int_{\Gamma_0(t, \mathbf{x})} f \left(\frac{e^{-\frac{\phi_0}{k_B T}}}{A} \bar{c}_0, \rho_s \right) ds_{\mathbf{y}}$.

Equation (5.23) is again a convection-diffusion equation with effective coefficients. Here, the effective transport velocity is given by $\tilde{\mathbf{V}}$, whereas $\mathbf{v} = \mathbf{v}^{\text{col}} + \mathbf{v}^{\text{hydr}}$ was the starting point of our investigations, cf. (5.1) and Section 2.1. Moreover, the redefined diffusion coefficient $\tilde{\mathbf{D}}$ is obtained as a rescaling of the diffusion tensor \mathbf{D} with the weighted porosity A and the properties, which have been stated in Theorem 5.5, transfer directly to $\tilde{\mathbf{D}}$.

5.5 Numerical Results

In this Section, we consider the derived model description in a radially symmetric setting, cf. Theorem 5.3. For this case, the effective coefficients $A, \hat{\mathbf{K}}, \mathbf{D}$ are computed numerically.

5.5.1 Representation of the interaction potential and the geometry in a radially symmetric setting

In case of a radially symmetric setting, a simplified description of the upscaling results in Theorem 5.3 and especially of the representation of the geometry is obtained. To this end, we assume a radially symmetric interaction potential Φ^{col} between the colloidal particles and the porous matrix as well as a circular shape of the local grains during evolution. First, we determine the representation of ϕ_0 and also of the evolution of the geometry explicitly. This is done analogously to [138], [139] with slight corrections:

For each point $\mathbf{x} \in \Omega$, we define the integer part $\mathbf{x}^M := \lfloor \mathbf{x} + (\frac{0.5}{\varepsilon}) \rfloor$ and the relative shift $\mathbf{x}^S = \mathbf{x} - \mathbf{x}^M$. Note as a remark, that \mathbf{x}^M denotes the midpoint (i, j) of the shifted unit cell Y^{ij} of which \mathbf{x} is an element, see also Figure 5.2. Then, it holds

$$\mathbf{x} = \varepsilon \left(\frac{\mathbf{x}}{\varepsilon} \right)^M + \varepsilon \left(\frac{\mathbf{x}}{\varepsilon} \right)^S$$

with $\left(\frac{\mathbf{x}}{\varepsilon} \right)^S \in Y$.

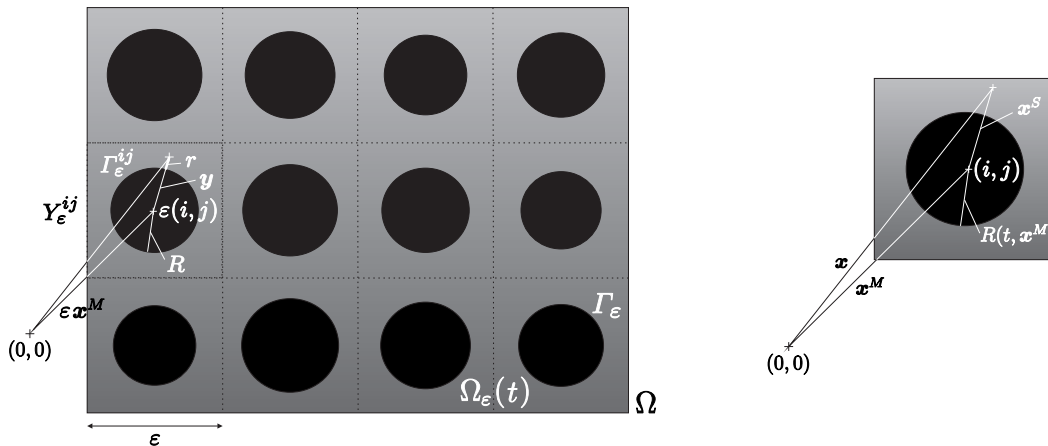


Figure 5.2: Locally periodic geometry; notation: scaled (left) and unscaled (right)

For the interaction potential, we assume for every Y_ε^{ij}

$$\phi_\varepsilon^{\text{col}}(t, \mathbf{x}) = \Phi^{\text{col}} \left(\frac{\text{dist}(\mathbf{x}, \Gamma_\varepsilon^{ij}(t, \mathbf{x}))}{\varepsilon} \right), \quad \mathbf{x} \in Y_\varepsilon^{ij} \quad (5.24)$$

with some given function Φ^{col} for the interaction potential.

We subsequently determine the representation of ϕ_0 in terms of Φ^{col} . To this end, we assume that a parametrization $\mathbf{k}_\varepsilon^{ij} : (t, s) \in (0, T) \times (0, 1) \rightarrow \mathbb{R}$ of the boundary Γ_ε^{ij}

exists, such that the following relation holds, [138]:

$$\begin{aligned} L_\varepsilon(t, \mathbf{k}_\varepsilon^{ij}(t, s)) &= 0, \quad t \geq 0 \\ \mathbf{k}_\varepsilon^{ij}(t, s) &= \varepsilon(i, j) + \varepsilon \mathbf{k}_0^{ij}(t, s) + \varepsilon^2 \mathbf{k}_1^{ij}(t, s) + \dots \end{aligned} \quad (5.25)$$

As shown in [138], $\mathbf{k}_0(t, s)$ locally parameterizes the zero level set L_0 , which means that $L_0(t, \mathbf{x}, \mathbf{k}_0) = 0$. Consequently, we also have a parametrization of the boundary Γ_0 .

Substituting the expansion (5.25), we obtain for $\mathbf{x} \in Y_\varepsilon^{ij}$:

$$\begin{aligned} \text{dist}(\mathbf{x}, \Gamma_\varepsilon^{ij}(t, \mathbf{x})) &= \min_{s \in (0,1)} |\mathbf{k}_\varepsilon^{ij}(t, s) - \mathbf{x}| = \min_{s \in (0,1)} \left| \varepsilon \left(\mathbf{k}_0^{ij}(t, s) - \left(\frac{\mathbf{x}}{\varepsilon} \right)^S \right) + O(\varepsilon^2) \right| \\ &= \varepsilon \text{dist} \left(\left(\frac{\mathbf{x}}{\varepsilon} \right)^S, \Gamma_0(t, \mathbf{x}) \right) + O(\varepsilon^2). \end{aligned}$$

Furthermore, in a *radially symmetric geometry*, for (5.24) it follows, by the derivations made above, that

$$\phi_\varepsilon^{\text{col}}(t, \mathbf{x}) = \Phi^{\text{col}} \left(\left| \left(\frac{\mathbf{x}}{\varepsilon} \right)^S \right| - R \left(t, \mathbf{x} - \varepsilon \left(\frac{\mathbf{x}}{\varepsilon} \right)^S \right) + O(\varepsilon) \right).$$

since in the radially symmetric setting, the local radius $R : (0, T) \times \Omega \rightarrow (0, \frac{1}{2})$ is used to parametrize the geometry completely. Taylor expansion around \mathbf{x} yields

$$R \left(t, \mathbf{x} - \varepsilon \left(\frac{\mathbf{x}}{\varepsilon} \right)^S \right) = R(t, \mathbf{x}) + O(\varepsilon)$$

and therefore, we obtain

$$\phi_\varepsilon^{\text{col}}(t, \mathbf{x}) = \Phi^{\text{col}} \left(\left| \left(\frac{\mathbf{x}}{\varepsilon} \right)^S \right| - R(t, \mathbf{x}) \right) + O(\varepsilon).$$

This allows to identify the representation of ϕ_0 in terms of the given radially symmetric interaction potential Φ^{col} :

$$\phi_0(t, \mathbf{x}, \mathbf{y}) = \Phi^{\text{col}}(|\mathbf{y}| - R(t, \mathbf{x})),$$

i.e., as a consequence of the circular grain geometry, the representation reduces to a function of the local separation distance $|\mathbf{y}| - R$.

In the radially symmetric case, the level set equation, which completely describes the evolution of the geometry, is reduced to the description of the evolution of the grain

radius $R : (0, T) \times \Omega \rightarrow (0, \frac{1}{2})$ which depends only the midpoints \mathbf{x}^M . It is determined directly by the following ordinary differential equation:

$$\partial_t R(t, \mathbf{x}) = \frac{m^{\text{col}}}{\rho_s} f(e^{-\phi_0(t, \mathbf{x}, R(t, \mathbf{x}))} u_0(t, \mathbf{x}), \rho_s).$$

5.5.2 Computation of effective coefficients

In this section, we compute the effective coefficients $A, \mathbf{K}, \hat{\mathbf{K}}, \mathbf{D}$ defined in Section 5.4.7 for a radially symmetric setting in dependence of the local grain radius R and porosity $\theta = |Y_{l,0}| = 1 - R^2\pi$, respectively, for different choices of the interaction potential. The second and third example are chosen according to well established power laws for repulsive or attractive particle-wall interaction potentials [41], [141].

$$1. \quad \phi_0(t, \mathbf{x}, \mathbf{y}) := \alpha - 2\alpha(|\mathbf{y}| - R(t, \mathbf{x})), \quad \text{for } \alpha \geq 0, \quad (5.26a)$$

$$2. \quad \phi_0(t, \mathbf{x}, \mathbf{y}) := \frac{1}{|\mathbf{y}| - R(t, \mathbf{x}) + \beta}, \quad \text{for } \beta \geq 0, \quad (5.26b)$$

$$3. \quad \phi_0(t, \mathbf{x}, \mathbf{y}) := \frac{1}{(|\mathbf{y}| - R(t, \mathbf{x}) + 1)^\gamma}, \quad \text{for } \gamma \geq 0. \quad (5.26c)$$

Recalling that $\mathbf{V} = -\frac{1}{\eta\rho_1} \hat{\mathbf{K}} \nabla_{\mathbf{x}} p_0$ and owing to a discretization by mixed finite elements, \mathbf{K}, \mathbf{D} , and $\hat{\mathbf{K}}$ are obtained directly by integrating the solutions of the cell problems (5.13) and the associated flux approximations $\zeta_j^1 := -e^{-\frac{\phi_0}{kT}} \nabla_{\mathbf{y}} \xi_j^1 - e^{-\frac{\phi_0}{kT}} \mathbf{w}_j$, $\zeta_j^2 := -e^{-\frac{\phi_0}{kT}} \nabla_{\mathbf{y}} \xi_j^2 - e^{-\frac{\phi_0}{kT}} \mathbf{e}_j$ of the cell problems (5.17) and (5.18), respectively.

$$\begin{aligned} \mathbf{D}(t, x) &= - \int_{Y_{1,0}(t,x)} [\zeta_1^2(t, x, y) | \zeta_2^2(t, x, y)] dy, \\ \mathbf{K}(t, x) &= - \int_{Y_{1,0}(t,x)} [\mathbf{w}_1(t, x, y) | \mathbf{w}_2(t, x, y)] dy, \\ \hat{\mathbf{K}}(t, x) &= - \int_{Y_{1,0}(t,x)} [\zeta_1^1(t, x, y) | \zeta_2^1(t, x, y)] dy. \end{aligned}$$

Here, the notation $[\mathbf{a} | \mathbf{b}]$ denotes the matrix consisting of columns \mathbf{a} and \mathbf{b} .

As we have demonstrated in Section 5.4.8, the averaged tensors are symmetric and positive definite. Moreover, in the radially symmetric setting, the tensors are in fact reduced to scalar coefficients, i.e.

$$\mathbf{D} = D_{11} \mathbf{E} \quad \mathbf{K} = K_{11} \mathbf{E}, \quad \hat{\mathbf{K}} = \hat{K}_{11} \mathbf{E}$$

with unity matrix \mathbf{E} . This is due to the fact that in an isotropic medium no direction is preferred for transport.

The computation results of the reference values of the effective coefficients (including K_{11} , cf. Remark 5.4) and the simulation results of the effective coefficients A , \hat{K}_{11} , and D_{11} are depicted in Figures 5.3–5.11. All numerical computations are done with the toolbox HyPHM, see Section 2.3 and [45].

The convergence to the reference values for small parameter value α , large parameter value β and large parameter value γ in (5.26), respectively, perfectly correspond to the analytical convergence of $\phi_0 \rightarrow 0$ in these limit cases. However, for other parameter values there is a clear dependence of the coefficients on the interaction potential.

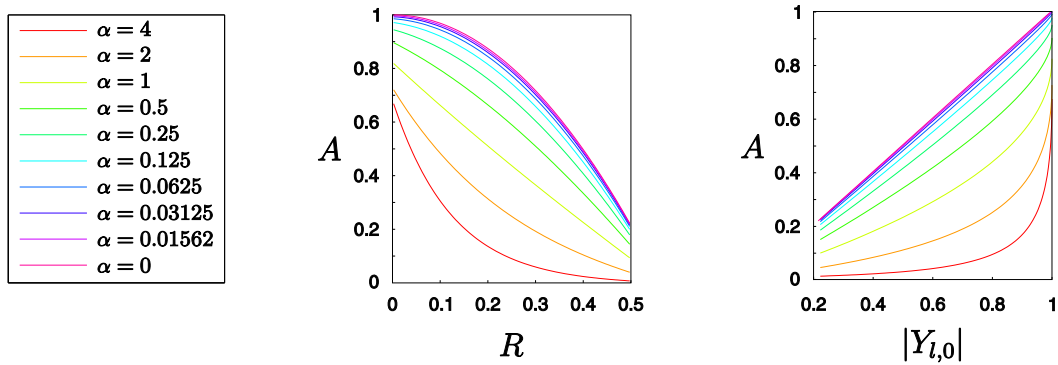


Figure 5.3: The computed coefficient A against the grain radius R and the porosity $\theta = |Y_{l,0}|$.

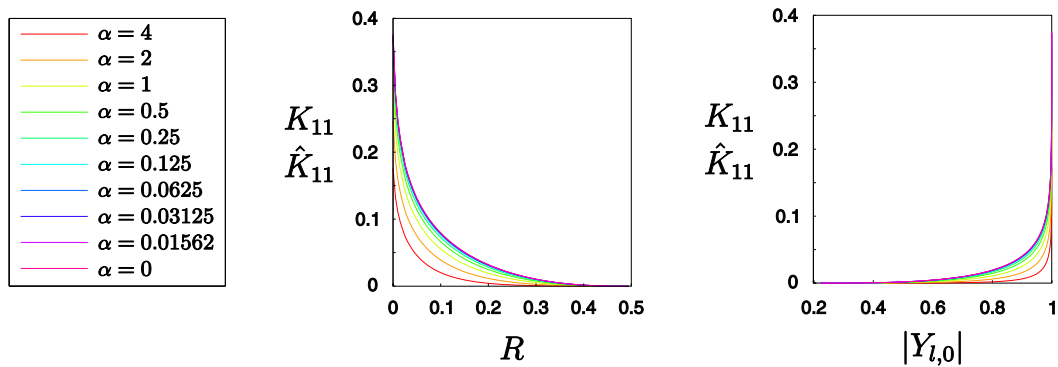


Figure 5.4: The computed coefficients K_{11} and \hat{K}_{11} against the grain radius R and the porosity $\theta = |Y_{l,0}|$.

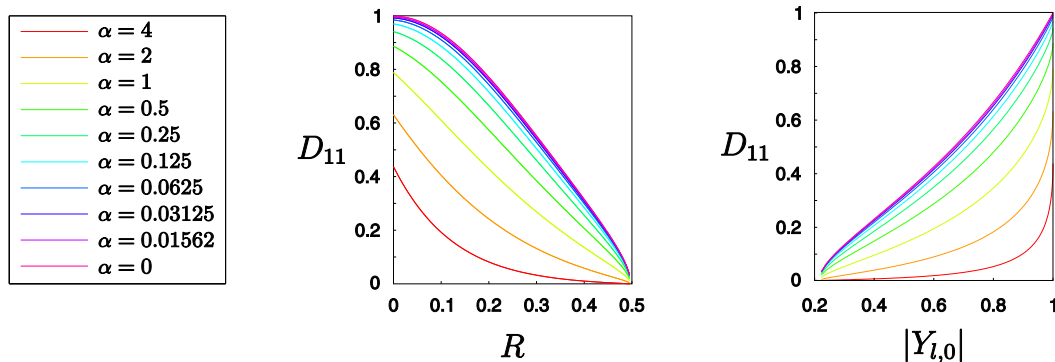


Figure 5.5: The computed coefficient D_{11} against the grain radius R and the porosity $\theta = |Y_{l,0}|$.

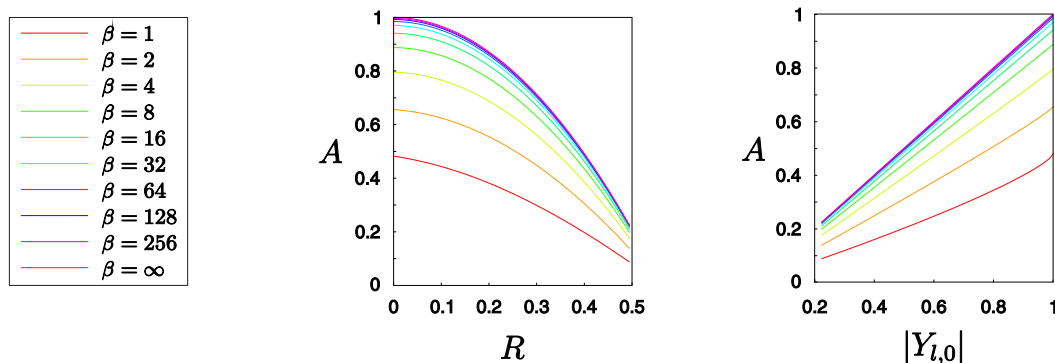


Figure 5.6: The computed coefficient A against the grain radius R and the porosity $\theta = |Y_{l,0}|$.

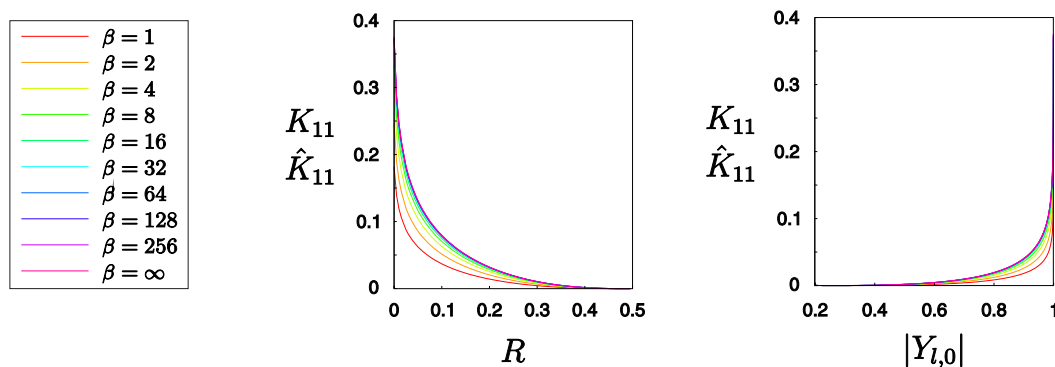


Figure 5.7: The computed coefficients K_{11} and \hat{K}_{11} against the grain radius R and the porosity $\theta = |Y_{l,0}|$.

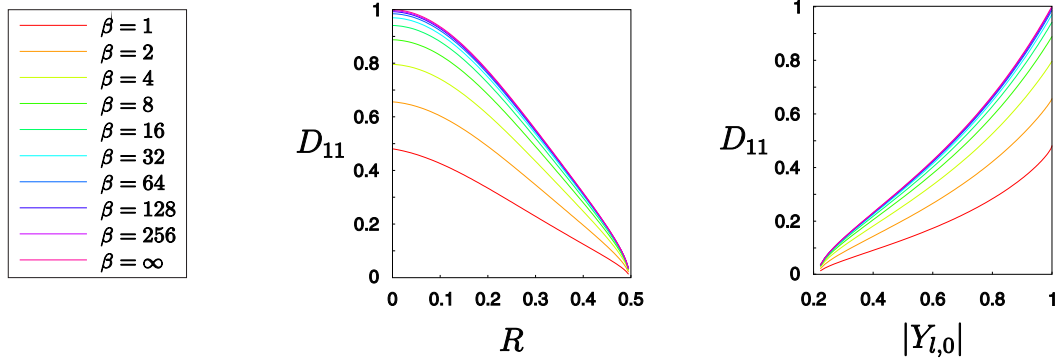


Figure 5.8: The computed coefficient D_{11} against the grain radius R and the porosity $\theta = |Y_{l,0}|$.

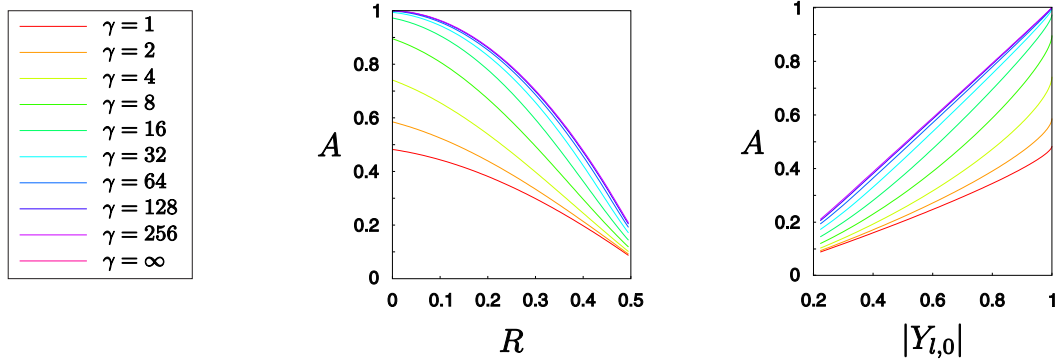


Figure 5.9: The computed coefficient A against the grain radius R and the porosity $\theta = |Y_{l,0}|$.

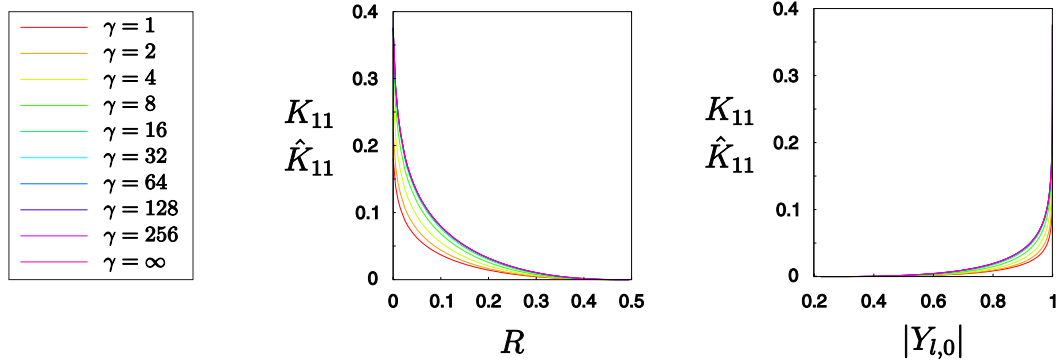


Figure 5.10: The computed coefficients K_{11} and \hat{K}_{11} against the grain radius R and the porosity $\theta = |Y_{l,0}|$.

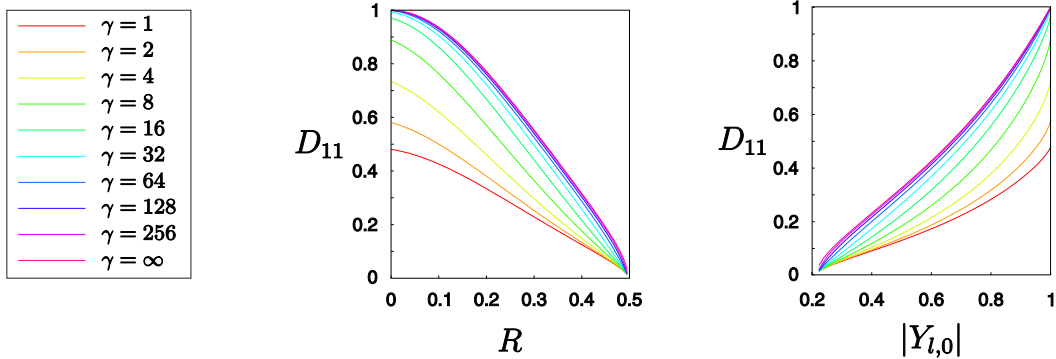


Figure 5.11: The computed coefficient D_{11} against the grain radius R and the porosity $\theta = |Y_{l,0}|$.

5.6 Concluding remarks

Using a level set formulation, we performed the periodic homogenization of a coupled model describing colloid and fluid dynamics within a porous medium including interaction with the porous matrix and an evolving microstructure. The obtained averaged model description consists of Darcy's law and a modified convection-diffusion equation. The supplementary cell problems and also the averaged coefficients depend on the geometry and the chosen interaction potential. These coefficients were computed numerically in a radially symmetric setting for varying porosity and radii, respectively, i.e. we considered a radially symmetric interaction potential between colloids and the porous matrix as well as a circular shape of the local grains during evolution. These results emphasize the fact that the multi-scale character and the interaction properties of colloidal particles within the porous matrix cannot be neglected in a reasonable model approach.

The particular strength of our model lies in the fact that it is applicable for further (non-) DLVO interaction forces and also combinations of such forces can be taken into account. However, even more effort needs to be undertaken to achieve a well-founded understanding of processes in a realistic 3D setting. Therefore, the methods applied in this study need to be further developed or different approaches have to be used. Despite of this drawback, our attempt can be seen as a first step toward capturing directly structural changes in a porous medium in a macroscopic model description. In this sense, in [112], numerical simulations of a heterogeneous multi-scale scenario with heterogeneous porosity were performed. For details on the discretization and numerical computations, we refer to Section 2.3, [46] and [112].

In [112], a locally periodic setting, which is generated by a random field is considered. In more detail, to each (discrete) point $\boldsymbol{x} \in \Omega$, a unit cell Y is associated with fluid phase $Y_l(t, \boldsymbol{x})$ and porosity $|Y_l(t, \boldsymbol{x})|$, which evolve in time and which represent the underlying locally periodic geometry of the porous matrix in the surrounding area. In particular, in the heterogeneous multi-scale scenario, the interaction potential and the surface reaction rate were chosen in such a way that pore clogging occurs. Several effects that are captured by our model such as the interplay between evolving microstructure due to attachment processes and fluid flow are highlighted in [112]. Moreover, the effects of porosity changes have been studied: A pressure difference between lower left corner and upper right corner of the computational domain is applied. Consequently, a water flux evolves in which the number density is transported. Then, a local reduction of the porosity results, which starts from the lower left corner according to the propagation of the number density and its interaction with the porous matrix. This also leads to a decrease of the fluid velocity since the pores are clogged locally. In this sense, the process of local pore clogging coming along with a change of the local water flux and porosity is emphasized.

Chapter 6

Discussion and Outlook

The scope of this thesis was the rigorous mathematical derivation of effective models of fluid flow and transport processes of charged colloidal particles based on microscopic modeling principles. A big challenge was to transfer information from the pore-scale to the macroscopic scale in a direct and reasonable way. Particular attention was laid on the following two aspects: Firstly, the spatial heterogeneous structure of a porous medium and secondly, the interplay and coupling of processes that arise in investigating fluid flow, colloidal particles, their transport and the porous matrix.

We started our considerations with the mathematical descriptions of fluid flow and transport of charged colloidal particles on different spatial scales. In particular, the Stokes-Nernst-Planck-Poisson system and the Darcy-Nernst-Planck-Poisson system were introduced and discussed to some extent. For both of these models, unique existence of weak solutions and physical properties of these solutions were established. To this end, a fixed point approach was applied and Moser's iteration was used in order to prove an L^∞ -estimate.

Based on existing upscaling methods, we performed the rigorous periodic homogenization of the Stokes-Nernst-Planck-Poisson system. In the derivation of equivalent effective models, we have demonstrated that suitable ε -independent a priori estimates hold. Guaranteeing the strong convergence of the number densities, we succeeded in deriving effective model descriptions using the method of two-scale convergence. Effective coefficients such as permeability, diffusion tensor and porosity were defined by means of so-called cell problems. In this way, also the geometrical structure enters the effective model description. We extended the existing convergence analysis by analyzing a quite large range of the parameter set $(\alpha_1, \alpha_2, \alpha_3, \beta, \gamma)$ and different (non homogeneous)

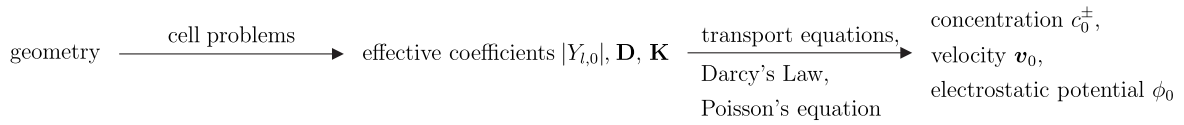


Figure 6.1: Schematic representation of the one-sided coupled two-scale system

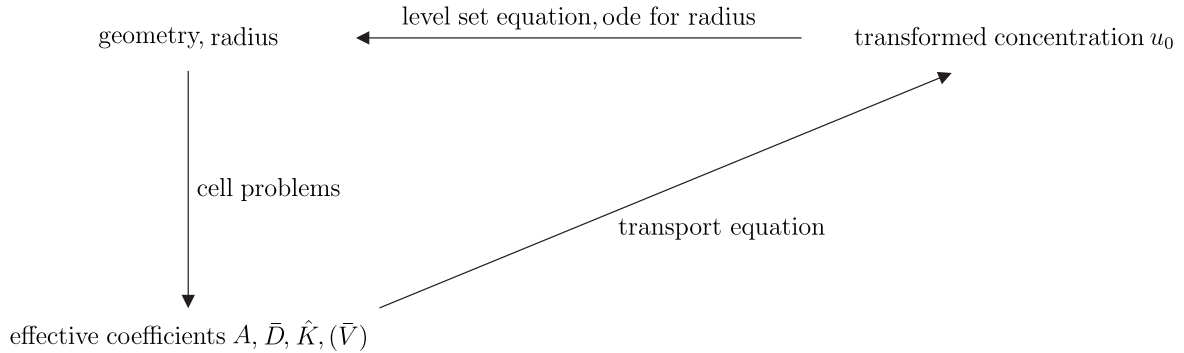


Figure 6.2: Schematic representation of the fully coupled two-scale system

boundary conditions. Although structurally different limit systems were obtained including also the fully coupled Darcy-Nernst-Planck-Poisson system, all these models have in common that they are only one sided coupled two-scale systems in the sense that effective coefficients can be precalculated, see Figure 6.1.

Another question that we addressed in this thesis was the integration of the interaction and chemical reactions of the colloidal particles with the porous matrix to the Stokes-Nernst-Planck system. In more detail, we provided an extension of the model that includes the evolution of the microstructure. Moreover, it is capable of changes in porosity and effects of pore clogging together with the back coupling to fluid flow and change in transport properties of the porous medium. Applying the method of two-scale asymptotic expansion in a level set framework, we were able to derive an effective model description also in this setting. In this sense, the existing theory was extended, since our attempt is a first step toward capturing directly structural changes in a porous medium in a macroscopic model description. In contrast to our results discussed above, a fully coupled two-scale system was obtained in the sense that effective coefficients cannot be precalculated independently of the macroscopic variables, see Figure 6.2.

All the results we have shown in this thesis emphasize the fact that the multi-scale character and the interplay of different processes at the pore-scale cannot be neglected in a reasonable macroscopic model approach.

Although the results obtained in this thesis lead to a deeper insight and a more profound understanding of the transport mechanism of colloidal particles on different

spatial scales, there is still considerable room for further improvements and future research.

Some aspects could not be answered in this thesis. Even though the methods employed in this thesis were very powerful, an improvement of the ε -independent regularity estimates needs to be achieved such that the volume additivity constraint could be omitted entirely. This issue could be clarified by an extension of the theoretical results provided in [61, 131]. Moreover, corrector/error estimates will be needed in order to compare the effective solutions/problem descriptions with the oscillatory solution/microscopic model. These considerations would also yield a possibility to compare the direct and the two-scale approach numerically, i.e. to identify whether the model error or the discretization error dominates the overall error estimate of a reasonable numerical scheme.

Having understood the dynamics of colloidal particles themselves in a porous medium and their influence on structural changes in the pore space by the investigations summarized above, another key question for the understanding of processes in the soil needs to be faced: the mobilization of substances, i.e. the interplay with contaminants. To this end, a combination of the provided models with mathematical models based on adsorption relations would open up new paths in the field of remediation.

Numerical simulations regarding realistic geoscientific or biological problems could be performed based on our analytical results. To this end, several extensions of the basic model equations need to be considered: the combination of different boundary conditions, the combination of the electrostatic forces with further (non-)DLVO forces, the integration of more than two species to the model, and further effects such as dispersion have to be taken into account in an overall mathematical model description. Multiple experimental observations and measurements are necessary in order to identify species dependent physical parameters explicitly and to provide reasonable functional dependencies on variables such as number densities of the species, temperature, pH-value, and so on.

Appendix A

Notation

A.1 Basic notation

\circ		composition
dist	$\text{dist}(\mathbf{x}, \mathbf{y}) = \ \mathbf{x} - \mathbf{y}\ $ $\text{dist}(\mathbf{x}, \Gamma) = \min_{\mathbf{y} \in \Gamma} \ \mathbf{x} - \mathbf{y}\ $	distance
δ_{ij}	$\delta_{ij} = \begin{cases} 0, & i \neq j \\ 1, & i = j \end{cases}$	Kronecker Delta
\mathbf{e}_j	$= (0, \dots, 0, \underbrace{1}_{j\text{-th position}}, 0, \dots, 0)$	j-th unity vector
\mathbf{E}	$\mathbf{E} = \begin{pmatrix} 1 & 0 & \dots & \dots & 0 \\ 0 & 1 & 0 & \dots & 0 \\ \vdots & \ddots & \ddots & \ddots & \vdots \\ \vdots & \ddots & 0 & 1 & 0 \\ 0 & \dots & \dots & 0 & 1 \end{pmatrix}$	unity matrix
min	$\min(x, y) = \begin{cases} x, & x \leq y \\ y, & x > y \end{cases}$	minimum
max	$\max(x, y) = \begin{cases} x, & x \geq y \\ y, & x < y \end{cases}$	maximum
O		Landau symbol
\prod	$\prod_{i=1}^k a_k = a_1 \cdot a_2 \cdot \dots \cdot a_k$	(in)finite product
\sum	$\sum_{i=1}^k a_k = a_1 + a_2 + \dots + a_k$	(in)finite sum
\cdot	$\mathbf{a} \cdot \mathbf{b} = \sum_{i=1}^n a_i b_i$	scalar product

$:$	$\mathbf{A} : \mathbf{B} = \sum_{i=1}^n \sum_{j=1}^n A_{ij} B_{ij}$	scalar product
$\mathbf{A}\mathbf{a}$	$\mathbf{A}\mathbf{a} = \left(\sum_{j=1}^n A_{1j} a_j, \dots, \sum_{j=1}^n A_{nj} a_j \right)^T$	matrix-vector product
$\mathbf{a} \cdot \mathbf{A}$	$\mathbf{a} \cdot \mathbf{A} = \left(\sum_{i=1}^n A_{i1} a_i, \dots, \sum_{i=1}^n A_{in} a_i \right)^T$	matrix-vector product
$\ \cdot\ $	$\ \mathbf{x}\ = \left(\sum_{i=1}^n x_i^2 \right)^{1/2}$	Euclidean norm
$ \cdot $		absolute value
$(\cdot)_-$	$(\varphi)_- = \min(0, \varphi)$	cut-off function
$(\cdot)_+$	$(\varphi)_+ = \max(0, \varphi)$	cut-off function
$[\cdot]$		floor function, largest integer not greater than \cdot
\rightarrow		strong convergence
\rightharpoonup		weak convergence
$\xrightarrow{*}$		weak-* convergence
$\xrightarrow{2}$		two-scale convergence

A.2 Domain related quantities

$\bar{\cdot}$		closure
\cdot_ε		ε -scaled quantity
\cdot_D		type Dirichlet
\cdot_F		type Flux
\cdot_N		type Neumann
\cdot_{NP}		type Nernst-Planck
\cdot_P		type Poisson
\cdot_{ij}		shifted 2D quantity related to mid point $(i, j) \in \mathbb{Z}^2$
\cdot_i		shifted quantity, encountered with $i \in I \subset \mathbb{N}$
Ω	$\Omega \subset \mathbb{R}^n$	computational domain
Ω_T	$\Omega_T = (0, T) \times \Omega$	time space cylinder
Ω_ε	$\Omega_\varepsilon \subset \Omega$	perforated computational domain
$\partial\Omega$		boundary of Ω , exterior boundary of Ω_ε
Γ_ε	$\partial\Omega_\varepsilon = \partial\Omega \cup \Gamma_\varepsilon$	interior boundary of Ω_ε , solid liquid interface
Y	$Y = [-\frac{1}{2}, +\frac{1}{2}]^n \subset \mathbb{R}^n$	unit cell
Y_l	$Y_l \subset \mathbb{R}^n$	liquid phase of unit cell
$ Y_l $	$ Y_l = \frac{ Y_l }{ Y }$	porosity of the porous medium
Y_s	$Y_s \subset \mathbb{R}^n$	solid phase of unit cell
∂Y		exterior boundary of Y
Γ	$\Gamma = \bar{Y}_s \cap \bar{Y}_l$	interior boundary of unit cell, solid liquid interface
χ	$\chi_\Omega(\mathbf{x}) = \begin{cases} 1, & \mathbf{x} \in \Omega \\ 0, & \mathbf{x} \notin \Omega \end{cases}$	characteristic function
ν		outer unit normal
τ		unit tangent

A.3 Function spaces

\mathbb{N}	$\mathbb{N} = \{1, 2, \dots\}$	set of natural numbers
\mathbb{N}_0	$\mathbb{N}_0 = \{0, 1, 2, \dots\}$	set of natural numbers including 0
\mathbb{R}		set of real numbers
\mathbb{R}_+	$\mathbb{R}_+ = \{x \in \mathbb{R} : x > 0\}$	set of real numbers
\mathbb{R}^n	$\mathbb{R}^n = \underbrace{\mathbb{R} \times \mathbb{R} \times \dots \times \mathbb{R}}_{n \text{ times}}; \mathbb{R}^1 = \mathbb{R}$	n -dimensional set of real numbers
\mathbb{Z}	$\mathbb{Z} = \{\dots, -2, -1, 0, 1, 2, \dots\}$	set of integer numbers
$C_{\text{per}}^\infty(\Omega)$		function space of infinitely differentiable and periodic functions
$\mathcal{D}(\Omega)$		function space of infinitely differentiable functions with compact support in Ω
$H^p(\Omega)$	$H^p(\Omega) = W^{p,2}(\Omega)$	Sobolev space
$H^{-1}(\Omega)$	$H^{-1}(\Omega) = (H_0^1(\Omega))'$	dual space of $H_0^1(\Omega)$
$H_{\text{div},0}^1(\Omega)$	$H_{\text{div},0}^1(\Omega) = \{\varphi \in (L^2(\Omega))^n, \nabla \cdot \varphi \in L^2(\Omega), \varphi \cdot \nu = 0 \text{ on } \partial\Omega_D\}$	function space containing functions whose divergence is in $L^2(\Omega)$
$L^p(\Omega)$	$L^p(\Omega) = \{\varphi : \Omega \rightarrow \mathbb{R} : \varphi \text{ Lebesgue measurable, } \ \varphi\ _{L^p(\Omega)} < \infty\}$	Lebesgue space, function space containing functions whose p -th power is Lebesgue integrable
$\ \cdot\ _{L^p(\Omega)}$	$\ \varphi\ _{L^p(\Omega)} = \left(\int_\Omega \varphi ^p d\mathbf{x}\right)^{1/p}$	L^p -norm, $p \neq \infty$
$\ \cdot\ _{L^\infty(\Omega)}$	$\ \varphi\ _{L^\infty(\Omega)} = \text{ess sup}_\Omega \varphi $	L^∞ -norm
$L^p(L^q)$	$L^p(L^q) = L^p(0, T; L^q(\Omega))$	Lebesgue space in time space cylinder
$V_0^1(\Omega)$	$V_0^1(\Omega) = \{\varphi \in H^1(\Omega) : \varphi = 0 \text{ on } \partial\Omega_D\}$	function space
$V_0^1(\Omega_\varepsilon)$	$V_0^1(\Omega_\varepsilon) = \{\varphi \in H^1(\Omega_\varepsilon) : \varphi = 0 \text{ on } \partial\Omega_D\}$	function space
$W^{p,q}(\Omega)$		Sobolev space, function space containing functions whose derivatives up to orders p are in L^q
$\ \cdot\ _{W^{p,q}(\Omega)}$	$\ \varphi\ _{W^{p,q}(\Omega)} = \left(\sum_{ \alpha \leq p} \int_\Omega D^\alpha \varphi ^q d\mathbf{x}\right)^{1/q}$	$W^{p,q}$ -norm, $q \neq \infty$
$\ \cdot\ _{W^{p,\infty}(\Omega)}$	$\ \varphi\ _{W^{p,\infty}(\Omega)} = \sum_{ \alpha \leq p} \text{ess sup}_\Omega D^\alpha \varphi $	$W^{p,\infty}$ -norm

$W^{p,q}(W^{r,s})$	$W^{p,q}(W^{r,s})$ $= W^{p,q}(0, T; W^{r,s}(\Omega))$	Sobolev space in time space cylinder
X		general function space
X'		dual space of function space X
$\langle \cdot, \cdot \rangle_{X',X}$		duality pairing
X_0		function space of functions having zero boundary data
X^n	$X^1 = X$ $X^n = \underbrace{X \times X \times \dots \times X}_{n \text{ times}}$	function space with functions whose n components belong to X

A.4 (Differential) operators

∂_i		partial derivative w.r.t. component i
∂_t		partial derivative with respect to time
∂_{x_i}		partial derivative with respect to x_i
∂_{y_i}		partial derivative with respect to y_i
$\frac{d}{dt}$		derivative with respect to time
$\delta \cdot$		small variation of \cdot
D		differential
Δ		difference
∇	$\nabla \varphi = (\partial_i \varphi)_{i=1, \dots, n}$	gradient
∇	$\nabla \varphi = (\partial_i \varphi_j)_{i,j=1, \dots, n}$	gradient
∇_ε		gradient of a two-scale functions
∇_x		gradient with respect to \mathbf{x}
∇_y		gradient with respect to \mathbf{y}
$\nabla \cdot$	$\nabla \cdot \varphi = \sum_{i=1}^n \partial_i \varphi_i$	divergence
$\nabla \cdot$	$\nabla \cdot \mathbf{A} = \left(\sum_{j=1}^n \partial_j A_{ij} \right)_{i=1, \dots, n}$	divergence
Δ	$\Delta \varphi = \sum_{i=1}^n \partial_i \partial_i \varphi$	Laplace operator
Δ	$\Delta \varphi = \left(\sum_{i=1}^n \partial_i \partial_i \varphi_j \right)_{j=1, \dots, n}$	Laplace operator
\mathcal{L}		differential operator
\mathcal{L}_ε		differential operator
$\bar{\mathcal{L}}$		averaged differential operator
$\int_0^T \cdot dt$		integration w.r.t. time over interval $(0, T)$
$\int_\Omega \cdot d\mathbf{x}$		integration w.r.t. space over domain Ω
$\int_Y \cdot d\mathbf{y}$		integration w.r.t. space over domain Y
$\int_\Gamma \cdot d\mathbf{y}$		surface integral over boundary Γ
E		extension operator
E_0		extension operator which extends functions by zero
E_p		extension operator of the pressure

A.5 Physical quantities

\cdot^0		initial value, i.e. physical quantity at $t = 0$
\cdot^0		physical quantity of order ε^0
\cdot^i		species index; physical quantity of order ε^i
\cdot_ε		physical quantity on pore-scale
$\bar{\cdot}$		y -averaged physical quantity
\cdot_{eq}		equilibrium value of physical quantity
\cdot_{col}		physical quantity related to colloids
\cdot_{el}		physical quantity related to electrostatics
\cdot_{hydr}		physical quantity related to hydrodynamics
\cdot_∞		bulk value of physical quantity
\cdot_\pm		physical quantity related to positively/negatively charged species
$\tilde{\cdot}$		modified/redefined physical quantity
$\hat{\cdot}$		limit of physical quantity
\mathbf{a}	$= (a_1, \dots, a_n) \in \mathbb{R}^n$	general vector with components a_i
\mathbf{A}	$\mathbf{A} = (A_{ij})_{i,j=1,\dots,n}$	general matrix with entries A_{ij}
A	–	weighted porosity
$\alpha_1, \alpha_2, \alpha_3$		scaling parameter
α_j		parameter in Moser iteration
β		scaling parameter
β_t, β_l		transversal/longitudinal dispersion coefficient
c	$1/\text{m}^3$	number density of species
d	m	grain radius
D	m^2/s	diffusivity of colloidal particles in the fluid
\mathbf{D}	m^2/s	effective diffusion tensor
e	C	elementary charge
\mathcal{E}	$\text{kg m}^2/\text{s}^2$	electrostatic energy
ε	–	scale parameter, ratio of pore size to domain size
$\varepsilon_0 \varepsilon_r$	$\text{C}^2 \text{s}^2/\text{kg}/\text{m}^3$	permittivity of vacuum times relative permittivity
η	m^2/s	kinematic viscosity of the fluid
f	$\text{kg}/\text{m}^2/\text{s}$	surface reaction rate
F	$\text{kg}/\text{m}^3/\text{s}$	effective production/consumption
	$\text{kg m}/\text{s}^2$	interaction force
γ		scaling parameter

\mathbf{j}	$(1/\text{m}^2/\text{s})$	(mass) flux
k, k_f, k_b	$1/\text{s}$	rate coefficient
$k_B T$	$\text{kg m}^2/\text{s}^2$	Boltzmann constant times absolute temperature
\mathbf{K}	m^2	effective permeability tensor
$\hat{\mathbf{K}}$	m^2	effective tensor
l, L	m	pore-scale/macroscale length
L	m	level set function
\mathbf{L}_{ij}		linear flux-force relation $\mathbf{j}_i = \sum_j \mathbf{L}_{ij} \mathbf{z}_j$
λ_D	m	Debye length
m	kg	(molecular) mass
μ	$\text{kg}/\text{m}/\text{s}, \text{kg m}^2/\text{s}^2$	dynamic viscosity of fluid; chemical potential
p	$\text{kg}/\text{m}/\text{s}^2$	pressure
π	—	solution of cell problem
ϕ	$\text{kg m}^2/\text{s}^2$	total (interaction) potential
ϕ^{el}	$\text{kg m}^2/\text{s}^2/\text{C}$	electrostatic potential
ϕ^{ion}	$\text{kg m}^2/\text{s}^2$	ionic potential
Ψ^*		dissipation functional
r	m	distance between particle and porous matrix
R	$1/\text{m}^3/\text{s}, \text{m}$	chemical reaction rate; grain radius
ρ_s	kg/m^3	density of the solid phase including attached particles
ρ	kg/m^3	density of the fluid
σ	C/m^2	(surface) charge density
t	s	time
T	s	end time
τ	—	tortuosity
θ	—	porosity
u	$1/\text{m}^3$	transformed number density
\mathbf{v}	m/s	velocity
\mathbf{V}	m/s	effective transport velocity
v_n	m/s	normal velocity of the solid-liquid interface
\mathbf{w}	—	solution of cell problem
\mathbf{x}	m	global space variable
\mathbf{x}^M	m	largest integer not greater than \mathbf{x}
\mathbf{x}^S	m	relative shift of \mathbf{x} , $\mathbf{x}^S = \mathbf{x} - \mathbf{x}^M$
X	—	chemical species

ξ	—	solution of cell problem
\mathbf{y}	m	microscopic space variable
z	—	charge number
\mathbf{z}	—	driving force in linear flux-force relation
		$\mathbf{j}_i = \sum_j \mathbf{L}_{ij} \mathbf{z}_j$
ζ	—	flux variable related to ξ

A.6 Dimensionless numbers and characteristic quantities

\cdot^*	dimensionless quantity
Pe	Pechlet number
Re	Reynolds number
St	Stouhal number
C	characteristic number density
K	characteristic reaction rate
L	characteristic length
P	characteristic pressure
Φ	characteristic potential
t_c	characteristic time
V	characteristic velocity

Bibliography

- [1] E. Acerbi et al. “An extension theorem from connected sets, and homogenization in general periodic domains.” In: *Nonlinear Analysis* 18.5 (Mar. 1992), pp. 481–496.
- [2] H.-D. Alber. “Evolving Microstructure and Homogenization.” In: *Continuum Mechanics and Thermodynamics* 12 (2000), pp. 235–286.
- [3] G. Allaire. “Homogenization and two-scale convergence.” In: *SIAM Journal on Mathematical Analysis* 23.6 (1992), pp. 1482–1518.
- [4] G. Allaire, A. Mikelić, and A. Piatnitski. “Homogenization of the linearized ionic transport equations in rigid periodic porous media.” In: *Journal of Mathematical Physics* 51 (2010), pp. 103–123.
- [5] G. Allaire and F. Murat. “Homogenization of the Neumann problem with non-isolated holes.” In: *Asymptotic Analysis* 7.2 (1993), pp. 81–95.
- [6] P. W. Atkins. *Physical Chemistry*. 3rd ed. W. H. Freeman and Company, 1985.
- [7] J. Auriault and P. Adler. “Taylor dispersion in porous media: Analysis by multiple scale expansions.” In: *Advances in Water Resources* 18 (1995), pp. 211–226.
- [8] J. Auriault and J. Lewandowska. “On the Cross-Effects of Coupled Macroscopic Transport Equations in Porous Media.” In: *Transport in Porous Media* 16 (1994), pp. 31–52.
- [9] J. Auriault and T. Strzelecki. “On the electro-osmotic flow in a saturated porous medium.” In: *International Journal of Engineering Science* 19.7 (1981), pp. 915–928.
- [10] J. Baer. *Dynamics of Fluids in Porous Media*. New York: Dover Publications, 1972.

-
- [11] M. Bause and P. Knabner. “Numerical Simulation of Contaminant Biodegradation by Higher Order Methods and Adaptive Time Stepping.” In: *Computing and Visualization in Science* 7 (2004), pp. 61–78.
- [12] L. Bedin and M. Thompson. “Existence theory for a Poisson-Nernst-Planck model of electrophoresis.” arXiv:1102.5370v1 [math.AP]. 2011.
- [13] H. M. Bekhit, M. A. El-Kordy, and A. E. Hassan. “Contaminant transport in groundwater in the presence of colloids and bacteria: Model development and verification.” In: *Journal of Contaminant Hydrology* 108.3-4 (2009), pp. 152–167.
- [14] H. M. Bekhit and A. E. Hassan. “Two-dimensional modeling of contaminant transport in porous media in the presence of colloids.” In: *Advances in Water Resources* 28.12 (2005), pp. 1320–1335.
- [15] A. Bensoussan, J.-L. Lions, and G. Papanicolau. *Asymptotic analysis of periodic structures*. North-Holland, 1978.
- [16] M. A. Biot. “General Theory of Three-Dimensional Consolidation.” In: *Journal of Applied Physics* 12.2 (1941), pp. 155–164.
- [17] X. Blanc, C. L. Bris, and P.-L. Lions. “Stochastic homogenization and random lattices.” In: *Journal de Mathématiques Pures et Appliquées* 88.1 (2007), pp. 34–63.
- [18] K. Bourbatache et al. “Modeling the Chlorides TRansport in Cementitious Materials by Periodic Homogenization.” In: *Transport in Porous Media* 22 (2012), pp. 1–23.
- [19] M. Burger, B. Schlake, and M.-T. Wolfram. “Mathematical modeling and simulation of nanopore blocking by precipitation.” In: *Journal of Physics: Condensed Matter* 22.45 (2010), 454101 (6pp).
- [20] M. Burger, B. Schlake, and M.-T. Wolfram. “Nonlinear Poisson-Nernst-Planck equations for ion flux through confined geometries.” In: *Nonlinearity* 25 (2012), pp. 961–990.
- [21] A. Chavarria-Krauser and M. Ptashnyk. “Homogenization of long-range auxin transport in plant tissues.” In: *Nonlinear Analysis: Real World Applications* 11.3 (2010), pp. 4524–4532.
- [22] Z. Chen. *Finite Element Methods and Their Applications*. Springer, 2005.

-
- [23] Y. S. Choi et al. “Electrodifusion of ions inside living cells.” In: *IMA Journal of Applied Mathematics* 62.3 (1999), pp. 207–226.
- [24] D. Cioranescu and P. Donato. *An Introduction to Homogenization*. Oxford University Press, 2000.
- [25] D. Cioranescu and J. Staint Jean Paulin. “Homogenization in open sets with holes.” In: *J. Math. Anal. Appl.* 71 (1979), pp. 590–607.
- [26] D. Cioranescu and J. Staint Jean Paulin. *Homogenization of Reticulated Structures*. Springer, 1999.
- [27] F. Ciucci and W. Lai. “Derivation of Micro/Macro Lithium Battery Models from Homogenization.” In: *Transport in Porous Media* 88 (2011), pp. 249–270.
- [28] M. Y. Corapcioglu and H. Choi. “Modeling colloid transport in unsaturated porous media and validation with laboratory column data.” In: *Water Resources Research* 32.12 (1996), pp. 3437–3449.
- [29] M. Y. Corapcioglu and S. Jiang. “Colloid-Facilitated Groundwater Contaminant Transport.” In: *Water Resources Research* 29.7 (1993), pp. 2215–2226.
- [30] M. Y. Corapcioglu and K. Song-Bae. “Contaminant transport in dual-porosity media with dissolved organic matter and bacteria present as mobile colloids.” In: *Journal of Contaminant Hydrology* 59.3-4 (2002), pp. 267–289.
- [31] S. Dargaville and T. W. Farrell. “Predicting Active Material Utilization in LiFePO₄ Electrodes Using a Multiscale Mathematical Model.” In: *Journal of The Electrochemical Society* 157.7 (2010), pp. 830–840.
- [32] B. Derjaguin and L. Landau. “Theory of the stability of strongly charged lyophobic sols and of the adhesion of strongly charged particles in solutions of electrolytes.” In: *Progress in Surface Science* 43.1-4 (1993), pp. 30–59.
- [33] E. DiBenedetto. *Degenerate Parabolic Equations*. New York: Springer, 1993.
- [34] P. Domenico and F. Schwartz. *Physical and Chemical Hydrogeology*. New York: Wiley, 1990.
- [35] W. E et al. “Heterogeneous multiscale methods: A review.” In: *Communications in Computational Physics* 2.3 (2007), pp. 367–450.
- [36] C. Eck. *A two-scale phase field model for liquid-solid phase transitions of binary mixtures with dendritic microstructure, habilitation thesis*. 2004.

- [37] C. Eck. “Analysis of a two-scale phase field model for liquid-solid phase transitions with equiaxed dendritic microstructure.” In: *Multiscale Modeling and Simulation* 3.1 (2004), pp. 28–49.
- [38] C. Eck. “Error estimates for a finite element discretisation of a two-scale phase field model.” In: *Multiscale Modeling and Simulation* 6.1 (2007), pp. 1–26.
- [39] C. Eck, H. Garcke, and P. Knabner. *Mathematische Modellierung*. Springer, 2008.
- [40] Y. Efendiev and T. Y. Hou. *Multiscale Finite Element Method – Theory and Application*. Springer, 2009.
- [41] M. Elimelech et al. *Particle Deposition and Aggregation, Measurement, Modelling and Simulation*. Butterworth-Heinemann, 1995.
- [42] H. Elman, D. Silvester, and A. Wathen. *Finite Elements and Fast Iterative Solvers with Applications in Incompressible Fluid Dynamics*. Oxford: Oxford University Press, 2005.
- [43] A. Ern and J. L. Guermond. *Theory and Practice of Finite Elements*. Applied Mathematical Sciences. Springer, 2004.
- [44] L. C. Evans. *Partial Differential Equations*. Vol. 19. Graduate Studies in Mathematics. Providence, Rhode Island: American Mathematical Society, 1998.
- [45] F. Frank. “HyPHM.” <http://www1.am.uni-erlangen.de/HyPHM>. retrieved on 1 Oct 2012.
- [46] F. Frank, N. Ray, and P. Knabner. “Numerical Investigation of a Homogenized Stokes-Nernst-Planck-Poisson Problem.” In: *Computating and Visualization in Science* 14.8 (accepted). (Preprint 352, Applied Mathematics, University of Erlangen-Nuremberg, 2012).
- [47] H. Gajewski and I. V. Skrypnik. “Existence and Uniqueness Results for Reaction-diffusion Processes of Electrically Charged Species.” In: *Nonlinear Elliptic and Parabolic Problems*. Ed. by H. Brezis, M. Chipot, and J. Escher. Vol. 64. Progress in Nonlinear Differential Equations and Their Applications. Birkhäuser Basel, 2005, pp. 151–188.
- [48] H. Gajewski. “On Existence, Uniqueness and Asymptotic Behaviour of Solutions of the Basic Equations for Carrier Transport in Semiconductors.” In: *Z. Angew. Math. u. Mech.* 65.2 (1985), pp. 101–108.

- [49] H. Gajewski and K. Gröger. “Reaction-Diffusion Processes of Electrically Charged Species.” In: *Math. Nachr.* 177.1 (1996), pp. 109–130.
- [50] H. Gajewski, K. Gröger, and K. Zacharias. *Nichtlineare Operatorgleichungen und Operatordifferentialgleichungen*. Akademie-Verlag, 1974.
- [51] H. Graaf. http://www.tu-chemnitz.de/physik/OSMP/Soft/ws0506_V14.pdf. retrieved on 1 Oct 2012.
- [52] P. Grisvard. *Elliptic Problems in Nonsmooth Domains*. Pitman, Monographs and Studies in Mathematics 24, 1985.
- [53] K. Gröger. “On steady-state carrier distributions in semiconductor devices.” In: *Aplikace matematiky* 32.1 (1987), pp. 49–56.
- [54] R. Helmig. *Multiphase Flow and Transport Processes in the Subsurface. A Contribution to the Modeling of Hydrosystems*. Ed. by U. Förstner, R. J. Murphy, and W. H. Rulken. Environmental Engineering. Springer, 1997.
- [55] M. Herz, N. Ray, and P. Knabner. “Existence and uniqueness of a global weak solution of a Darcy-Nernst-Planck-Poisson system.” In: *GAMM-Mitteilungen* 35.2 (2012). (Preprint 359, Applied Mathematics, University of Erlangen-Nuremberg), pp. 191–208.
- [56] T. Hofmann. “Die Welt der vernachlässigten Dimensionen, Kolloide.” In: *Chem. Unserer Zeit* 38 (2004), pp. 24–35.
- [57] U. Hornung and W. Jäger. “Diffusion, convection, adsorption and reaction of chemicals in porous media.” In: *Journal of Differential Equations* 92 (1991), pp. 199–225.
- [58] U. Hornung (editor). *Homogenization and Porous Media*. Springer, 1997.
- [59] IUPAC. *Compendium of Chemical Terminology, 2nd ed. (the “Gold Book”)*. Compiled by A. D. McNaught and A. Wilkinson, XML on-line corrected version: <http://goldbook.iupac.org> (2006-) created by M. Nic, J. Jirat, B. Kosata; updates compiled by A. Jenkins. ISBN 0-9678550-9-8. doi:10.1351/goldbook. Last update: 2012-08-19; version: 2.3.2. DOI of this term: doi:10.1351/goldbook.C01171. original PDF version: <http://www.iupac.org/goldbook/C01171.pdf>. retrieved on 1 Oct 2012.
- [60] M. Kato. “Numerical analysis of the Nernst-Planck-Poisson system.” In: *Journal of Theoretical Biology* 177.3 (1995), pp. 299–304.

- [61] C. E. Kenig, F. Lin, and Z. Shen. “Homogenization of elliptic systems with Neumann boundary conditions.” arXiv:1010.6114v1 [math.AP]. 2010.
- [62] W. Kinzelbach and R. Rausch. *Grundwassermodellierung. Eine Einführung mit Übungen*. Gebrüder Borntraeger, 1995.
- [63] B. J. Kirby. *Micro- and Nanoscale Fluid Mechanics. Transport in Microfluidic Devices*. Cambridge University Press, 2010.
- [64] P. Knabner. *Mathematische Modelle für Transport und Sorption gelöster Stoffe in porösen Medien, habilitation thesis*. Ed. by B. Brosowski and E. Martensen. 1991.
- [65] P. Knabner and L. Angermann. *Numerical Methods for Elliptic and Parabolic Partial Differential Equations*. Vol. 44. Texts in Applied Mathematics. New York: Springer, 2003.
- [66] P. Knabner, K. U. Totsche, and I. Kögel-Knabner. “The modeling of reactive solute transport with sorption to mobile and immobile sorbents - Part I: experimental evidence and model development.” In: *Water Resources Research* 32.6 (1996), pp. 1611–1622.
- [67] P. Knabner, C. J. van Duijn, and S. Hengst. “An Analysis of Crystal Dissolution Fronts in Flows through Porous Media - Part 1: Compatible Boundary Conditions.” In: *Advances in Water Resources* 18 (1995), pp. 171–185.
- [68] M. Kojic, N. Filipovic, and A. Tsuda. “A mesoscopic scale model for fluids and coupling dissipative particle dynamics with continuum finite element method.” In: *Comput. Methods Appl. Mech. Eng.* 197 (2008), pp. 821–833.
- [69] S. M. Kozlov. “The averaging of random operators.” In: *Mathematics of the USSR-Sbornik* 109 (1979), pp. 188–202.
- [70] S. Kräutle. *General Multi-Species Reactive Transport Problems in Porous Media: Efficient Numerical Approaches and Existence of Global Solutions, habilitation thesis*. 2008.
- [71] P. Kulkarni, R. Sureshkurma, and P. Biswas. “Hierarchical Approach to Model Multilayer Colloidal Deposition in porous Media.” In: *Envir. Sci. Technol.* 39 (2005), pp. 6361–6370.
- [72] W. Lai and F. Ciucci. “Mathematical modeling of porous battery electrodes. Revisit of Newman’s model.” In: *Electrochimica Acta* 56.11 (2011), pp. 4369–4377.

- [73] C. Le Bris. “Some Numerical Approaches for Weakly Random Homogenization.” In: *Numerical Mathematics and Advanced Applications 2009*. Ed. by G. Kreiss et al. Springer Berlin Heidelberg, 2010, pp. 29–45.
- [74] P. C. Lichtner, C. I. Steefel, and E. H. Oelkers. *Reactive transport in porous media*. Reviews in mineralogy. Mineralogical Society of America, 1996.
- [75] G. M. Lieberman. *Second order parabolic differential equations*. World Science Publishing, 1996.
- [76] Y. Liu et al. “Transport of *Cryptosporidium parvum* Oocysts in a Silicon Micro-model.” In: *Environmental Science & Technology* 46.3 (2012), pp. 1471–1479. eprint: <http://pubs.acs.org/doi/pdf/10.1021/es202567t>.
- [77] D. J. Logan. *Transport Modeling in Hydrogeochemical Systems*. Ed. by S. Antman et al. Vol. 15. Interdisciplinary applied mathematics. Springer, 2001.
- [78] J. R. Looker. *The Electrokinetics of Porous Colloidal Particles, PhD thesis*. 2006.
- [79] L. Lührmann. *Modellierung des kolloidgetragenen Schadstofftransports unter Berücksichtigung von Sorptions- und Filtrationsprozessen*. 1999.
- [80] J. H. Maasliyah and S. Bhattacharjee. *Electrokinetic and colloid transport phenomena*. John Wiley & Sons, 2006.
- [81] A. D. MacGillivray. “Nernst-Planck Equations and the Electroneutrality and Donnan Equilibrium Assumptions.” In: *Journal of Chem. Physics* 48.7 (1968), pp. 2903–2907.
- [82] A. D. MacGillivray and D. Hare. “Applicability of Goldman’s constant field assumption to biological systems.” In: *Journal of Theoretical Biology* 25.1 (1969), pp. 113–126.
- [83] R. V. Magan and R. Sureshkumar. “Multiscale-linking simulation of irreversible colloidal deposition in the presence of DLVO interactions.” In: *Journal of Colloid and Interface Science* 297 (2006), pp. 389–406.
- [84] A. Marciniak-Czochra and M. Ptashnyk. “Derivation of a macroscopic receptor-based model using homogenization technique.” In: *SIAM J. Math. Anal.* 40 (2008), pp. 215–237.
- [85] S. Marino, M. Shapiro, and P. M. Adler. “Coupled transport in heterogeneous media.” In: *J. Colloid Interface Sci.* 223 (2001), pp. 292–304.

- [86] P. A. Markovich. *The Stationary Semiconductor Device Equations*. Springer, 1986.
- [87] K. U. Mayer. *A numerical Model for Multicomponent Reactive Transport in Variably Saturated Porous Media, PhD thesis*. 1999.
- [88] J. E. McCarthy and Z. J. M. “Subsurface transportcontaminants – Mobile colloids in the subsurface environment may alter the transport of contaminants.” In: *Environ. Sci. Technol.* 23.5 (1989), pp. 496–502.
- [89] A. Mielke. “A gradient structure for the reaction-diffusion system and for the energy-drift-diffusion systems.” In: *WIAS Preprint, Berlin* 1485 (2010), pp. 1–17.
- [90] P. Ming and X. Yue. “Numerical methods for multiscale elliptic problems.” In: *Journal of Computational Physics* 214.1 (2006), pp. 421–445.
- [91] Y. Mori, J. W. Jerome, and C. S. Peskin. “A Three-Dimensional Model of Cellular Electrical Activity.” In: *Bulletin of the Institute of Mathematics. Academia Sinica* 2.2 (2007), pp. 367–390.
- [92] J. Moser. “A Harnack Inequality for Parabolic Differential Equations.” In: *Comm. Pure and Appl. Math.* XVII (1964), pp. 101–134.
- [93] J. Moser. “A new Proof of de Giorgi’s Theorem Concerning the Regularity Problem for elliptic Differential Equations.” In: *Comm. Pure and Appl. Math.* XIII (1960), pp. 457–468.
- [94] C. Moyne and M. A. Murad. “A Two-scale Model for coupled Electro-Chemo-Mechanical Phenomena and Onsager’s Reciprocity Relation in Expansive Clays: I Homogenization Analysis.” In: *Transp. in Porous Media* 62.3 (2006), pp. 333–380.
- [95] C. Moyne and M. A. Murad. “Electro-Chemo-Mechanical Couplings in swelling Clays derived from a micro/macro-homogenization procedure.” In: *International Journal of Solids and Structures* 39 (2006), pp. 6159–6190.
- [96] M. A. Murad and C. Moyne. “A dual-porosity model for ionic solute transport in expansive clays.” In: *Computational Geosciences* 12.1 (2008), pp. 47–82.
- [97] M. Neuss-Radu. “Some extensions of two-scale convergence.” In: *Comptes Rendus de l’Académie des Sciences. Série 1, Mathématique* 332 (1996), pp. 899–904.

- [98] M. Neuss-Radu and W. Jäger. *Homogenization of thin porous layers and applications to ion transport through channels of biological membranes*. Report. Reactive Flow and Transport Through Complex Systems (Organised by C. J. van Duijn, A. Mikelic, C. Schwab). Mathematisches Forschungsinstitut Oberwolfach, 2005, pp. 2809–2812.
- [99] J. Newman and W. Tiedemann. “Porous-electrode theory with battery applications.” In: *American Institute of Chemical Engineers* 21 (1975), pp. 25–41.
- [100] G. Nguetseng. “A general convergence result for a functional related to the theory of homogenization.” In: *SIAM J. Math. Anal.* 20 (1989), pp. 608–629.
- [101] A. L. Noell et al. “The role of silica colloids on facilitated cesium transport through glass bead columns and modeling.” In: *Journal of Contaminant Hydrology* 31 (1998), pp. 23–56.
- [102] R. O’Brian and L. R. White. “Electrophoretic Mobility of a Spherical Colloidal Particle.” In: *J. Chem. Soc., Faraday Trans. 2* 74 (1978), pp. 1607–1622.
- [103] L. Onsager. “Reciprocal Relations in Irreversible Processes. I.” In: *Phys. Rev.* 37 (4 1931), pp. 405–426.
- [104] G. Papanicolaou and S. R. S. Varadhan. “Boundary value problems with rapidly oscillating random coefficients.” In: vol. 27. *Seria Colloquia Mathematica Societatis Janos Bolyai*. North Holland, 1981, pp. 835–873.
- [105] M. Peter. *Coupled reaction-diffusion systems and evolving microstructure: mathematical modelling and homogenisation, PhD thesis*. 2006.
- [106] M. A. Peter and M. Böhm. “Different choices of scaling in homogenization of diffusion and interfacial exchange in a porous medium.” In: *Math. Meth. Appl. Sci.* 31 (2008), pp. 1257–1282.
- [107] A. Prechtel et al. “Simulation of carrier-facilitated transport of phenanthrene in a layered soil profile.” In: *Journal of Contaminant Hydrology* 56.3-4 (2002), pp. 209–225.
- [108] R. F. Probstein. *Physicochemical Hydrodynamics: An Introduction*. Wiley-Interscience, 2003.
- [109] A. Quateroni. *Modellistica Numerica per Problemi Differenziali*. Springer, 2003.

- [110] N. Ray, A. Muntean, and P. Knabner. “Rigorous homogenization of a Stokes-Nernst-Planck-Poisson system.” In: *Journal of Mathematical Analysis and Applications* 390 (2012). (CASA-Report 11-55, Technische Universität Eindhoven, 2011), pp. 374–393.
- [111] N. Ray et al. “Colloid and Fluid Dynamics in Porous Media including an Evolving Microstructure.” Preprint 351, Applied Mathematics, University of Erlangen-Nuremberg. 2011.
- [112] N. Ray et al. “Multiscale Modeling of Colloid and Fluid Dynamics in Porous Media Including an Evolving Microstructure.” In: *Transport in Porous Media* 95.3 (2012), pp. 669–696.
- [113] N. Ray et al. “Variable Choices of Scaling in the Homogenization of a Nernst-Planck-Poisson Problem.” Preprint 344, Applied Mathematics, University of Erlangen-Nuremberg. 2010.
- [114] W. Ren. “Analytical and numerical study of coupled atomistic-continuum methods for fluids.” In: *Journal of Computational Physics* 227 (2007), pp. 1353–1371.
- [115] L. A. Richards. “Capillary Conduction of Liquids through Porous Mediums.” In: *Journal of Applied Physics* 1.5 (1931), pp. 318–333.
- [116] K. Roth, H.-J. Vogel, and R. Kasteel. “The scaleway: A conceptual framework for upscaling soil properties.” In: *In Modelling of Transport Processes in Soils* 227 (1999), pp. 477–490.
- [117] T. Roubíček. “Incompressible Fluid Mixtures of Ionized Constitutents.” In: *Trends in Applic. of Math. to Mechanics*. Ed. by Y. Wang and K. Hutter. Shaker, 2005, pp. 429–440.
- [118] T. Roubíček. “Incompressible ionized fluid mixtures.” In: *Continuum Mechanics and Thermodynamics* 17.7 (2006), pp. 493–509.
- [119] T. Roubíček. *Nonlinear partial differential Equations with Applications*. Birkhäuser, 2005.
- [120] J. N. Ryan and M. Elimelech. “Colloid Mobilization and transport in groundwater.” In: *Colloids and Surfaces A Physicochemical and Engineering Aspects* 107 (1996), pp. 1–56.
- [121] I. Samohýl. “Application of Truesdell’s model of mixture to an ionic liquid mixture.” In: *Comp. and Math. with Appl.* 53.2 (2007), pp. 182–197.

- [122] E. Samson, J. Marchand, and J. J. Beaudoin. “Describing ion diffusion mechanisms in cement-based materials using the homogenization technique.” In: *Cement and Concrete Research* 29.8 (1999), pp. 1341–1345.
- [123] E. Sánchez-Palancia. *Nonhomogeneous media and vibration theory*. Springer, 1980.
- [124] A. E. Scheidegger. “General Theory of Dispersion in Porous Media.” In: *Journal of Geophysical Research* 66.10 (1961), pp. 3273–3278.
- [125] M. Schmuck. “Analysis of the Navier-Stokes-Nernst-Planck-Poisson System.” In: *Mathematical Models and Methods in Applied Sciences* 19.6 (2008), pp. 993–1014.
- [126] M. Schmuck. *Modeling, Analysis and Numerics in Electrohydrodynamics, PhD thesis*. 2008.
- [127] M. Schmuck. “Modeling and deriving porous media Stokes-Poisson-Nernst-Planck equations by a multiple-scale approach.” In: *Comm. Math. Sci.* 9.3 (2011), pp. 685–710.
- [128] L. Schreyer Bennethum and J. H. Cushman. “Multicomponent, Multiphase Thermodynamics of Swelling Porous Media with Electroquasistatics: I. Macroscopic Field Equations.” In: *Transport in Porous Media* 47 (2002), pp. 309–336.
- [129] L. Schreyer Bennethum and J. H. Cushman. “Multicomponent, Multiphase Thermodynamics of Swelling Porous Media with Electroquasistatics: II. Constitutive Theory.” In: *Transport in Porous Media* 47 (2002), pp. 337–362.
- [130] Z. Schuss, B. Nadler, and R. Eisenberg. “Derivation of Poisson and Nernst-Planck equations in a bath and channel from a molecular model.” In: *Comm. Math. Sci.* 9.3 (2011), pp. 685–710.
- [131] Z. Shen. “ W_p^1 estimates for elliptic homogenization problems in non-smooth domains.” In: *Indiana Univ. Math. J.* 57.5 (2008), pp. 2283–2298.
- [132] R. E. Showalter. *Monotone Operators in Banach Space and Nonlinear Partial Differential Equations*. Vol. 49. Mathematical Surveys and Monographs. American Mathematical Society, 1997.
- [133] D. Smith et al. “Theoretical Analysis of Anion Exclusion and Diffusive Transport Through Platy-Clay Soils.” In: *Transport in Porous Media* 57.3 (2004), pp. 251–277.

-
- [134] D. L. Sparks. *Environmental soil chemistry*. Academic Press, 1995.
- [135] W. Stumm and J. J. Morgan. *Aquatic chemistry. Chemical Equilibria and Rates in Natural Waters*. Ed. by J. L. Schoor and A. Zehnder. Environmental science and technology. John Wiley and sons, 1996.
- [136] S. Timmann. *Repititorium der Funktionentheorie*. Binomi, 1998.
- [137] C. J. van Duijn and P. Knabner. “Crystal Dissolution in Porous Media Flow.” In: *ZAMM* 76 (1996), pp. 329–332.
- [138] T. van Noorden. “Crystal precipitation and dissolution in a porous medium: effective equations and numerical experiments.” In: *Multiscale Modeling and Simulation* 7 (2009), pp. 1220–1236.
- [139] T. van Noorden and A. Muntean. “Homogenization of a locally-periodic medium with areas of low and high diffusivity.” In: *European Journal of Applied Mathematics* 22 (2011), pp. 493–516.
- [140] W. van Roosbroeck. “Theory of flow of electrons and holes in germanium and other semiconductors.” In: *Bell System Technical Journal* 29.4 (1950), pp. 560–607.
- [141] T. G. Van de Ven. *Colloidal Hydrodynamics*. Academic Press, 1989.
- [142] E. J. W. Verway and J. T. G. Overbeek. *Theory of the stability of lyophobic colloids*. Dover Publications, 1999.
- [143] S. Whitaker. *The Method of Volume Averaging. Theory and Applications of Transport in Porous Media*. Springer, 1998.
- [144] E. Zeidler. *Nonlinear Functional Analysis and its Applications I: Fixed Point Theorems*. Springer, 1986.

Hiermit erkläre ich, daß ich diese Arbeit selbständig und nur unter Verwendung der angegebenen Hilfsmittel angefertigt habe.

Erlangen, den 10. Juni 2013

Nadja Ray

Curriculum Vitae

ANGABEN ZUR PERSON

Name Nadja Ray
 Adresse Buckenhofer Weg 8
 91058 Erlangen
 Tel.: 09131/4002626
 nadjaray@web.de
 Geburtsdatum/-ort geboren am 11.09.1983 in Erlangen
 Familienstand verheiratet, keine Kinder
 Staatsangehörigkeit deutsch

AUSBILDUNGSDATEN

Schulbildung

09/1989 - 08/1993 Grundschule Bruck (Sandbergschule), Erlangen
 09/1993 - 06/2002 Emmy-Noether-Gymnasium, Erlangen (Abitur, Note 1.1)

Studium

10/2002 - 03/2008 Diplom-Mathematik, Universität Erlangen-Nürnberg
 (Diplom mit Auszeichnung, Note 1.05)
 Studienschwerpunkt Mathematische Modellierung und
 Angewandte Analysis, Nebenfach Theoretische Physik

Promotion

seit 12/2008 Promotion am Lehrstuhl für Angewandte Mathematik I
 Universität Erlangen-Nürnberg
 Thema: "Kolloidgetragener Schadstofftransport in porösen
 Medien – Modellierung und Analysis"
 Betreuer: Prof. Dr. Peter Knabner

AUSLANDSAUFENTHALTE

- 02/2006 - 06/2006 Auslands-Semester in Florenz/Italien
(Erasmus-Programm)
- 09/2010 - 10/2010 Forschungsaufenthalt in Eindhoven/Niederlande
- 04/2012 Forschungsaufenthalt in Bergen/Norwegen

STIPENDIEN

- 02/2003 - 03/2008 Studienstiftung des Deutschen Volkes
- 12/2008 - 11/2011 Deutsche Telekom Stiftung
- 01/2009 - 09/2011 Studienstiftung des Deutschen Volkes (ideelle Förderung)
- 12/2011 - 09/2012 Stipendienprogramm zur "Förderung der Chancengleichheit für Frauen in Forschung und Lehre" an der Universität Erlangen-Nürnberg

WISSENSCHAFTLICHE TÄTIGKEITEN**an der Universität Erlangen-Nürnberg**

- 04/2008 - 11/2008 Mitarbeiterin am Lehrstuhl für Angewandte Mathematik I
Sprechstunde Mathematik für Ingenieure I-IV
- seit 10/2012 Mitarbeiterin am Lehrstuhl für Angewandte Mathematik I
und am Lehrstuhl für Informatik 9
Übung Mathematik für Ingenieure 3C

VERÖFFENTLICHUNGEN

N. Ray et al. "Variable Choices of Scaling in the Homogenization of a Nernst-Planck-Poisson Problem." Preprint 344, Applied Mathematics, University of Erlangen-Nuremberg, 2010.

N. Ray, F. A. Radu, and P. Knabner. "Drug release from collagen matrices and transport phenomena in porous media including an evolving microstructure." In: *Proceedings of the 11th International Conference on Mathematical Methods in Science and Engineering, Alicante 26-30 June 2011*, 2011.

N. Ray, A. Muntean, and P. Knabner. "Rigorous homogenization of a Stokes-Nernst-Planck-Poisson system." In: *Journal of Mathematical Analysis and Applications* 390 (2012), pp. 374-393, (CASA-Report 11-55, Technische Universität Eindhoven, 2011).

N. Ray et al. “Colloid and Fluid Dynamics in Porous Media including an Evolving Microstructure.” Preprint 351, Applied Mathematics, University of Erlangen-Nuremberg, 2011.

N. Ray et al. “Multiscale Modeling of Colloid and Fluid Dynamics in Porous Media Including an Evolving Microstructure.” In: *Transport in Porous Media* 95.3 (2012), pp. 669-696.

M. Herz, N. Ray, and P. Knabner. “Existence and uniqueness of a global weak solution of a Darcy-Nernst-Planck-Poisson system.” In: *GAMM-Mitteilungen* 35.2 (2012), pp. 191-208, (Preprint 359, Applied Mathematics, University of Erlangen-Nuremberg, 2012).

N. Ray et al. “Drug release from collagen matrices including an evolving microstructure.” In: *Zeitschrift für Angewandte Mathematik und Mechanik* (2013), (Preprint 356, Applied Mathematics, University of Erlangen-Nuremberg, 2012).

F. Frank, N. Ray, and P. Knabner. “Numerical Investigation of a Homogenized Stokes-Nernst-Planck-Poisson Problem.” Accepted in: *Computing and Visualization* 14.8, (Preprint 352, Applied Mathematics, University of Erlangen-Nuremberg, 2012).